Illinois U Library

The American Mineralogist

Journal of the Mineralogical Society of America

Vol. 40 MAY–JUNE, 1955 Nos. 5 and 6

Contents

Relationship between light absorption and composition in a solid solution series . . . . . F. Donald Bloss 371
A compilation and classification of immersion media of high index of refraction . . . . . Robert Meyrowitz 398
Synthetic asbestos investigations, II: *X*-ray and other data on synthetic fluor-richterite, -edenite, and -boron edenite . . . J. A. Kohn and J. E. Comeforo 410
Differential thermal analysis and cell dimensions of some natural magnetites . . . . . E. R. Schmidt and F. H. S. Vermaas 422
Preliminary report on investigations of minerals of columbium and tantalum and of certain associated minerals . . . . . Richard W. Hutchinson 432
A second occurrence of the mineral sinhalite ($2\,MgO \cdot Al_2O_3 \cdot B_2O_3$) . . . . . Waldemar T. Schaller and Fred A. Hildebrand 453
Concentration of heavy accessories from large rock samples . . H. W. Fairbairn 458
Goldichite, a new hydrous potassium ferric sulfate from the San Rafael Swell, Utah . . . . . A. Rosenzweig and Eugene B. Gross 469
Radon leakage from radioactive minerals . . . . . Bruno J. Giletti and J. Laurence Kulp 481
Wavellite spherulites in the Bone Valley formation of central Florida . . . . . M. H. Bergendahl 497
Scawtite from Crestmore, California . . . . . Joseph Murdoch 505
A chemical, optical and *x*-ray study of scawtite from Ballycraigy, Larne, N. Ireland . . . . . J. D. C. McConnell 510
Notes and news: Studies of uranium minerals (XVII): Synthetic schroeckingerite . . . . . Virginia Ross 515
A discussion on "Mechanism of solution of quartz in pure water at elevated temperatures and pressures" . . . . . W. S. Fyfe 520
Directional hardness variation in tungsten carbide (WC) monocrystals . . . . . J. A. Kohn, Perry G. Cotter and R. A. Potter 522
Hornblende in diorite pegmatite near Camp Irwin, San Bernardino County, California . . . . . Robert D. Allen and Henry Kramer 527
Lattice spacings in clear crystalline quartz and their variability . . . . . H. D. Keith 530

(*continued on cover 2*)

EDITOR: WALTER F. HUNT
ASSISTANT EDITOR: LEWIS S. RAMSDELL
BOARD OF ASSOCIATE EDITORS:
ELBURT F. OSBORN
IAN CAMPBELL
WILLIAM F. BRADLEY
ADOLF PABST (1955)
BRIAN MASON (1955–56)
FRANCIS J. TURNER (1955–57)

Published bi-monthly by the Society

(*contents continued*)

Absorption spectra of smoky quartz from an Arkansas vein deposit and from a Sierran miarolitic granite . . . . Royal R. Marshall 535
A new parallel ruler for adapting the universal stage for petrofabric analysis . . . . A. W. Kleeman 537
Activation of photoluminescence in artificial calcite by stannous ion . . . . Stewart J. Carlson 540
On the stability and hydrothermal synthesis of benitoite . . . . D. E. Rase and Rustum Roy 542
Faults in gypsum accessory plates . . . . William T. Holser 544
Book reviews 546
New mineral names 551

Mineralogical Society of America

ASSOCIATED WITH THE GEOLOGICAL SOCIETY OF AMERICA

President: **Harry H. Hess,** Princeton University, Princeton, New Jersey.
Vice-President: **Clifford Frondel,** Harvard University, Cambridge 38, Massachusetts.
Secretary: **C. S. Hurlbut, Jr.,** Harvard University, Cambridge 38, Massachusetts.
Treasurer: **Earl Ingerson,** U. S. Geological Survey, Washington 25, D. C.
Editor: Walter **F. Hunt,** University of Michigan, Ann Arbor, Michigan.
Councillors: **Victor T. Allen,** Institute of Geophysical Technology, St. Louis, Missouri.
C. Osborne Hutton, Stanford University, Palo Alto, California.
Felix Chayes, Geophysical Laboratory, Washington, D. C.
Leonard G. Berry, Queen's University, Kingston, Ontario, Canada.
Sterling B. Hendricks, U. S. Department of Agriculture, Beltsville, Maryland.

The enlarged issues of this journal for 1955 are made possible by a grant from the Penrose Fund of the Geological Society of America.

The American Mineralogist—Journal of the Mineralogical Society of America

A journal containing articles on mineralogy, crystallography, petrography, and allied sciences, is issued every two months. Contributions are invited from everyone. Office of Publication, Mineralogical Laboratory, Ann Arbor, Michigan.

The general conduct of the journal is in the hands of the editor, **Walter F. Hunt,** Ann Arbor, Michigan, to whom all manuscripts should be submitted. To assist the editor the council of the Mineralogical Society has appointed **Lewis S. Ramsdell,** Ann Arbor, Michigan, assistant editor, and the following board of associate editors:

William F. Bradley, Illinois State Geological Survey, Urbana, Illinois.
Ian Campbell, California Institute of Technology, Pasadena 4, California.
Brian H. Mason, American Museum of Natural History, New York, N. Y.
Elburt F. Osborn, Pennsylvania State University, University Park, Pennsylvania.
Adolf Pabst, University of California, Berkeley 4, California.
Francis J. Turner, University of California, Berkeley 4, California.

It will expedite publication if two copies of each manuscript are submitted to the editor.

Sent to all members and fellows of the Mineralogical Society of America. Membership dues $4.00 annually, fellowship dues $5.00 annually. Subscriptions for libraries, colleges, institutions, companies and similar organizations $6.00 annually.

Entered as second class matter at the post office at Menasha, Wis., under Act of March 3, 1879. Acceptance for mailing at the special rate of postage provided for in section 1103, Act of Oct. 3, 1917, paragraph 4 section 429 P. L. & R. authorized March 13, 1922.

Notice of change of address, orders, and remittances should be sent to Dr. Earl Ingerson, U. S. Geological Survey, Washington 25, D. C.

Printed by the George Banta Publishing Company, Menasha, Wisconsin
Printed in the United States of America

THE AMERICAN MINERALOGIST

JOURNAL OF THE MINERALOGICAL SOCIETY OF AMERICA

Vol. 40 MAY–JUNE, 1955 Nos. 5 and 6

RELATIONSHIP BETWEEN LIGHT ABSORPTION AND COMPOSITION IN A SOLID SOLUTION SERIES*

F. DONALD BLOSS, *University of Tennessee, Knoxville, Tenn.*

ABSTRACT

Using a spectrophotometer improvised from a monochromator, polarizing microscope, and a photomultiplier tube, light absorbance measurements were made for the γ' direction on a (110) face for crystals of varying nickel content in the solid solution series between $Ni(NH_4)_2(SO_4)_2 \cdot 6H_2O$ and $Mg(NH_4)_2(SO_4)_2 \cdot 6H_2O$. Measured absorbance values were found to confirm the Beer-Lambert law within the limits of measurement. On the basis of this law, compositions predicted from absorbance per centimeter values of different crystals were accurate to within 3.0 mol per cent (of the compositions predicted from density values) for 75% of the crystals measured.

Calculations to obviate the effects of opaque inclusions and internal cleavages in the measured crystals when predicting composition from absorbance measurements are discussed.

INTRODUCTION

Previous Investigations

Absorption spectrophotometry rarely has been used to determine the chemical composition of a mixed crystal in a solid solution series; on the other hand, the analysis of liquid solutions by colorimetric methods has found increasing use. To the writer's knowledge Malmqvist (1929, p. 224) was one of the first to realize the possibility of correlating chemical composition and light absorption in a solid solution series and thereby using light absorption measurements to aid in ascertaining the chemical composition of a mixed crystal.

In his work on crystals of varying compositions in the epidote series, Malmqvist attempted to establish for this series the applicability of Beer's law, an expression of the relationship between light absorption and chemical composition in solutions (much used by chemists in the colorimetric analysis of liquids). His conclusion that Beer's law can well be used for this series (Malmqvist, p. 275) is unfortunately based on all-too-meager data, namely a comparison for two crystals of piedmontite of the amounts of MnO calculated to be present on the basis of: (*a*) refractive index measurements and (*b*) absorption measurements at the wavelengths 5893 and 6563 Å.

---

* An investigation conducted in the laboratories of the Department of Geology of the University of Chicago as part of a Ph.D. thesis by the author.

Tromnau (1934, pp. 355, 368) attempted to determine the relationship between light absorption and chemical composition for some artificial cobalt-colored spinels but, unfortunately, single crystals with sufficient cobalt content to be analyzable proved too opaque whereas crystals sufficiently transparent did not possess enough cobalt for an accurate analysis. In 1936, J. Evers (Rehberg, 1949, p. 1) concluded in an unpublished dissertation that light absorption was a function of chromium content in a series of synthetic spinels but he was unable to determine the nature of this correlation.

One of the first published accounts of a successful confirmation of Beer's law for a solid solution series, that of C. H. Rehberg (1949), became accessible to the writer only after the experimental work of this present paper was well under way. Rehberg performed spectrophotometric measurements on some mixed crystals of the solid solution series between common alum and chrome alum. Using a graphical method of analyzing his data, he found fairly close conformation to Beer's law and further expressed the opinion (1949, p. 18) that Beer's law would probably hold for all solid solutions.

Rehberg's work was excellent but a few points of minor criticism should perhaps be considered: (1) his published graphs were drawn on too small a scale and visual deviations from linearity were thereby suppressed, (2) crystals grown from the same solution were assumed to possess the same composition,* (3) light losses due to reflection were not considered by Rehberg, and (4) the wide (200 Å) spectral band used further reduced accuracy.

In spite of the last three objections, Rehberg's data on absorption enable predictions of composition within an accuracy of 5 mol per cent, if one corrects the typographical errors in his Table 5 (Rehberg, 1949, p. 12) for the 41.9 mol per cent crystal at wavelengths: 540, 560, 580, and 600 mu.

---

* The present writer found variations of up to 3 mol per cent in the composition of mixed crystals of the same crop when grown by evaporation from aqueous solutions of nickel ammonium sulfate and magnesium ammonium sulfate (under conditions of controlled temperature and humidity). Possibly this effect is not so severe for the chrome-alum crystals used by Rehberg; however, the method of extrapolating an analysis of a sibling crystal to provide the composition of the crystal being spectrophotometrically analyzed introduces undesirable uncertainties.

Selection of the Solid Solution Series to be Studied

Artificially grown mixed crystals of the solid solution series between nickel ammonium sulfate, $Ni(NH_4)_2(SO_4)_2 \cdot 6H_2O$, and magnesium ammonium sulfate, $Mg(NH_4)_2(SO_4)_2 \cdot 6H_2O$, were chosen for study because of the following advantages: (1) crystals free of impurities could be obtained, (2) composition of *individual* crystals, as was anticipated, could be accurately predicted (Bloss, 1952, eq. 6) from their densities, and (3) the series was monoclinic and therefore analogous to several important mineral solid solutions to which it is hoped this work may be extended. The first two advantages enumerated were especially helpful in permitting an adequate test of the relationship between light absorption and concentration of colorant without excessive complications.

EXPERIMENTAL DETAILS

A full description of the experimental details appears in an unpublished doctoral dissertation (Bloss, 1951); to orient the reader, however, a synoptic presentation follows.

Growth of Crystals and Determination of Their Composition

The crystals were grown by evaporation (at a controlled temperature and humidity) from saturated aqueous solutions containing nickel ammonium sulfate and magnesium ammonium sulfate in varying proportions. From the previously established equation relating density to composition for this series (Bloss, 1952, p. 970, eq. 6), the composition of small single crystals could be calculated from their density values as measured with a Berman micro-balance. Therefore, the composition of each individual crystal selected for the spectrophotometric work was known with confidence to within one mol per cent (Bloss, 1952, p. 971, Table 4). The measured densities and predicted compositions of the crystals used in the spectrophotometric work are listed in Table 1.

Spectrophotometric Apparatus and Procedures

Arrangement and function of apparatus. A 1000 candle power Pointolite bulb, housed at *L* of Fig. 1, served as a source of continuous visible radiation. The collecting lens, *CL*, gathered and focused the light upon the entrance slit, *ES*, of the monochromator, *MO*, which was actually a converted Bausch and Lomb Laboratory Wave-length Spectrometer with a constant deviation prism of the Pellin-Broca type. An empty cooling cell, *CC*, located between *CL* and *ES*, served as a convenient means of controlling light intensity; rotation of the cell about an axis parallel to the brass rod upon which it was mounted altered the percentage of

TABLE 1. COMPOSITION OF CRYSTALS STUDIED

Code Number of Crystal	Density Measurements		$Ni(NH_4)_2(SO_4)_2 \cdot 6H_2O$ Content of Crystals[a]	
	Average of 3 Determinations	Deviation	Mol Per Cent	Mols Per Liter[b]
0-19	—	—	0.00	0.0000
0-1	1.7512	.0005	15.30	0.7323
0-3	1.7638	.0004	21.61	1.0356
0-9	1.7802	.0001	29.83	1.4318
0-10	1.7824	.0001	30.93	1.4850
0-12	1.8069	.0005	43.14	2.0762
0-11	1.8071	.0001	43.24	2.0810
0-7	1.8537	.0004	66.31	3.2059
0-8	1.8539	.0003	66.41	3.2107
0-17	1.8851	.0010	81.74	3.9640
0-5	1.9013	.0003	89.67	4.3554
0-22	—	—	100.00	4.8671
0-23	—	—	100.00	4.8671

[a] With the exception of 0-19, 0-22, and 0-23 which were grown from pure solutions and therefore of known composition, compositions were calculated from the densities using the formula

$$h(\rho) = -1028.0653 + 689.6492\rho - 53.5518\rho^2$$

previously established for this solid solution series (Bloss, 1952, p. 970) to relate composition in terms of mol per cent of $Ni(NH_4)_2(SO_4)_2 \cdot 6H_2O$) as a function, $h(\rho)$, of the crystal's density, ρ.

[b] The formula for the conversion of mol per cent to mols per liter is

$$C = \frac{n\rho}{n(N - M) + M}$$

where C represents the mols nickel ammonium sulfate present in a liter volume of a crystal containing n mol per cent nickel ammonium sulfate and having a density of ρ. M and N refer to 360.62 and 394.99 grams, respectively, the gram molecular weights for magnesium ammonium sulfate and nickel ammonium sulfate.

light transmitted through the two parallel glass planes of the cell. After dispersion by *MO*, the light leaves the exit slit, *XS*, and is directed upon the substage mirror of the polarizing microscope. By means of the substage lenses, the image of slit *XS* is focused, now in plane polarized light, into the plane of the microscope stage.

The cable release mount *CR*, a one-eighth inch thick circular disc of brass with a 0.5 mm. diameter hole at its center (Fig. 2), is screwed onto the microscope stage so that its opening, which acts as a fixed diaphragm, is centered in the field of view of the microscope. Actuation of the cable release causes *CH*, a removable rectangular piece of brass through which is drilled a 1 mm. diameter hole, to slide centripetally until stopped by the set screw, *SS* (which may be so adjusted that the hole in *CH*, in its arrested position, lies directly over the central hole in *CR*). Upon cessation of pressure on the cable release, *CH* moves centrifugally to a rest position entirely clear of *CR*'s central hole. Thus a crystal mounted on crystal holder, *CH*, can be made to move into or out of the path of a light beam passing through the central hole in *CR*.

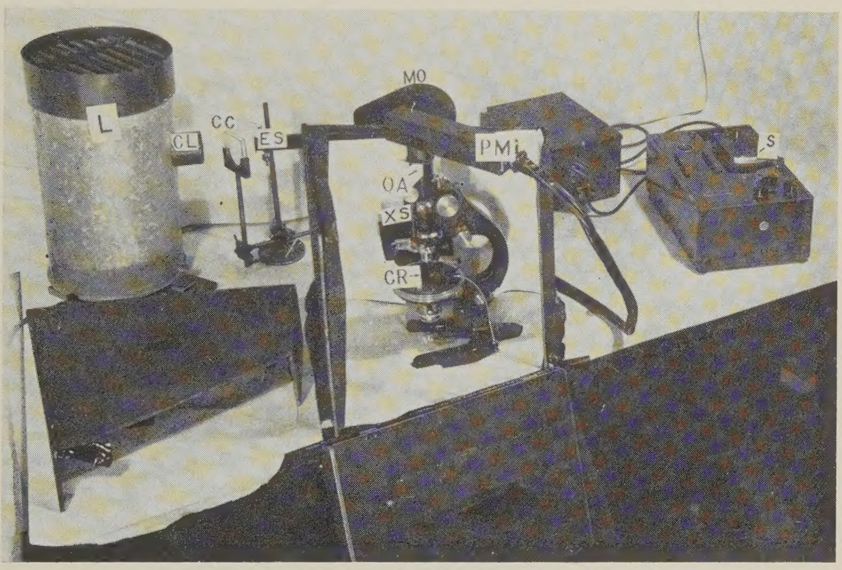

FIG. 1. Arrangement of apparatus for spectrophotometric measurements. For illustrative purposes, the light proof enclosure for the microscope has been opened and pieces of gray paper taped over its dull black finish (and that of the table). Lamp, spectrometer, and microscope were securely fastened to the table to maintain proper alignment. The ordinary substage mirror of the microscope was replaced by a first surface mirror.

Light entering the objective of the microscope follows the usual optical path (analyzer out). The ocular adapter, *OA* of Fig. 1, is essentially a brass tube which fits snugly over the ocular; its upper end is threaded and screws into the housing of the photomultiplier tube, *PM*. Both joints are light tight. Within *OA* a piece of frosted glass is mounted to coincide with the exit pupil. It is essential; without it a light spot at the center of the field of view caused a larger photoelectric response than did a spot of equal area and intensity more peripherally located, an effect probably caused by the curvature of the photomultiplier tube. The intensity of response of the photomultiplier tube to the diffused light from the frosted glass was read in terms of the arbitrary units of the linearly responding scale, S, of the Photovolt Model 512-M photometer used for this work.

Measurements of light absorption. One of the numbered crystal holders, CH, upon which a crystal is mounted (Fig. 2), is coupled to the motivating mechanism of the cable release by means of the small coupling pin so that the crystal can be readily moved into or out from the path of the light beam. With the crystal in (nicols crossed, sodium light), the micro-

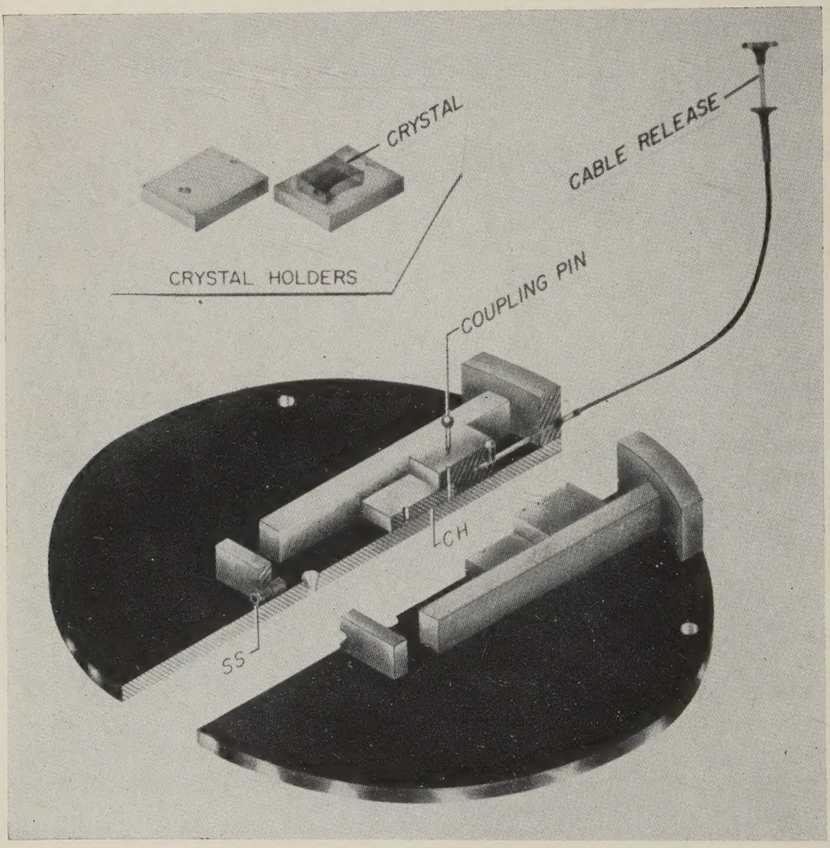

FIG. 2. Isometric sectional view of the cable release mount (CR in Fig. 1). The centrally located, slightly conical hole was 0.5 mm. in diameter (for illustrative purposes both its size and conic shape have been exaggerated); the holes in the crystal holders were 1.0 mm. in diameter. Several extra crystal holders were available and a quick interchange with CH, the crystal holder in place, was possible simply by withdrawing the coupling pin and substituting a crystal holder with a different crystal mounted on it. Two extra crystal holders are shown to the upper left, one with a crystal plate already mounted on it.

scope stage is rotated until a minimum reading on scale S indicates an extinction position. With the crystal at the desired extinction position and the analyzer out, the intensity readings on scale S are, for a given wavelength, successively recorded for the crystal inserted into and for it withdrawn from the optical path. Minimization of the interval between insertion and withdrawal decreases the possibility of variation in the intensity of the light source (in response to line voltage fluctuations) between these two readings.

In some instances, however, the intensity fluctuations were so rapid as to inevitably affect the accuracy of the readings. Fortunately the effect was random so that the four or five pairs of readings normally taken for each wavelength generally yielded an average of a higher order of accuracy. Each set of readings was secured as follows: first a reading was taken for the unimpeded beam, next for the crystal-transmitted beam, and lastly for the unimpeded beam again. If the third reading agreed with the first, the results were accepted and the first and second readings were recorded as a pair. Prior, however, to running the series of absorption measurements for the several different wavelengths, the monochromator was set at a wavelength for which the crystal transmitted around 50 to 70 per cent of the light. Set screw SS, Fig. 2, was then adjusted until successive absorption measurements showed a maximum light transmission for a certain position. This was done for each crystal measured so that its clearest portion would always be used.

A second set of observations was often made two or three days later. Eight to ten weeks later some of the crystals were ground to a new thickness and the set of observations was repeated.

Thickness Measurements

After completion of the absorption measurements on a crystal, the thickness of that portion of it over the hole in CH was measured using a micrometer calipers in conjunction with a dial indicator. The dial indicator permitted the same contact pressure to be attained during all measurements. Measurements are believed to be accurate to within .003 cm.

Discussion of Beer's Law

Statement of Beer's Law; Definitions

Beer's law, generally but possibly erroneously believed to have been formulated by Beer (Pfeiffer and Liebhafsky, 1951, p. 123), reads for a solution containing n light-absorbing components through which monochromatic light is transmitted

$$\mathrm{A} = \log \frac{I_0}{I} = (\epsilon_a C_a + \epsilon_b C_b + \cdots \epsilon_n C_n)d \qquad \text{Eq. (1).}$$

The value log I_0/I or A is termed absorbance* (Brode, 1950, p. 199); I_0 and I respectively indicate the intensity of the light beam *immediately after entrance into* and *immediately prior to exit from* the solution; C represents the concentration in mols per liter of the respective colorants in the solution; d is the distance in centimeters that the light beam travels through the solution; ϵ represents the molar absorbance of the respective colorants for the light used.

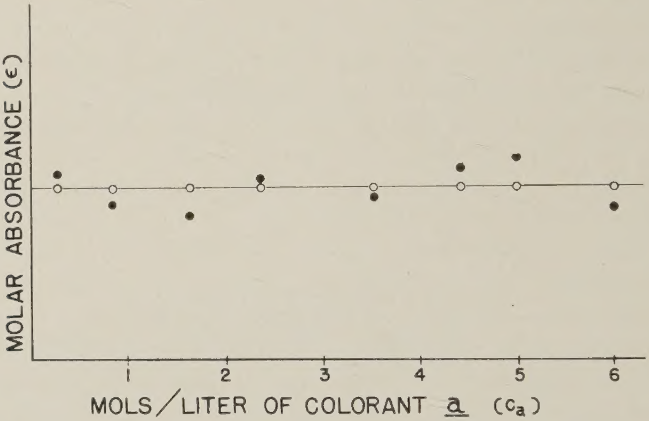

FIG. 3. Hypothetical relationship between molar absorbance (for a given wavelength) and concentration of colorant for eight crystals of a solid solution series between colorant a and a colorless material (monochromatic light assumed). Small circles represent points as would be ideally observed; filled circles represent points when observed with some experimental error.

The value ϵ_a, to be more explicit, represents the absorbance per centimeter of light travel produced by a one-mol-per-liter concentration of colorant a in the solution. In general the value of ϵ differs for different colorants and for different wavelengths of light. For p, a perfectly transparent colorless material, ϵ_p would equal zero for all portions of the visible spectrum. Therefore, for a series of solutions of varying proportions of a perfectly transparent colorless material plus just one particular colorant, Eq. (1) reduces to

$$\text{Log} \frac{I_{0\lambda_1}}{I_{\lambda_1}} = \epsilon_a C_a d \qquad \text{Eq. (2)}$$

(for light of wavelength, λ_1).

Method of Statistically Testing Beer's Law

To establish the validity of Beer's law for a series of solutions of a given colorant, a, it is necessary to prove that ϵ_a has the same value for all concentrations. Figure 3 graphically expresses such a relationship (hypothetical) for eight different concentrations between colorant a and a colorless solvent; ideally expressed (circles) the data would fall along a perfectly horizontal line. Unfortunately, experimental errors occur and solid circles might better represent the empirical data. Herein arises the necessity for statistical analysis to determine whether the trend of the data deviates sufficiently from parallelism to the abscissa to permit a flat rejection of Beer's law.

---

* Log I_0/I is often termed optical density and given the symbol D.

By the method of least squares, one can calculate for each particular wavelength the values of the parameters, $\hat{\alpha}$ and $\hat{\beta}$, of the straight line, $\epsilon_a = \hat{\alpha} + \hat{\beta} C_a$, which best follows the trend of the data. If Beer's law is not valid for the series of solutions of colorant a, the value of $\hat{\beta}$ will deviate significantly from zero.

Statistical methods permit the calculation of a certain range to either side of the calculated value, $\hat{\beta}$, to thereby establish an interval around $\hat{\beta}$ within which the true value, β_t, would fall in 19 out of 20 such samplings of the data. This interval, the 0.95 confidence interval,* becomes increasingly confined as experimental accuracy or number of observation increases. The value zero may fall outside of this 0.95 confidence interval, whereupon a rejection of Beer's law would have a 19 out of 20 chance of being the correct choice, or it may fall within this interval, whereupon the chances are 19 out of 20 that Beer's law is valid within the limits of measurement. In the latter event, the possibility still remains that future investigations may, through greater accuracy or larger number of observations, permit calculation of a narrower 0.95 confidence interval which will exclude zero.

EMPIRICAL DATA AND RELATED CALCULATIONS

Preliminary Examinations and Confinement of Data

A crystal of the colorless magnesium-rich end member, $Mg(NH_4)_2(SO_4)_2 \cdot 6H_2O$, and of the deep green nickel-rich end member, $Ni(NH_4)_2(SO_4)_2 \cdot 6H_2O$, were each mounted, lying on a (110) face, on a crystal holder. Their absorbance values for the two extinction positions measured for different wavelengths† are graphically expressed in Fig. 4. Conclusions from these preliminary examinations were: (1) the light absorption by the colorless end member is extremely small for either extinction position, (2) absorption by the green end member is relatively large, especially for the longer wavelengths, (3) the green colors respectively transmitted by the α' and γ' vibration directions of the nickel end member, although visually indistinguishable, are readily differentiated when the absorption curves are compared—an effect for convenience referred to as cryptopleochroism.

---

* Discussion of confidence intervals and of the statistical quantity t used in its calculation may be found in Snedecor (1946, pp. 41–42, 62–66).

† The spectral band isolated by the monochromator was determined to be approximately 35Å wide in the region of the sodium doublet; its width varied slightly, however, as other regions in the visible spectrum were isolated. Each spectral band of light used is here designated by the wavelength setting of the monochromator.

Since the absorption curves for the α' and γ' vibration directions were so similar (possibly an outgrowth of the almost isometric nature of the internal structure of crystals in this series), the measurements of light absorbance were confined to the γ' vibration direction for those crystals studied.

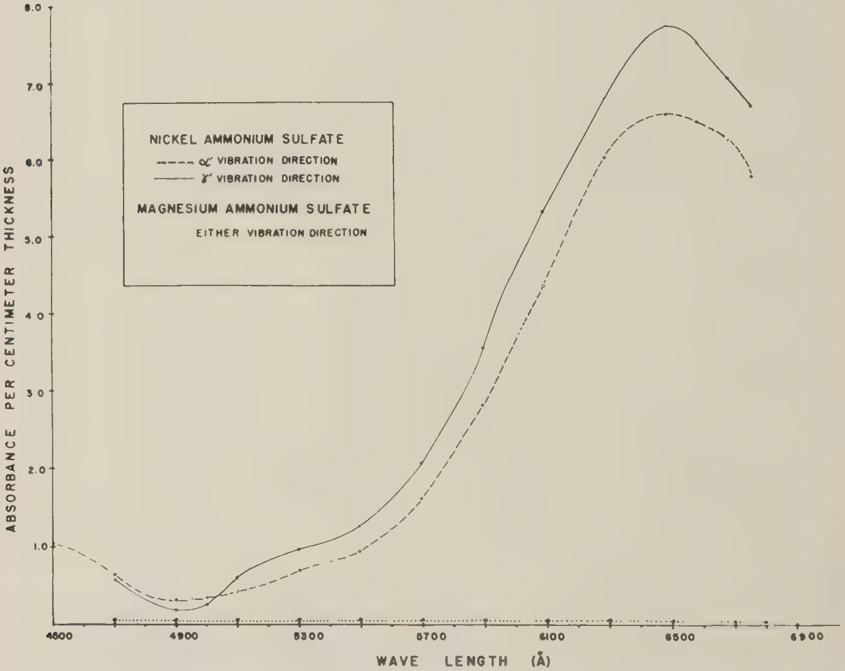

FIG. 4. Absorption curves for α' and γ' directions on a (110) face for nickel ammonium sulfate and for magnesium ammonium sulfate.

Compositions of the Crystals Examined Spectrophotometrically

In addition to the preceding two crystals, another crystal of the nickel-rich end member as well as the ten crystals whose compositions were previously stated in Table 1 were examined spectrophotometrically. Several were ground to new thicknesses and the spectrophotometric measurements were repeated.

Reflectional Losses at Interfaces

If one considers the reflectional losses at the air-crystal and crystal-air interfaces, it is apparent from Fig. 5 that the light intensity values measured as the crystal was slid into and out of the light beam are not I and I_0 as previously defined but rather, I' and I_0', where

$$I_0 = I_0' - I_0'R \quad \text{and} \quad I' = I - IR$$

and R is the coefficient of reflection for normal incidence. The relationship between the observed ratio I_0'/I' and the desired ratio I_0/I is therefore

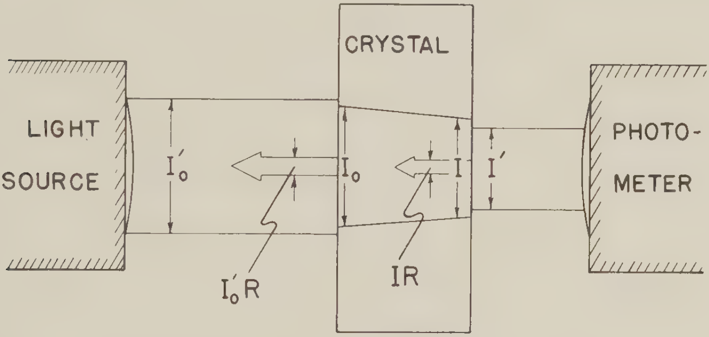

FIG. 5. Relationship between I_0', I_0, I, and I', respectively, the intensity of the light incident upon an absorbing crystal, immediately after entering the crystal, immediately prior to leaving, and immediately after leaving. R represents the coefficient of reflection for normal incidence. Reflection losses at interfaces are shown by arrows pointing left; width of beam or arrow diagrammatically indicates intensity of the light. Photometer measures I' when crystal is in path of light beam, I_0' when it is not.

$$\frac{I_0}{I} = \frac{I_0'}{I'}(1 - R)^2 \qquad \text{Eq. (3).}$$

For the crystal series and vibration direction investigated R may be calculated from the basic equation (Wood, 1934, p. 411) to be

$$R = \frac{(\gamma' - 1)^2}{(\gamma' + 1)^2} \qquad \text{Eq. (4).}$$

For the two end members the values of γ' and subsequently the values of R were calculated for wavelengths 4700, 4900, 5000, 5100, 5300, 5500, 5700, 5900, 6100, 6300, 6500, 6600, 6700, and 6800 Å using Tutton's (1905, pp. 1136–37; 1916, pp. 7–9) data. The values of R for intermediate

TABLE 2. CORRECTION VALUES $(1-R)^2$ FOR AIR-CRYSTAL REFLECTION LOSSES (NORMAL INCIDENCE ON (110) FACE)

Crystal	Mol. % Nickel Ammonium Sulfate	Wavelengths (Angstrom Units)													
		4700	4900	5000	5100	5300	5500	5700	5900	6100	6300	6500	6600	6700	6800
0-19	0.00	0.9270	0.9272	0.9274	0.9276	0.9279	0.9280	0.9282	0.9284	0.9285	0.9287	0.9288	0.9291	0.9292	0.9293
0-1	15.30	.9259	.9261	.9263	.9265	.9268	.9269	.9271	.9273	.9274	.9276	.9277	.9280	.9280	.9282
0-3	21.61	.9255	.9257	.9259	.9261	.9264	.9265	.9267	.9269	.9270	.9272	.9273	.9275	.9276	.9277
0-9	29.83	.9249	.9251	.9253	.9255	.9258	.9259	.9261	.9263	.9264	.9266	.9267	.9269	.9270	.9271
0-10	30.93	.9249	.9251	.9253	.9255	.9258	.9259	.9261	.9263	.9264	.9266	.9267	.9269	.9270	.9271
0-12	43.14	.9240	.9242	.9244	.9246	.9249	.9250	.9252	.9254	.9255	.9257	.9258	.9260	.9261	.9262
0-11	43.24	.9240	.9242	.9244	.9246	.9249	.9250	.9252	.9254	.9255	.9257	.9258	.9260	.9261	.9262
0-7	66.31	.9226	.9228	.9230	.9232	.9235	.9236	.9238	.9240	.9241	.9243	.9244	.9246	.9247	.9248
0-8	66.41	.9226	.9228	.9230	.9232	.9235	.9236	.9238	.9240	.9241	.9243	.9244	.9246	.9247	.9248
0-17	81.74	.9217	.9219	.9221	.9223	.9226	.9227	.9229	.9231	.9232	.9234	.9235	.9237	.9238	.9249
0-5	89.67	.9212	.9214	.9216	.9218	.9221	.9222	.9224	.9226	.9227	.9229	.9230	.9232	.9233	.9234
0-22	100.00	0.9204	0.9206	0.9208	0.9210	0.9213	0.9214	0.9216	0.9218	0.9219	0.9220	0.9221	0.9223	0.9224	0.9225

members in the series were secured, with sufficient accuracy, by interpolation between the end member values.

The computed values of $(1-R)^2$ for the crystals studied and wavelengths used are given in Table 2.

The Reflection-Corrected Empirical Data

Table 3 presents the empirically determined apparent opacity values, I_0'/I', multiplied by the pertinent $(1-R)^2$ values of Table 2; these values thus represent the true opacity, I_0/I. Each of the I_0'/I' values upon which they were based represents the average of at least three such ratios; for values where precision seemed below average up to eight or nine I_0'/I' values were obtained and averaged.

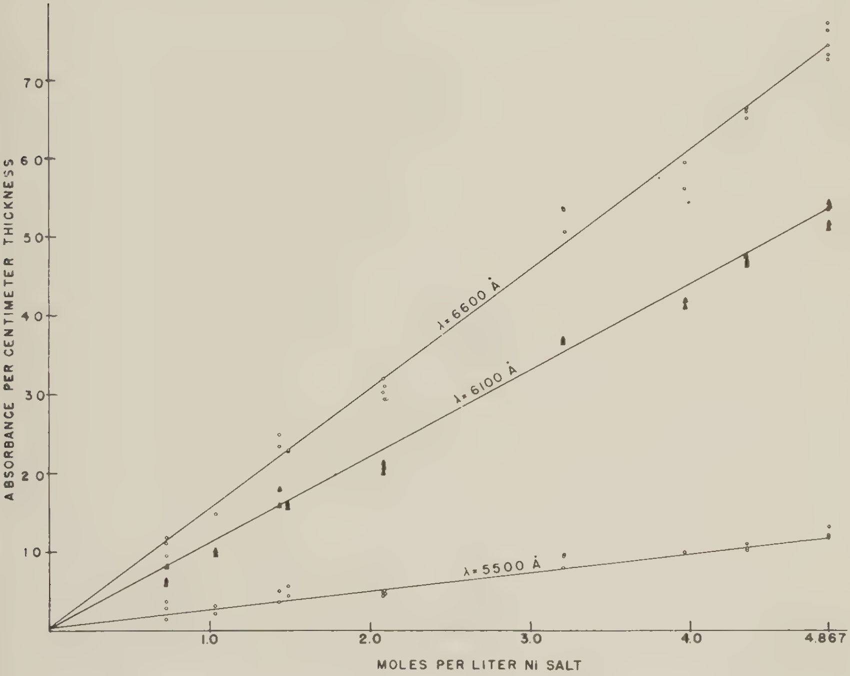

FIG. 6. Absorbance of crystals per centimeter thickness for wavelengths 5500, 6100, and 6600 Å, respectively, plotted against nickel ammonium sulfate content. The straight lines denote the first degree equations of best fit (as determined by the method of least squares).

Calculation of Absorbance per Centimeter

The logarithm to the base 10 of each value in Table 3 (i.e., the ab-

TABLE 3. REFLECTION-CORRECTED VALUES OF OPACITY* FOR γ' DIRECTION ON (110) FACE

Crystal	Mol % Nickel Ammonium Sulfate	Thickness (cm)	Trial	Wavelengths (Angstrom Units)													
				4700	4900	5000	5100	5300	5500	5700	5900	6100	6300	6500	6600	6700	6800
0-19	0.00	0.347	1	1.04	1.03	1.03	1.02	1.04	1.03	1.03	1.02	1.02	1.02	1.02	1.03	1.03	1.02
0-1	15.30	.160	1	1.09	1.10	1.11	1.12	1.13	1.15	1.16	1.25	1.35	1.50	1.54	1.55	1.58	1.54
			2	1.08	1.07	1.07	1.08	1.10	1.11	1.15	1.31	1.33	1.44	1.49	1.51	1.48	1.47
		.147	3			1.00	1.01	1.03	1.04	1.07	1.14	1.24	1.32	1.38	1.38	1.37	1.36
0-3	21.61	.184	1	1.09	1.08	1.08	1.09	1.11	1.14	1.19	1.32	1.54	1.76	1.88	1.88	1.86	1.81
			2	1.07	1.04	1.06	1.06	1.08	1.10	1.16	1.29	1.51	1.71	1.86	1.89	1.84	1.76
0-9	29.83	.210	1	1.08	1.06	1.06	1.09	1.15	1.20	1.33	1.64	2.16	2.72	3.12	3.12	3.09	2.85
		.190	2			1.12	1.14	1.19	1.25	1.37	1.67	2.20	2.80	3.09	2.98	2.94	2.85
0-10	30.93	.185	1	1.24	1.17	1.19	1.20	1.25	1.28	1.39	1.60	2.00	2.39	2.68	2.66	2.53	2.47
		.170	2			1.10	1.11	1.15	1.19	1.29	1.50	1.84	2.23	2.45	2.44	2.40	2.36
0-12	43.14	.121	1	1.08	1.06	1.07	1.08	1.11	1.15	1.25	1.45	1.79	2.15	2.36	2.44	2.31	2.29
		.111	2			1.04	1.06	1.09	1.12	1.21	1.38	1.67	2.03	2.20	2.18	2.20	2.16
0-11	43.24	.134	1	1.07	1.04	1.05	1.07	1.12	1.15	1.26	1.49	1.89	2.26	2.53	2.49	2.40	2.37
		.129	2			1.06	1.07	1.13	1.16	1.27	1.50	1.88	2.27	2.50	2.52	2.50	2.50
0-7	66.31	.131	1	1.17	1.13	1.17	1.18	1.25	1.33	1.55	2.11	3.06	4.29	5.24	5.05	4.90	4.82
		.120	2			1.08	1.10	1.19	1.25	1.45	1.94	2.77	3.97	4.59	4.42	4.36	4.37
0-8	66.41	.164	1	1.18	1.13	1.17	1.19	1.34	1.44	1.74	2.51	3.99	6.19	7.54	6.85	6.58	5.77
0-17	81.74	.183	1	1.21	1.14	1.16	1.21	1.36	1.49	1.94	3.19	5.70	9.72	12.14	10.82	9.64	8.41
		.158	2			1.17	1.23	1.34	1.45	1.81	2.74	4.61	7.70	9.31	8.81	8.09	7.17
0-5	89.67	.161	1	1.24	1.16	1.16	1.25	1.39	1.51	1.91	3.04	5.73	9.24	11.08	11.91	10.74	9.15
			2	1.25	1.14	1.16	1.22	1.36	1.48	1.89	3.02	5.66	10.00	11.76	11.38	10.00	8.47
		.111	3			1.10	1.13	1.21	1.30	1.56	2.08	3.39	4.94	5.78	5.46	5.17	4.90
0-22	100.00	.134	1	1.20	1.12	1.15	1.19	1.32	1.45	1.84	2.88	4.97	8.95	10.39	9.68	9.13	8.76
			2	1.23	1.16	1.19	1.23	1.37	1.51	1.86	2.99	5.38	9.03	13.06	10.95	10.80	9.23
		.102	3			1.09	1.13	1.23	1.32	1.60	2.28	3.61	5.58	6.18	6.11	5.53	5.42
0-23	100.00	.146	1	1.21	1.14	1.17	1.23	1.39	1.54	2.00	3.29	5.97	9.69	13.27	12.42	10.62	9.39
			2	1.18	1.11	1.14	1.23	1.35	1.49	1.92	3.15	5.60	9.50	10.90	11.63	10.21	8.32
		0.1235	3			1.14	1.18	1.31	1.42	1.76	2.65	4.68	7.65	8.84	8.66	8.03	7.37

---

* Each of these values represents the product of the average of at least three to four observed opacity values, I_0'/I', times the appropriate reflection correction value, $(1-R)^2$, of Table 5.

sorbance) was next divided by the thickness of the crystal to yield the absorbance per centimeter of the crystal for each of the wavelengths used. Results are given in Table 4. Figures 6 and 7 express the results graphically for several wavelengths.

Calculation of the Molar Absorbance (ϵ_{ni}) for $Ni(NH_4)_2(SO_4)_2 \cdot 6H_2O$ in the Mixed Crystals

A problem encountered in this calculation stemmed from the fact that accurate spectrophotometric measurements could not be made on the pure, highly transparent $Mg(NH_4)_2(SO_4)_2 \cdot 6H_2O$ crystals since accuracy decreases sharply as complete transparency is approached. The individual absorbance per centimeter values for crystal 0–19 in Table 4 are thus questionable. As a result the amount of absorbance per centimeter contributed by the $Mg(NH_4)_2(SO_4)_2 \cdot 6H_2O$ components of the solid solutions could not be accurately assessed and therefore their ϵ_{ni} values could not be accurately calculated.

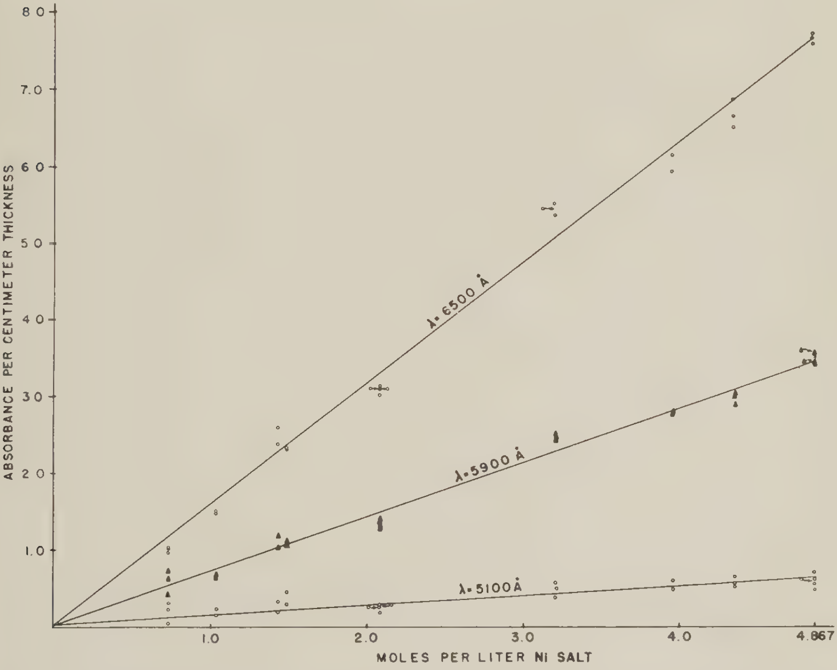

FIG. 7. Absorbance of crystals per centimeter thickness for wavelengths 5100, 5900, and 6500 Å, respectively, plotted against nickel ammonium sulfate content.

Two assumptions were made which are thought to be extremes be-

TABLE 4. ABSORBANCE PER CENTIMETER THICKNESS* FOR γ' DIRECTION ON (110) FACE OF MIXED CRYSTALS OF $(NH_4)_2(Mg, Ni)(SO_4)_2 \cdot 6H_2O$

Crystal	Concentration of Nickel Ammonium Sulfate in Crystal		Thickness (cm)	Trial	Wavelengths (Angstrom Units)													
	Mol %	Mols per Liter	(4)	(5)	4700 (6)	4900 (7)	5000 (8)	5100 (9)	5300 (10)	5500 (11)	5700 (12)	5900 (13)	6100 (14)	6300 (15)	6500 (16)	6600 (17)	6700 (18)	6800 (19)
0-19	0.00	0.000	0.347	1	0.048	0.038	0.037	0.030	0.044	0.035	0.035	0.027	0.026	0.027	0.019	0.037	0.037	0.025
0-1	15.30	0.732	1.60	1	.236	.259	.283	.295	.339	.377	.408	.610	.817	1.093	1.169	1.186	1.238	1.172
				2	.216	.184	.181	.211	.251	.283	.370	.733	.780	0.994	1.082	1.110	1.059	1.037
			.147	3			.000	.029	.068	.136	.204	.408	0.612	0.816	0.952	0.952	0.952	0.884
0-3	21.61	1.036	.184	1	.199	.175	.179	.212	.248	.309	.409	.657	1.022	1.334	1.494	1.490	1.465	1.395
				2	.153	.088	.129	.126	.175	.216	.350	0.607	0.970	1.265	1.458	1.496	1.443	1.333
0-9	29.83	1.432	.210	1	.153	.115	.117	.171	.282	.374	.593	1.021	1.594	2.073	2.356	2.354	2.334	2.167
			.190	2			.259	.300	.398	.510	.720	1.172	1.802	2.354	2.579	2.496	2.465	2.394
0-10	30.93	1.485	.185	1	.514	.373	.414	.428	.516	.574	.773	1.105	1.624	2.042	2.312	2.296	2.180	2.119
			.170	2			.244	.267	.357	.445	.651	1.036	1.558	2.049	2.289	2.279	2.236	2.194
0-12	43.14	2.076	.121	1	.286	.209	.246	.260	.362	.495	.787	1.334	2.080	2.741	3.076	3.207	3.010	2.968
			.111	2			.153	.227	.335	.441	.743	1.255	1.997	2.758	3.071	3.036	3.071	3.000
0-11	43.24	2.081	.134	1	.210	.140	.158	.222	.359	.459	.746	1.286	2.055	2.641	3.002	2.953	2.841	2.798
			.129	2			.196	.228	.412	.500	0.805	1.365	2.126	2.760	3.085	3.112	3.085	3.085
0-7	66.31	3.206	.131	1	.521	.405	.521	.543	.742	.955	1.451	2.475	3.711	4.827	5.492	5.369	5.265	5.213
			.120	2			.278	.345	.630	.808	1.345	2.398	3.688	4.990	5.515	5.378	5.329	5.338
0-8	66.41	3.221	.164	1	.447	.312	.413	.461	.765	.966	1.471	2.440	3.664	4.828	5.350	5.096	4.988	4.639
0-17	81.74	3.964	.183	1	.450	.309	.356	.450	.723	0.814	1.576	2.750	4.131	5.396	5.924	5.652	5.378	5.054
			.158	2			.408	.569	.804	1.022	1.631	2.771	4.201	5.611	6.133	5.981	5.747	5.415
0-5	89.67	4.355	.161	1	.582	.391	.403	.611	.879	1.110	1.743	2.998	4.709	5.997	6.487	6.683	6.405	5.972
				2	.595	.346	.409	.529	.821	1.048	1.720	2.978	4.673	6.208	6.645	6.555	6.207	5.759
			.111	3			.373	.478	.746	1.026	1.740	2.866	4.777	6.250	6.864	6.641	6.428	6.218
0-22	100.00	4.867	.134	1	.580	.359	.439	.569	0.905	1.200	1.980	3.427	5.199	7.102	7.586	7.358	7.169	7.033
				2	.663	.473	.553	.666	1.018	1.327	2.013	3.549	5.455	7.132	8.328	7.757	7.712	7.204
			.102	3			.365	.518	0.877	1.177	1.991	3.492	5.439	7.284	7.717	7.668	7.246	7.161
0-23	100.00	4.867	.146	1	.572	.392	.464	.604	.969	1.275	2.065	3.545	5.314	6.757	7.691	7.494	7.027	6.663
				2	0.495	0.310	.382	.621	.886	1.176	1.939	3.410	5.126	6.695	7.104	7.298	6.912	6.301
			0.123	3			0.461	0.582	0.950	1.233	1.988	3.428	5.427	7.156	7.663	7.591	7.326	7.024

---

* These values are secured through division of the logarithm of the corresponding value in Table 6 by the thickness in centimeters of the crystal in question, i.e.,

$$\frac{A}{d} = \frac{1}{d} \log \frac{I_0'}{I'} (1-R)^2$$

tween which the actual situation lies: (*a*) the $Mg(NH_4)_2(SO_4)_2 \cdot 6H_2O$ portions of these crystals absorbed no light, (*b*) their absorbance per centimeter value is 0.033, i. e. the arithmetric mean of the values for all wavelengths given for crystal 0–19 in Table 4. The first is of course a low estimate, the second is possibly high, perhaps produced by small unnoticed flaws in 0–19. It was decided therefore to calculate two sets of ϵ_{ni} values, one for each of the assumptions.

TABLE 5. CALCULATED VALUES OF ϵ_{ni} THE MOLAR ABSORBANCE OF $Ni(NH_4)_2(SO_4)_2 \cdot 6H_2O$ AT SEVERAL WAVELENGTHS (UNDER THE ASSUMPTION THAT E_{mg}, THE MOLAR ABSORBANCE OF $Mg(NH_4)_2(SO_4)_2 \cdot 6H_2O$, EQUALS ZERO)

Crystal	Trial	Wavelength in Angstroms								
		5500	5700	5900	6100	6300	6500	6600	6700	6800
0-1	(1)	.515	.557	.833	1.116	1.493	1.597	1.620	1.691	1.601
	(2)	.387	.505	1.001	1.066	1.358	1.478	1.516	1.447	1.417
	(3)	.186	.279	.557	.836	1.115	1.301	1.301	1.301	1.208
0-3	(1)	.298	.395	.634	.986	1.288	1.442	1.438	1.414	1.347
	(2)	.208	.338	.586	.936	1.221	1.407	1.444	1.393	1.287
0-9	(1)	.261	.414	.713	1.113	1.448	1.645	1.644	1.630	1.513
	(2)	.356	.503	.818	1.258	1.644	1.801	1.743	1.721	1.672
0-10	(1)	.387	.521	.744	1.094	1.375	1.557	1.546	1.468	1.427
	(2)	.300	.438	.698	1.049	1.380	1.541	1.535	1.506	1.477
0-12	(1)	.238	.379	.643	1.002	1.320	1.482	1.545	1.450	1.430
	(2)	.212	.358	.605	.962	1.329	1.479	1.462	1.479	1.445
0-11	(1)	.221	.358	.618	.988	1.269	1.443	1.419	1.365	1.345
	(2)	.240	.387	.656	1.022	1.326	1.482	1.495	1.482	1.482
0-17	(1)	.205	.398	.694	1.042	1.361	1.494	1.426	1.357	1.275
	(2)	.258	.411	.699	1.060	1.415	1.547	1.509	1.450	1.366
0-5	(1)	.355	.400	.688	1.081	1.377	1.490	1.135	1.471	1.371
	(2)	.241	.395	.684	1.073	1.425	1.526	1.505	1.425	1.322
	(3)	.236	.400	.658	1.097	1.435	1.576	1.525	1.476	1.428
0-22	(1)	.247	.407	.704	1.068	1.459	1.559	1.512	1.473	1.445
	(2)	.273	.414	.724	1.121	1.465	1.711	1.594	1.585	1.480
	(3)	.242	.409	.717	1.118	1.497	1.586	1.576	1.489	1.471
0-23	(1)	.262	.424	.728	1.092	1.388	1.580	1.540	1.444	1.369
	(2)	.242	.398	.701	1.053	1.376	1.460	1.499	1.420	1.295
	(3)	.253	.408	.704	1.115	1.470	1.574	1.560	1.505	1.443
Av. Value ϵ_{ni}		.273	.415	.706	1.065	1.399	1.549	1.533	1.491	1.430
Av. Value ϵ_{ni} for 0-22, 0-23		.253	.410	.715	1.095	1.443	1.578	1.547	1.486	1.417

TABLE 6. CALCULATED VALUES OF ϵ_{ni} THE MOLAR ABSORBANCE OF $Ni(NH_4)_2(SO_4)_2 \cdot 6H_2O$ AT SEVERAL WAVELENGTHS (UNDER THE ASSUMPTION THAT ϵ_{mg}, THE MOLAR ABSORBANCE OF $Mg(NH_4)_2(SO_4)_2 \cdot 6H_2O$, EQUALS 0.007 FOR ALL WAVELENGTHS

Crystal	Trial	Wavelength in Angstroms								
		5500	5700	5900	6100	6300	6500	6600	6700	6800
0-1	(1)	0.477	0.519	0.795	1.078	1.455	1.559	1.582	1.653	1.563
	(2)	.348	.467	.963	1.027	1.320	1.440	1.478	1.408	1.378
	(3)	.148	.240	.519	.798	1.077	1.262	1.262	1.262	1.169
0-3	(1)	.273	.370	.609	.961	1.263	1.417	1.413	1.389	1.321
	(2)	.183	.313	.561	.911	1.196	1.382	1.419	1.368	1.262
0-9	(1)	.245	.398	.697	1.097	1.431	1.629	1.628	1.614	1.497
	(2)	.340	.487	.802	1.242	1.628	1.785	1.727	1.705	1.656
0-10	(1)	.371	.505	.729	1.078	1.360	1.541	1.531	1.452	1.411
	(2)	.284	.423	.682	1.034	1.364	1.526	1.519	1.490	1.462
0-12	(1)	.229	.370	.633	.993	1.311	1.473	1.536	1.441	1.421
	(2)	.203	.349	.595	.953	1.319	1.470	1.453	1.470	1.436
0-11	(1)	.211	.349	.609	.978	1.260	1.433	1.410	1.356	1.335
	(2)	.231	.378	.647	1.012	1.317	1.473	1.486	1.473	1.473
0-17	(1)	.204	.396	.692	1.041	1.360	1.493	1.424	1.355	1.273
	(2)	.256	.410	.698	1.058	1.414	1.546	1.507	1.448	1.365
0-5	(1)	.254	.400	.688	1.081	1.376	1.489	1.534	1.470	1.371
	(2)	.240	.394	.683	1.072	1.425	1.525	1.504	1.425	1.322
	(3)	.235	.399	.657	1.096	1.434	1.575	1.524	1.475	1.427
0-22	(1)	.247	.407	.704	1.068	1.459	1.559	1.512	1.473	1.445
	(2)	.273	.414	.729	1.121	1.465	1.711	1.594	1.585	1.480
	(3)	.242	.409	.717	1.118	1.497	1.586	1.576	1.489	1.471
0-23	(1)	.262	.424	.728	1.092	1.388	1.580	1.540	1.444	1.369
	(2)	.242	.398	.701	1.053	1.376	1.460	1.499	1.420	1.295
	(3)	0.253	0.408	0.704	1.115	1.470	1.574	1.560	1.505	1.443
Av. Value of ϵ_{ni}		0.260	0.401	.689	1.045	1.374	1.520	1.509	1.465	1.402
Av. Value of ϵ_{ni} for 0-22-23		0.253	0.410	0.714	1.094	1.442	1.578	1.547	1.486	1.417

Calculation of ϵ_{ni} Assuming $Mg(NH_4)_2(SO_4)_2 \cdot 6H_2O$ Is Perfectly Transparent

Under this assumption the values of ϵ_{ni} at the several wavelengths were determined by dividing the values of Table 4 by the concentration of $Ni(NH_4)_2(SO_4)_2 \cdot 6H_2O$ (in mols per liter) for that particular crystal. The results of these calculations are presented in Table 5.

Calculation of ϵ_{ni} Assuming Absorbance per Centimeter for $Mg(NH_4)_2(SO_4)_2 \cdot 6H_2O$ is 0.033.

Assuming A/d for pure $Mg(NH_4)_2(SO_4)_2 \cdot 6H_2O$ to be 0.033 and calculating C_{mg} for the pure end member to be 4.773 mols per liter, then from Eq. (2)

$$\epsilon_{mg} = \frac{\frac{A}{d}}{C_{mg}} = \frac{0.033}{4.773} = 0.007 \qquad \text{Eq. (5).}$$

To compute ϵ_{ni} values under the above assumption, Beer's law is written as for a two color component series, i.e.,

$$\frac{A}{d} = \epsilon_{mg}C_{mg} + \epsilon_{ni}\,C_{ni} = .007C_{mg} + \epsilon_{ni}\,C_{ni}$$

which becomes if solved for ϵ_{ni}

$$\epsilon_{ni} = \frac{\frac{A}{d} - .007\,C_{mg}}{C_{ni}} \qquad \text{Eq. (6).}$$

The quantity A/d, of course, merely represents the absorbance per centimeter values of Table 4. Thus if C_{mg} is calculated for each of the solid solutions and since C_{ni} is already known, the values for ϵ_{ni} were then calculable. The values thus calculated appear in Table 6.

TESTING THE DATA WITH RESPECT TO BEER'S LAW

There now remained the necessity of statistically fitting a straight line to the data of both Table 5 and Table 6 to determine whether the slope of the trend line for the data would be zero (if graphed like the hypothetical example in Fig. 3). The general equation for the line could be written

$$\epsilon_{ni} = \hat{\alpha} + \hat{\beta}C_{ni} \qquad \text{Eq. (7).}$$

As was previously discussed the value of $\hat{\beta}$ should equal zero or closely approach it, if Beer's law holds for this solid solution series.

Accordingly, the values of $\hat{\alpha}$ and $\hat{\beta}$ were calculated by the method of least squares using the data of both Tables 5 and 6. The regressions† carried out were in terms of ϵ_{ni} values upon C_{ni}, i. e., the lines were fitted under the assumption that C_{ni} was the independent variable, ϵ_{ni}, the dependent variable. Table 7 presents the results of these statistical calculations.

---

† In statistical terminology regression signifies the process of fitting a line to the data which accurately follows their trend yet, at least in part, lacks their chance errors.

TABLE 7. SUMMARY OF STATISTICALLY DERIVED VALUES OF PARAMETERS $\widehat{\alpha}$ AND $\widehat{\beta}$

	Regression of ϵ_{ni} Values (of Table 5) on Composition					Regression of ϵ_{ni} Values (of Table 6) on Composition				
	$\widehat{\alpha}$	$\widehat{\beta}$	Standard Error of $\widehat{\beta}$	Standard Error of $\widehat{\beta}$ times t[a]	Interval[b] in which β_t is likely to fall	$\widehat{\alpha}$	$\widehat{\beta}$	Standard Error of β	Standard Error of β times t	Interval[b] in which β_t is likely to fall
5500	.322	−.0174	.0086	.0178	+.004 to −.0352	.290	−.0105	.0084	.0174	+.0069 to −.0279
5700	.431	−.0064	.0075	.0155	+.0091 to −.0219	.396	+.0017	.0075	.0155	+.0172 to −.0138
5900	.712	−.0041	.0115	.0238	+.0197 to −.0353	.681	+.0029	.0112	.0232	+.0261 to −.0203
6100	1.010	+.0161	.0098	.0203	+.0364 to −.0042	.979	+.0231	.0099	.0205	+.0436 to +.0026
6300	1.318	+.0233	.0125	.0259	+.0492 to −.0026	1.287	+.0304	.0126	.0261	+.0565 to +.0043
6500	1.488	−.0154	.0125	.0259	+.0413 to −.0105	1.456	+.0224	.0127	.0263	+.0487 to −.0039
6600	1.505	+.0053	.0183	.0379	+.0432 to −.0326	1.474	+.0122	.0112	.0232	+.0354 to −.0110
6700	1.494	−.0060	.0125	.0259	+.0199 to −.0319	1.462	+.0011	.0126	.0261	+.0272 to −.0250
6800	1.441	−.0096	.0147	.0311	+.0215 to −.0407	0.409	−.0025	.0133	.0275	+.0250 to −.0300

[a] The statistical quantity t refers to "student's" t distribution (Mood, 1950, p. 206; Rider, 1939, pp. 88–98).

[b] This is actually the 0.95 confidence interval which will generally, for 19 out of 20 such collections of data, embrace the true value, β_t. The possibility still remains that in 1 out of 20 times, a capricious distribution of the data might occur such that the calculated confidence interval actually would not embrace the value β_t.

Salient points of Table 7 are: (1) the $\hat{\beta}$ values of the left hand column differ from the corresponding ones of the right hand column by .007, the assumed value of ϵ_{mg}, (2) the values of $\hat{\beta}$ are in all cases very small and with two exceptions, never differ from zero by more than t times their standard error (the 0.95 confidence interval).

The first of the above points had been anticipated; if $Mg(NH_4)_2(SO_4)_2 \cdot 6H_2O$ actually absorbed appreciable light (but was assumed to absorb none at all) the result would be that for crystals almost pure with respect to Mg but very low in Ni, ϵ_{ni} would be calculated high by the amount, ϵ_{mg}. For crystals increasingly higher in Ni this discrepancy would decrease so that it vanished for pure $Ni(NH_4)_2(SO_4)_2 \cdot 6H_2O$ crystals. Thus the line $\epsilon_{ni} = \hat{\alpha} + \hat{\beta}\ C_{ni}$ would automatically be given a negative slope equal to $-\epsilon_{mg}$ (i. e. $\hat{\beta} = -\epsilon_{mg}$).

The consistency of this difference between the $\hat{\beta}$ values in the right and left hand columns of Table 7 served as a check on the accuracy of the statistical calculations.

The second of the salient points of Table 7 permits the conclusion that the light absorption data substantiate the validity of Beer's law for this solid solution series (within the limits of measurement). In view of the small sample size, the two exceptions out of 18 samplings are not disturbing; in fact this ratio is not much different from the 1 misleading sample out of 20 which is expectable according to statistical theory (for a 0.95 confidence interval).

APPLICATIONS

Determination of Composition from Light Absorbance

For clear crystals of a solid solution series to which Beer's law is applicable, general equation (1) may be applied; the molar absorbance values, i.e., ϵ values, may be determined from measurements of the absorbance per centimeter values, A/d, of as many crystals of known composition as there are color-producing components in the series. Substitution of this data in eq. (1) yields a set of equations which may be solved simultaneously to determine the molar absorbance values ϵ_a, ϵ_b, etc., of the various colorants involved. With these molar absorbance values established for the specific colorants and light wavelengths used, the compositions of unknown crystals of the series can be determined if their absorbance per centimeter values are measured for as many wavelengths as there are possible colorants.

The above methods of calculation, however, assume the absence of any opaque inclusions, bubbles, internal cleavages, or other flawed areas in the crystal. Obviously, such flawed areas would cause a crystal to intercept a larger amount of light than if it were perfectly clear. Therefore if eq. 1 were directly applied as previously suggested, the crystal's composition would be calculated to have greater amounts of the light absorbing components than it actually had.

This difficulty can be overcome if the usually tenable assumption can be made that the flawed areas block off essentially the same fraction of light, i.e., k, regardless of light wavelength used. Under this assumption the apparent opacity I_0'/I' would be related to the true opacity I_0/I by the equation

$$\frac{I_0'}{I'} = \frac{I_0}{I(1-k)(1-R)^2} \qquad \text{Eq. (8).}$$

The apparent and true absorbance values, A' and A, respectively, would therefore be related as follows

$$A' = A - \log(1-k) - 2\log(1-R) \qquad \text{Eq. (9).}$$

Since for different wavelengths of light the value of $\log(1-k)$ and of $\log(1-R)$ changes but slightly, the difference between the apparent absorbance at two different wavelengths, i.e., $A_{\lambda_1}' - A_{\lambda_2}'$, equals the difference between the true absorbance, $A_{\lambda_1} - A_{\lambda 2}$, at those wavelengths. As a result a "difference" version of eq. 1 may be written

$$A_{\lambda_1}' - A_{\lambda_2}' = (\epsilon_{a\lambda_1} - \epsilon_{a\lambda_2})C_a + (\epsilon_{b\lambda_1} - \epsilon_{b\lambda_2})C_b + \cdots \qquad \text{Eq. (10)}$$

and used for turbid or flawed crystals just as eq. 1 was used for clear crystals. Numerous *colored* inclusions in the crystal area examined spectrophotometrically would, of course, produce erroneous results by either method of calculation.

Empirical Results for the Series Studied

When light absorbance per centimeter values are established for several crystals of known composition in a solid solution series, it is possible to fit a first degree equation to these values by the method of least squares. If the intent in deriving the equation is to predict a crystal's absorbance per centimeter when its composition is known, absorbance per centimeter should be treated as the dependent variable, composition as the independent variable. For the nickel-magnesium ammonium sulfate crystals studied, an equation of the form

$$\frac{A}{d} = f(C_{\mathrm{ni}}) = \hat{\alpha} + \hat{\beta}C_{\mathrm{ni}} \qquad \text{Eq. (11)}$$

would therefore be secured. The values of the constants $\hat{\alpha}$ and $\hat{\beta}$ are secured for each wavelength's data by the least square calculations. The values of ϵ_{ni} and ϵ_{mg} are calculated to be, for a particular wavelength (or spectral band),

$$\epsilon_{\mathrm{ni}} = \frac{\hat{\alpha}}{4.867} + \hat{\beta} \qquad \text{Eq. (12)}$$

and

$$\epsilon_{\mathrm{mg}} = \frac{\hat{\alpha}}{4.773} \qquad \text{Eq. (13)}$$

where 4.867 represents the C_{ni} value of the pure nickel end member and 4.773 represents the C_{mg} value for the pure magnesium end member.

However, if the intent in deriving the equations is to predict composition from measured absorbance data, it is statistically preferable (though less natural) to regard absorbance per centimeter as the independent variable and composition as the dependent variable. The form of the derived equation for the data at each wavelength would be

$$C_{ni} = f\left(\frac{A}{d}\right) = \hat{\alpha} + \hat{\beta}\frac{A}{d} \qquad \text{Eq. (14).}$$

Thus, when the values of the constants $\hat{\alpha}$ and $\hat{\beta}$ have been calculated, the compositions of unknown crystals may be predicted, (in terms of mols of nickel ammonium sulfate per liter of crystal volume) from their measured A/d values.

This second method was applied to the data of Table 4 for the A/d values measured at the 5900 Å, 6500 Å, and 6600 Å wavelengths* and the following equations were derived:

$$C_{ni} = -0.0047 + 1.4157\frac{A_{5900}}{d} \qquad \text{Eq. (15)}$$

$$C_{ni} = 0.0188 + 0.6324\frac{A_{6500}}{d} \qquad \text{Eq. (16)}$$

and

$$C_{ni} = -0.0056 + 0.6491\frac{A_{6600}}{d} \qquad \text{Eq. (17).}$$

In a similar manner equations were fitted to the difference between the A/d values of Table 4 for wavelengths 6500 and 5900 Å, 6600 and 5900 Å, and 6600 and 5000 Å. The following equations based on the "differential absorption" between two different wavelength bands were thereby secured and theoretically should obviate the effects of flaws and turbid areas in the crystal:

$$C_{ni} = 0.0505 + 1.1359\frac{A_{6500} - A_{5900}}{d} \qquad \text{Eq. (18)}$$

$$C_{ni} = 0.8190 + 1.1921\frac{A_{6600} - A_{5900}}{d} \qquad \text{Eq. (19)}$$

$$C_{ni} = 0.0368 + 0.6857\frac{A_{6600} - A_{5000}}{d} \qquad \text{Eq. (20).}$$

By way of statistical comparison of equations 15–20, the residual sum of the squares for each were calculated to be 0.830, 0.786, 0.458, 1.511,

---

* Actually spectral bands of approximately 35 Å width centered at these wavelengths were used.

TABLE 8

Crystal	Mol %*	Trial	Deviations in Mol Per Cent of Compositions Predicted By Substitution of Absorption Measurements of Table 4 into Eqs. 15–20.							
			Substitution of $\frac{A_\lambda}{d}$ Values				Substitution of $\frac{A_{\lambda_1}-A_{\lambda_2}}{d}$ Values			
			Eq. 15, $\frac{A_{5900}}{d}$	Eq. 16, $\frac{A_{6500}}{d}$	Eq. 17, $\frac{A_{6600}}{d}$	Algebraic Average	Eq. 18, $\frac{A_{6500}-A_{5900}}{d}$	Eq. 19, $\frac{A_{6600-5900}}{d}$	Eq. 20, $\frac{A_{6600}-A_{5000}}{d}$	Algebraic Average
0-19	0.00	(1)	0.68	0.64	0.39	0.57	0.86	0.35	0.76	0.66
0-1	15.30	(1)	2.55	0.53	0.66	0.10	−0.95	−0.82	−1.56	−2.21
		(2)	6.18	−0.60	−0.35		−5.86	−5.69	−1.19	
		(3)	−3.27	−2.28	−2.47		−1.32	−1.60	−0.86	
0-3	21.61	(1)	−2.28	−1.48	−1.52	−2.07	−0.72	−0.78	−2.06	−0.77
		(2)	−3.74	−1.95	−1.46		−0.39	0.60	−1.27	
0-9	29.83	(1)	0.18	1.58	1.85	2.73	2.77	3.33	2.86	3.23
		(2)	4.56	4.48	3.74		4.46	3.10	2.86	
0-10	30.93	(1)	3.60	−0.08	0.00	0.40	−1.29	−1.23	−3.25	−1.18
		(2)	−0.47	−0.39	0.23		−0.23	0.04	−1.09	
0-12	43.14	(1)	−3.95	−2.30	0.00	−2.86	−0.97	3.33	−0.18	0.49
		(2)	−6.25	−2.36	−2.28		0.97	1.07	−1.27	
0-11	43.24	(1)	−5.45	−3.37	−3.49	−3.18	−1.66	−1.83	−2.63	−1.41
		(2)	−3.14	−2.28	−1.38		−1.58	0.14	−0.92	
0-7	66.31	(1)	6.02	5.88	5.61	5.55	5.59	5.12	3.19	5.96
		(2)	3.86	6.17	5.73		7.91	7.21	6.74	
0-8	66.41	(1)	4.91	3.93	1.87	3.57	2.98	−0.82	0.76	0.97
0-17	81.74	(1)	−1.56	−4.09	−6.19	−2.66	−6.33	−10.25	−6.08	−4.91
		(2)	−0.95	−1.38	−1.81		−1.94	−2.71	−2.18	
0-5	89.67	(1)	−2.36	−4.81	−0.47	−2.52	−7.00	0.84	−0.25	−0.63
		(2)	−2.96	−2.76	−2.18		−2.86	−1.77	−2.14	
		(3)	−6.21	0.10	−1.03		4.87	3.08	−0.41	
0-22	100.00	(1)	−0.41	−1.05	−1.99	1.77	−1.89	−3.62	−1.77	1.82
		(2)	3.14	8.59	3.33		12.58	3.16	2.26	
		(3)	1.48	0.66	2.14		−0.35	2.38	3.66	
0-23	100.00	(1)	3.02	0.31	−0.18	−0.80	−2.20	−3.16	−0.18	−2.40
		(2)	−0.90	−7.32	−2.79		−12.74	−4.66	−1.81	
		(3)	−0.39	−0.04	1.11		−0.14	2.08	1.21	

* Of $Ni(NH_4)_2(SO_4)_2 \cdot 6H_2O$ in crystals as calculated from density.

0.819, and 0.443, respectively. From this it can be seen that the empirical data deviate least from equations 17 and 20, most from equation 18.

The relative accuracy of equations 15–20 in predicting composition from light absorbance measurements for this series is indicated in Table

8; for each equation the composition in mols per liter of nickel ammonium sulfate, i.e., C_{ni} was calculated by substituting into it the A/d values of Table 4 (or their differences in the case of equations 18–20). The deviation of the values thereby secured from either the known or density-calculated composition values† is given in terms of mol per cent of the nickel end member. Whereas individual calculations indicated discrepancies up to 12.74 mol per cent, algebraic averages for several calculations were within 3 mol per cent of the density-calculated composition in over 75% of the cases.

These deviations have several possible explanations. Positive deviations from the density-calculated composition may have been caused by opacities or internal reflections in the crystal or by the grinding off during preparation of the crystal (but after the density measurement) of less dense, more transparent, magnesium-rich outer zones. Random deviations could be caused by photometric errors such as nonlinearity in response of the spectrophotometer, fluctuation in intensity of light source, or by errors in reading the scale.

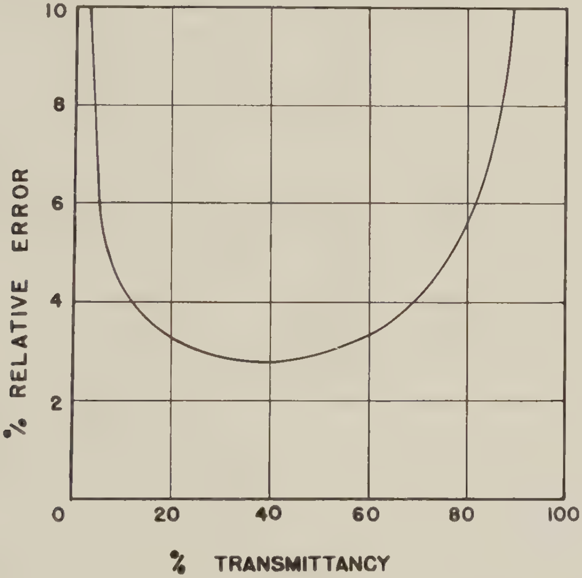

Fig. 8. Relative analysis error as a function of transmittancy (Ayres, 1949, p. 652). Note how relative error increases greatly for crystals with very high or very low transmittancy.

In general photometric errors cause a relatively greater error in prediction of composition for crystals outside the 20 to 60% transmittancy ($=I/I_0$) range (Fig. 8); theoretically the relative error is at a minimum for transmittancies of about 36.8%. However, even for crystals of thicknesses and color concentrations such that they transmit 36.8% of the light, an error of 1 division in the photometer scale reading would result in a concentration error of about 2.7% of the actual value. (Ayres, 1949, p. 652). Table 8 should thus show greatest deviations for the nickel-rich crystals since transmittancy was occasionally around 70 to 90%. This trend does seem to exist but, by the same token, the later trials at lesser thicknesses for these crystals should yield increasingly accurate results as the 20 to 60% transmittancy range is approached or attained (assuming the crystals are not zoned), an effect which is not apparent.

---

† For crystals of this series the density calculated values are likely to be within 1 mol per cent of the analyzed values (see Bloss, 1952, Table 4).

For eqs. 18 and 19 the "absorption difference" method of calculation proved rather unsuccessful, perhaps because the difference in absorption between the wavelengths involved was not as large as for the more successful eq. 20. (As this absorbance difference decreases, the $\hat{\beta}$ parameter necessarily becomes larger in value and this, in turn, may serve to magnify the effect of random photometric errors.) Eq. 20 did exhibit a superiority which was definite with respect to equations 15 and 16, but only slight with respect to equation 17.

CONCLUSIONS

1. Beer's law holds within the limits of measurement for the solid solution series between $Ni(NH_4)_2(SO_4)_2 \cdot 6H_2O$ and $Mg(NH_4)_2 \cdot (SO_4)_2 \cdot 6H_2O$.
2. Light absorption is at a maximum for wavelengths in the 6500 Å unit region and at a minimum for wavelengths in the region of 4900 Å for the α' and γ' vibration directions for crystals of $Ni(NH_4)_2(SO_4)_2 \cdot 6H_2O$ lying on a (110) face.
3. For the solid solution series studied light absorption measurements at several wavelengths generally permit prediction of composition to within 3 mol per cent.
4. The method can be used even though none of the pure end members of the solid solution series are available (since ϵ values may be computed for these end members from absorbance measurements on crystals of known but intermediate compositions).
5. Difference in absorbance per centimeter measurements for the wavelengths of maximum and minimum absorption of a crystal may be substituted into the equation for Beer's law to obviate the effects of flaws, cleavages, or opacities in the crystals. Random errors may be increased, however, by this method of calculation.
6. The method can well be used to determine concentrations of colorants for small idiochromatic crystals of the geologically important solid solution series.

ACKNOWLEDGMENTS

Sincere thanks are extended to the Department of Geology of the University of Chicago for the Rollin D. Salisbury fellowship awarded the writer. In particular the writer is indebted to Professors D. Jerome Fisher and Hans Ramberg for their excellent guidance and counsel throughout this work. Mr. William Schmidt constructed portions of the equipment used and suggested several improvements in their design.

The writer is further grateful to Professor Fisher and to Dr. John Dean of the Department of Chemistry of the University of Tennessee for their critical readings of the manuscript. All views expressed, however, are the responsibility of the writer.

REFERENCES

AYRES, GILBERT H. (1949), Evaluation of accuracy in photometric analysis: *Anal. Chem.*, **21,** 652–657.

BLOSS, F. DONALD. (1951), Relationship between light absorption and composition in the solid solutional series between $Ni(NH_4)_2(SO_4)_2 \cdot 6H_2O$ and $Mg(NH_4)_2(SO_4)_2 \cdot 6H_2O$; *Ph.D. Thesis*, Department of Geology, University of Chicago.

———. (1952), Relationship between density and composition in mol per cent for some solid solution series: *Am. Mineral.*, **37,** 966–981.

BRODE, WALLACE R. (1950), Spectrophotometry and Colorimetry, Physical Methods in Chemical Analysis, Edited by Walter G. Berl, Vol. 1, Academic Press, Inc., New York.

MALMQVIST, DAVID (1929), Studien innerhalb der Epidotgruppe mit besonderer Rucksicht auf die manganhaltigen Gleider: *Upsala Univ., Geol. Inst. Bull.*, **22,** 223–280.

MOOD, ALEXANDER M. (1950), Introduction to the Theory of Statistics, McGraw-Hill Book Co., Inc., New York.

PFEIFFER, HEINZ G., AND LIEBHAFSKY, HERMAN A. (1951), The origins of Beer's law: *Jour. Chem. Education,* **28,** 123–125.

REHBERG, C. H. (1949), Die Lichtdurchlassigkeit der Chromaluminiumalaune und ihrer Losungen: *Neues Jahrb., Mineral., Geologie und Pal., Abh., Abt. A,* **80,** 1–35.

RIDER, PAUL R. (1939), An Introduction to Modern Statistical Methods, John Wiley and Sons, Inc., New York.

SNEDECOR, GEORGE W. (1946), Statistical methods, The Iowa State College Press, Ames, Iowa.

TROMNAU, HANS-WERNER (1934), Chemische und physikalische Untersuchungen and synthetischen mit Kobalt gefarbten Spinellen: *Neues Jahrb., Mineral., Geologie* and Pal., *Beil.-Bd., Abt. A,* **68,** 365–375.

TUTTON, A. E. H. (1905), The relation of ammonia to the alkali metals. A study of ammonium magnesium and ammonium zinc sulphates and selenates: *Jour. Chem. Society (London), Trans.*, **87,** 1123–1183.

———. (1916), The monoclinic double sulphates containing ammonium: *Philosophical Trans. Royal Society, Series A,* **216,** 1–62.

WOOD, ROBERT W. (1934), Physical optics, The Macmillan Company, New York.

Manuscript received June 9, 1954.

A COMPILATION AND CLASSIFICATION OF IMMERSION MEDIA OF HIGH INDEX OF REFRACTION*

Robert Meyrowitz, *U. S. Geological Survey, Washington 25, D. C.*

Abstract

The composition of more than 100 media whose indices of refraction are stated to be equal to or greater than that of methylene iodide, $n=1.74$, are classified in four groups: (1) pure liquids, (2) liquid solutions, (3) pure solids, and (4) solids (2 or more components). Many liquid immersion media are not adequate for routine use in the mineralogical laboratory because of their reactivity with the immersed phase, their instability and toxicity. Five new liquids whose indices of refraction are 1.99–2.07 have been discovered. They are arsenic tribromide solutions of various mixtures containing sulfur, selenium, arsenic disulfide, arsenic trisulfide, and mercuric sulfide.

Introduction

The use of immersion media in the identification of crystalline material is well established, and satisfactory immersion liquids have long been available for indices of refraction below $n=1.74$. The unsatisfactory nature of available high index liquids prompted a study of the possibility of developing new and better liquids, and some have already been reported (Meyrowitz and Larsen, 1951; Meyrowitz, 1952). Five new liquids (II B 6, 7, 8, 9, 10), have since been discovered. Their preparation and properties will be described in future publications.

In the course of this work, the literature on proposed media of high index of refraction has been reviewed. The present paper is a compilation of all such media, classified into four categories:

I. Pure liquids;
II. Liquid solutions, further subdivided by solvents;
III. Pure solids;
IV. Solids (2 or more components).

These media are arranged alphabetically and the corresponding indices of refraction are those found in the original references. In this paper is reported the highest index for that composition. Where a complete series of media has been made, the range of indices is given. The chemical formulas of the more uncommon compounds are given. A question mark (?) after the name of a compound indicates either an ambiguity in the naming of a compound or that the name is obsolete and/or the compound cannot be identified.

Most of the solid media have been proposed by biologists and botanists as mounting media for diatoms and other biological specimens.

---

* Publication authorized by the Director, U. S. Geological Survey.

Desirable properties of high index media for routine use in the mineralogical laboratory are:

(1) They should be liquids. (2) They should be stable (the maximum change in index of refraction should not be more than a few units in the third decimal place in one year). (3) They should not constitute a health or safety hazard. (4) They should be inert to all minerals.

Although embedding media are neither as convenient nor as accurate as liquid immersion media (Larsen and Berman, 1934, p. 13), their use is necessary if indices above 2.1 are to be measured.

High Index Media

I. *Pure liquids*

A. Methylene iodide, CH_2I_2, $n=1.74$ (Brauns, 1886, p. 77).

B. Phenyldi-iodoarsine, $C_6H_5AsI_2$, $n=1.85$ (Gryszkiewicz-Trochimowski and Sikorski, 1928, p. 411–412).

C. Selenium monobromide, Se_2Br_2, $n=2.1$ (Borgström, 1929, p. 61); $n=1.96$ (Anderson and Payne, 1934, p. 67).

Phenylsulfide, $(C_6H_5)_2S$, and dimethylmercury, $(CH_3)_2Hg$, have not been included in the list of media. The index of phenylsulfide was reported to be 1.95 (Pulfrich, 1890, p. 65; Zirkel, 1893, p. 40; Behrens, 1898, p. 46), although Abbe (1879*A*, p. 41, 1879*B*, p. 649) listed it as 1.62. However, as early as 1898, Schroeder van der Kolk (1898, p. 13) warned that it did not always have an index of 1.95, and later the index was corrected to 1.63 by Schroeder van der Kolk and Beekman (1906, p. 10). This was confirmed by Himmelbauer (1909) and by Vogel and Cowan (1943, p. 22). Johannsen (1918, p. 260) has suggested that this confusion is a result of a typographical error, an inverted "6" in the original reference. It is possible that the compound or mixture reported to have an index of 1.95 is something other than phenylsulfide. Bolland (1910, p. 389) has listed in his series of immersion liquids used in the identification of crystalline chemical compounds, a substance having a refractive index of 1.95 which he calls "phenylensulfid." A number of compounds might be confused with phenylsulfide, $(C_6H_5)_2S$, (diphenylsulfide). They are phenyldisulfide, $(C_6H_5)_2S_2$, (diphenyldisulfide); diphenylene disulfide, $(C_6H_4)_2S_2$, (thianthrene); diphenylene sulfide, $(C_6H_4)_2S$, (dibenzthiophene); and diphenylene 2:2 disulfide, $(C_6H_4)_2S_2$. However, all except phenylsulfide are solids.

Dimethylmercury (quecksilbermethyl) was listed as having an index of 1.93 (Pulfrich, 1890, p. 65; Zirkel, 1893, p. 40; Behrens, 1898, p. 47). This index is incorrect and should have been 1.53 (Marvel and Calvery, 1923, p. 823). Pulfrich (1890), Zirkel (1893) and Behrens (1898) have all listed the incorrect indices of both phenylsulfide and dimethylmercury;

all probably used the same, but faulty, original reference or each used the earlier work and accepted it as being reliable.

II. *Liquid solutions*

A. Aniline, $C_6H_5NH_2$, and quinoline, C_9H_7N, combined as a solvent.
1. Mercuric iodide (Pulfrich, 1890, p. 66; Zirkel, 1893, p. 40; Schroeder van der Kolk, 1898, p. 12); $n=1.8$ (Wright, 1911, p. 98).

Aniline darkens on exposure to air and light; it is flammable and poisonous. Quinoline darkens on storage and has a penetrating odor.

B. Arsenic tribromide as a solvent.
1. Arsenic disulfide, As_2S_2 (Smith, 1885, p. 162); $n=1.88$ (Borgström, 1929, p. 60).
2. Arsenic disulfide and arsenic triiodide; $n=1.96$ (Borgström, 1929, p. 61).
3. Arsenic disulfide and selenium (Borgström, 1933, p. 29); $n=2.11$ (Meyrowitz and Larsen, 1951, p. 749).
4. Arsenic disulfide and sulfur (Smith, 1886*A*, p. 76; Meates, 1886*B*, p. 357; Kolbe, 1927, p. 205); $n=2.00$ (Meyrowitz and Larsen, 1951, p. 748).
5. Arsenic trisulfide and selenium, $n=1.97$, red but is transparent to red, yellow, and green light (Borgström, 1933, p. 29); $n=2.04$ (Meyrowitz, unpublished data).
6. Arsenic trisulfide and sulfur, $n=2.07$ (Meyrowitz, unpublished data).
7. Sulfur, mercuric sulfide, and arsenic disulfide, $n=1.99$ (Meyrowitz, unpublished data).
8. Sulfur, mercuric sulfide, and arsenic trisulfide, $n=2.01$ (Meyrowitz, unpublished data).
9. Sulfur, selenium, and arsenic disulfide, $n=2.02$ (Meyrowitz, unpublished data).
10. Sulfur, selenium, and arsenic trisulfide, $n=2.00$ (Meyrowitz, unpublished data).

Solutions containing arsenic tribromide attack the lead-glass prisms of refractometers (Alexander, 1934, p. 181), will corrode metal, and are by their nature, poisonous and reactive toward some minerals (Meyrowitz and Larsen, 1951, p. 747). Although arsenic tribromide liquids hydrolyze in contact with water vapor, they are relatively stable (Meyrowitz and Larsen, 1951, p. 747; Meyrowitz, 1952, p. 853–855).

C. α-Bromonaphthalene, $C_{10}H_7Br$, as a solvent.
1. Arsenic tribromide, $n=1.72$ (Pulfrich, 1890, p. 65; Behrens, 1898, p. 46).
2. Arsenic tribromide and sulfur, $n=1.66$–1.81 (Meyrowitz, 1952, p. 854).
3. Arsenic tribromide, sulfur, and arsenic disulfide, $n=1.66$–2.02 (Meyrowitz, 1952. p. 855–856).
4. Phenyldi-iodoarsine, $n=1.85$ (Bosazza, 1940, p. 300).

D. Cacodyl selenide, $[(CH_3)_2As]_2Se$, as a solvent.
1. Selenium, $n=1.83$ (Anderson, 1934, p. 221).

Cacodyl selenide has a repugnant and extremely penetrating odor.

E. Carbon disulfide, CS_2, as a solvent.
1. Phosphorus, $n=2.01$ (Gladstone and Dale, 1859, p. 32; Stephenson, 1873, p. 2; Stephenson, 1880, p. 565; Retgers, 1893, p. 134).
2. Sulfur, $n=1.75$ (Stephenson, 1880, p. 565; Behrens, 1898, p. 50).
3. Sulfur and phosphorus, $n=2.07$ (Borgström, 1929, p. 62).

Carbon disulfide is highly volatile, very flammable and poisonous.

Solutions containing white phosphorus must be kept in the dark as light causes the conversion of the white phosphorus to the red form, which is insoluble (Madan, 1898*A*, p. 102; 1898*B*, p. 280; West, 1936, p. 247). Because of its poisonous nature and the ease with which finely divided white phosphorus undergoes spontaneous combustion it must be handled with care (Borgström, 1929, p. 62; Milton, 1948, p. 512–513; Burri, 1950, p. 225). The elements, sulfur and phosphorus, dissolved in carbon disulfide will combine chemically, frequently with explosive violence, when the mixture is heated (Thorne and Roberts, 1949, p. 751). Mixtures of sulfur and phosphorus in methylene iodide should be stored in the cold. The free iodine liberated as a result of the slow decomposition of methylene iodide probably increases the danger of explosion, for it has been reported that iodine in a mixture of sulfur and phosphorus in carbon disulfide lowers the temperature at which the elements will combine (Thorne and Roberts, 1949, p. 751). These liquids (II *J* 14.) should be kept under water (Borgström, 1929, p. 62; West, 1936, p. 247). Although hydrogen sulfide gas is evolved when these liquids are stored under water (West, 1936, p. 248), it has been shown that solutions of phosphorus and sulfur in methylene iodide are relatively stable on long storage (Brunn and Barth, 1947).

F. Diethylselenium, $(C_2H_5)_2Se$, as a solvent.
   1. Sulfur and selenium, $n = 1.90$ (Marpmann, 1898, p. 8).

Diethylselenium has an obnoxious odor.

G. Dimethylmercury, $(CH_3)_2Hg$, as a solvent.
   1. Phosphorus, $n = 1.93$ (Retgers, 1893, p. 134).

Dimethylmercury is volatile, flammable, and a deadly poison.

H. Glycerol, $C_3H_8O_3$, as a solvent.
   1. Potassium iodide and mercuric iodide, $n = 1.78$–1.80 (Amann, 1896, p. 21).

I. α-Iodonaphthalene as a solvent.
   1. Iodoform, $n = 1.81$ (Bryant, 1943, p. 97, 101).

J. Methylene iodide as a solvent.
   1. Antimony tribromide, $n = 1.83$ (Zirkel, 1893, p. 48; Borgström, 1933, p. 28).
   2. Antimony tribromide, arsenic disulfide, sulfur, and antimony trisulfide, $n = 1.96$ (Wright, 1911, p. 98).
   3. Antimony tribromide and stannic iodide, $n = 1.86$ (Borgström, 1933, p. 28).
   4. Antimony triiodide, $n = 1.76$ (Merwin, 1913, p. 36).
   5. Antimony triiodide and stannic iodide, $n = 1.83$ (Merwin, 1913, p. 36).
   6. Arsenic tribromide, $n = 1.78$ (Borgström, 1933, p. 58).
   7. Arsenic tribromide and arsenic disulfide, $n = 1.90$ (Borgström, 1929, p. 60–61).
   8. Arsenic tribromide, arsenic disulfide and arsenic triiodide, unstable (Borgström, 1929, p. 61).
   9. Arsenic tribromide and sulfur, $n = 1.74$–1.81 (Meyrowitz and Larsen, 1951, p. 747–748).
   10. Arsenic trisulfide, $n = 1.74$–2.28 (Merwin, 1913, p. 36–37; Weinzierl, 1919/1920, p. 182; Bryant, 1932, p. 3761).

Kolbe (1927, p. 205) reports Weinzierl as having proposed a medium of arsenic disulfide (realgar) dissolved in methylene iodide which does not have the index (2.2–2.4) given by Weinzierl (1919/1920, p. 182). Kolbe says this solution has an index of 1.73 (methylene iodide). Kolbe is in error, because Weinzierl's article describes a solution, not of arsenic disulfide, but of arsenic trisulfide in methylene iodide.

11. Phenyldi-iodoarsine, $n=1.74$–1.85 (Bryant, 1943, p. 97).
12. Phosphorus, $n=1.95$ (Madan, 1898A, p. 101; Gavelin, 1916, p. 293).
13. Phosphorus and iodine, $n=1.95$ (Zirkel, 1893, p. 40).
14. Phosphorus and sulfur, $n=1.78$–2.06 (West, 1936, p. 246).
15. Selenium monobromide, $n=1.97$ (Anderson and Payne, 1934, p. 67).
16. Selenium monobromide and sulfur, $n=1.95$ (De Ment, 1949, p. 102).
17. Selenium monobromide, sulfur, and tetraiodoethylene, C_2I_4, $n>1.90$ (De Ment, 1949, p. 102).
18. Selenium monobromide, sulfur, tetraiodoethylene, antimony triiodide, and/or arsenic sulfide (?), $n=1.96$ (De Ment, 1949, p. 102).
19. Stannic iodide, $n=1.78$ (Merwin, 1913, p. 36).
20. Stannic iodide, arsenic triiodide, and antimony triiodide (Davies and Hartshorne, 1934, p. 1831).
21. Stannic iodide, arsenic triiodide, antimony triiodide, and iodoform (Larsen, Witt, and Poe, 1948, p. 5).
22. Stannic iodide, arsenic triiodide, antimony triiodide, and sulfur, $n=1.85$ (Merwin, 1913, p. 36).
23. Stannic iodide, arsenic triiodide, antimony triiodide, sulfur, and iodoform, $n=1.87$ (Merwin, 1913, p. 36).
24. Stannic iodide, arsenic triiodide, iodoform, sulfur, and arsenic sulfide (?), $n=1.85$ (McCormick, 1936, p. 9).

Solutions of iodides in methylene iodide are unstable and relatively dark in color (Borgström, 1929, p. 58; Jelley, 1934, p. 242; Larsen, Witt, and Poe, 1948, p. 5; Burri, 1950, p. 225).

25. Stannic iodide, arsenic triiodide, and iodoform, $n=1.84$ (Merwin, 1913, p. 36).
26. Stannic iodide and sulfur, $n=1.82$ (Merwin, 1913, p. 36).
27. Sulfur, $n=1.78$, (Bertrand, 1888 p. 31; Madan, 1898*A*, p. 101; Wright, 1911, p. 98).
28. Sulfur and arsenic, $n=1.85$–2.01 (Bryant, 1938, p. 1397).

Solutions of sulfur and arsenic in methylene iodide are unstable (H. E. Merwin, personal communication) as are solutions of arsenic trisulfide in methylene iodide (Merwin, 1913, p. 37).

29. Sulfur and arsenic trisulfide, $n=1.9$ (Plato, 1942, p. 238).
30. Sulfur and iodine, $n>1.85$ (Bertrand, 1888); $n=1.82$ (Johannsen, 1918, p. 252).
31. Sulfur and iodoform, $n=1.81$ (McCormick, 1936, p. 9).
32. Sulfur and tetraiodoethylene, $n=1.81$ (Anderson, 1933, p. 203).
33. Sulfur, tetraiodoethylene, antimony triiodide, and arsenic sulfide (?), $n=1.96$ (De Ment, 1949, p. 102).
34. Sulfur, tetraiodoethylene, and stannic iodide, $n=1.83$, tends to attack the glass parts of refractometers (Anderson, 1933, p. 203).

The frequent use of methylene iodide as a solvent in the preparation of high index immersion liquids is due primarily to its high index of refraction and its ability to dissolve relatively large amounts of solids. The volatility of methylene iodide is less than that of carbon disulfide but more than that of α-bromonaphthalene. It is inert to most minerals but has the disadvantage of decomposing slowly on exposure to light, air, and water, becoming dark because of the liberation of free iodine. Copper shot or wire placed in the liquid has been used to preserve its light color. As its usefulness as a heavy liquid for mineral separation and as a high index immersion liquid depends on its purity, the commercially produced reagent, although now available with reasonable purity, should be tested to verify that its index of refraction ($n_D^{25° C.}$) is 1.737.

K. Phenyldi-iodoarsine as a solvent.
  1. Arsenic sulfides, $n=1.93$ (Borgström, 1951, p. 240).
  2. Arsenic trisulfide and selenium, $n=1.95$ (Borgström, 1951, p. 240).

Borgström (1951, p. 239–240) has urged the use of phenyldi-iodoarsine as a solvent in mixtures in order to obtain high index liquids. It has a blistering action on the skin (Anderson and Payne, 1934, p. 66) and is known to attack the soft glass of refractometers (Anderson and Payne, 1936, p. 168).

L. Phosphorus as a solvent.
  1. Selenium, $n=2.2$–2.5 (Retgers, 1894, p. 424); $n=2.17$ (Borgström, 1929, p. 62).
  2. Sulfur, $n=2.2$–2.5 (Retgers, 1894, p. 424); $n=2.07$ (Borgström, 1929, p. 62).
  3. Sulfur and selenium (Borgström, 1929, p. 62).

Solutions of selenium in phosphorus cannot be stored under water because they decompose, as is shown by the appearance of red flakes of selenium in the protective water layer (Borgström, 1929, p. 63).

M. Selenium monobromide as a solvent.
  1. Selenium, $n>2.02$ (Borgström, 1929, p. 61; Anderson and Payne, 1934, p. 67).
  2. Selenium, methylene iodide, sulfur, tetraiodoethylene, $n>1.90$ (Anderson and Payne, 1934, p. 67).

Selenium monobromide is unstable, decomposing with the separation of selenium, and it is almost opaque except in thin film (Borgström, 1929, p. 61). It is unpleasant to handle (Anderson and Payne, 1940, p. 580).

N. Water as a solvent.
  1. Barium mercuric iodide, $n=1.79$ (Rohrbach, 1883, p. 172; Schroeder van der Kolk, 1898, p. 12).
  2. Mercuric nitrate-mercuric iodide, $n=1.80$ (Zirkel, 1893, p. 40).
  3. Potassium mercuric iodide, $n=1.73$ (Goldschmidt, 1881, p. 234; Stephenson, 1882, p. 167; Merwin, 1911, p. 427).

III. *Pure solids*

A. Antimony pentasulfide (Morris, 1885*B*, p. 132).
B. Antimony triiodide (Morris, 1885*B*, p. 130).
C. Antimony trisulfide (Morris, 1885*B*, p. 132).
D. Arsenic (Hanna and Grant, 1939, p. 175).
E. Arsenic disulfide, $n=2.45$, (Gifford, 1892, p. 174; Marpmann, 1897, p. 338; Hanna and Grant, 1939, p. 175).
F. Arsenic selenide, As_2Se_3 (Merwin in Larsen and Berman, 1934, p. 17).
G. Arsenic tribromide, $n=1.78$ (Abbe, 1879*A*, p. 42, 1879*B*, p. 650; Rohrbach, 1883, p. 172; Pulfrich, 1890, p. 65; Zirkel, 1893, p. 40; Madan, 1898*B*, p. 273; Borgström, 1929, p. 58–59).
H. Arsenic triiodide (Morris, 1885*B*, p. 129).
I. Chloro-chromic acid, (?), CrO_2Cl_2 (Morris, 1885*B*, p. 128).
J. Chromic acid, CrO_3 (Morris, 1885*B*, p. 127).
K. Cyanogen iodide, CNI (Morris, 1885*B*, p. 130).
L. Lead chromate (Gladstone and Dale, 1859, p. 30).
M. Mercuric iodide (Morris, 1885*B*, p. 130).
N. Phosphorus, $n=2.1$ (Gladstone and Dale, 1859, p. 30–31; Stephenson, 1873, p. 2; Damien, 1881, p. 269, 271; Retgers, 1893, p. 131).
O. Selenium (Hanna and Grant, 1939, p. 175).
P. Selenium tetrachloride (Morris, 1885*B*, p. 131).
Q. Silver bromide (Morris, 1885*B*, p. 130), $n=2.25$ (De Ment, 1949, p. 102).
R. Silver chloride, $n=2.07$ (De Ment, 1949, p. 102).
S. Silver iodide (Morris, 1885*B*, p. 130).
T. Sulfur, $n=2.1$ (Stephenson, 1880, p. 565; Morris, 1885*B*, p. 125; Marpmann, 1897, p. 338; Schroeder van der Kolk, 1899, p. 627).
U. Tellurium (Morris, 1885*A*; p. 76; Hanna and Grant, 1939, p. 175).
V. Tellurium chloride (Morris, 1885*B*, p. 130).
W. Thallium monobromide, $n=2.42$ (De Ment, 1949, p. 102).
X. Thallium monochloride (Morris, 1885*B*, p. 131), $n=2.25$ (De Ment, 1949, p. 102).
Y. Thallium monoiodide (Morris, 1885*B*, p. 131).

IV. *Solids* (*2 or more components*)

A. Antimony tribromide, glycerol and
  1. Boracic acid, H_3BO_3, $n>1.7$ (Smith, 1886*B*, p. 3; 1886*C*, p. 13–14).
  2. Arsenious acid, $n=$approximately 2 (Smith, 1886*A*, p. 76; Strasburger and Koernicke, 1923, p. 441).

B. Arsenic tribromide and arsenic disulfide, $n=2.4$ (Smith, 1885, p. 162, 1886*A*, p. 76; Meates, 1886*B* p. 357; Van Heurck, 1886–1887, p. 22–23).
C. Antimony trichloride and arsenic (Morris, 1885*B*, p. 129).
D. Arsenic disulfide and
  1. Mercuric iodide (Morris, 1885*B*, p. 132).
  2. Sodium tetraborate, $Na_2B_4O_7$ (Marpmann, 1897, p. 338).

E. Lead chromate and chromic acid (Morris, 1885*B*, p. 127).
F. Piperine, $C_{17}H_{19}NO_3$ and
  1. Antimony tribromide, $n=$approx. 1.70 (Van Heurck, 1907, p. 60).
  2. Antimony triiodide and arsenic triiodide, $n=1.68$–2.10 (Merwin, 1913, p. 37; Billiet, 1925, p. 113–114; Fisk, 1930, p. 263–266).
  3. Mercuric iodide (Morris, 1885*B*, p. 126).

G. Selenium and
  1. Arsenic (Marpmann, 1898, p. 6–7).
  2. Arsenic disulfide, $n > 2.5$ (Jones, 1914, p. 25).
  3. Arsenic triselenide, $n = 2.72–3.17$ (Merwin in Larsen and Berman, 1934, p. 17).

The melt containing selenium and arsenic trisulfide described by Burri (1950, p. 226) is incorrect and will be corrected in a future edition of his book (Burri, personal communication). It should be "selenium and arsenic selenide."

H. Sulfur and
  1. Arsenic (Meates, 1886*A*; p. 171; Marpmann, 1898, p. 7).
  2. Arsenic disulfide (Morris, 1885*B*, p. 132; Gifford, 1892, p. 174).
  3. Arsenic disulfide and mercuric iodide (Morris, 1886, p. 100).
  4. Arsenic trisulfide, $n = 2.1–2.6$ (Merwin, 1913, p. 37).
  5. Arsenious acid and bromine (Nelson, 1892, p. 123).
  6. Selenium (Morris, 1885*B*, p. 125; Marpmann, 1898, p. 7); $n = 1.99–2.92$ (Merwin and Larsen, 1912, p. 42; Billiet, 1925, p. 113–115).

I. Synthetic resins
  1. Aniline, $C_6H_5NH_2$, formaldehyde, CH_2O, and sulfur, $n =$ approx. 1.80 (Hanna, 1930, p. 424–425).
  2. Hyrax (derivative of naphthalene, $C_{10}H_8$), $n = 1.82$ (Hanna, 1930, p. 425).
  3. Naphthalene, formaldehyde, acetic acid and sulfuric acid, $n = 1.76–1.80$ (Fleming, 1943, p. 35–36).

J. Tellurium and arsenic selenide (Merwin in Larsen and Berman, 1934, p. 17).

K. Thallium monobromide and thallium monoiodide, $n = 2.4–2.8$ (Barth, 1929, p. 358–361).

L. Thallium monochloride and
  1. Stannic chloride (Morris, 1885*B*, p. 131).
  2. Valerianate (?) of quinine (Morris, 1885*B*, p. 131).

Acknowledgments

The author is indebted to a number of his colleagues in the U. S. Geological Survey for their assistance in the literature search and in the preparation of this paper. The help of Donald W. Hastie and Elmer Chovan of the Library of the U. S. Geological Survey proved invaluable. Thanks are due to Esper S. Larsen, Jr., and John C. Rabbitt for their encouragement in the conception and initiation of this compilation of immersion media of high index of refraction. Dr. H. E. Merwin of the Geophysical Laboratory of the Carnegie Institution of Washington critically read the manuscript.

REFERENCES

ABBE, E. (1879*A*), Ueber die Bestimmung der Brechungs-Verhältnisse fester Körper mittelst des Refraktometers: *Gesell. Med. Naturw. Jena Sitzungsber.*, 35–44.

——— (1879*B*), Ueber die Bestimmung der Brechungs-Verhältnisse fester Körper mittelst des Refraktometers: *Repertorium Experimental-Physik*, **15**, 643–652.

Alexander, A. E. (1934), Caution against the use of Borgström's liquids with the lead-glass prisms: *Am. Mineral.*, **19,** 181.

Amann, Jules (1896), Conservirungsflussigkeiten und Einschlussmedien für Moose-, Chloro- und Cyanophyceen: *Zeits. Wiss. Mikros.*, **13,** 18–21.

Anderson, B. W. (1933), Modern methods of gem testing. I.: *Gemmologist*, **2,** 199–204.

——— (1934), The refractometer and other refractive index methods: *Gemmologist* **3,** 216–222.

Anderson, B. W., and Payne, C. J. (1934), Liquids of high refractive index: *Nature*, **133,** 66–67.

——— (1936), Liquids of high refractive index: *Nature*, **138,** 168.

——— (1940), New refractometers employing diamond and other minerals: *Mineral. Mag.*, **25,** 579–583.

Barth, Tom (1929), Some new immersion melts of high refraction: *Am. Mineral.* **14,** 358–361.

Behrens, Wilhelm, (1898), Tabellen zum Gebrauch bei Mikroskopischen Arbeiten, 3d Ed., Leipzig.

Bertrand, Emile (1888), Liquides d'indices supérieurs á 1.8: *Soc. franç. minéralogie Bull.*, **11,** 31.

Billiet, Valere (1925), Over de bepaling van becquereliet, janthiniet, curiet, kasoliet, fourmarieriet, parsonsiet en dumontiet door middel van de immersie-methode van Becke: *Natuurw. Tijdschr.*, **7,** 112–116.

Bolland, A. (1910), Mikrochemische Studien. IV. Die Brechungsindices krystallinischer chemischer Individuen nach der Einbettungsmethode vom Standpunkte der analytischen Praxis: *Monatsh. Chemie*, **31,** 387–420.

Borgström, L. H. (1929) Ein Beitrag zum Entwicklung der Immersionsmethode: *Comm. géol. Finlande Bull.*, **87,** 58–63.

——— (1933), Beitrag zur Entwicklung der Immersionsmethode. II. Vervendung von Antimonbromid. Versuche mit Selen: *Comm. géol. Finlande Bull.*, **101,** 28–29.

——— (1951), Fenyldijodarsin, en vatska med myket hög brytingsexponent: *Comm. géol. Finlande Bull.*, **154,** 239–240.

Bosazza, V. L. (1940), Notes on refractive index liquids: *Am. Mineral.*, **25,** 299–301.

Brauns, R. (1886), Über die Verwendbarkeit des Methylenjodids bei petrographischen und optischen Untersuchungen: *Neues Jahrb.*, **1886,** *Band II*, 72–78.

Bruun, B., and Barth, T. (1947), Stability on storage of the high refractive index liquids of C. D. West: *Am. Mineral.*, **32,** 92–93.

Bryant, W. M. D. (1932), Optical properties of some derivatives of lower aliphatic alcohols and aldehydes: *Am. Chem. Soc. Jour.*, **54,** 3758–3765.

——— (1938), Optical crystallographic studies with the polarizing microscope. I. Identification and semiquantitative determination of acetic and propionic p-bromoanilides in their binary mixtures: *Am. Chem. Soc. Jour.*, **60,** 1394–1399.

——— (1943), Optical crystallographic studies with the polarizing microscope, IV. Axial dispersion with sign. Other dispersion measurements: *Am. Chem. Soc. Jour.*, **65,** 96–102.

Burri, Conrad (1950), Das Polarisationsmikroskop, Basel.

Damien, B. C. (1881), Recherches sur le Pouvoir Réfringent des Liquides: *Ecolê Normale Superior, Paris, Annales Scientific*, 2d Ser., **10,** 233–280.

Davies, E. S., and Hartshorne, N. H. (1934), Identification of some aromatic nitro-compounds by optical crystallographic methods: *Chem. Soc. London Jour.*, II, 1830–1836.

De Ment, Jack (1949), Silicon carbide refractometer: *Mineral.*, **17,** 99–104.

FISK, H. G. (1930), Preparation and purification of the tri-iodides of antimony and arsenic for use in immersion media of high refractive index: *Am. Mineral.*, **15**, 263–266.

FLEMING, W. D. (1943), Synthetic mounting medium of high refractive index: *Royal Micros. Soc. Jour.*, **63**, 34–37.

GAVELIN, AXEL (1916), Über Hogbomit: *Upsala Univ., Geol. Inst. Bull.*, **15**, 289–316.

GIFFORD, J. W., (1892), The resolution of Amphipleura pellucida: *Royal Micros. Soc. Jour.*, 173–174.

GLADSTONE, J. H., AND DALE, T. P. (1859), On some optical properties of phosphorus: *Philos. Mag.*, **18**, 30–33.

GOLDSCHMIDT, V. (1881), Über Verwendbarkeit einer Kaliumquecksilberjodidlosung bei mineralogischen und petrographischen Untersuchungen: *Neues Jahrb., Beilage-Band*, **1**, 179–238.

GRYSZKIEWICZ-TROCHIMOWSKI, E., AND SIKORSKI, S. F. (1928), Sur les properties optiques de' l arsenic. II.: *Roczniki Chemji*, **8**, 405–422.

HANNA, G. D. (1930), Hyrax, a new mounting medium for diatoms: *Royal Micros. Soc. Jour.*, **48**, 424–426.

HANNA, G. D., AND GRANT, W. M. (1939), Preliminary note on a technique for mounting diatoms in realgar and other substances: *Royal Micros. Soc. Jour.*, 3d Ser., **59**, 174–176.

HIMMELBAUER, ALFRED (1909), Bemerkungen über das Phenylsulfid: *Centralbl. Mineralogie*, **1909**, 396.

JELLEY, E. E. (1934), A microrefractometer and its use in chemical microscopy: *Royal Micros. Soc. Jour.*, **54**, 234–235.

JOHANNSEN, ALBERT (1918), Manual of Petrographic Methods: 2d Ed., New York.

JONES, CHAPMAN (1914), On media of high refractive power for photo-micrography: *Royal Photog. Soc. Journ.*, **54**, 14–25.

KOLBE, R. W. (1927), Über Einschlussmittel für Diatomeen: *Zeits. Wiss. Mikros.*, **44**, 196–211.

LARSEN, E. S., JR., AND BERMAN, H., (1934), The Microscopic Determination of Non-opaque Minerals: *U. S. Geol. Survey Bull.* **848**.

LARSEN, J., WITT, N. F., AND POE, C. F., (1948), Optical crystallographic identification of some amino acids with 2-nitroindandion-1, 3: *Mikrochem. ver. Mikrochim. Acta*, **34**, 1–13.

MCCORMICK, R. B. (1936), Advanced and refined technique in the petrographic study of crystalline refractories: *Am. Ceramic Soc. Jour.*, **19**, 7–13.

MADAN, H. G. (1898*A*), Note on some of the properties of methylene di-iodide: *Chem. Soc. London Proc.*, **14**, 101–102.

——— (1898*B*), On some organic substances of high refractivity, available for mounting specimens for examination under the microscope: *Royal Micros. Soc. Jour.*, 273–281.

MARPMANN, G. (1897), Über die Anwendung von Zimmtöl, Cassiaöl and von anderen Einschlussmitteln in der Mikroskopie: *Zeits. angew. Mikros.*, **2**, 335–338.

——— (1898), Das Selen als Einschlussmittel fur Diatomaceen: *Zeits. angew. Mikros.*, **4**, 6–8.

MARVEL, C. S., AND CALVERY, H. O. (1923), The preparation of dialkyl mercury compounds from the Grignard reagent. II. The relative stability of the carbon-mercury linkage in dialkyl mercury compounds: *Am. Chem. Soc. Jour.*, **45**, 820–823.

MEATES, W. C. (1886*A*), Mounting medium: *Royal Micros. Soc. Jour.*, **6**, 171.

——— (1886*B*), New medium of high refractive index: *Royal Micros. Soc. Jour.*, **6**, 357.

MERWIN, H. E. (1911), A method of determining the density of minerals by means of Rohrbach's solution having a standard refractive index: *Am. Jour. Sci.*, 4th Ser., **32**, 425–428.

——— (1913), Media of high refraction for refractive index determinations with the microscope; also a set of permanent standard media of lower refraction: *Washington Acad. Sci. Jour.*, **3**, 35–40.

Merwin, H. E., and Larsen, E. S. (1912), Mixtures of amorphous sulfur and selenium as immersion media for the determination of high refractive indices with the microscope: *Am. Jour. Sci.*, 4th Ser., **34**, 42–47.

Meyrowitz, Robert (1952), A new series of immersion liquids: *Am. Mineral.*, **37**, 853–856.

Meyrowitz, R., and Larsen, E. S., Jr. (1951), Immersion liquids of high refractive index: *Am. Mineral.*, **36**, 746–750.

Milton, Charles (1948), Fire hazard with C. D. West's high refractive index liquids: *Am. Mineral.*, **33**, 512–513.

Morris, William (1885*A*), Proceedings of the Microscopical Section of the Royal Society of New South Wales: *Australasian Med. Gaz.*, **5**, 76.

——— (1885*B*), Notes on experiments in mounting the Amphipleura pellucida in media having a higher refractive index than Canada balsam: *Royal Soc. New South Wales Jour.*, **19**, 121–133.

——— (1886), Proceedings of the Microscopical Section of the Royal Society of New South Wales: *Australasian Med. Gaz.*, **5**, 100.

Nelson, E. M. (1892), The Rev. Father Thompson's high refractive medium: *Quekett Micr. Club Jour.*, Ser. II, **5**, 123.

Plato, W. (1942), Mikroskop-Refraktometer für Flüssigkeiten und seine Anwendung zur Bestimmung von rohen und geschliffenen Steinen: *Zeits. Wiss. Mikros.*, **58**, 228–239.

Pulfrich, C. (1890), Das Totalreflektometer und das Refraktometer für Chemiker, Leipzig.

Retgers, J. W. (1893), Der Phosphor als stark lichtbrechendes Medium zu petrographischen Zwecken: *Neues Jahrb.*, **1893**, Band II, 130–134.

——— (1894), Der Phosphor als stark lichtbrechendes Medium zu petrographischen Zwecken. Druckfehler-Berichtigungen: *Neues Jahrb.*, **1894**, Band I, 424.

Rohrbach, Carl (1883), Über eine neue Flüssigkeit von hohem specifischen Gewicht, hohem Brechungsexponenten und grosser Dispersion: *Annalen der Physik und Chemie, N. F.*, **20**, 169–174.

Schroeder van der Kolk, J. L. C. (1898), Kurze Anleitung zur Mikroskopischen Krystallbestimmung, Wiesbaden.

——— (1899), Tabellen zur mikroskopischen Bestimmung der Mineralien nach ihrem Brechungsindex: *Zeits. anal. Chemie*, **38**, 615–662.

Schroeder van der Kolk, J. L. C., and Beekman, E. H. M. (1906), Tabellen zur Mikroskopischen Bestimmung der Mineralien nach ihrem Brechungsindex, Zweite Auflage, Wiesbaden.

Smith, H. L. (1885), Mounting media of high refractive index: *Am. Monthly Micros. Jour.*, **6**, 161–163.

——— (1886*A*), High-refractive media: *New York Micros. Soc. Jour.*, **2**, 75–77.

——— (1886*B*), A new mounting medium of high refractive index: *Am. Monthly Micros. Jour.*, **7**, 3–4.

——— (1886*C*), A new high-refractive mounting medium: *New York Micros. Soc. Jour.*, **2**, 13–16.

Stephenson, J. W. (1873), Observations on the optical appearances presented by the inner and outer layers of *Coscinodiscus* when examined in bisulfide of carbon and in air: *Monthly Micros. Jour.*, **10**, 1–5.

——— (1880), On the visibility of minute objects mounted in phosphorus, solution of sulfur, bisulfide of carbon and other media: *Royal Micros. Soc. Jour.*, **3**, 564–567.

——— (1882), On mounting objects in phosphorus, and in a solution of biniodide of mercury and iodide of potassium: *Royal Micros. Soc. Jour.*, Ser. II, **2**, 163–169.

STRASBURGER, E., AND KOERNICKE, M. (1923), Das Botanische Prakticum, 7th Ed., Jena.

THORNE, P. C. L., AND ROBERTS, E. R. (1949), Fritz Ephraim-Inorganic Chemistry, 5th Ed., New York, N. Y.

VAN HEURCK, HENRI (1886–1887), Nouvelle préparation du médium á haut indice (2.4) et note sur le liquidambar: *Soc. belge Micros. Bull.*, **13**, 20–24.

——— (1907), Les mediums á haut indice: *Soc. belge Micros. Annales*, **28**, 56–63.

VOGEL, A. I., AND COWAN, D. M. (1943), Physical properties and chemical constitution. VII. Alkyl sulphides, disulphides, sulphites, sulphates, and orthophosphates: *Chem. Soc. London Jour.*, 16–24.

WEINZIERL, F. I. (1919/1920), Ein neues Einschlussmittel fur Diatomeen: *Mikrokosmos*, **13**, 182–183.

WEST, C. D. (1936), Immersion liquids of high refractive index: *Am. Mineral.*, **21**, 245–249.

WRIGHT, F. E. (1911), The methods of petrographic-microscopic research: *Carnegie Inst. Wash. Pub.* **158.**

ZIRKEL, FERDINAND (1893), Lehrbuch der Petrographie, Erster Band, Zweite Auflage, Leipzig.

Manuscript received June 1, 1954.

SYNTHETIC ASBESTOS INVESTIGATIONS, II: X-RAY AND OTHER DATA ON SYNTHETIC FLUOR-RICHTERITE, -EDENITE, AND -BORON EDENITE*

J. A. Kohn† and J. E. Comeforo,‡ *Electrotechnical Laboratory, U. S. Bureau of Mines, Norris, Tennessee.*

Abstract

As a portion of a general research program on the synthesis of asbestiform minerals, *x*-ray and other data have been obtained on the following chemically analyzed synthetic fluor-amphiboles: richterite, $Na(CaNa)Mg_5(Si_4O_{11})_2F_2$, edenite, $NaCa_2Mg_5(Si_{3.5}Al_{0.5}O_{11})_2F_2$, boron edenite, $NaCa_2Mg_5(Si_{3.5}B_{0.5}O_{11})_2F_2$. Comparisons are made with the values previously reported for fluor-tremolite, $Ca_2Mg_5(Si_4O_{11})_2F_2$.

A detailed indexing of *x*-ray powder diffraction patterns has been made in the range up to 76° 2*θ*, and accurate unit cell dimensions have been determined. The observed cell-dimension variations are discussed with reference to ionic location and polarization. The synthesis and analysis of additional specified compositions are needed to elucidate the factors controlling fibrosity and flexibility in layered and allied silicate structures.

Introduction

During an extensive study of the synthesis of fluor-amphiboles from melts, over 100 different batch compositions were investigated; the effect of fluoride concentration and various isomorphic substitutions in the batch on the development of asbestiform amphibole were evaluated (1). Concurrently, some of the fundamental constants of various "end-members" of the monoclinic fluor-amphiboles were determined.

In the present study, the optical and *x*-ray constants of synthetic fluor-richterite, $Na(CaNa)Mg_5(Si_4O_{11})_2F_2$, fluor-edenite, $NaCa_2Mg_5(Si_{3.5}Al_{0.5}O_{11})_2F_2$, and a boron-containing fluor-edenite, $NaCa_2Mg_5(Si_{3.5}B_{0.5}O_{11})_2F_2$, have been evaluated and are compared with the values previously measured for synthetic fluor-tremolite, $Ca_2Mg_5(Si_4O_{11})_2F_2$ (2).

Experimental Procedure

The method of synthesis and the techniques employed were the same as previously reported (2); that is, a batch corresponding to the composition of the desired fluor-amphibole was melted and cooled, during which time the amphibole devitrified. Graphite crucibles with screw-on covers were used to minimize the extent of volatilization and to prevent the introduction of impurities that might enter the amphibole structure or otherwise cause a deviation from the desired composition.

---

* A contribution from the Synthetic Minerals Section, Industrial Minerals Branch, U. S. Bureau of Mines, Norris, Tennessee.

† Present address, Chemical-Physics Branch, Signal Corps Engineering Laboratory, Fort Monmouth (Hexagon), New Jersey.

‡ Present address, Sylvania Electric Products Inc., Woburn, Mass.

The percentage of each raw material used in compounding the synthetic fluor-amphiboles is given in Table 1. To eliminate the presence of carbonates, hydroxides, or other compounds that decompose with liberation of gases, certain components were initially reacted to form stable, anhydrous, nonvolatile materials, such as $Na_2MgSi_3O_8$ (as glass), $CaSiO_3$, and MgB_2O_4. Others, such as the clay and silicic acid, were dehydrated before use. In every instance, the particle size of the ingredients was minus-100 mesh. After dry mixing in a glass jar with rubber balls, the batches were packed in the crucibles to hand tightness.

TABLE 1. FLUOR-AMPHIBOLE BATCH COMPOSITIONS (WEIGHT—PER CENT)

Raw Material	Richterite	Edenite	Boron edenite
$Na_2MgSi_3O_8$*	34.4	16.9	17.2
$CaSiO_3$*	14.1	27.7	28.2
MgF_2 (tech. grade)	7.6	7.5	7.6
MgO†	14.7	16.9	14.8
MgB_2O_4*	—	—	6.7
Dehydrated Georgia clay ($Al_2Si_2O_7$)	—	13.2	—
Dehydrated silicic acid† (SiO_2)	29.2	17.9	25.6
	100.0	100.1	100.1

* Prepared from reagent-grade chemicals.

† Reagent-grade chemicals.

The batches were fired to 1350° C., maintained at this temperature for 5 hours, and then cooled at 36° C. per hour to 1100° C., at which temperature the furnace was turned off. The resulting crystalline reaction products, consisting primarily of brittle, acicular crystals of fluor-amphibole (at least 80%), were ground to minus-200 mesh. Beneficiation was carried out by heavy-liquid separation using tetrabromoethane and methylene iodide (adjusted to 2.97 and 3.10 gm./cc., respectively) until fractions containing at least 95% fluor-amphibole (microscopically determined) were obtained. Each of these samples was divided into four aliquot portions: The first was examined petrographically, and the optical constants determined; the second was chemically analyzed; the third was used for the x-ray study; and the last portion was filed.

RESULTS

(1) *Chemical Composition*

The beneficiated samples of the synthetic fluor-amphiboles were examined petrographically, and in no case was the estimate of the total

Table 2. Chemical Analyses of Synthetic Fluor-amphiboles*

Constituent	Fluor-richterite		Fluor-edenite		Fluor-boron edenite	
	Theoretical	Actual	Theoretical	Actual	Theoretical	Actual
SiO_2	58.45	58.88	50.17	51.09	51.16	52.21
Al_2O_3	.00	—	6.08	6.47	.00	—
B_2O_3	.00	—	.00	—	4.24	3.91
Fe_2O_3	.00	0.17	.00	.21	.00	.24
MgO	24.51	24.24	24.05	23.06	24.52	24.09
CaO	6.82	7.00	13.38	12.30	13.64	12.69
Na_2O	7.54	7.20	3.70	4.26	3.77	3.99
F^-	4.62	4.74	4.53	4.89	4.62	4.85
O=F	−1.94	−2.00	−1.91	−2.06	−1.95	−2.04
	100.00	100.23	100.00	100.22	100.00	99.94

* Analysts: H. R. Shell, R. L. Craig; samples No. 3848, 3867, and 3850, respectively. Analytical data based on samples dried at 110° C.

impurities greater than 4%. The fluor-richterite sample contained less than 1% impurity, mostly CaF_2. In the case of fluor-edenite, the major contaminant was 1–2% pyroxene, probably diopside. The remaining impurity concentration was less than ½%. The extraneous phases in fluor-boron edenite totaled less than 4%, of which approximately 3% was forsterite.

The chemical analyses of the beneficiated samples are given in Table

Table 3. Comparisons of Theoretical and Empirical Ionic Ratios of Synthetic Fluor-Amphiboles

	(WO_{12})	(XO_8)	(YO_6)	(ZO_4)	
			Richterite		
Theoretical	Na	(CaNa)	Mg_5	Si_8	$O_{22}F_2$
Calculated*	$Na_{0.93}$	$(Ca_{1.03}Na_{0.97})$	$Mg_{4.93}$	$Si_{8.04}$	$O_{22}F_{2.04}$
			Edenite		
Theoretical	Na	Ca_2	Mg_5	(Si_7Al)	$O_{22}F_2$
Calculated*	$Na_{0.99}$	$(Ca_{1.84}Na_{0.16})$	$(Mg_{4.79}Al_{0.18})$	$(Si_{7.12}Al_{0.88})$	$O_{22}F_{2.15}$
			Boron edenite		
Theoretical	Na	Ca_2	Mg_5	(Si_7B)	$O_{22}F_2$
Calculated*	$Na_{0.93}$	$(Ca_{1.87}Na_{0.13})$	$Mg_{4.92}$	$(Si_{7.16}B_{0.92})$	$O_{22}F_{2.10}$

* Calculated from chemical analysis on basis of 22 oxygen atoms. No attempt was made to correct for the small amounts of impurities present.

2. A comparison between the theoretical and empirical formulas of the three fluor-amphiboles appears in Table 3.

(2) *Optical Properties*

Comparisons of the optical constants reported on various naturally occurring richterites and edenites with those measured on the synthetic fluor-amphiboles are rendered difficult because the natural minerals invariably contain significant amounts of cations other than those required for theoretical compositions (3, 4). For this reason, the observed differences cannot be attributed entirely to complete replacement of hydroxyl by fluoride.

The refractive indices of the synthetic fluor-amphiboles were measured at room temperature with a petrographic microscope, using the oil-immersion technique. The results obtained are compared in Table 4 with those previously measured for synthetic fluor-tremolite.

TABLE 4. SYNTHETIC FLUOR-AMPHIBOLE OPTICAL CONSTANTS*

	Tremolite	Richterite†	Edenite‡	Boron-edenite
X	1.581	1.603	1.605	1.588
Y	1.593	1.614	1.617	1.598
Z	1.602	1.622	1.624	1.605
$Z \wedge c$	21°	22°	18°	12°
2V	86½°	72°	69°	75°
Sign	(−)	(−)	(−)	(−)

* Determinations by M. V. Denny; maximum error for X, Y, and Z is ±0.002; 2V determined by means of a 5-axis universal stage, using sodium (*D*) light.

† A natural richterite ("soda-tremolite") described by Larsen (3) was not used for comparison of optical properties owing to the presence of 3.91% Fe_2O_3 and 2.44% FeO.

‡ A natural, biaxial positive edenite described by Palache (4) was not used for comparison of optical properties owing to the presence of 1.02% Fe_2O_3 and 3.38% FeO.

(3) *X-ray Data*

No *x*-ray data are available in the literature on relatively pure synthetic or natural amphiboles of the types herein concerned. In the present study, accurate unit cell dimensions have been obtained, and complete diffraction data are given in the range up to 76° 2θ. The three synthetic fluor-amphiboles studied are monoclinic, with a bimolecular unit cell.

All *x*-ray diffraction data were recorded using a chart operation in conjunction with a Philips high-angle goniometer (diffractometer). The synthetic fluor-amphibole samples were packed in the usual rectangular aluminum holders. The instrumental setting used was as follows: scale factor, 16 (unless rescanning a very strong maximum); multiplier, 1.0

(giving a counting rate of 800 counts per second, full scale); time constant, 4 seconds; Geiger overvoltage, 300 volts; divergence slit, 1°; scanning speed, $\frac{1}{4}$° per minute; chart scale, $\frac{1}{2}$ inch per degree.

Both before and after each chart operation involving a fluor-amphibole pattern, appropriate silicon maxima were recorded using the silicon standard compact furnished with the instrument. Corrections ranged from 0.005° to 0.055° and were read from a curve plotting instrumental correction against 2θ.

A low-power microscope fitted with a movable-hair ocular, used in conjunction with a photographically processed slide of 200 lines per inch, permitted very accurate 2θ readings of the diffraction maxima. For those peaks directly concerned with the calculation of the unit-cell dimensions, 2θ readings to the third decimal place were obtained. For all other maxima, measurements were taken to 0.005°. Following the procedure established by Donnay and Donnay (5), the peaks were bisected at approximately two-thirds of the peak height to obtain the readings.

In the case of fluor-tremolite, the positions of the maxima directly involved in the calculation of the cell dimensions were determined by a counting operation in conjunction with the Philips unit. For the present study, a chart operation was found to be of approximately the same accuracy (see Table 8) and substantially less time-consuming. After the complete pattern of the fluor-amphibole under investigation was obtained by scanning down-scale from 76° 2θ, four sharp, unambiguously-indexed maxima in the higher 2θ range were selected. Each chosen peak was then scanned four additional times. 2θ values averaged from the 5 separate measurements were used for a solution of the quadratic form (6). The unit-cell dimensions thus derived were refined until close agreement was obtained between the calculated and observed 2θ values of various selected maxima. The final cell dimensions are given in Table 9 and compared with those previously obtained for synthetic fluor-tremolite.

Following the last cell-dimension refinement, the positions of all reflections permissible by the space group symmetry ($C\ 2/m$) were calculated in the range up to 76° 2θ (approximately 250 potential maxima in each case). The diffraction data for all resolved maxima (and a few significant doublets) in this range are tabulated in Tables 5, 6, and 7 for synthetic fluor-richterite, -edenite, and -boron edenite, respectively. Results bearing on the accuracy of the diffraction data, and ultimately upon the unit-cell dimensions adopted, are collected in Table 8, and compared with the values for synthetic fluor-tremolite. In the present study, no diffraction maximum showed a deviation in 2θ of more than 0.02° from the calculated value, and the average deviation was in the order of 10^{-4} degrees.

Table 5. X-Ray Diffraction Data (Powder) for Synthetic Fluor-Richterite
(*Space Group C 2/m*)

hkl	2θ obs.	2θ calc.*	$\Delta 2\theta$	Meas. Int.	*d* calc.
020	9.865°	9.855°	−0.01°	3	8.979 Å
110	10.51	10.515	+ .005	>100	8.409
130	17.49	17.50	+ .01	2	5.067
$11\bar{1}$	18.25	18.255	+ .005	3	4.860
200	18.635	18.645	+ .01	11	4.759
040	19.76	19.775	+ .015	10	4.489
220	21.115	21.13	+ .015	4	4.205
111	22.275	22.265	− .01	2	3.993
$13\bar{1}$	23.03	23.045	+ .015	4	3.859
131	26.34	26.345	+ .005	10	3.380
150	26.505	26.505	0	3	3.360
240	27.285	27.285	0	60	3.265
310	28.54	28.55	+ .01	≫100	3.124
221	30.325	30.33	+ .005	11	2.944
$15\bar{1}$	30.505	30.52	+ .015	3	2.926
330	31.91	31.91	0	76	2.803
331	32.91	32.89	− .02	9	2.721
151	33.15	33.15	0	20	2.700
061	34.73	34.715	− .015	7	2.582
$20\bar{2}$	35.555	35.535	− .02	6	2.524
350	37.805	37.805	0	11	2.378
$35\bar{1}$	38.68	38.665	− .015	7	2.327
$42\bar{1}$	38.885	38.875	− .01	5	2.315
$17\bar{1}$	39.385	39.365	− .02	7	2.287
171	41.515	41.50	− .015	3	2.174
132	41.63	41.64	+ .01	3	2.167
261	41.81	41.81	0	8	2.159
202	44.20	44.195	− .005	3	2.048
351	44.905	44.91	+ .005	5	2.017
370	45.435	45.43	− .005	5	1.9947
190	46.465	46.46	− .005	3	1.9528
510	48.03	48.025	− .005	29	1.8928
$19\bar{1}$	49.06	49.05	− .01	3	1.8556
530	50.275	50.255	− .02	8	1.8139
0·10·0	50.815	50.80	− .015	2	1.7957
$51\bar{2}$	52.575	52.585	+ .01	2	1.7389
461	55.67	55.67	0	16	1.6496
480	56.295	56.295	0	6	1.6327
1·11·0	57.20	57.205	+ .005	10	1.6090
600	58.10	58.105	+ .005	9	1.5862
$55\bar{2}$	58.695	58.715	+ .02	3	1.5711
620	59.105	59.09	− .015	2	1.5620
551	61.68	61.675	− .005	6	1.5026
0·12·0	61.96	61.955	− .005	7	1.4964
442	63.10	63.10	0	1	1.4721
3·11·0	64.08	64.095	+ .015	5	1.4516
$66\bar{1}$	64.975	64.98	+ .005	11	1.4340
512	68.545	68.555	+ .01	6	1.3676
$60\bar{3}$ 532	70.355	70.355 70.355	—	1	1.3370 1.3369
263	70.575	70.575	0	1	1.3333
$75\bar{1}$	72.23	72.23	0	3	1.3068
$2\cdot12\cdot\bar{2}$	73.495	73.505	+ .01	4	1.2872

* Using λ $CuK\alpha_1$ (1.54050 A) above 25° 2θ and λ CuK_α (1.5418 A) below 25° 2θ.

TABLE 6. X-RAY DIFFRACTION DATA (POWDER) FOR SYNTHETIC FLUOR-EDENITE
(*Space Group C 2/m*)

hkl	2θ obs.	2θ calc.*	Δ2θ	Meas. Int.	*d* calc.
020	9.825°	9.825°	0°	4	9.002 Å
110	10.515	10.515	0	81	8.413
$11\bar{1}$	18.15	18.17	+ .02	2	4.882
200	18.64	18.645	+ .005	3	4.759
040	19.71	19.725	+ .015	6	4.501
220	21.095	21.115	+ .02	6	4.208
131	26.37	26.37	—	10	3.377
041		26.375			3.376
240	27.24	27.245	+ .005	42	3.270
310	28.54	28.54	0	99	3.125
221	30.395	30.405	—	19	2.937
$15\bar{1}$		30.415			2.936
330	31.87	31.875	+ .005	37	2.805
$33\bar{1}$	32.74	32.735	− .005	7	2.733
151	33.135	33.14	+ .015	15	2.701
061	34.645	34.645	0	7	2.587
$20\bar{2}$	35.37	35.36	− .01	11	2.536
170	36.145	36.145	0	1	2.483
$40\bar{1}$	37.35	37.35	0	2	2.406
350	37.76	37.755	− .005	8	2.381
$35\bar{1}$	38.51	38.50	− .01	7	2.336
$42\bar{1}$	38.70	38.71	+ .01	7	2.324
$17\bar{1}$	39.24	39.24	0	5	2.294
261	41.815	41.815	0	9	2.158
351	44.95	44.96	+ .01	8	2.014
370	45.36	45.35	− .01	3	1.9980
190	46.325	46.34	+ .015	2	1.9577
510	48.02	48.015	− .005	12	1.8932
$46\bar{1}$	48.47	48.46	− .01	1	1.8769
530	50.25	50.235	− .015	6	1.8146
0·10·0	50.665	50.66	− .005	1	1.8004
550	54.485	54.475	− .01	2	1.6830
461	55.735	55.72	− .015	12	1.6481
480	56.205	56.21	+ .005	4	1.6351
1·11·0	57.03	57.045	+ .015	3	1.6130
600	58.095	58.09	− .005	4	1.5865
402	59.46	59.445	− .015	2	1.5535
551	61.79	61.77	—	12	1.5006
0·12·0		61.78			1.5003
$2\cdot 10\cdot \bar{2}$	63.305	63.29	− .015	1	1.4681
3·11·0	63.95	63.945	− .005	2	1.4546
$66\bar{1}$	64.76	64.77	+ .01	11	1.4381
512	68.80	68.785	− .015	5	1.3636
710	69.24	69.23	− .01	2	1.3560
$75\bar{1}$	72.01	72.015	+ .005	3	1.3102
$2\cdot 12\cdot \bar{2}$	73.235	73.24	+ .005	2	1.2913

* Using λ CuKα_1 (1.54050 Å) above 25° 2θ and λ CuK$_\alpha$ (1.5418 Å) below 25° 2θ.

TABLE 7. X-RAY DIFFRACTION DATA (POWDER) FOR SYNTHETIC FLUOR-BORON EDENITE
(*Space Group C 2/m*)

hkl	2θ obs.	2θ calc.*	$\Delta 2\theta$	Meas. Int.	*d* calc.
020	9.845°	9.85°	+0.005°	4	8.979 Å
110	10.54	10.54	0	95	8.395
130	17.50	17.515	+ .015	3	5.064
$11\bar{1}$	18.255	18.255	0	2	4.860
200	18.675	18.685	+ .01	8	4.748
040	19.755	19.775	+ .02	6	4.489
220	21.155	21.165	+ .01	5	4.198
111	22.325	22.305	− .02	2	3.986
$13\bar{1}$	23.04	23.045	+ .005	3	3.859
131	26.39	26.38	− .01	7	3.376
240	27.31	27.315	+ .005	35	3.262
310	28.61	28.61	0	≫100	3.118
221	30.405	30.395	− .01	16	2.939
330	31.955	31.955	0	29	2.798
331	32.925	32.91	− .015	9	2.719
151	33.18	33.175	− .005	20	2.698
350	37.85	37.85	—	6	2.375
400		37.86			2.374
$35\bar{1}$	38.675	38.68	+ .005	8	2.326
$42\bar{1}$	38.915	38.92	+ .005	6	2.312
$17\bar{1}$	39.375	39.365	− .01	4	2.287
261	41.86	41.855	− .005	7	2.156
351	45.00	44.985	− .015	5	2.013
370	45.47	45.47	—	5	1.9931
222		45.47			1.9929
190	46.48	46.465	− .015	2	1.9526
510	48.13	48.13	0	19	1.8888
$19\bar{1}$	49.04	49.05	+ .01	2	1.8556
530	50.37	50.36	− .01	9	1.8104
0·10·0	50.805	50.80	− .005	2	1.7957
461	55.76	55.77	+ .01	8	1.6469
$60\bar{1}$	56.36	56.355	—	5	1.6312
480		56.36			1.6311
1·11·0	57.185	57.205	+ .02	3	1.6089
600	58.235	58.24	+ .005	7	1.5828
620	59.235	59.225	− .01	2	1.5588
402	59.39	59.39	0	2	1.5549
0·12·0	61.96	61.955	− .005	5	1.4964
3·11·0	64.115	64.13	+ .015	2	1.4509
$66\bar{1}$	65.065	65.065	0	13	1.3423
512	68.765	68.735	—	3	1.3645
$73\bar{1}$		68.77			1.3639
710	69.41	69.41	0	3	1.3528
730	71.205	71.205	0	2	1.3231
$75\bar{1}$	72.355	72.345	− .01	3	1.3050
$2\cdot 12\cdot \bar{2}$	73.50	73.51	+ .01	2	1.2872

* Using λ $\mathrm{CuK}\alpha_1$ (1.54050 Å) above 25° 2θ and λ CuK_α (1.5418 Å) below 25° 2θ.

TABLE 8. ACCURACY OF SYNTHETIC FLUOR-AMPHIBOLE DIFFRACTION DATA

	Maximum Deviation (degrees)	Average Deviation (degrees)	Contributing Peaks (number)
Tremolite	0.03	$+2.3\times10^{-4}$	41
Richterite	.02	-4.0×10^{-4}	51
Edenite	.02	-2.5×10^{-4}	40
Boron edenite	.02	$+1.3\times10^{-4}$	38

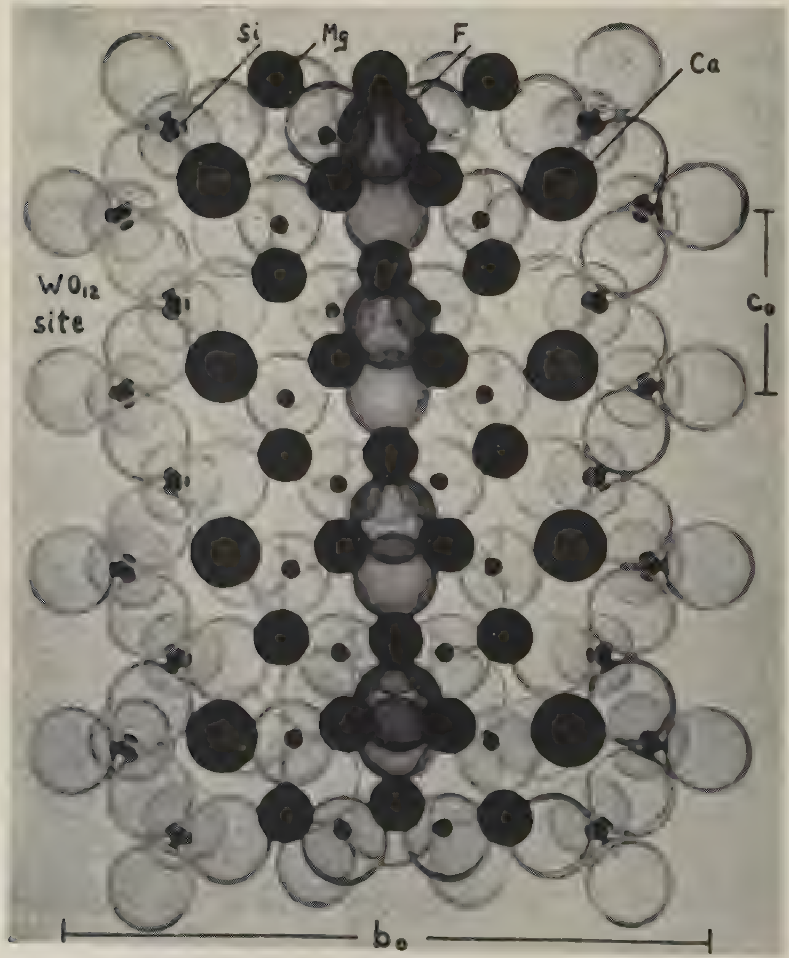

FIG. 1. Plastic-ball model (8) of a portion of the fluor-termolite structure, with $[d_{100}]$ perpendicular to the plane of the figure.

DISCUSSION

A model of a portion of the fluor-tremolite structure, as derived by Warren (7), is depicted in Fig. 1 to supplement the following discussion.

In richterite, $Na(CaNa)Mg_5(Si_4O_{11})_2F_2$, the substitution of 2 Na^+ for 1 Ca^{++} presents two geometrical possibilities for the sites occupied by these cations. Specifically, 1 Na^+ can fill the 12-fold vacant sites known to exist in tremolite (environment similar to the 12-fold positions in mica), while the remaining Na^+ proxies for Ca^{++} in 8-fold coordination. On the other hand, both Na^+ ions may replace Ca^{++} in the (XO_8) positions, with Ca^{++} occupying the (WO_{12}) vacant sites. In tremolite, where the Ca^{++} ions are more or less free to choose between 12- and 8-fold coordination, the latter is preferred, although in calcium phlogopite, $Ca_2Mg_6(Si_3AlO_{10})_2F_4$, where no such option exists, Ca^{++} does occupy the position of 12-fold coordination. Thus it would seem that in the particular structural environment presented by the tremolite arrangement, Ca^{++} is more stable in the (XO_8) position. Since the structural environment of richterite does not differ radically from that of tremolite, it seems logical to assume that, where possible, Ca^{++} will again seek positions of 8-fold coordination. Thus it is indicated that Na^+ occupies the (WO_{12}) vacant sites, and the (XO_8) positions are shared by both Na^+ and Ca^{++}. This double coordination of Na^+ is not unusual, as shown by eckermannite, $NaNa_2Mg_4Al(Si_4O_{11})_2(OH,F)_2$, where the (WO_{12}) and (XO_8) positions are filled by this cation.

TABLE 9. MONOCLINIC CELL DIMENSIONS OF SYNTHETIC FLUOR-AMPHIBOLES*

	Tremolite	Richterite	Edenite	Boron edenite
a_0	9.781 Å	9.823	9.847	9.807
b_0	18.007	17.957	18.004	17.957
c_0	5.267	5.268	5.282	5.266
β	75°29′	75°40′	75°10′	75°33′
Calculated Density	3.021 g/cm³	3.035	3.077	3.042

* Maximum errors are as follows: a_0, ±0.005; b_0, ±0.004; c_0, ±0.006; β, ±5′; calculated density (D_x), ±0.006.

The change in unit-cell dimensions between tremolite and richterite, as shown in Table 9, can be explained by either of the above assumptions. Both would result in an increased a dimension because of filling of the vacant sites, since $[d_{100}]$ parallels the principal axis of the (WO_{12}) coordination polyhedron. With the limited data available, the contraction along b can be ascribed to substitution of a slightly smaller ion (Na^+ for

Ca^{++}) in positions between the double chains. Regardless of the actual location of the Na^+ and Ca^{++} ions, no noticeable change in the *c* direction would result, as the latter parallels the elogation of the Si_4O_{11} chains and is essenitally uninfluenced by the occupants of the (WO_{12}) and (XO_8) positions. Knowledge of the cell dimensions of fluor-eckermannite and various richterites, especially those in which Mn^{++}, Ba^{++}, or Sr^{++} replace Ca^{++}, might resolve this question without recourse to a detailed structural analysis.

Edenite, $NaCa_2Mg_5(Si_{3.5}Al_{0.5}O_{11})_2F_2$, is derived from tremolite by substituting one Al^{+3} for Si^{+4} in tetrahedral coordination and restoring electrical neutrality by filling the (WO_{12}) sites with Na^+. In boron edenite, $NaCa_2Mg_5(Si_{3.5}B_{0.5}O_{11})_2F_2$, B^{+3} replaces Al^{+3} in the (ZO_4) positions. As with richterite, filling of the 12-fold sites in both edenites increases the *a* dimension relative to that observed in tremolite (cf. Table 9). This direction is also influenced by the substitution in 4-fold coordination. Thus the *a* dimension of aluminum edenite is larger than that of boron edenite, owing to the larger $(AlO_4)^{-5}$ grouping. It was expected that this difference in tetrahedron size between $(AlO_4)^{-5}$ and $(BO_4)^{-5}$ would also be reflected in the *b* direction, with aluminum edenite exhibiting the larger *b* dimension. The observed data bear out this expectation. When compared with fluor-tremolite, however, the *b* dimension of aluminum edenite remains essentially the same. This may be due either to a cushioning effect along *b* (perpendicular to the direction of the double chains) or to a distortion of the $(AlO_4)^{-5}$ grouping, which would not be unexpected with a trivalent ion in 4-fold coordination.

The *c* dimension of aluminum edenite is increased relative to that of tremolite owing to the effect of the larger $(AlO_4)^{-5}$ grouping on the direction of the double chains. In boron edenite a contraction (relative to tremolite) was expected along *c*, because of the probable smaller size of the $(BO_4)^{-5}$ grouping in comparison to $(SiO_4)^{-4}$.* This contraction, however, did not materialize, which intimates a distortion on the $(BO_4)^{-5}$ tetrahedron. Such a distortion would be in keeping with the relative ease of polarization of this group. The indicated distortions of both the $(AlO_4)^{-5}$ and $(BO_4)^{-5}$ groups are such that the tetrahedra seem attenuated (relative to *b*) along the *c* direction.

In the discussion of the fluor-richterite composition, certain isomorphic substitutions were suggested as offering promise in correlating unit-cell dimensions with ionic location. Continuing in this vein, the effect of polarization of the tetrahedra could be clarified by the synthesis and analysis of amphiboles and micas in which various cations, such as Be^{++}, Ge^{+4}, and V^{+3}, substitute for Si^{+4}. In a number of instances such compositions have been prepared in this laboratory, but samples pure enough for investigation have not been obtained. Likewise, additional data are needed to understand fully the effect of the replacement of $(OH)^-$ by F^-, (10) which is basic to the study of fluor-silicates.

---

* Analogous to the relative sizes of the $(BO_4)^{-5}$ and $(SiO_4)^{-4}$ tetrahedra in danburite, $CaB_2Si_2O_8$(9).

When such data become available, it may be possible to comprehend the relationships existing among the many layered and allied silicate minerals. This, in turn, by clarifying the directional distribution of bond strengths, especially those perpendicular to the layers or chains, would shed light on the ultimate problems of fibrosity and flexibility and their relation to crystal structure.

Acknowledgments

The authors are indebted to their associates in the Electrotechnical Laboratory who have contributed to this investigation: to H. R. Shell and R. L. Craig for the chemical analyses; to M. V. Denny for the optical determinations and the photograph; to Mrs. G. M. Huff for many of the calculations involved in the cell dimension determinations; and to R. A. Hatch for his critical review and helpful suggestions.

References

1. Comeforo, J. E., Eitel, Wilhelm, and Hatch, R. A. (1954), Synthetic asbestos investigations, III: The effect of isomorphic substitutions and fluoride concentration on the synthesis of fluor-amphiboles: To be published as *U. S. Bur. Mines. Rept. Invest.*
2. Comeforo, J. E. and Kohn, J. A., (1954), Synthetic asbestos investigations, I: Study of synthetic fluor-tremolite: *Am. Mineral.*, **39,** 537–548.
3. Larsen, E. S. (1942), Alkalic rocks of Iron Hill, Gunnison County, Colo.: *U. S. Geol. Surv. Prof. Paper* **197A,** 64 pp.
4. Palache, C. (1935), The minerals of Franklin and Sterling Hill, Sussex County, New Jersey: *U. S. Geol. Surv. Prof. Paper* **180,** 135 pp. (particularly p. 73).
5. Donnay, Gabrielle, and Donnay, J. D. H. (1952), The symmetry change in the high-temperature alkali-feldspar series: *Am. J. Sci., Bowen Vol.*, 115–132 (particularly p. 118).
6. (1944), Internationale Tabellen zur Bestimmung von Kristallstrukturen: Gebrüder Borntraeger, Berlin, vol. II, revised ed., 454.
7. Warren, B. E. (1929), The structure of tremolite, $H_2Ca_2Mg_5(SiO_3)_8$: *Z. Krist.*, **72,** 44.
8. Hatch, R. A., Comeforo, J. E., and Pace, N. A. (1952), Transparent, plastic-ball, crystal structure models: *Am. Mineral.*, **37,** 58–67.
9. Hermann, C., et al (1937), Strukturbericht, vol. II (1928–1932), 153–155.
10. Kohn, J. A., and Hatch, R. A. (1955), Synthetic mica investigations, VI: *X*-ray and optical data on synthetic fluor-phlogopite: *Am. Mineral.*, **40,** 10–21.

Manuscript received May 20, 1954.

DIFFERENTIAL THERMAL ANALYSIS AND CELL DIMENSIONS OF SOME NATURAL MAGNETITES*

E. R. Schmidt and F. H. S. Vermaas,
Union Geological Survey, Pretoria, South Africa.

Abstract

The *DTA* curve of magnetite is characterized by two exothermic peaks.

X-ray examination of the products obtained by differential thermal analysis showed that both exothermic reactions are caused by oxidation of ferrous iron. The intensity of the first peak decreases with increasing particle size indicating that the intensity of the first peak is directly proportional to the total surface area of the particles.

The first reaction is caused by the oxidation of Fe^{2+} on the surface of the particles resulting in the formation of a protective film of Fe_2O_3 around the particles. The second reaction is caused by the oxidation of the remaining magnetite by diffusion of oxygen into the magnetite structure after the protective film of Fe_2O_3 had become porous by recrystallization of the Fe_2O_3 at higher temperatures. It appears that the transition from ferromagnetism to paramagnetism promotes the diffusion of oxygen into the lattice as the second exothermic peak follows the transition temperature, (Curie point) immediately.

Some new lattice measurements of magnetite are also presented and an attempt was made to correlate cell-edge dimensions with magnesium content. There seems to be a tendency for the cell-edge to decrease with an increase in magnesium content.

I. Introduction

In a general survey of the thermal behaviour of various minerals by means of differential thermal analysis it was found that magnetite gave a very distinctive curve showing two exothermic reactions.

In an attempt to interpret this interesting phenomenon, the effect of particle size on the differential thermal curve was determined. *X*-ray determinations were also made of the lattice parameters (a_0) of the unheated magnetites as well as after heating to a temperature where the first reaction had stopped but before the second one began. The resulting data provided a basis for a satisfactory explanation of the two reactions.

II. Description of Magnetite Samples

Five magnetite samples from the Transvaal were investigated as well as the classical material from Mineville, U.S.A. They may be described as follows:

(*a*) *Sibasa, Zoutpansberg District.* Geological associations unknown.

(*b*) *de Roodepoort 67, Ermelo District.* Material from this locality was described by Wagner (1) as bedded magnetic iron ore which is interstratified with sandstones and shales belonging to the Middle Ecca Series of the Karroo System (Carboniferous). These rocks are intruded by sills of dolerite which have metamorphosed the ore as well as the associated rocks. The ore consists of a finely granular aggregate of magnetite accompanied by secondary limonite. According to Wagner it is probable that the ore was originally a bedded sideritic ironstone.

---

* Published with the consent of the Department of Mines.

(c) *Barberton Chrysotile Mine, Barberton.* Magnetite veins which cut the chrysotile-bearing serpentine body. Hydrothermal origin.

(d) *Witbank 59, Ermelo District.* Geological associations unknown. The sample was coarsely fibrous and is probably a pseudomorph of magnetite after an asbestiform mineral.

(e) *Phalaborwa, Phalaborwa Complex.* At the present the general opinion is that the magnetite is of magmatic origin.

(f) *Mineville, U.S.A.* U. S. Bureau of Standards, Sample No. 29*a*.

All the samples were carefully cleaned of impurities by hand picking, washing in water and by the use of a hand magnet. Microscopic examination showed that all the material used in this study was essentially free from all impurities. Tyler sieves were used for separating the various sizes.

III. DIFFERENTIAL THERMAL ANALYSIS

The *DTA* apparatus used in this investigation consisted of the following components:

1. A horizontal alundum tube furnace wound with Kanthal A wire, similar in construction to the one described by Gruver (2).
2. A Variac (General Radio Co. Type V20HM) continuously adjustable transformer used as the manual power control for the heating rate of the furnace.
3. A spotlight galvanometer (30 mm. per microampere sensitivity) for measurements of the e.m.f. from the differential thermocouple.
4. A nickel block sample holder, two inches long and one and a half inches in diameter, with two drilled cavities for holding the sample and inert material.
5. A temperature thermocouple and a differential thermocouple both made of Pt-Pt 13% Rh wire, 0.3 mm. in diameter.
6. An ordinary pyrometer for measuring the temperature of the inert material (Al_2O_3).

All samples were lightly tamped in the sample holder before the analyses. A cover was not used over the sample holder because the magnitude of the thermal reactions is suppressed considerably by its use. The heating rate used was 15° C. per minute and apart from the 50 ohms internal resistance of the galvanometer no additional external resistance was used in the circuit.

DTA curves of five magnetite samples from different localities are shown in Fig. 1. All the curves are characterized by a sharp exothermic peak at 360 to 375° C. which is followed by a broad exothermic peak beginning at 580° C. and having a varying maximum peak temperature. The intensity of the first peak varies in different samples of magnetite but the temperature of 580° C. where the second reaction begins is very characteristic for all samples examined. It was found that samples ground

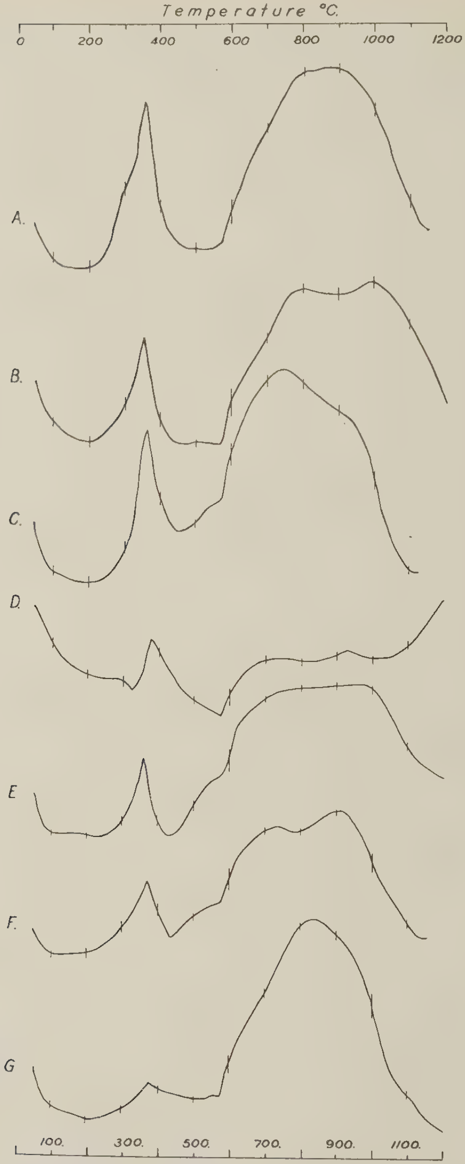

FIG. 1. *DTA* curves of magnetites from different localities. *A*. Sibasa. Grain size (−200) mesh. *B*. Sibasa, Grain size (−100) mesh. *C*. De Roodepoort. Grain size (−200) mesh. *D*. De Roodepoort. Grain size (−200) mesh, with cover on sample holder. *E*. Barberton. Grain size (−200) mesh. *F*. Witbank. Grain size (−200) mesh. *G*. Phalaborwa. Grain size (−200) mesh.

to −200 mesh gave better defined second peaks than those ground to −100 mesh. (cf. curves *A* and *B*, Fig. 1). In curve *B* there is a doubling of the second exothermic peak which is characteristic of samples of larger particle size. The phenomenon is also seen in Fig. 1 curve *F*. In this instance it is due to the fact that the sample was coarsely fibrous so that larger particles than −200 mesh were able to pass through the sieve.

In Fig. 1 curves *A* and *G* the curve is horizontal between the two exothermic reactions but in Fig. 1 curves *C*, *E* and *F* however, the second reaction starts immediately after the first one. In all the curves the second reaction is greatly accelerated at a temperature of 580° C.

The effect of using a cover over the sample holder can be seen by comparing curves *C* and *D* in Fig. 1. In curve *D* the second exothermic reaction is nearly completely suppressed and the height of the first peak is about half of that in the curve *C*.

In Fig. 2 the effect of particle size on the *DTA* curves are illustrated. A constant weight of 6.5 gms. were used for all the examples. The height of the first exothermic peak decreases with an increase in particle size, and that of the second peak increases with an increase in particle size. There is also a tendency for the second peak to split into two peaks in samples coarser than 325 mesh especially when the particle size range is kept in narrow limits. (cf. Fig. 1, *E* and Fig. 2, *C*). Curve *F*, Fig. 2 was obtained on a standard magnetite sample from Mineville, U.S.A., of the National Bureau of Standards of the U.S. Department of Commerce (Sample 29*a*). It was included in Fig. 2 to illustrate the effect of an extremely small particle size on the *DTA* curve. The intensity of the first peak is greater and that of the second peak smaller than in all the other curves in Fig. 2.

IV. The Oxidation of Natural Magnetite

Both exothermic reactions as recorded by *DTA* analysis are due to the oxidation of ferrous iron in the magnetite structure. This was established as follows:

(*a*) *X*-ray photographs of magnetite heated until just beyond the first peak (±510° C.), revealed that it consisted of a mixture of magnetite and hematite. The relative intensities of the magnetite reflections remained the same, although the intensity of the pattern as a whole was slightly lower and the six strongest lines of hematite appeared. Lattice determinations of magnetites thus heated were identical to that of the original material.

(*b*) Magnetite of −115+150 mesh size was heated up to 980° C. under normal conditions in the differential thermal analyzer. At this temperature nitrogen was introduced into the furnace and heating continued until 1200° C. The *DTA* curve indicated that oxidation was stopped immediately after the introduction of the nitrogen. The material so obtained, when ground to −325 mesh after cooling in a nitrogen atmosphere, consisted of a mixture of magnetite and hematite and when

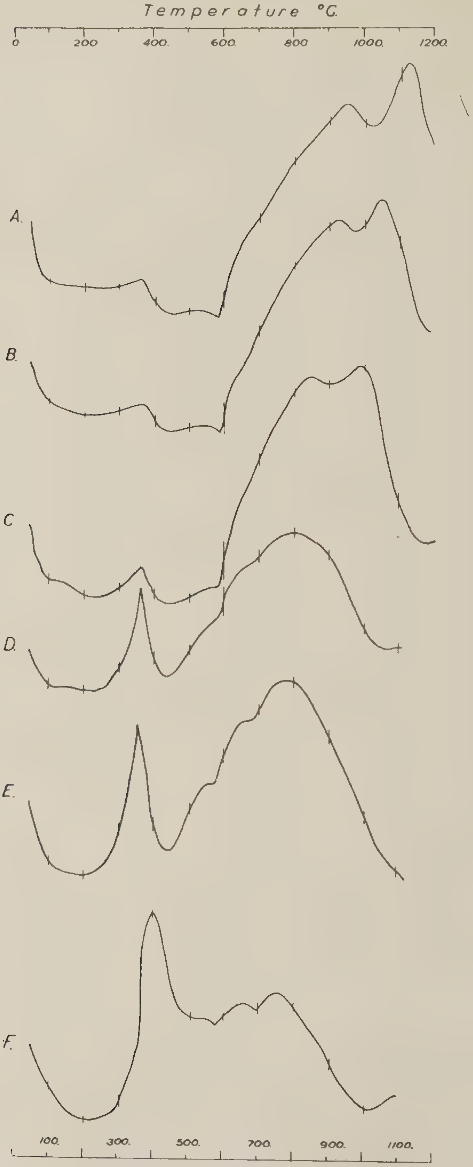

FIG. 2. *DTA* curves of magnetites showing the effect of grain size. *A*. Barberton. Grain size. (−115+150) mesh. *B*. Barberton. Grain size (−150+200) mesh. *C*. Barberton. Grain size (−200+325) mesh. *D*. Barberton. Grain size (−325) mesh. *E*. Barberton. The smallest grain size that could be obtained by hand grinding. *F*. Mineville. Extremely fine-grained; particles even smaller than *E*.

subjected to differential thermal analysis, again showed the two characteristic peaks for magnetite although these were less intense.

(*c*) When magnetite was heated in an oxidizing atmosphere until the *DTA* curve showed that the second reaction was complete, no magnetite was detected in the oxidized material. In Fig. 2 curves *A* and *B* this reaction had not yet been completed at 1200° C. (due to the large particle size). In these two cases magnetite was again detected in the end products.

(*d*) The formation of gamma Fe_2O_3 under the heating conditions used can be eliminated as this phase was never detected at any stage.

A. Interpretation of the first exothermic reaction

Gheith (3) recently ascribed the first sharp exothermic peak to the recrystallization of the extremely fine magnetite particles present in his samples. He mentions that such a recrystallization is due to the "high force of crystallization" of magnetite. Such an interpretation is not in accordance with the fact that *x*-ray examination of an extremely fine magnetite powder revealed a very high order of crystallization, the photographs showing no line broadening. Furthermore, the presence of hematite in material heated beyond the first peak is regarded as ample evidence that the first peak represents only an oxidation reaction.

When magnetite was heated to beyond the first peak (510° C) and then again rerun, the *DTA* curve showed only the second peak. On the other hand, when magnetite previously heated to beyond the first peak was ground and rerun the first peak was again recorded on the curve. This fact is significant because it indicates that the first reaction is arrested by the formation of a protective film of hematite around the magnetite particles. Furthermore, the observation that the intensity of the first peak increases with decreasing particle size is in accordance with the fact that in a constant weight of material the total surface area increases with decreasing particle size. The intensity of the first peak is therefore directly proportional to the total surface area of the particles. On the above mentioned evidence the authors have interpreted the first peak on the *DTA* curve as follows:

The *first* exothermic reaction is caused by the oxidation of Fe^{2+} on the surface of the particles resulting in the formation of a thin protective film of hematite around a core of unaltered magnetite.

B. Interpretation of the second exothermic reaction

The temperature of 580° C. where the second reaction begins, remains absolutely constant for all the samples examined and is preceded by a very small endothermic peak, the intensity of which is depressed by the second exothermic reaction. It is interesting to note that the so-called Curie point, where the ferromagnetism of magnetite changes to paramagnetism occurs at 590° C. (4).

In order to investigate whether the change from ferromagnetism to paramagnetism could be detected on the differential thermal analyzer, a sample of magnetite was examined in an atmosphere of nitrogen. The curve indicated that no oxidation took place; the two exothermic peaks were absent but a well defined endothermic peak at 585° C. was recorded. On cooling, this peak was again recorded at 585°C. (now exothermic) indicating that a reversible transition had taken place corresponding to a change from ferromagnetism to paramagnetism and vice versa. According to Mason (4) these changes are not accompanied by any structural alteration. It appears that the transition from ferromagnetism to paramagnetism promotes the diffusion of oxygen into the lattice as the second exothermic reaction follows the transition temperature immediately. The second peak on the *DTA* curve has therefore been interpreted as follows:

The *second* exothermic reaction is caused by the oxidation of the remaining magnetite at a temperature where the diffusion of oxygen into the magnetite structure becomes possible after the protective film of hematite had become porous by recrystallization at higher temperatures. However, the most important factor governing the second oxidation reaction is that the process of diffusion of oxygen into the lattice is promoted when a transition from ferromagnetism to paramagnetism takes place. By such a process it is understood that the oxygen diffuses into the lattice forming Fe_2O_3 immediately. Oxidation therefore, progresses from the surface of the grains towards the core. The intensity of the second peak increases with increasing particle size because the intensity of the first peak decreases with increasing particle size so that relatively more magnetite remains unoxidized after the first reaction is completed. The tendency for the second peak to split into two peaks in samples coarser than 325 mesh is difficult to explain and needs further investigation.

V. X-RAY EXAMINATION

X-ray powder diffraction patterns were obtained by using 57.3 mm. diameter cameras in which the film is mounted according to the Straumanis method. Unfiltered cobalt radiation was used. The method of mounting the samples in the camera and measuring the films is that usually employed in this Laboratory (5) and (6).

Values for the lattice parameter (a_0), calculated from the high angle lines were obtained by the graphical extrapolation method described by Henry, Lipson and Wooster (7). In this method the different values of the cell-edge (a) are plotted against the function

$$\frac{1}{2} \times \left(\frac{\cos^2 \theta}{\sin \theta} + \frac{\cos^2 \theta}{\theta} \right)$$

and the value for a_0 recorded where this function is equal to 0.

The results of lattice measurements are listed in Table 1.

TABLE 1. LATTICE MEASUREMENTS OF MAGNETITES

Locality	a_0 (Å)
Sibasa, Zoutpansberg district	8.394 (±0.001)
de Roodepoort 67, Ermelo district	8.389 (±0.003)
Barberton Chrysotile Mine, Barberton	8.398 (±0.001)
Witbank 59, Ermelo district	8.386 (±0.001)
Phalaborwa, Letaba district	8.387 (±0.002)
Mineville, U.S.A.	8.392 (±0.001)

In the literature measurements of the length of the cell-edge vary from 8.36 Å to 8.42 Å (4). The most recent values for artificial magnetite are probably those published by Tombs and Rooksby (8) and Abrahams and Calhoun (9). All these authors give a value of 8.394 Å.

The relatively large variation of the lattice parameters of the magnetites examined, suggested a variation of the cube-edge due to a variation in chemical composition. Qualitative spectrographic analyses showed that the only elements likely to affect the size of the unit-cell are aluminum, magnesium, and in the Witbank sample, also nickel.

Quantitative spectrographic analyses of magnesium and aluminum were carried out according to the Jaycox Method (10). The nickel content of the Witbank sample was determined chemically. FeO determinations varied between 25% and 28% indicating an excess of Fe_2O_3 of approximately the same order for all the samples examined. No definite relationship could be established between FeO content and unit-cell size.

In Table 2 spectrochemical and chemical data are given for the magnetites examined:

TABLE 2. SPECTROCHEMICAL AND CHEMICAL DATA OF MAGNETITES

Locality	MgO%	Al_2O_3%	NiO%
Sibasa	1.48	0.38	—
de Roodepoort	1.73	0.45	—
Barberton	0.67	0.09	—
Witbank	1.05	0.07	1.76*
Phalaborwa	2.55	0.75	—
Mineville†	0.095	0.46	—

* Analyst: A. Kruger, Division of Chemical Services, Pretoria.

† U.S. Bureau of Standards Analysis (Sample 29*a*).

In Fig. 3 values for a_0 are plotted against the molecular proportion of MgO; for the Witbank sample the molecular proportion of (MgO+NiO) is used. The ionic radii of Mg^{2+} and Ni^{2+} are approximately the same and their influence on the size of the lattice parameter will therefore be of similar magnitude.

The replacement of Fe^{2+} (ionic radius 0.74 Å) by Mg^{2+} and/or Ni^{2+} (ionic radii 0.66 and 0.69 Å resp.) causes a contraction of the unit-cell of magnetite. Figure 3 indicates such a tendency, although it is obvious that much more results are needed to establish the exact magnitude of this shrinkage. No satisfactory explanation can be offered for the anomalous position of the Mineville sample on the curve.

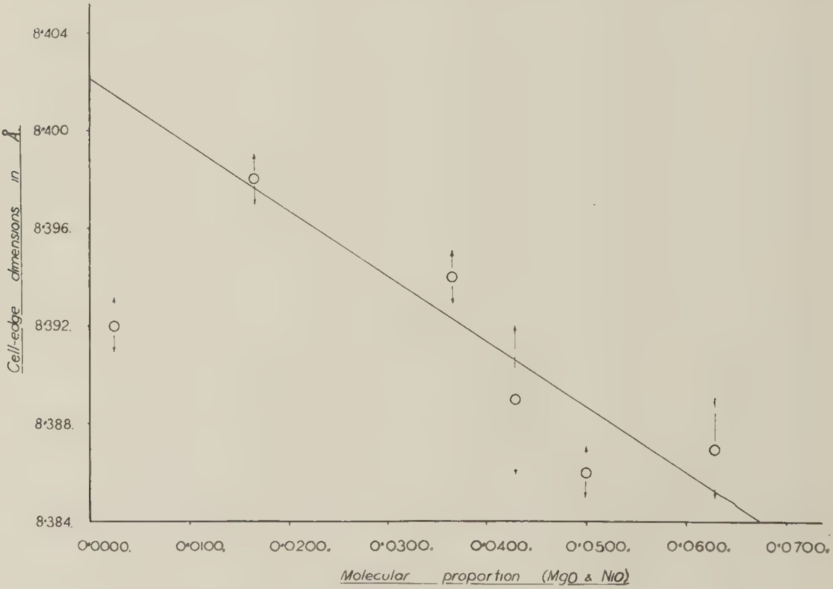

FIG. 3. Graphical representation of the variation of the cell-edge (a_0) with the molecular proportion of (MgO+NiO).

In compiling the curve, the possible effects of an excess of Fe_2O_3, or a replacement of Fe^{3+} by Al^{3+} on the unit-cell dimensions, were not considered because FeO-determinations on all samples indicated an excess of Fe_2O_3 of approximately the same order and a very low alumina content.

If the shrinkage of the unit-cell as indicated by the curve is correct then a magnesium-free magnetite should have a cube-edge of 8.402 Å (±0.002). The corresponding calculated specific gravity of such a magnetite is 5.187.

VI. CONCLUSIONS

1. A differential thermal analysis and *x*-ray study of magnetite indicated that on heating, magnetite is oxidized in two distinct stages.
2. The first reaction is ascribed to the oxidation of Fe^{2+} on the surface of the magnetite particles.
3. The second reaction is ascribed to the oxidation of the magnetite particles by a process of diffusion of oxygen into the magnetite structure.
4. Some new precision lattice determinations of natural magnetites are given. There seems to be a tendency for the size of the unit-cell of magnetite to decrease with a replacement of Fe^{2+} by Mg^{2+}.

ACKNOWLEDGMENTS

The authors wish to thank Dr. R. Haul of the South African Council for Scientific and Industrial Research, Pretoria, for the interest shown in the work as well as for reviewing the manuscript. The National Chemical Laboratory of the C.S.I.R. is gratefully acknowledged for the FeO determinations and Mr. H. D. Russell of this Laboratory for the quantitative spectrographic analyses.

REFERENCES

1. WAGNER, P. A., The iron deposits of the Union of South Africa: *Geol. Surv. Memoir No.* **26** (1928).
2. GRUVER, R. M., Precision method of thermal analysis: *Jour. Am. Ceram. Soc.*, **31**, No. 12, 323–328 (1948).
3. GHEITH, M. A., Differential thermal analysis of certain iron oxides and oxide hydrates: *Am. Jour. Sci.*, **250**, 677–695 (1952).
4. MASON, B., Mineralogical aspects of the system FeO-Fe_2O_3-MnO-Mn_2O_3: *Geol. För. Förh. Stockholm*, **65**, 97–180 (1943).
5. WASSERSTEIN, B., Precision lattice measurements of galena: *Am. Mineral.*, **36**, 102–115 (1951).
6. VERMAAS, F. H. S., South African scheelites and an *x*-ray method for determining members of the scheelite-powellite series: *Am. Mineral.*, **37**, 719–735 (1952).
7. HENRY, N. F. M., LIPSON, H., AND WOOSTER, W. A., The interpretation of *x*-ray diffraction photographs: Macmillan and Co. Ltd., London (1951).
8. TOMBS, N. C., AND ROOKSBY, H. P., Structure transition and antiferromagnetism in magnetite: *Acta Cryst.*, **4**, Pt. 5, 474–475 (1951).
9. ABRAHAMS, S. C., AND CALHOUN, B. A., Low temperature transition in magnetite: *Acta Cryst.*, **6**, Pt. 1., 105–106 (1953).
10. JAYCOX, E. K., Spectrochemical analysis of ceramics and other non-metallic materials: *Jour. Opt. Soc. Am.*, **37**, 162 (1947).

Manuscript received May 7, 1954.

PRELIMINARY REPORT ON INVESTIGATIONS OF MINERALS OF COLUMBIUM AND TANTALUM AND OF CERTAIN ASSOCIATED MINERALS

Richard W. Hutchinson,* *University of Wisconsin, Madison, Wisconsin.*

Abstract

This paper is a progress report of an investigation of columbium and tantalum minerals. The rotation properties of the columbite-tantalite series have been investigated in detail and the results and their application to identification are discussed. The optical properties of some other columbium-tantalum minerals including yttrotantalite, bismutotantalite, stibiotantalite, tapiolite and ilmenorutile are also discussed so far as they have been determined. The relationship between the orthorhombic columbite-tantalite series and the tetragonal mossite-tapiolite series is critically examined. All specimens of ilmenorutile so far studied were found to be intergrowths of two minerals, columbite and rutile. Related features of this intergrowth are discussed. Some optical properties of minerals commonly associated with columbium-tantalum minerals have also been determined and have been of value in the investigation. Data for these minerals are presented.

Introduction

An investigation of the opaque minerals of columbium and tantalum was begun in 1952 in the Laboratory of Economic Geology at the University of Wisconsin. This report summarizes the results of the first year's investigations, and although research is not yet complete, certain interesting features have been found that warrant publication of a progress report.

The identification of columbium and tantalum minerals is a problem of many years' standing. The minerals can be distinguished by a combination of *x*-ray and chemical techniques, but these methods are time-consuming and are not readily applicable to the identification of small grains, or of mixtures of columbium-tantalum minerals with other opaque minerals. The present investigation was designed especially to obtain information regarding the optical properties of the columbium-tantalum minerals in the hope that these would facilitate identification. Particular attention was paid to their rotation properties, which were unknown yet seemed to offer promise of being useful in identification. It was hoped that if the rotation properties (5)[1] of members of the isomorphous columbite-tantalite series were functions of the Cb-Ta content, it would be possible to determine the $Cb_2O_5:Ta_2O_5$ ratio of a given sample by optical methods.

---

* Present address, American Metal Co. of Canada, Ltd., 25 Adelaide St. W., Toronto, Ontario, Canada.

[1] Numbers in parentheses refer to the bibliography at the end of the paper.

Of the minerals studied, tapiolite and ilmenorutile proved to be particularly interesting, and they are discussed in some detail in this report. Study of tapiolite led to an examination of the relationships between the tetragonal mossite-tapiolite series and the orthorhombic columbite-tantalite series, and certain tentative conclusions are presented. Ilmenorutile in our specimens proved to be an intergrowth of columbite and rutile. This intergrowth is described and its origin is discussed.

During the investigation it became apparent that optical information was needed for certain minerals that are commonly associated with the columbium-tantalum minerals. Studies of these minerals were made and the results are also presented in this report.

Suitable samples of the various columbium-tantalum minerals were difficult to obtain, and this factor was one of the major problems of the investigation. All available samples required checking by means of *x*-ray diffraction techniques, and in some cases chemical determinations had to be procured.

ACKNOWLEDGMENTS

The investigation was made possible by the grant to the writer of the Union Carbide and Carbon Fellowship for 1952–53, and this support is gratefully acknowledged. Thanks are due to Mr. H. Rush Spedden of Union Carbide and Carbon Research Laboratories, Inc., at Niagara Falls, New York, who furnished specimens for study and arranged for the chemical determinations. These determinations were carried out under the supervision of Dr. W. D. Forgeng, of the same organization, to whom sincere thanks are also extended.

Dr. Cornelius Hurlbut, of Harvard University, assisted the writer with precise specific gravity determinations, and Dr. Clifford Frondel, of the same University, furnished several specimens from the collections under his care. Mr. J. G. Farmer of the Electrometallurgical Company at Niagara Falls also supplied material for study.

Mr. H. E. Abendroth and Mr. E. R. Bottoms assisted in the preparation of polished surfaces.

Mr. T. Hurst and Mr. C. L. Hall of the African Manganese Co., Ltd., in London, England, and Mr. J. D. Pollett, Director of the Geological Survey of Sierra Leone, supplied information concerning the occurrences of ilmenorutile in Sierra Leone. Mr. F. A. Behr of the North American Philips Co., Inc., at Mount Vernon, New York, furnished data regarding the sensitivity and accuracy of the chemical determinations. Sincere thanks are extended to these gentlemen for their assistance.

The investigation was carried out in the Laboratory of Economic Geol-

ogy at the University of Wisconsin under the supervision of Dr. E. N. Cameron. Dr. Cameron has furnished much of the material studied, has helped the writer during the investigation, and has given helpful advice and criticism in the preparation of this report. Sincere thanks are also due to Mr. S. W. Bailey, of the University of Wisconsion Geology Department, for his assistance with the *x*-ray determinations which were essential to the study.

Columbite-Tantalite and Related Minerals

Methods and Scope of the Investigation

Twenty-nine specimens of columbite-tantalite were obtained for study of the optical properties of the orthorhombic series (Fe,Mn)-Cb_2O_6-(Fe, Mn)Ta_2O_6. For each crystal or specimen permitting it, three oriented (critical) sections were cut, mounted in bakelite, and polished. Optical studies of all these surfaces were completed in the manner outlined by Cameron *et al.* (5, 6). The rotation properties of these specimens as determined are summarized in Table 1. In order to relate the optical properties to chemical composition, chemical analyses of some of the specimens were obtained.

The chemical determinations were done by *x*-ray fluorescence analysis and the results, expressed in terms of oxides of the elements, are shown in Table 2. The lower sensitivity ranges of this analytical method for the elements shown in the analyses are as follows,

	Per Cent
Cb	0.05 to 0.1
Ta	0.1 to 0.2
Fe	0.01 to 0.05
Mn	0.01 to 0.1
Sn	0.2
Zr	0.02 to 0.05
Y	0.03 to 0.05
W	2.0
Ti	5.0

The notation *n.d.* on Table 2 indicates that titanium was present in amounts less than the sensitivity for this element.

The accuracies of the quantitative results shown in Table 2 can be expressed in per cent of the amounts of the elements present (% P.E.). For the elements that are present in amounts near the sensitivity limits shown above, accuracies of ±10% P.E. may be expected. For the elements present in higher concentrations (Cb, Ta, Fe and Mn), the determinations should be accurate to ±1% P.E.

The compositional range covered by the specimens studied is shown

TABLE 1. ROTATION PROPERTIES OF COLUMBITE-TANTALITE

Univ. Wis. Ref. No.	Mineral Designation and Locality	S.G.	DR_r	A_r			DA_r	Amount of Dispersion
				Red	White	Blue		
50-50- 1	Columbite, E. E. Smith Mine, Alexandria, New Hampshire	5.789	ess. nil	1.5	1.3	.9	$r>v$, distinct	.6
50-10- 1	Tantalite,* Etta Mine, Keystone, South Dakota	7.041	ess. nil	1.5	1.4	1.1	$r>v$, weak	.4
50-12- 3	Columbite-tantalite,* Rough and Ready Mine, Tinton, South Dakota	6.392	ess. nil	1.5	1.4	1.1	$r>v$, weak	.4
50-10-11	Columbite-tantalite, Peerless Mine, Keystone, South Dakota	5.979	ess. nil	1.5	1.3	.9	$r>v$, distinct	.6
51-27- 1	Columbite,* Van der Made Claim, Erongo Schlucht, S. W. Africa	5.607	ess. nil	1.5	1.5	1.3	ess. nil	.2
51-27- 8	Columbite,* Van der Made Main Pegmatite, Erongo Schlucht, S. W. Africa	5.660	ess. nil	1.6	1.5	1.3	$r>v$, very weak	.3
51-32- 1	Columbite, Krom River Beryl Deposit, Umeis Farm, Warmbad District, S. W. Africa	5.503	ess. nil	1.5	1.3	1.0	$r>v$, weak	.5
51-30- 3	Columbite, Spencer #11 Claim, Farm Daawib East, S. W. Africa	5.732	ess. nil	1.5	1.4	1.0	$r>v$, weak	.5
50-51- 1	Columbite,* DeStaffany Ta-Be Mine, Great Slave Lake, N.W.T., Canada	5.808	ess. nil	1.5	1.3	.8	$r>v$, strong	.7
50-52- 1	Columbite,* Quartz Creek Pegmatite District, Gunnison County, Colorado	5.691	ess. nil	1.6	1.4	.9	$r>v$, strong	.7
53-85- 2	Columbite, Naipa Pegmatite, Alto Ligonha, Portuguese East Africa	—	ess. nil	1.3	1.2	.9	$r>v$, weak	.4
53-85- 4	Columbite, Marige Pegmatite, Alto Ligonha, Portuguese East Africa	—	ess. nil	1.3	1.2	.8	$r>v$, weak	.5
53-85- 1	Columbite, Muiane Pegmatite, Alto Ligonha, Portuguese East Africa	—	ess. nil	1.4	1.3	.9	$r>v$, distinct	.5
53-85- 3	Columbite, Nahora Pegmatite, Alto Ligonha, Portuguese East Africa	—	ess. nil	1.3	1.2	.8	$r>v$, weak	.4
53-80- 1	Columbite, Mirruccu Area, Alto Ligonha, Portuguese East Africa	—	ess. nil	1.4	1.3	.9	$r>v$, strong	.6

TABLE 1—*(continued)*

Univ. Wis. Ref. No.	Mineral Designation and Locality	S.G.	DR_r	A_r			DA_r	Amount of Dispersion
				Red	White	Blue		
53-13- 1	Columbite, Umeis Farm, S. W. Africa	—	ess. nil	1.3	1.2	.9	$r>v$, weak	.4
49-11-13	Tantalite,* Old Mike Pegmatite, Custer County, South Dakota	—	ess. nil	1.3	1.2	.9	$r>v$, weak	.4
53- 8- 1	Yttrotantalite,* Renders Claim, Bikita, Rhodesia	5.85	none, sample is isotropic, metamict with internal reflections					
53-10- 1	Yttrotantalite, Johnson Claim, Bikita, Rhodesia		none, sample is isotropic, metamict with internal reflections					
53-11- 1	Columbite, Warmbad District, S. W. Africa	—	ess. nil	1.0	.9	.7	$r>v$, weak	.3
53-83- 1	Columbite, Lot 26136, Union Carbide	—	ess. nil	1.4	1.3	1.1	$r>v$, weak	.3
53-83- 3	Columbite, Lot 6424, Union Carbide	—	ess. nil	1.5	1.3	.9	$r>v$, strong	.6
53-83- 2	Columbite, Lot 6262, Union Carbide	—	ess. nil	1.3	1.2	.9	$r>v$, weak	.4
53-83- 4	Columbite, Lot 6425, Union Carbide	—	ess. nil	1.5	1.4	.9	$r>v$, strong	.6
53-84- 3	Manganotantalite, Wodgina, West Australia	—	ess. nil	1.1	1.0	.9	ess. nil	.2
53-84- 4	Manganotantalite, Pilbara, West Australia	—	ess. nil	.7	.6	?	ess. nil	?
53-84- 1	Bismutotantalite, Uganda	—	ess. nil	?	small	?	$r>v$, distinct	?
53-84- 2	Stibiotantalite, Mesa Verde, California	—	ess. nil	1.3	1.2	.8	$r>v$, distinct	.4
H.L.-16	Columbite, Hidden Lake, N.W.T., Canada	—	ess. nil	1.5	1.4	.9	$r>v$, strong	.6

* Indicates specimen has been analyzed and is listed in Table 2.

TABLE 2. ANALYSES OF SPECIMENS

Univ. Wis. Ref. No.	Mineral	Locality	S.G.	Per Cent Composition by Elemental Oxides											
				Cb_2O_5	Ta_2O_5	Cb:Ta ratio	FeO	MnO	Fe:Mn ratio	SnO_2	WO_3	ZrO_2	Y_2O_3	Rare Earths	TiO_2
50-52-1	Columbite	Quartz Creek Pegmatite District, Gunnison County, Colorado	5.691	73	10	7.30:1	9.5	6	1.58:1	—	<2	—	—	—	n.d.
51-27-8	Columbite	Van der Made Main Pegmatite, Erongo Schlucht, Southwest Africa	5.660	70	10	7.00:1	7.5	9	1:1.20		<2	—	—	—	n.d.
50-51-1	Columbite	DeStaffany Ta-Be Mine, Great Slave Lake, N.W.T., Canada	5.808	59	23	2.56:1	11	4	2.75:1	—	<2	tr.	—	—	n.d.
51-27-1	Columbite	Van der Made Claim, Erongo Schlucht, Southwest Africa	5.607	56	26	2.15:1	—	16	zero	—	<2	—	—	—	n.d.
50-12-3	Columbite-tantalite	Rough and Ready Mine, Tinton, South Dakota	6.392	37	45	1:1.22	6	7	1:1.11	—	<2	—	—	—	n.d.
50-10-1	Tantalite	Etta Mine, Keystone, South Dakota	7.041	18	63	1:3.50	5	8	1:1.60	3.0	<2	—	—	—	n.d.
49-11-13	Tantalite	Old Mike Pegmatite, Custer County, South Dakota	—	15	65	1:4.33	8.5	3.5	2.43:1	3.5	<2	tr.	—	—	n.d.
50-53-1	Tapiolite	Peg Tantalum Mine, Ross Lake, N.W.T., Canada	7.550	9	73	1:8.11	14	.7	20.0:1	—	<2	—	—	—	n.d.
53- 8-1	Yttro-tantalite	Renders Claim,* Bikita, Rhodesia	5.85	1	56	1:56	5	1	5:1	2	<2	tr.	12	5–10	<6

* In addition to listed oxides this specimen contains U_3O_8.

by the analyses. Samples approaching the theoretical end-members were most difficult to obtain. Columbite from Gunnison County, Colorado (Table 2) has a $Cb_2O_5:Ta_2O_5$ ratio of 7.3:1. Tantalite from the Old Mike pegmatite, Custer County, South Dakota has a $Cb_2O_5:Ta_2O_5$ ratio of 1:4.33. These two specimens are the nearest approaches to the end-members of the series in the material studied. The compositions of several intermediate members of the series are also listed in Table 2. It was impossible to obtain chemical determinations for all the specimens, but the samples submitted for analyses were carefully selected on the basis of specific gravities and variations in optical properties, in order to cover as wide a compositional range as possible.

A few samples of some rare varieties of tantalite, including manganese-, yttrium-, rare-earth-, antimony-, and bismuth-rich types were also obtained. Their identification was first checked, wherever possible, by *x*-ray diffraction powder photographs. Their optical properties were then investigated using oriented polished surfaces.

Difficulty in procuring specimens of these varieties of columbite-tantalite was again a problem. Only one of these samples, yttrotantalite from Bikita, Rhodesia, has been analyzed. Its composition is indicated in Table 2. Because of these difficulties, data obtained for the rare varieties of columbite-tantalite are too incomplete to justify any final conclusions, but the results of the limited studies are discussed briefly.

Rotation Properties

(*a*) Apparent Angle of Rotation in White Light

Tables 1 and 2 clearly indicate that in white light there is essentially no variation in the apparent angle of rotation in the isomorphous series columbite-tantalite, because none of the specimens studied shows significant differences in the apparent angle of rotation between Cb- and Ta-rich varieties. The angle of rotation in white light for columbite from Gunnison County, Colorado, is 1.4 degrees while the rotation angle for tantalite from the Old Mike pegmatite is 1.2 degrees. All other specimens studied also have angles of rotation that lie in the range from 1.2 to 1.5 degrees for white light in air. This variation is within the limits of experimental error (5, p. 746).

(*b*) Dispersion

Significant variations in strength, or amount, of dispersion of the apparent angle of rotation were found and are recorded in Table 1. Qualitatively the variation in strength of dispersion is shown by varying intensity of color fringes in the polarization figures of different columbite-tantalites. It was quantitatively determined by measuring the apparent angles of rotation for monochromatic red and monochromatic blue light. The difference between the two values obtained is the amount of dispersion. The amount of dispersion varies from .2 to .7 degree. This is a significant and measurable difference. Thus far, oil immersion methods have been attempted only on a limited scale, but immersion in oil of R.I. 1.515 increases the range of the variation to .3 to 1.1 degrees.

This variation is apparently not due to varying $Cb_2O_5:Ta_2O_5$ ratios, for samples of columbite-tantalite with widely varying ratios have similar dispersions. Table 2 shows that the specimen (51-27-8) from the Van der Made main pegmatite, Southwest Africa has a $Cb_2O_5:Ta_2O_5$ ratio of 7:1, while tantalite from the Etta Mine at Keystone, South Dakota, has a ratio of 1:3.5. Table 1 shows that both specimens have very similar dispersions. The analyses indicate that the amount of dispersion is related to the FeO content, or more specifically to the FeO:MnO ratio. When the ratio of FeO to MnO is high (greater than unity), the amount of dispersion tends to be high (.5 to .7 degree), and the color fringes in the polarization figure at the 45-degree position are strong. Columbite from Gunnison County, Colorado, and from Great Slave Lake in Canada are examples. Table 2 shows that both these specimens have high FeO:MnO ratios, and Table 1 shows that they have strong dispersions. One apparent exception is tantalite from the Old Mike pegmatite which has a high FeO:MnO ratio of 2.43:1 as shown in Table 2, but has only an intermediate dispersion. This discrepancy is explained, however, by the high content of tin which presumably substitutes for manganese in the sample. If the tin content is computed with manganese, the ratio (of $FeO:MnO+SnO_2$) becomes 1.2:1, and this figure is in agreement with the intermediate dispersion.

When the ratio of FeO:MnO is low (less than unity), dispersion is correspondingly weak (.2 to .4 degree) and color fringes in the polarization figure are weak or absent. Specimen 51-27-1 from the Van der Made Claim, Southwest Africa, is an excellent example. Table 2 shows that it contains essentially no iron whatever but is rich in manganese, and Table 1 records that it has essentially no dispersion. Samples in which the FeO:MnO ratio is near unity have intermediate dispersions (.4 or .5 degree). The analyzed specimen from Tinton, South Dakota, has an FeO:MnO ratio near unity, and an intermediate dispersion of .4 degree is shown for the sample in Table 1.

An independent test of this relationship was carried out on additional samples for which approximate analyses were available. It was possible to select, on the basis of strength of dispersion alone, which of these samples were FeO-rich and which were high in MnO.

Additional samples of both iron and manganese varieties are being obtained and will be studied to substantiate this relationship further. It seems probable that with additional data (especially using oil immersion) an empirical scale can be set up that will make it possible to determine the FeO:MnO ratio of a given sample from its amount of dispersion.

Conclusions

(*a*) The apparent angle of rotation does not vary significantly with composition in the columbite-tantalite series.

(*b*) The amount of dispersion in the columbite-tantalite series appears to vary with the FeO:MnO ratio. Additional samples, analyses and measurements are required to substantiate the relationship.

(*c*) Comparison of chemical analyses and specific gravities clearly shows that specific gravity alone can be used only in a general way to place a given sample in the columbite-tantalite series, because both FeO:MnO and Cb_2O_5:Ta_2O_5 ratios affect the specific gravity.

Yttrotantalite

Two specimens of yttrotantalite were obtained and studied. Optically both are noticeably different from normal tantalite. They are isotropic or very weakly anisotropic, and neither sample shows the degree of anisotropism common to normal tantalite. Internal reflections are much stronger than those usually encountered in tantalite and they interfere drastically with the determination of rotation properties.

It was suspected that both crystals were partially, or wholly, metamict in nature and perhaps radioactive. Tests with a simple Geiger counter showed that both samples are strongly radioactive. *X*-ray diffraction powder patterns of both specimens, in general, match that of yttrotantalite. In both cases, however, there are broad diffuse bands instead of sharp lines. This suggests a partial breakdown of the crystal structure.

An analysis of one of the samples was subsequently obtained and is given in Table 2. It reveals appreciable amounts of yttrium, rare-earths and uranium, thus accounting for the radioactivity and metamict properties. In polished surface the specimen is notably impure and contains tiny inclusions of other unidentified minerals. Whether these mineral impurities contain the radioactive elements disclosed by the analysis is not known.

No general conclusions are justified on the basis of the two specimens studied, but it appears that the yttrotantalite is partially metamict as indicated by Dana (9, p. 763). This could result normally from the presence of the rare-earth elements and uranium that are present in the sample. The metamict condition would explain the isotropism of the specimens in reflected light.

Bismutotantalite and Stibiotantalite

A single sample of each of these minerals was obtained and studied. Microscopic examination showed that both are impure and contain varying amounts of an unidentified mineral that appears to replace them along cracks and fissures. Stibiotantalite is semi-transparent and is softer than normal tantalite with stronger internal reflections, lower anisotropism and stronger dispersion. Bismutotantalite also is softer and has lower anisotropism and stronger internal reflections than tantalite. Thus stibiotantalite and bismutotantalite are similar to each other in optical properties in reflected light, and Dana (8, p. 697) states that for bismutotantalite, "angles show similarity to those of stibiotantalite." Since the antimony variety is semi-transparent, oriented thin sections must be prepared for the determination of its optical properties in transmitted light.

X-ray diffraction powder photographs of both samples were taken. The specimen of stibiotantalite gives a pattern that matches the *A.S.T.M.* index card for that mineral. No card is available for bismutotantalite, but its pattern resembles the pattern of stibiotantalite more closely than it does the pattern of normal tantalite. The similarity in *x*-ray patterns is also reported by Dana (9, p. 770). For the two specimens studied, the resemblance between *x*-ray powder patterns was especially close with regard to the positions of the strong lines. Weaker lines in the bismutotantalite pattern were closer in position to the corresponding lines of normal tantalite. The crystal structure of stibiotantalite is known (10; 20, p. 227), and is different from that of normal tantalite (2; 22). In bismutotantalite, as in stibiotantalite, a trivalent cation takes the place of the bivalent iron and manganese cations found in normal tantalite. In view of this fact and of the observations given above, it seems likely that bismutotantalite is very similar in crystal structure to stibiotantalite. It is evident, however, that additional studies of the varieties containing the trivalent cations are needed.

Manganotantalite

Two samples designated as manganotantalite from West Australia were secured and investigated. Their optical and rotation properties, as well as their *x*-ray diffraction powder photographs are similar to those of the ordinary columbite-tantalites studied. It is interesting to note that in these two samples dispersion of the apparent angle of rotation is weak as shown in Table 1. Although no analyses of these samples are available, the weak dispersion is in accordance with a high manganese content (or low FeO:MnO ratio), and therefore supports the designation of these specimens as manganotantalites.

MOSSITE-TAPIOLITE

Methods and Scope of the Investigation

It was desired to investigate the optical properties of the mossite-tapiolite series in a manner similar to that outlined for the columbite-tantalite series. Unfortunately very few specimens of the tetragonal series were available. Only three proven samples were obtained, but one other, from the Old Mike pegmatite, has optical properties that warrant its assignment to this group. The rotation properties of these specimens were determined and are summarized in Table 3.

TABLE 3. ROTATION PROPERTIES OF SOME TAPIOLITES

Univ. Wis. Ref. No.	Mineral	Locality	S.G.	DR_r	A_r			DA_r	Amount Dispers.
					Red	White	Blue		
B.B. 4	Tapiolite	Best Bet Pegmatite, Drever Lake, N.W.T., Canada	—	ess. nil.	2.9	2.7	1.6	$r>v$, strong	1.3
Peg. M-3	Tapiolite	Peg Tantalum Mines, Ross Lake, N.W.T., Canada	—	ess. nil	2.0	1.8	.9	$r>v$, strong	1.1
49-11-13	Tapiolite	Old Mike Pegmatite,* Custer County, South Dakota	—	ess. nil	1.8	1.5	?	$r>v$, strong	n.d.
50-53-1	Tapiolite	Peg Tantalum Mines,† Ross Lake, N.W.T., Canada	7.550	ess. nil	1.9	1.7	.8	$r>v$, strong	1.1

* This tapiolite occurs as inclusions in tantalite.

† Indicates specimen has been analyzed and is listed in Table 2.

One of the samples was analyzed, and its composition as shown in Table 2 indicates that it is a tapiolite. Another of the samples studied consists of inclusions in the specimen of tantalite from the Old Mike pegmatite. Inasmuch as the host tantalite has a low $Cb_2O_5:Ta_2O_5$ ratio (Table 2) it seems likely that the inclusions (if they could be analyzed) would also prove to be tantalum-rich. The composition of the other two specimens is not known. Thus it is evident that the writer is in no position to discuss the relation between optical properties and composition in the mossite-tapiolite series, but the results of the limited studies are briefly presented.

The search for specimens of the mossite-tapiolite series, together with x-ray work on available samples and a study of the literature, led, however, to a critical examination of the relationship between the tetragonal mossite-tapiolite series and the orthorhombic columbite-tantalite series. Certain aspects of this subject are of interest and are discussed below.

Rotation Properties

(*a*) Distinction of Mossite-Tapiolite from Columbite-Tantalite

Polarization figures and rotation properties offer a simple, quick and effective technique for distinguishing between tapiolite and columbite-tantalite in polished surfaces. Previously the similarity of the two minerals has made their distinction a matter of extreme difficulty. The physical and chemical properties of the two minerals are almost identical, and *x*-ray work on small impure grains in polished surfaces is difficult. The two minerals can be rapidly distinguished, however, by their rotation properties and relative reflectivities (Table 4).

(*b*) Angle of Rotation and Dispersion

Significant and measurable differences in the apparent angle of rotation in air were found for the various specimens of tapiolite. The values of the angle recorded in Table 3 range from 1.7 to 2.9 degrees. Variations in the strength of dispersion similar to those described for columbite-tantalite have also been encountered. Tapiolite from Ross Lake, Northwest Territories, and from the Old Mike pegmatite have strong blue and pink color fringes in their polarization figures at the 45-degree position. Tapiolite from Drever Lake in the Northwest Territories has blue and yellow color fringes.

Although it is impossible at present to relate the variations in rotation angles and dispersion to changing composition in the mossite-tapiolite series, it is interesting to note that those tapiolites that occur in iron-rich tantalite have high dispersion. Strength of dispersion may be related to the FeO:MnO ratio. Investigations using *x*-ray diffraction precession photographs of tapiolite from Ross Lake, Northwest Territories, have shown that this material (specimen 50-53-1, Tables 2 and 3) is disordered and has a rutile structure. Goldschmidt reported (13, p. 17; 14) that tapiolite is ordered, with tri-rutile structure and a superlattice. Thus it seems that there are two distinct forms of the tetragonal mineral tapiolite, and the observed variation in optical properties may be related to the degree of ordering.

Relationship between the Orthorhombic Columbite-Tantalite Series and the Tetragonal Mossite-Tapiolite Series

In the Ta-rich tantalites examined from the Old Mike pegmatite and from the Etta Mine, inclusions of tetragonal mossite-tapiolite were found; but inclusions belonging to the tetragonal series were never dis-

Table 4. Rotation Properties of Minerals

Mineral	Cryst. System	Dispersion of Reflection Rotation	Apparent Angle of Rotation			Dispersion of Apparent Angle of Rotation	Reflectivity relative and listed in descending order	
			Red	White	Blue			
Hematite	hex.	$r>v$, weak		2.4		$v>r$, distinct	creamy-white	highest
Rutile	tet.	$r>v$, weak to distinct	3.2	2.9	2.4	$r>v$, weak or masked		nearly equal to hematite
Ilmenite	hex.	$v>r$, distinct	2.2	2.9	3.1	$v>r$, distinct		definitely lower than rutile
Tapiolite	tet.	ess. nil	2.9	2.8	1.7	$r>v$, strong	orange-cream	nearly equal to ilmenite
Columbite-tantalite	orth.	ess. nil.	1.5	1.4	1.0	$r>v$, weak to strong		slightly lower than tapiolite
Euxenite	iso.	ess. nil		none		none		definitely lower than columbite
Cassiterite	tet.	ess. nil		1.9		$r>v$, weak often masked	grayish-cream	nearly equal to to euxenite
Ferberite	mono.	ess. nil	2.6	2.3	1.6	$r>v$, distinct		very close to cassiterite
Monazite	mono.	all dispersions and rotation properties masked by internal reflections					gray	low, definitely lower than ferberite, cassiterite
Zircon	tet.	all dispersions and rotation properties masked by internal reflections						lowest

covered in any of the numerous Cb-rich columbites. Columbium is a much more abundant element than tantalum (19, pp. 604–605) and this is reflected in the fact that columbite is much more abundant than tantalite. By the same standard mossite should be much commoner than tapiolite. This is not the case. Dana (9, p. 775) lists only two occurrences of mossite. The first of these was described by Brögger (3) and is the original material from Moss, near Obstfold, Norway, from which the mineral takes its name. The analysis of this specimen given in Dana's table (9, p. 776) shows only combined columbium-tantalum content. A

Often Associated With Cb-Ta Minerals

Internal Reflections	Separation of Isogyres in % of Field Diameter	Description of Figure upon Rotation of Analyzer, Mineral in Crossed Position	Description of Figure in 45-degree Position, Polarizer and Analyzer Crossed
rare, weak & reddish if present	35%	black isogyres, weak violet fringes on concave side, deep green on convex side, center of field yellow	black isogyres, violet fringes on concave side, blue-green fringe on convex side, center of field yellow
numerous, strong & reddish	40%	gray to reddish isogyres, narrow pink fringe on concave sides, narrow blue fringe on convex sides	black to reddish isogyres (if internal reflections present), concave sides pale blue, convex sides pink (or masked)
very rare	30%	black isogyres, weak blue fringe on concave side, pink fringe on convex	black isogyres, distinct pink fringe on concave sides, green-blue fringe on convex
none	35%	black isogyres, no distinct color fringes	black or dark green-blue isogyres, blue green fringe on concave side, yellow convex
rare, weak & reddish	20%	black isogyres, fringes indistinct	black isogyres, concave side pale blue, convex sides pink, fringes weak to strong
none or very rare	none	black isogyres, no color fringes	black cross, no separation of isogyres
numerous & varied white, gray, brown, red	30%	black isogyres, essentially no color fringes (or pink concave, blue convex and very weak)	black isogyres, fringes very weak often masked by internal reflections-appear blue concave, pink convex but this weak and possibly due to internal reflections
rare	30%	black isogyres, no color fringes	black isogyres, fringes distinct—concave side blue, convex orangey-pink
numerous & strong, always present, white, brown, red, patchy	cannot tell	figure unobtainable, internal reflections flood field	figure unobtainable, internal reflections flood field
strong & always present, reddish	cannot tell	figure unobtainable, internal reflections flood field	figure unobtainable, internal reflections flood field

later analysis of this material in 1906 (23) revealed a Ta_2O_5 content of 52% and a Cb_2O_5 content of 31%. This material is therefore tantalum-rich and should properly be called tapiolite. Schaller believed (21, p. 16) that the mineral name mossite proposed by Brögger for this specimen should be dropped because the sample is a columbic tapiolite. The second sample listed by Dana is a "mangano-mossite" from West Australia and it is described (9, p. 776) as doubtful, and possibly a columbite.

All these features lead one to question the existence of mossite and of a complete tetragonal mossite-tapiolite series. The suggestion is advanced here that there may be no complete tetragonal series of composition $(Fe,Mn)Cb_2O_6$-$(Fe,Mn)Ta_2O_6$ but only an orthorhombic series. In the high tantalum ranges, the orthorhombic form may revert to tetragonal symmetry in the mineral tapiolite. This would explain the anomalous features described above including the absence of mossite inclusions in columbite and the over-all rarity of mossite despite the relative abundance of columbium.

Dana stated (9, p. 776) that it has not been established that the natural tetragonal series extends to a high columbium member. Brandt (2, p. 6) reported that if a mineral analysis gives more than 25 atom per cent of columbium, a columbite phase must exist. She further stated that if larger amounts of tantalum are found in an iron-manganese mineral either orthorhombic or tetragonal compounds can be formed. Apparently synthesis of the high tantalum members can yield either tetragonal tapiolite or orthorhombic tantalite, but at the high columbium end only an orthorhombic member has been obtained. This lends support to our hypothesis which is also in accordance with the geologic occurrence of columbite, tantalite and tapiolite. Columbite forms early in pegmatites while tantalite and tapiolite are later (7, pp. 69 and 99). This may be explained by the greater relative abundance of columbium, which, in the course of differentiation, causes the early crystallization of columbium-rich compounds. Tantalum becomes enriched to the point of crystallization at a later time and results in the formation of tantalite or (because of the enrichment in tantalum relative to columbium) tapiolite.

Polymorphism

The cause of polymorphism in the proposed columbite-tantalite-tapiolite series is not now understood. Order-disorder cannot be the solution as it would mean that tapiolite (the higher symmetry and supposedly disordered form) would be early while tantalite (the low symmetry and ordered form) would be late. This is the reverse of the geologic occurrence of these minerals in pegmatites. It is also known that a superlattice is present in some tapiolite (24, p. 17; 13, p. 17) and this indicates that it is, in fact, an ordered structure and finally rules out order-disorder as a cause of polymorphism.

If the radius ratio of the quinquevalent columbium and tantalum ions to the oxygen ion fell on the borderline between two different co-ordination ranges, the small size difference of the columbium and tantalum ions might cause a change of symmetry in the Ta-rich range. In actual fact, however, the radius ratio (of quinquevalent columbium and tantalum ions to the oxygen ion) lie centrally in the octahedral co-ordination range.

It may be significant that tapiolite has a tri-rutile or rutile structure based on the mineral rutile while columbite-tantalite is based on the brookite structure (2, p. 4; 13; 17) The cause of polymorphism in tapiolite-tantalite may be similar, or comparable, to the cause in the case of rutile-brookite but this has not been determined. Heating and cooling experiments to determine whether orthorhombic tantalite can be converted to tetragonal tapiolite at high temperatures, and vice versa, would be of interest in studying the polymorphic relationships. Additional syntheses of the columbite-tantalite-tapiolite minerals would also be of value.

Summary and Conclusions

(*a*) Tapiolite can be distinguished quickly and readily from the columbite-tantalites in polished surfaces by the use of polarization figures and rotation properties.

(*b*) The apparent angle of rotation varies significantly in the different specimens of tapiolite studied. This variation may be related to compositional differences or to the degree of ordering.

(*c*) Strength of dispersion also varies in the different tapiolites studied. This variation may be related to varying FeO:MnO ratios in the specimens investigated.

(*d*) The existence of the mineral mossite, and of a complete tetragonal mossite-tapiolite series is questioned. It is proposed that only a single series of composition $(Fe,Mn)Cb_2O_6$-$(Fe,Mn)Ta_2O_6$ occurs in nature and includes the minerals columbite, tantalite and tapiolite. This proposal is an hypothesis only, and should be critically examined in the light of further information.

(*e*) The cause of polymorphism in tantalite-tapiolite is not understood. Additional work, including heating and cooling and synthesis experiments, is needed to determine the cause of the dimorphic relationship.

(*f*) A second distinct form of tapiolite was encountered in this study. Goldschmidt previously described (13, p. 17) an ordered form with tri-rutile structure and a superlattice. The analyzed specimen from Ross Lake, however, is a disordered form with rutile structure. The relationship between degree of ordering and optical properties needs further investigation.

ILMENORUTILE

General Statement

The name ilmenorutile was orginally proposed by Koksharov (16, pp. 352–355) for what he called "a new variety of rutile." Later analyses apparently showed that this material contained appreciable columbium and minor tantalum. Dana (9, p. 558) described ilmenorutile as columbian rutile, and this is the accepted definition at the present time.

A number of specimens believed to be ilmenorutile were obtained and studied. The first two samples received were crystals from M'ba, French Cameroons and from the Tonkolili District, Sierra Leone. Oriented polished surfaces of these crystals were prepared. Subsequently twenty additional sand samples from pits alongside streams, also from Sierra Leone, were obtained. These were believed to contain ilmenorutile and polished surfaces of them were prepared. The results of the studies of these materials to date are presented below.

Observations and Discussion

The crystals from M'ba, French Cameroons and from the Tonkolili District of Sierra Leone proved to be complex, intricate intergrowths of columbite and rutile. Identification of the constituent minerals was first accomplished using rotation properties and polarization figures on polished surfaces. The identification was later substantiated by means of *x*-ray diffraction powder photographs. The *x*-ray patterns obtained showed strong rutile lines and weak columbite lines. There was no apparent shift in position of the rutile lines (from the pattern of "normal" rutile) of the kind often resulting from substitutional solid solution.

Examination of a number of the concentrates in polished surfaces revealed that the non-magnetic portion of each sample[1] also contained some mineral grains that are intergrowths of columbite and rutile. These intergrowths, therefore, account for at least part of the columbium content of these specimens. In addition to the intergrowths, each non-magnetic fraction contains numerous grains of homogeneous rutile.

From one of the non-magnetic samples of concentrates, several grains were selected, and individual *x*-ray diffraction powder photographs of these grains were taken. These photographs showed that there was no visible shift of the rutile lines between a grain of pure rutile and a grain containing the intergrowth of columbite and rutile. In both cases the rutile lines agreed with the *A.S.T.M.* index card for normal rutile and with the pattern of a different check sample of our own rutile. This is, at best, a rough experiment but it indicates that little columbium is contained in solid solution in either the homogeneous rutile grain, or in the grain of rutile that has the columbite intergrowth. If columbium is present in the rutile, it is in insufficient amounts to cause a shift in position of the lines of the rutile powder pattern.

Data at hand, therefore, suggest that ilmenorutile as a distinct mineral is not present in the material studied, but only intergrowths of columbite with ordinary rutile. This fact raises some doubt about the existence of ilmenorutile as an independent mineral, and led the writer to an examination of the literature in this regard.

---

[1] Each of the concentrate specimens had been divided into magnetic and non-magnetic fractions.

Prior (18, pp. 88–89) concluded that strüverite was an independent mineral and was related to ilmenorutile. He considered strüverite from Italy to be a solid solution of the tapiolite molecule with the rutile molecule. He also believed that ilmenorutiles from Norway and Russia were solid solutions of the mossite molecule with rutile. His conclusions and formulae, however, were based on chemical analyses and thus do not take into account the possibility of mineral intergrowths.

Schaller (21, p. 38) stated that ilmenorutile was a distinct mineral subspecies of rutile in which Fe, Cb and Ta were present in isomorphous mixtures. This conclusion also was based on chemical analyses, and likewise does not allow for the presence of fine mineral intergrowths.

A more recent article in a bulletin of the *Imperial Institute of London* (15) described ilmenorutile from the Tonkolili District of Sierra Leone as a distinct columbium-bearing variety of rutile. The optical properties of the specimen in transmitted light are discussed, but the sample was not apparently examined in reflected light or by *x*-ray diffraction methods. All our specimens from this area contain the intergrowth of columbite and rutile.

X-ray information concerning the mineral ilmenorutile is scarce. Wyckoff (24, p. 17) indicated that columbium is present in ilmenorutile in solid solution and is disordered. Ando and Nitta published the results (1) of some *x*-ray studies of Japanese ilmenorutile but their article was not available to the writer. Hence the results of their investigation are not considered here.

The nature of the intergrowth in the samples studied is of interest. In the two crystalline specimens of ilmenorutile the following features were observed.

(1). Rutile is invariably the more abundant component of the intergrowth and constitutes the host mineral. For this reason the intergrowth may be described as columbite in rutile.

(2). Grains and blebs of columbite are of irregular shape and have various orientations, but are rather evenly distributed throughout the host crystals of rutile.

In the samples of concentrates, the following features have been noted.

(1). Rutile is invariably the more abundant component of the intergrowth and constitutes the host mineral.

(2). The orientation of intergrown columbite grains varies in a single grain of rutile, so far as can be determined.

(3). The size of the intergrown columbite grains varies in a single grain of the host from tiny to large (relative to the size of the host grain).

(4). The shape of intergrown columbite grains is extremely irregular.

(5). The distribution of columbite intergrowths varies within a single rutile grain. Portions of one rutile grain may contain more columbite than other portions.

(6). Columbite intergrowths generally occur in the more cracked and pitted grains of rutile. Perfect unpitted and unfractured grains of rutile tend to be homogeneous and lack columbite intergrowths. This is a generalization and exceptions were encountered. Whether the imperfections are earlier or later than the intergrowth is not known.

The origin of the intergrowth is yet another problem. No information is available to the writer concerning the geologic occurrence of the ilmenorutile studied from M'ba, French Cameroons. The specimens from the Tonkolili District of Sierra Leone are reported to occur in alluvial stream gravels (15). The following information concerning the possible derivation of the ilmenorutile has been summarized from additional references (4; 11; 12).

The streams in which the alluvium is found drain an area of crystalline rocks, including various granites and a belt of schists and migmatites. Ilmenorutile is thought to occur in sugary quartz veins, in different kinds of medium- and coarse-grained granite, near migmatitic fringes of the schist belt. It may also occur in pegmatites. Unfortunately this information is not of direct aid in understanding the origin of the intergrowth.

The laboratory findings are, likewise, inconclusive. The irregular physical characteristics of the intergrowth are unlike those of many other intergrowths of unmixed origin. If unmixing is the answer, then we would expect to find some content of columbium still in solid solution in rutile from grains showing the intergrowth. Present x-ray experiments do not indicate that this is the case, but more detailed x-ray studies are essential. Thus the observations to date do not seem to support an unmixing origin but it may be argued that they do not exclude it entirely.

Other possible explanations would be that the intergrowth is of replacement origin, or that it is the result of simultaneous (eutectic) crystallization. Observation (1) above would satisfy either of these possibilities. Replacement of rutile by minor amounts of columbite could result in this feature, but so could eutectic crystallization. The fact that some grains of rutile contain the intergrowth, whereas others are homogeneous could also be due either to replacement or to eutectic crystallization where rutile was the initial pure phase to crystallize. Observation (6) above would support a replacement origin only if we could be certain that it is a causative feature.

Conclusions

(*a*) In the specimens studied, ilmenorutile is not an independent mineral but is an intergrowth of two distinct mineral phases, namely columbite and rutile.

(*b*) The origin of the observed intergrowth is not known. Unmixing seems unlikely to be the answer but is not excluded. Either replacement or eutectic crystallization could also account for the observed features.

(*c*) Further work is needed to determine whether ilmenorutile occurs as an independent mineral in nature, and to determine the origin of the intergrowth.

OPTICAL PROPERTIES OF MINERALS ASSOCIATED WITH COLUMBIUM-TANTALUM MINERALS

General discussion

During the course of the optical investigations of columbium-tantalum minerals it became apparent that the distinction of these minerals from certain of their common associates was a problem. It was decided to investigate the optic properies of these minerals, and especially their rotation properties, in the hope that the problem could be simplified. The minerals investigated, in addition to columbite, tantalite and tapiolite were hematite, ilmenite, rutile, cassiterite, euxenite, monazite, zircon and ferberite.

Some of the optical properties of these minerals, including their apparent angles of rotation in air, dispersions and relative reflectivities have been determined and are summarized in Table 4. Since most of these minerals are known to vary in composition, the data given apply only to the specific material studied. Additional data for other compositional members may later be found to modify or extend the range of properties given. Nevertheless, it was found that the properties so far measured and recorded are extremely valuable in the distinction and identification of the various oxides. They permit simple and rapid identification in polished surfaces, and are of special value where work with mixtures of the minerals is involved.

REFERENCES

1. ANDO, R., AND NITTA, I., *X*-ray study of some Japanese minerals, II, ilmenorutile at Tesirogi, Hukusima Prefecture: *Jour. Chem. Soc. Japan*, **62,** 978 (1941).
2. BRANDT, KARIN, *X*-ray studies on ABO_4 compounds of rutile type and AB_2O_6 compounds of columbite type: *Arkiv. for Kemi., Min. och Geol., Bd.* **17A,** N:o 15 (1943).
3. BRÖGGER, W. C., Über den Mossit und über das Krystallsystem des Tantalit (Skogbolite aus Finnland): *Vidensk. Akad. Oslo, Mat.-Nat. Kl.* (1897).
4. Colonial Geology and Mineral Resources, Vol. **4,** No. 1, p. 72.

5. Cameron, E. N., and Green, L. H., Polarization figures and rotation properties in reflected light and their application to the identification of the ore minerals: *Ec. Geol.*, **45,** 719–754 (1950).
6. Cameron, E. N., Hutchinson, R. W., and Green, L. H., Sources of error in the measurement of rotation properties with the ore microscope: *Ec. Geol.*, **48,** 574–590 (1953).
7. Cameron, E. N., Jahns, R. H., McNair, A. H., and Page, L. R., The internal structure of granitic pegmatites: *Ec. Geol., Mono.* **2,** (1949).
8. Dana's Textbook of Mineralogy 4th ed., Edited by W. E. Ford, John Wiley and Sons, New York (1932).
9. Dana's System of Mineralogy 7th ed., Vol. 1, Edited by Palache, Berman and Frondel, John Wiley and Sons, New York (1944).
10. Dihlstrom, K., Über den Bau des wahren Antimontetroxyds und des damit isomorphen Stibiotantalit $SbTaO_4$: *Zeits. Anorg, Chem., Ch.* **239,** 57–65 (1938).
11. Geological Survey of Sierra Leone, Annual Report (**1952**) pp. 14–18.
12. Geological Survey of Sierra Leone, Annual Report (**1949**) pp. 4–5.
13. Goldschmidt, V. M., Geochemische Verteilungsgesetze der Elemente, VI, Über die Krystallstrukturen vom Rutiltypus mit bemerken zur Geochemie Zweiwertiger und Vierwertiger Elemente: *Vidensk. Akad. Oslo, Mat.-Nat. Kl., Skr.* (1926), Vol. **1,** Paper I.
14. Goldschmidt, V. M., Geochemische Verteilungsgesetze der Elemente, VII, Die Gesetze der Krystallochemie: *Vidensk. Akad. Oslo, Mat.-Nat. Kl., Skr.* (1926), Vol. **1,** Paper II.
15. Ilmenorutile from Sierra Leone, *Imperial Institute of London Bulletin*, **42,** 45–47 (1944).
16. Koksharov, N., *Materialien zur Mineralogie Russlands*, **2,** (1854).
17. Prior, G. T., Note on a connexion between the molecular volume and chemical composition of some crystallographically similar minerals: *Mineral. Mag.*, **13,** 217–223 (1903).
18. Prior, G. T., and Zambonini, F., On struverite and its relation to ilmenorutile: *Mineral. Mag.*, **15,** No. 68, 78–89 (1908).
19. Rankama, K., and Sahama, Th. G., Geochemistry, Univ. of Chicago Press (1950).
20. Rosen, O., and Westgren, A., Minerals of the Varutrask pegmatite, XII, On the structure and composition of minerals belonging to the pyrochlore-atopite group and on *x*-ray analysis of stibio-microlite: *Geol. För. Förh.*, Mar.-April (**1938**).
21. Schaller, W. T., Mineralogical Note, Series 2, A study of the rutile group: *U.S.G.S. Bulletin* **509,** 1–39 (1912).
22. Sturdivant, J. H., The crystal structure of columbite: *Zeits. Kryst.*, Bd. **75,** 1/2 (1930).
23. Thesen, analysis in Brögger, W. C., Die Mineralien der Sudnorwegischen Granitpermatitgange, I, Niobate, Tantalate, Titanate und Titanoniobate: *Vidensk. Akad. Oslo, Mat.-Nat. Kl.* **6,** 52 (1906).
24. Wyckoff, R. W. G., Crystal Structures, Vol. II, Chap. IX, text 1951.

Manuscript received May 20, 1954.

A SECOND OCCURRENCE OF THE MINERAL SINHALITE ($2MgO \cdot Al_2O_3 \cdot B_2O_3$)*

Waldemar T. Schaller and Fred A. Hildebrand,
U. S. Geological Survey, Washington 25, D.C.

Abstract

The undetermined *mineral B* occurring with serendibite in Warren County, New York, is identified with the recently described new mineral sinhalite from Ceylon.

In their paper on serendibite from Warren County, New York, Larsen and Schaller (1932) described two associated undetermined minerals, which they referred to as *mineral A* and *mineral B*. The recently described new mineral sinhalite ($2MgO \cdot Al_2O_3 \cdot B_2O_3$) from Ceylon (Claringbull and Hey, 1952) recalled to one of us these two undetermined minerals from New York State and suggested the possibility of *mineral B* being sinhalite. A comparison of the properties of these two minerals shows their identity, thus giving a second occurrence for sinhalite.

The type of occurrence and mineral association of serendibite from the two localities are the same: essentially a contact metamorphosed limestone. Serendibite from Ceylon occurs as thin layers in contact zones between limestone and a granulite (composed mainly of quartz and feldspar); but it is more common where blue spinel, apatite, scapolite, and plagioclase are present in addition to abundant diopside. It would be interesting to examine the serendibite material from Ceylon to see if any sinhalite occurs with it as it does with the New York serendibite. The serendibite from New York State likewise is in thin layers of a contact zone between limestone and an intrusive granite and is of hydrothermal contact-metamorphic origin. The associated sinhalite is of similar origin.

Mineral B, according to Larsen and Schaller (1932, p. 461), " . . . is closely associated with serendibite in the specimen that yielded the serendibite for analysis, but was not found in other specimens." In an unpublished notation, *mineral B* is referred to by Larsen as "white olivine"—a remarkably prophetic observation, made about 1920, as sinhalite may be considered as an olivine with boron proxying for silicon and one aluminum proxying for one magnesium, to balance the charges:

Olivine	$MgMgSiO_4$
Sinhalite	$AlMgBO_4$

The pertinent properties of *mineral B* from New York and of sinhalite from Ceylon follow:

---

* Publication authorized by the Director, U. S. Geological Survey.

	Mineral B	*Sinhalite* (Average values)
Specific gravity	>3.20	3.48
Sign	Minus (−)	Minus (−)
2V	Rather large	55°–56°
α	1.665	1.668
β	1.692	1.698
γ	1.705	1.706
Birefringence	0.040	0.038

Table 1. X-Ray Powder Diffraction Data for Sinhalite

Present Work Warren County, N. Y. Cu/Ni λ: $K_\alpha=1.5418$ Å, $K\alpha_1=1.54050$ film 6350[1]		*Data of Claringbull and Hey* (1952) *Ceylon* Cu-K_α radiation (λ=1.542 Å)			
		No. 18[2]		No. 5[2]	
d_{hkl} (Å)	I^3	*d* (Å)	*I*	*d* (Å)	*I*
7.7	2	—	—	—	—
7.1	3	—	—	—	—
4.96	9	4.97	m	4.93	ms
3.99	7	4.00	mw	3.97	mw
3.74	6	3.77	w	3.73	vw
3.53	2	—	—	—	—
3.45	6	3.45	vw	3.43	vvw
3.27	8(?)	3.26	s	3.24	s
2.84	4	2.84	vvw	2.82	vvw
2.69	1	—	—	—	—
2.63	9	2.64	ms	2.62	s
2.47	6	2.47	vvw	2.46	vw
2.39	8	2.40	m	2.38	ms
2.32	7(?)	2.32	m	2.30	ms
2.27	4	2.27	vvw	—	—
2.15	10(?)	2.15	vs	2.14	vvs
1.929	5	1.94	vvw	1.93	vw
1.877	4	1.876	vw	1.868	vw
1.804	3	1.824	vvw	1.801	vvw
1.771	3(?)	1.785	vvw	1.764	vvw
1.740	2	—	—	—	—

---

[1] Pattern taken with 114.56-mm. camera using the Straumanis technique and ethyl cellulose rod-shaped mounts. Back reflection lines were obtained and film shrinkage was found to be negligible.

[2] Patterns were taken with 6-cm. camera.

[3] The question mark (?) after intensities of these sinhalite lines indicates that coincident diopside lines make the observed intensities questionable. Calibrated strips were used for intensity measurements. B, broad; VB, very broad.

TABLE 1—(*continued*)

Present Work Warren County, N. Y. Cu/Ni λ: $K_\alpha = 1.5418$ Å, $K\alpha_1 = 1.54050$ film 6350[1]		*Data of Claringbull and Hey* (1952) *Ceylon* Cu-K_α radiation ($\lambda = 1.542$ Å)			
		No. 18[2]		No. 5[2]	
d_{hkl} (Å)	I[3]	d (Å)	I	d (Å)	I
1.716	6	1.716	w	1.705	w
1.631	9(?)	1.632	s	1.621	vs
1.588	5	1.592	vvw	1.576	vvwb
1.570	4(?)	1.568	vvw		
1.540	5	1.541	w	1.534	w
1.523	6(?)	1.524	w	1.514	w
1.508	3(?)	—	—	—	—
1.427	7B(?)	1.427	m	1.420	ms
1.389	4	1.387	vvw	1.384	vw
1.368	1	—	—	1.360	vvw
1.346	6	1.347	vw	1.340	w
1.326	3(?)	1.324	vvw	1.320	vvw
1.307	1				
1.280	4				
1.249	6				
1.236	2				
1.187	3				
1.143	2				
1.135	3				
1.096	2B				
1.086	2				
1.081	3				
1.073	4(?)				
1.057	2				
1.045	3				
1.011	3B				
0.998	4B				
0.977	3B				
0.969	1				
0.952	1B				
0.935	3VB				
0.923	2B				
0.900 (α_1)	3				
0.8897	1				
0.8007 (α_1)	3VB				
0.8584	2				
0.8555 (α_1)	4				
0.8393	2				
0.8358 (α_1)?	3				
0.8244	2				
0.8215 (α_1)?	3				

Three x-ray powder diffraction patterns of *mineral B*, taken by and filed with the Geochemistry and Petrology Branch, U. S. Geological Survey, are as follows: Films 6350 and 7205 were taken from the same rod-shaped mount of material previously analyzed. This material contained the most admixed diopside, as indicated by the higher percentage of SiO_2. The x-ray diffraction data for sinhalite from New York State, shown in Table 1, were obtained from film 6350. Film 7205 is shown in Fig. 1. Another film, number 6336 (not shown in this report), was taken of a second sample, which had the least SiO_2. The x-ray powder diffraction pattern (film 7205) of *mineral B* is identical with that given for sinhalite from Ceylon (Fig. 1, plate 27, Claringbull and Hey, 1952), as shown in Fig. 1. X-ray diffraction data for sinhalite are shown in Table 1.

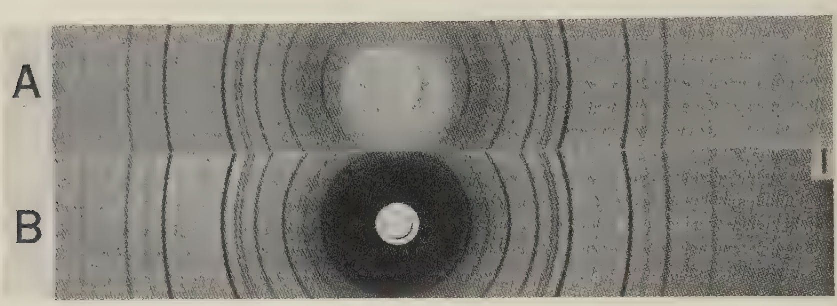

FIG. 1. X-ray diffraction patterns of sinhalite. A, sinhalite from Warren County, New York, film 7205 taken with a 57.3-mm. camera. Broken lines are attributed to diopside. B, sinhalite from Ceylon (reproduced from Fig. 1, plate 27, Claringbull and Hey, 1952). The print used in Fig. 1A was slightly enlarged to correspond with the reproduction in Fig. 1B.

The only remaining material of the analyzed samples of *mineral B* was the exceedingly minute quantity clinging to the sides of the small glass sample tubes. Most of the obvious, colored impurities (greenish serendibite, blue spinel) were removed by hand picking before the samples were x-rayed. The samples were too small to permit removal of all the associated minerals, particularly of diopside, the most abundant mineral. This purified material was then x-rayed; the resulting pattern is shown in Fig. 1A. The broken lines shown in Fig. 1A are due to the presence of admixed diopside. As all the samples were used for the powder diffraction patterns, there is now no more of the analyzed material available.

The very poor, partial analyses of *mineral B*, made on a small quantity of material, are of value only in indicating that the mineral is not a silicate, and in indicating the presence of much Al_2O_3 and MgO. Boron was not tested for and it is not known how much the presence of boron affected the values for Al_2O_3 and MgO given in the old analyses. The samples analyzed contained as impurities diopside, serendibite, spinel, and possibly other minerals. Attempts to interpret the old analyses given for *mineral B* on the basis of assigning the silica to associated minerals were futile.

The undetermined *mineral A*, associated with *mineral B*, remains unidentified.

REFERENCES

CLARINGBULL, G. F., AND HEY, M. H. (1952), Sinhalite ($MgAlBO_4$), a new mineral: *Mineral. Mag.*, **29**, 841–849.

LARSEN, E. S., AND SCHALLER, W. T. (1932), Serendibite from Warren County, New York, and its paragenesis: *Am. Mineral.*, **17**, 457–465.

Manuscript received June 1, 1954.

CONCENTRATION OF HEAVY ACCESSORIES FROM LARGE ROCK SAMPLES

H. W. Fairbairn, *Department of Geology and Geophysics, Massachusetts Institute of Technology, Cambridge, Massachusetts.*

Abstract

Concentration of heavy accessories from large rock samples (circa 50 lb.) requires, in the interest of efficiency, some modification of standard techniques currently used for small samples. To this end a continuous flow heavy-liquid separator has been designed which reduces handling and economizes on time. An improved method is described for recovery of heavy liquids by adding water directly to the filtered, but unwashed, sand. A number of additional points in technique are also included as well as an appendix listing the major items of equipment needed for work with large samples.

Introduction

Recent developments in geochronology, using zircon concentrates from igneous rocks (Larsen et al., 1952; Hurley and Fairbairn, 1953) require in many cases the processing of samples of fifty pounds or more. The concentration of these heavy accessories by crushing, grinding, sizing, heavy-liquid separation, and magnetic separation is a well known technique, but many details of the operation, as currently described (see texts listed), are suitable for small samples only. The present paper reconsiders the whole matter and reports on certain labor-saving modifications which, by laboratory standards, make processing of large samples reasonably efficient. Although developed for a special purpose, they have general application and will be useful for concentrating accessories from a variety of rocks.

Preparation of the Sand

Quantitative separation of the components of a rock, either by heavy-liquid or magnetic means, depends to a large degree on close sizing of the rock particles, or sand. In a poorly-sized sand smaller, heavy grains tend to be rafted up by larger, lighter, grains and conversely, lighter grains may be dragged down to contaminate the sink fraction.* Preparation of an adequately sized sand is therefore essential and, for large samples, consists of the steps outlined below.

The field sample must first be reduced to fragments small enough to be fed into a laboratory jaw breaker. This can be done by hand or, more rapidly, with a hydraulic-type chisel. The material is then passed through the breaker twice, setting the jaws to a smaller opening for the second pass. The product from the breaker, now a coarse sand, goes through a disc grinder, two or three times depending on the rock, with closer settings of the discs between each run. To avoid an undue proportion of very fine dust (as well as a lowering of grinding efficiency) the sand is screened between each grinding operation. A continuous-discharge vibrating screen with two 12″×30″ screen beds gives (1) a +40 oversize product which is returned to the disc grinder, (2) a +200 product which is set aside, (3) a −200 product which is usually discarded. When grinding is completed, the stock of +200 sand is passed through the screen at least twice to remove remaining fines. From a 50-lb. sample, if all the oversize is reduced, up to 30 lbs. of −40 +200 sand may thus be obtained.

---

* See p. 466 for details of an experiment bearing on this.

Magnetic Separation

To reduce as far as possible the volume of sink resulting from heavy-liquid separation, preliminary magnetic separation of major constituents such as biotite and hornblende is always advisable. A continuous-flow induced-roll separator, fitted with an auxiliary device for removing magnetite, accomplishes this most efficiently (Fig. 1). On a platform just above the roll separator a vibrating feed, equipped with a large hopper, passes a thin layer of the +200 sand forward to the triangular receptacle on the front of the roll separator. Before leaving the conveyor, however, this thin layer of grains passes under a slowly moving transverse belt, above which is suspended a row of Alnico horseshoe magnets. High-magnetic material (magnetite, iron filings, etc.) is lifted to the belt, passes over an aluminum pulley and is dropped into a receptacle beneath. Low-magnetic minerals are next separated from non-magnetic by the strong field of the roll separator, and the products are collected in two pails attached to the frame. An air cleaner (not shown) removes the inevitable dust.

Lacking this equipment, a Frantz separator, set up for vertical feed, will remove biotite, but not ordinary hornblende or pyroxene. The removal of these latter two minerals with the Frantz inclined feed is possible, but hardly practicable for a large sample of mafic rock. The equipment described above provides an adequate solution.

Heavy-Liquid Separation

Since the major part of most common rocks is non-magnetic quartz and feldspar, removal of this fraction from its associated heavy accessories is at best a time-consuming process. If a sand much finer than −200 must be processed, a large centrifuge will be necessary equipment. For +200 sand, with which this paper is concerned, gravity settling is adequate. To eliminate some of the handling, however, as well as to

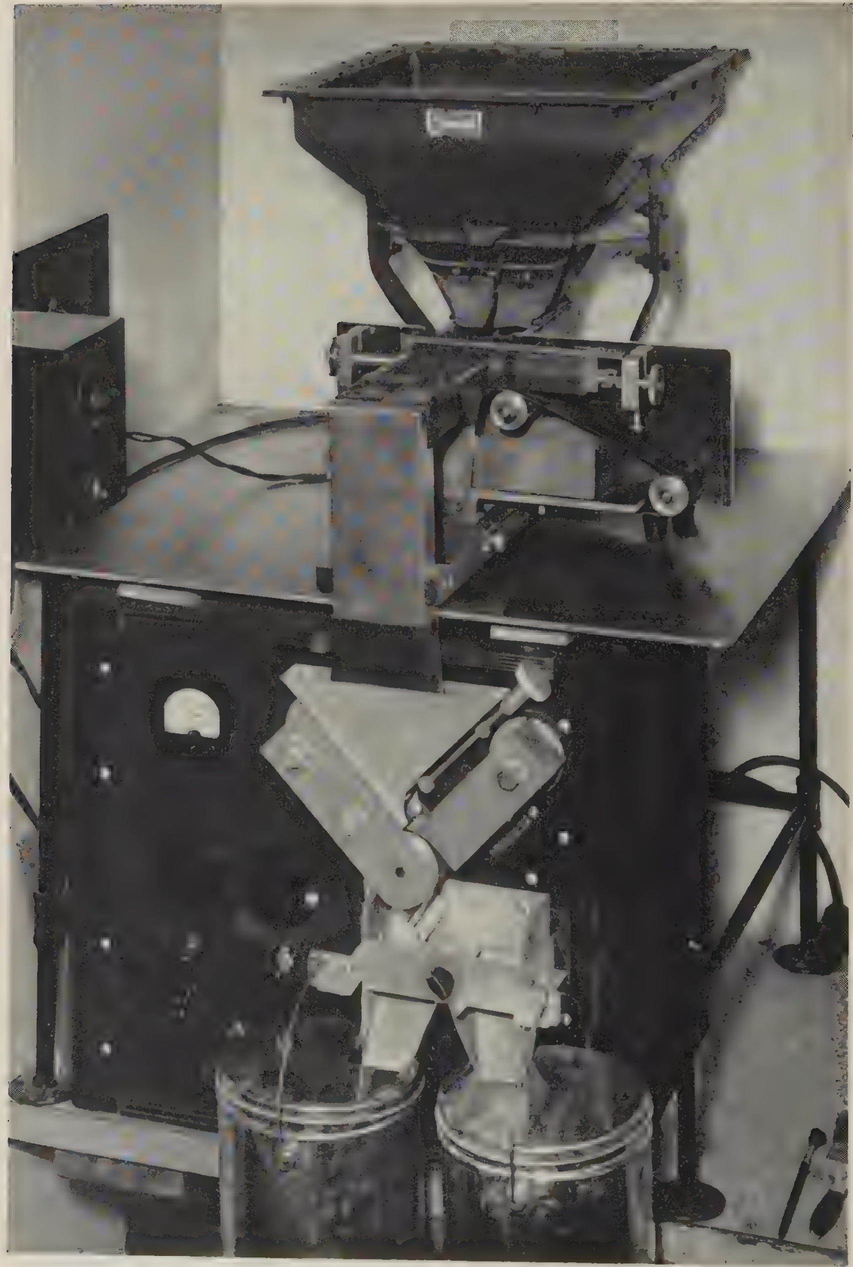

FIG. 1. Induced-roll magnetic separator (Carpco) with auxiliary vibrating feed and device for removing magnetite.

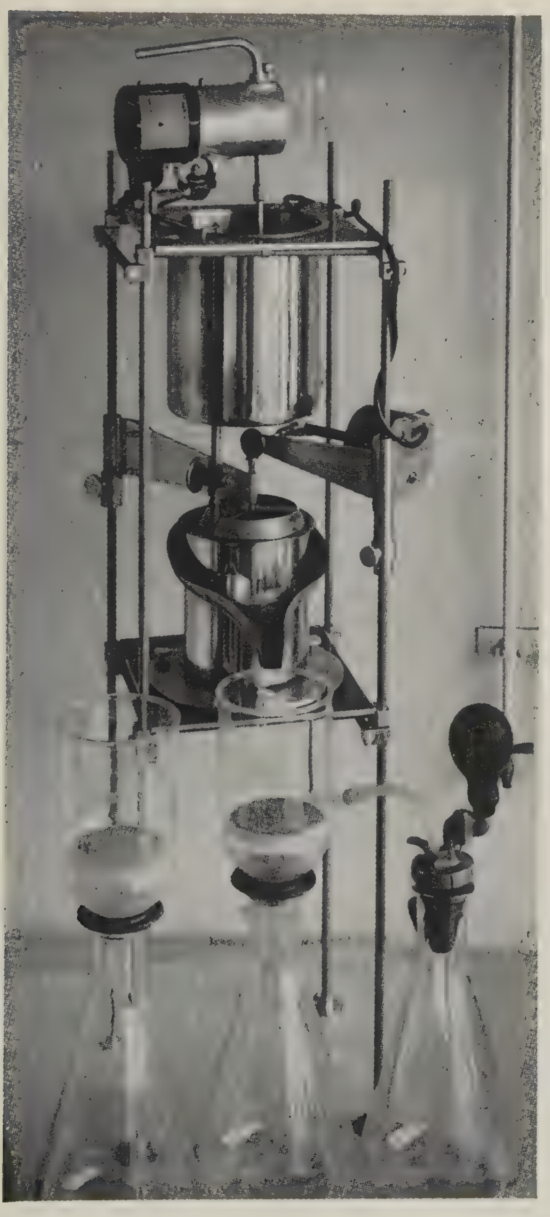

FIG. 2. Heavy-liquid separator for large samples. See text for description.

economize somewhat on time, a heavy-liquid separator, designed for use with large samples, has proved its worth in recent tests.

A 9-quart stainless steel beaker at the top of the assembly shown in Fig. 2 is filled with a 2:1 mixture of tetrabromoethane (acetylene tetrabromide) and sand. The mixture is kept in constant motion by a 4-propeller stirrer (with a lid on the beaker to prevent splashing), and leaks slowly through a conical valve in the bottom of the beaker. This valve has a screw adjustment outside the beaker so that, as the head of fluid falls, the opening may be increased to maintain uniform flow. The liquid-sand mixture leaves the beaker through a wide-diameter brass* tube (to prevent clogging) and is fed into a 4-quart stainless steel beaker below, near the wall and at a point about one inch from the bottom. This beaker is previously filled with tetrabromoethane. The rising quartz-feldspar-muscovite fraction is removed from the beaker by a jig. This consists of a horizontal collar with inclined sides which is given an up-and-down motion into the liquid by a cam directly above. This action moves the floating sand over the edge into an inclined drain which encircles the beaker. Vacuum filtering is carried out in 2-liter fritted-disc Büchner funnels. When the run is completed, the heavy accessories zircon, mona-

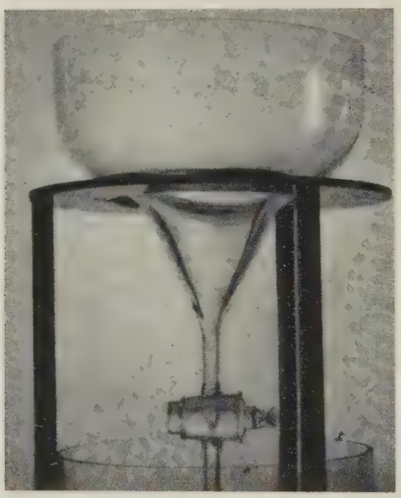

FIG. 3. Separatory funnel used either (1) for concentration of heavy accessories from small samples, or (2) for recovery of tetrabromoethane from acetone washings. Constructed from a 5-gal. Pyrex carboy, as described in text.

---

* Aluminum, iron, and rubber are unsatisfactory materials for use with tetrabromoethane.

zite, apatite, sphene, etc. are collected from the bottom of the separation beaker and fractionated further by magnetic and heavy-liquid treatment. The filter flasks are emptied by means of a rubber bulb pump (Fig. 2, lower right).

For methylene iodide separations, or for tetrabromoethane separations with only a few pounds of sand, separatory funnels of the design shown in Fig. 3 have been found very satisfactory. The one illustrated is made by cutting off the bottom of a 5-gal. Pyrex carboy, drawing out the neck, and fitting to this a stopcock. This funnel design has the advantage over conventional funnels that, for equivalent volumes of sand, the thickness of the layer is much reduced and rapid collection of the heavy accessories is thus facilitated. The disadvantage of a fairly flat shoulder, which catches much of the sink, is not a serious handicap as rotary stirring will displace the sink towards the center.

Smaller models of this funnel have been found to be exceedingly useful.

Recovery of Liquids

With large samples a considerable volume (about 3 gallons) of heavy liquid is required for the initial separation. Although the cost of the tetrabromoethane used by the writer is only a small fraction of the cost of bromoform used in many laboratories,* nevertheless it is uneconomical not to recover most of it. Furthermore, if unwashed sand is discarded, disposal becomes a problem as the liquid is toxic.†

As a result of some experimentation, the following procedure for recovery of tetrabromoethane has been found incomparably more efficient than any other known to the writer. The method applies equally well to bromoform.

The funnel which receives float from the separation beaker (Fig. 2) should be filled with sand to not more than half capacity. After the liquid has been pumped through to the flask the vacuum is disconnected and about one-half liter water is added to the sand.‡ This is stirred in thoroughly and thus displaces an additional amount of heavy liquid to the bottom which had not been removed by the initial pumping. This liquid and the overlying water are now pumped through to the flask.

---

* $0.55 per pound as against $2.00 a pound or, by volume $3.50 per liter and $14.00 per liter (approx.). These are commercial grades, obtainable from Dow Chemical Co., Midland, Mich.

† Although the catalog of harmful effects attributed to the liquid, as compiled by Sax in "Handbook of Dangerous Materials," makes alarming reading, in an adequately ventilated laboratory the amount of the vapor in the air can easily be kept below the critical concentration of 5 parts per million.

‡ This seems to have been first suggested by Smithson (1934).

The flask can later be emptied with a convenient hand pump (Fig. 2) and the undiluted heavy liquid then separated from the water.

The funnel is then transferred to another filter flask and, without vacuum, about one-half liter acetone is stirred into the sand. This is now pumped out and the sand is then discarded. Although additional washing of this type with acetone would be necessary to remove the heavy liquid quantitatively, this should not be done unless the quartz-feldspar sand is required for some other investigation.*

Since the sand before washing with acetone contains water as well as tetrabromoethane, the acetone will dissolve preferentially in the water and excess will go with the heavy liquid. The filter flask will thus have a layer of partly concentrated tetrabromoethane overlain by an acetone-water solution. This lighter fraction may be discarded. The heavy layer is transferred to a large beaker and a stream of water passed through it. A mineral fragment placed in the liquid will serve as density control and will float after a few minutes' washing.†

Following are some figures relevant to the procedure just outlined.

	Tetrabromoethane	Bromoform
Vol. of liquid required to saturate given vol. of sand	100 cc.	100 cc.
Vol. of liquid recovered in first filtration	48 cc.	79 cc.
Vol. of liquid recovered after addition of water.	33 cc.	8
Vol. of liquid recovered from heavy layer in filtrate after one acetone wash	11 cc.	n.d.
Vol. liquid recovered from upper layer in filtrate after one acetone wash	1 cc.	n.d.
Total recovery (disregarding final 1 cc. from upper layer)	92 cc.	n.d.

The greater viscosity of tetrabromoethane over bromoform shows clearly in the above tests and, if the water stage of Smithson were omitted, use of tetrabromoethane would involve a bigger recovery problem than would bromoform (only 48 cc. recovered directly compared with 79 cc.). However, use of water as described above neutralizes this advantage and, as tetrabromoethane is much the cheaper liquid, a loss of 8% can be tolerated.‡

---

* A test made on a *second* wash showed that, disregarding the time required, the cost of the acetone used was about three times the cost of the tetrabromoethane which could be recovered.

† The writer uses lepidolite (2.80) in order to hasten fractionation of heavy accessories. If the liquid is required to be at maximum density a piece of aragonite (2.94) should be used.

‡ This is not of course 8% of the liquid used for the separation, but only 8% of the liquid needed to saturate the sand.

For general acetone washings, where Smithson's method is not used, the usual laborious flask-shaking method of recovery may be avoided if 400 cc. aliquots of the wash material are fed slowly with gentle stirring into a large separatory funnel (Fig. 3) containing at least 6 liters of water. The recovered heavy liquid is withdrawn through the bottom, the funnel is drained, re-filled with fresh water, and another 400 cc. of acetone wash is added. The recovered heavy liquid can then be brought to full strength by passing water through it, as already noted.

Bromoform is soluble in water at 30° to the extent of 1 cc./liter H_2O. The writer has not found any similar data for tetrabromoethane, but from tests made the solubility would appear to be much less than for bromoform. Losses from this source using the recovery method above are therefore small. On the other hand, methylene iodide is moderately soluble (4cc./liter H_2O) and, in view of the cost of the liquid,* recovery of its acetone washings with water is not recommended. Evaporation at room temperature, using an electric fan and with a fragment of sillimanite ($D=3.20$) for density control, is preferable. Losses can be kept under 5%.

There are no shortcuts for recovery of diluted Clerici solution. Since it decomposes all too readily and is an expensive mixture,* evaporation at room temperature with the aid of an electric fan is the safest procedure. Fortunately it is needed in small quantities only. Willemite ($D=4.2$) may be used as density indicator.

DECOLORIZATION

Heavy liquids (except Clerici solution) tend to discolor with use and in contact with iron-rich minerals, particularly magnetite, will decompose as well. The latter can be prevented by immediate washing of such mixtures. Ordinary discoloration can be removed in a number of ways, one method being as follows. The liquid, diluted well with acetone (at least 5:1), is gently heated and a small amount of finely ground bone charcoal is stirred into it. When most of the acetone is gone, the liquid is filtered with a double thickness of paper and the decolorized liquid collected for final recovery with water. Decoloration need seldom be carried out for tetrabromoethane; for methylene iodide on the other hand deep color handicaps observation of the sink and the above decolorization method provides a remedy.

EFFICIENCY OF SEPARATIONS

No comprehensive experiments have been carried out to test efficiency of separation, as the goal of the writer's investigation did not require strictly quantitative separation of heavy accessories. However, a few tests have been made as recorded below.

---

* About $0.20 per cc. for methylene iodide; $0.50 per cc. for Clerici solution.

The need for closely sized sand in heavy liquid separations has already been pointed out. As an example of this, 100 mg. zircon was added to a prepared mixture of about 3 lbs. of quartz, feldspar, biotite, the entire sample having been sized to −40 +200. The mixture was placed in tetrabromoethane in a large separatory funnel of the kind shown in Fig. 2. After an initial stirring of a few seconds the sink contained 53 mg. zircon; after a second, 15 mg.; after a third, 8 mg.; and after a fourth, 5 mg., totalling 80 mg. recovery. The later sinks contained an increasing proportion of smaller grains. For quantitative separation, therefore, it is apparent that much closer sizing than −40 +200 would be necessary. For ordinary work, however, semi-quantitative fractionation is usually adequate.

The efficiency of fractionation of the new heavy-liquid separator (Fig. 2) is unknown but is believed to be very high if the flow rate is kept low. A sample of float, concentrated at a rate of flow of about 5–6 liters per hour, was transferred to a large Pyrex separator (Fig. 3). After repeated stirrings, and finally standing overnight, no trace of a sink fraction could be found.

No tests have been made with methylene iodide, but since it has lower viscosity than other heavy liquids in common use, separations are believed to be fairly complete. Clerici solution on the other hand is relatively viscous and small-diameter heavy accessories which should normally sink are commonly rafted up by large-diameter fragments belonging to the float. Close sizing is therefore highly important here, as well as patience while particles settle slowly through the column, if losses of hardly won heavy accessories are to be avoided.

From a few tests made with the Frantz magnetic separator it would appear that recovery of non-magnetics is about 100%. Sizing is important here also and the magnetic and non-magnetic products obtained at given settings should be rerun at least once for quantitative recovery.

Concluding Remarks

The foregoing account of concentration procedure for large samples is intended to amplify the established procedures used for small samples. Since the general method is used in a great many laboratories it may well be that apparatus and procedures for processing of large samples have been developed but not reported in the literature. If such is the case, and also if any pertinent published information has been missed, the writer would like to be informed.

ACKNOWLEDGMENTS

I am indebted to my colleague P. M. Hurley for providing the incentive to investigate these heavy accessory methods from the standpoint of large samples. Discussions with E. S. Larsen, Jr., who has pioneered much of the work on zircon concentration in igneous rocks, and with his staff at the Geological Survey, Washington, have likewise been of considerable help. John Solo, John Annese, and John Gower assisted in designing, and provided the necessary manual skill in assembly of the screen unit, heavy-liquid separator, and auxiliary belt separator. Last, but not least, the financial support of the Office of Naval Research under *Contract N5-ori-07857* is gratefully acknowledged.

APPENDIX

As an aid to readers who may wish to work with large samples, the following details concerning equipment are appended. Many of the units may be purchased through local supply houses.

1. Hydraulic Rock Chisel, Ward's Nat. Science Establishment, Rochester, N. Y.
2. Laboratory Jaw Breaker, Denver Fire Clay Co., Denver, Colo.
3. Laboratory Disc Grinder, Denver Fire Clay Co., Denver, Colo.
4. Laboratory model Low-Head Vibrating Screen, Allis-Chalmers Co., Milwaukee, Wis. A second screen can be fitted on the apparatus so as to increase its utility. This equipment, together with the breaker and grinder, should be in a separate room with adequate dust removal facilities.
5. Induced Roll Magnetic Separator (Carpco), Separations Engineering Corp., 110 E. 42nd St., New York 17, N. Y.
6. Isodynamic Magnetic Separator. S. G. Frantz Co., N. J. If a choice must be made between this separator and the one above, the Frantz equipment should be selected because of its greater versatility.
7. Heavy-Liquid Separator (described in text)
    - (a) 4 qt. and 9 qt. Stainless Steel Beakers, The Vollrath Co., Sheboygan, Wis. It is recommended that beakers of this type be used instead of glass beakers for the entire laboratory operation.
    - (b) "Lightnin'" Portable Mixer, Model F, with Ring Stand Clamp, and 3 extra Propellers, Mixing Equipment Co. Inc., 135 Mt. Read Boulevard, Rochester 11, N. Y.
    - (c) "Slo-Speed" Motor (to operate cam) Serial E-6, Cat. 75765, 85 RPM at full load, Precision Scientific Co., Chicago, Ill.
    - (d) Pneumatic Acid Pump, with plastic tubing, Thompson Mfg. Co., Erie, Penn.
    - (e) 2-liter Funnels, Büchner type, with fritted glass disc (coarse), Corning Glass works, Corning, N. Y.
    - (f) 4-liter Pyrex Filter Flasks, Corning Glass Works, Corning, N. Y.
    - (g) Flexaframe Rod, Connectors, and Feet, Fisher Scientific Co., Pittsburgh 19, Penn.
8. Vibrating Feed, Model 1-B, Jeffrey Mfg. Co., Columbus 16, Ohio

The services of a competent shop man for about 10 days will be needed for the various units described in this paper. There are no very critical dimensions, but the writer will be glad to furnish further details on request.

REFERENCES

1. HURLEY, P. M., AND FAIRBAIRN, H. W. (1953), Radiation damage in zircon: A possible age method: *Bull. Geol. Soc. Am.*, **64,** 659.
2. KRUMBEIN, W. C., AND PETTIJOHN, J. F. (1938), Manual of Sedimentary Petrography Ch. 14. (Appleton-Century).
3. LARSEN JR., E. S., KEEVIL, N. B., HARRISON, H. C. (1952), Method for determining the age of igneous rocks using the accessory minerals: *Bull. Geol. Soc. Am.*, **64,** 659.
4. MILNER, H. B. (1940), Sedimentary Petrography, 3rd ed. (Murby).
5. SMITHSON, F. (1934), The recovery of bromoform: *Geol. Mag.*, **71,** 240.
6. TWENHOFEL, W. H., AND TYLER, S. A. (1941), Methods of Study of Sediments (McGraw-Hill).

Manuscript received June 3, 1954.

GOLDICHITE, A NEW HYDROUS POTASSIUM FERRIC SULFATE FROM THE SAN RAFAEL SWELL, UTAH*

A. Rosenzweig, *University of Minnesota, Minneapolis, Minnesota,*†
AND
Eugene B. Gross, *Exploration Division, U. S. Atomic Energy Commission, Grand Junction, Colorado.*

Abstract

Goldichite, a new hydrous potassium ferric sulfate from the Dexter No. 7 Mine, Calf Mesa, San Rafael Swell, Utah, has the composition $KFe(SO_4)_2 \cdot 4H_2O$. It occurs as radiating clusters of pale-green crystals or fine-grained crystalline encrustations. It is associated with coquimbite, halotrichite, roemerite, alunogen, copiapite, fibroferrite, melanterite and other sulfates, which comprise the cementing material of a talus slope below a small, pyrite-rich uranium deposit in the Triassic Shinarump conglomerate. Crystals are commonly singly terminated, monoclinic-prismatic laths parallel {100} with forms {100}, {110}, and {011}. The space group is $P2_1/c$ and the cell constants are: $a_0 = 10.45$ Å, $b_0 = 10.55$ Å, $c_0 = 9.15$ Å, $\beta = 101°49'$. The cell contains 4 molecules; the density is 2.43 (observed) and 2.419 (calculated). The mineral is biaxial positive, with $2V = 82°$ (calculated), $\alpha = 1.582$, $\beta = 1.602$, $\gamma = 1.629$; $X = b$, $Z \wedge c = 11°$.

The mineral is named in honor of Samuel S. Goldich, Professor of Geology at the University of Minnesota.

Introduction

The new mineral goldichite, a hydrous potassium ferric sulfate, was first observed in a suite of sulfate minerals from the Dexter No. 7 Mine, Calf Mesa, San Rafael Swell, Utah, submitted to the authors for identification by R. L. Akright of the Atomic Energy Commission. The large number of unusual minerals in this suite prompted the authors to visit the locality early in 1953. A large number of samples were collected, including several of the suspected new mineral. Additional specimens were collected by John W. Gruner and Deane K. Smith, Jr., of the University of Minnesota during the summer of 1953.

The Dexter No. 7 Mine is located along the southeast rim of Calf Mesa, which is in the northwestern end of the San Rafael Swell in Emery County, Utah. The locality is approximately 30 miles west of Greenriver, Utah, as shown in the index map (Fig. 1). The mine is owned by Harold Olsen, Nolan Olsen and Leonard Wilson, who have operated it intermittently for its uranium content. At the time of the authors' visit the property was not being operated, and previous mining activity did not appear to have been extensive.

The mineral is named in honor of Dr. Samuel S. Goldich, Professor

---

* Work done by and on behalf of the Raw Materials Division, U. S. Atomic Energy Commission.

† Formerly with U. S. Atomic Energy Commission, Grand Junction, Colorado. Present address, Dept. of Geology, University of New Mexico, Albuquerque, New Mexico.

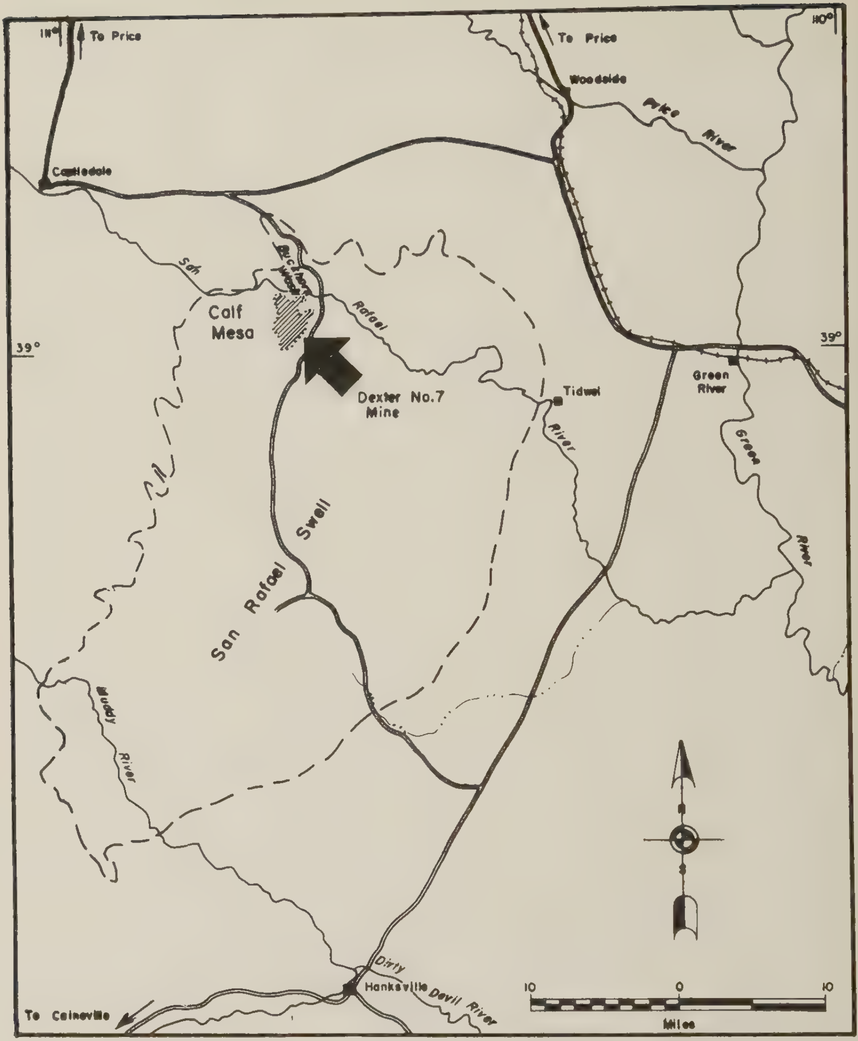

FIG. 1. Index map of Dexter No. 7 Mine and San Rafael Swell, Utah. (Drafted by Exploration Division, U. S. Atomic Energy Commission, Grand Junction, Colorado).

of Geology at the University of Minnesota, in recognition of his contributions to mineralogy and petrology, both in teaching and directing the Rock Analysis Laboratory at the University of Minnesota.

OCCURRENCE

The Dexter No. 7 deposit is in the Triassic Shinarump conglomerate which caps Calf Mesa. The ore horizon is about 25 feet above the contact of the Shinarump and the underlying Moenkopi formation (Akright, 1953). The shales and mudstones of the Moenkopi formation form a steep slope below the Shinarump cliff. Directly below the ore horizon, and extending down over the Moenkopi slope, is a talus breccia composed of fragments of the Shinarump conglomerate. The talus is crusted over with fine-grained material making it almost indistinguishable from the Moenkopi slope. A trench has been cut into this talus directly below the workings, and it is here that the sulfates are found cementing the talus fragments. The minerals of this suite, in addition to goldichite, are coquimbite, halotrichite, roemerite, alunogen, copiapite, melanterite, fibroferrite, voltaite, butlerite, parabutlerite, chalcanthite and diadochite. The essential minerals of the uranium deposit are metazeunerite, pyrite and chalcopyrite. The greatest percentage of the uranium is found in an asphalt-like carbonaceous material of indeterminate nature, wherein it may be present as extremely minute grains of uraninite as is common in other deposits in the San Rafael Swell (Rosenzweig, Gruner and Gardiner, 1954, p. 351).

Goldichite occurs as small laths in radiating clusters and as encrustations of very minute crystals in the near surface zone of the talus. It is closely associated with platy masses of white alunogen, purple crystals of coquimbite and bright yellow, small crystals of copiapite.

CRYSTALLOGRAPHY

Crystals of goldichite are small laths elongated parallel to the *c*-axis [001], and flattened parallel to the orthopinacoid {100}. The prism {110} and clinodome {011} are present on all crystals, and are nearly ideal in their development. Most crystals are singly terminated, but some, especially the minute ones making up the encrustations, are doubly terminated. The larger crystals have striated prism zones, while the smaller ones show smooth, highly reflecting faces. Single crystals range in size up to 2.5 mm. parallel to *c*, 1.0 mm. parallel to *b*, and 0.4 mm. parallel to *a*. Crystals up to 4 mm. in length are found in parallel and radiating growths. Figure 2 shows the natural habit of both the larger and smaller crystals, the latter being almost ideal in their development.

Morphological measurements were made on six crystals. The small number of faces observed makes the determination of crystal class uncertain, but the appearance of the clinodome {011} on both terminations and the presence of a mirror plane strongly suggests the class to be monoclinic-prismatic. This is conclusively borne out by the *x*-ray data. Morphological data are given in Table 1. Due to the poor quality of reflections from the striated zone, it was necessary to calculate the crystallographic elements from the *x*-ray data. These are given in Table 2.

TABLE 1. MORPHOLOGICAL DATA

Form	No. of Obs.	Quality	Average ϕ	Average ρ
100	12	fair	90°19′	89°52′
120	1	v. poor	29°52′	90°12′
110	20	fair	45°30′	89°55′
210	2	v. poor	62°37′	89°50′
011	17	good	13°43′	41°36′

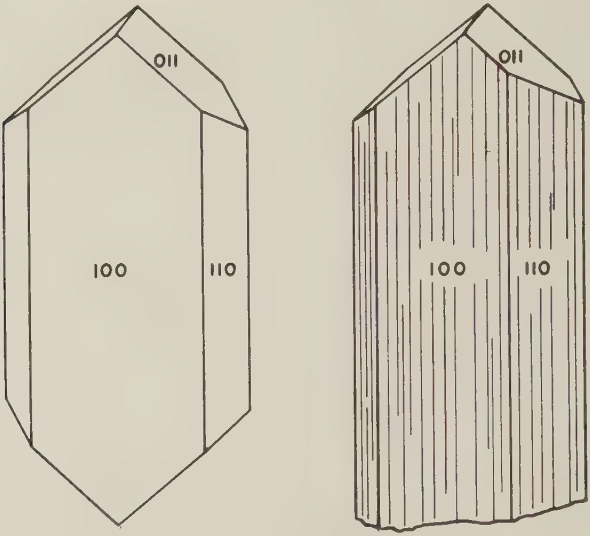

FIG. 2. Goldichite; nearly ideal development of small crystals (left); habit of the larger crystals (right).

TABLE 2. CRYSTALLOGRAPHIC ELEMENTS AND ANGLE TABLE (CALCULATED FROM X-RAY DATA)

Monoclinic prismatic—$2/m(C_{2h})$

$a:b:c=0.9924:1:0.8689;\ \beta=101°49'$
$p_0:q_0:r_0=0.8755:0.8505:1$
$r_2:p_2:q_2=1.176:1.029:1:\ \mu=78°11'$
$p_0'=0.8945;\ q_0'=0.8689;\ x_0'=0.2092$

Forms	ϕ	ρ	ϕ_2	$\rho_2=B$	C	A
100	90°00′	90°00′	0°00′	90°00′	78°11′	0°00′
120	27°14′	90°00′	0°00′	27°14′	84°37′	62°46′
110	45°50′	90°00′	0°00′	45°50′	81°33′	44°10′
210	64°06′	90°00′	0°00′	64°06′	79°23′	25°54′
011	13°42′	41°29′	78°11′	30°47′	59°13′	80°58′

TABLE 3. *X*-RAY DIFFRACTION DATA

Single crystal data—MoK_α radiation; MoK_α=0.7107 Å

a_0=10.45 Å	cell volume=986 Å^3
b_0=10.53	cell contents 4
c_0= 9.15	cell weight=1432.6
β=101° 49′	

Powder diffraction data—FeK_α radiation; FeK_α=1.9373 Å, camera diam. 57.3 mm.

I	*d meas.* Å	*probable index*	*d calc.* Å
8	10.29	100	10.23
9	7.35	110	7.34
7	6.85	011	6.82
	6.16	$\bar{1}11$	6.15
4	4.31	$\bar{1}21$	4.32
6	4.00	121	3.998
1	3.825	102	3.822
		211	3.816
2	3.670	220	3.668
1	3.553	$\bar{2}12$	3.550
6	3.403	022	3.409
		300	3.408
5	3.247	310	3.243
10	3.068	202	3.070
		$\bar{2}22$	3.067
4	3.014	$\bar{3}02$	3.026
	2.945	212	2.948
5	2.856	320	2.860
		032	2.761
1	2.752	$\bar{1}32$	2.755
		$\bar{2}13$	2.747
		231	2.665
6	2.656	222	2.652
		321	2.599
	2.595	023	2.597

TABLE 3—(*continued*)

Powder diffraction data—FeK_α radiation, camera diam. 57.3 mm.

I	*d meas.* Å	*probable index*	*d calc.* Å
		132	2.585
	2.560	400	2.556
		140	2.549
3	2.440	$\bar{4}02$	2.445
		330	2.445
1	2.320	$\bar{2}41$	2.318
		213	2.317
2	2.273	033	2.274
		042	2.268
		$\bar{1}42$	2.265
		$\bar{4}22$	2.218
	2.214	241	2.214
	2.156	$\bar{2}42$	2.159
		104	2.100
1	2.094	$\bar{1}24$	2.098
	2.021*		
1	2.002		
	1.901		
1	1.880		
	1.841		
	1.788		
1	1.763		
	1.714		
1	1.671		

* Large number of choices renders indexing meaningless.

Agreement between measured and calculated angles is good except for the rare forms {120} and {210}.

Space group and unit cell dimensions were determined from precession photographs using MoK_α radiation. Pictures were taken of the 0-, 1-, and 2- level with the *c* axis precessing and the beam parallel to *b*, and of the 0- level with the *c*-axis precessing and the beam parallel to a^*. Symmetry of the photographs shows the crystals to be monoclinic, and systematic extinctions indicate the space group to be $P2_1/c$. Powder photographs were taken using FeK_α radiation. Spacings calculated from the cell constants, and measured from the powder photographs are in good agreement. The large number of choices makes the indexing of all but the larger spacings rather uncertain. Both single crystal and powder data are given in Table 3.

PHYSICAL PROPERTIES

Goldichite is pale yellowish green in color. By artificial light the crystals assume a distinct lavender tint. This same color phenomenon was observed by the senior author on crystals of the ferric sulfate, kornelite. Goldichite has one excellent cleavage parallel to {100}; the hardness is approximately 2.5.

The density measured on the Berman balance is 2.43; that calculated from the *x*-ray data is 2.419. The optical properties of goldichite are as follows:

$$\left.\begin{array}{l}\alpha=1.582\pm0.002\\ \beta=1.602\pm0.002\\ \gamma=1.629\pm0.002\end{array}\right\} Na_D$$

$$(+)\ 2V=82^\circ \text{ (calculated)}$$

$$X=b$$

$$Z\wedge c=11^\circ$$

CHEMICAL PROPERTIES

Goldichite is a hydrous potassium ferric sulfate with formula $KFe(SO_4)_2\cdot 4H_2O$. The chemical analysis is given in Table 4. Although

TABLE 4

	$KFe(SO_4)_2\cdot 4H_2O$	Goldichite	ratios
K_2O	13.11	12.87	
Na_2O		0.09	1
Rb_2O		0.03	
Fe_2O_3	22.24	22.16	1
TiO_2		0.02	
Al_2O_3		0.32	
SO_3	44.58	43.65	3.94
H_2O	20.07	20.35	8.16
Insol.		0.23	
	100.00	99.72	

MnO, MgO, CaO, SrO, BaO, Cs_2O each less than 0.01 per cent. S. S. Goldich, analyst. Rb_2O, Cs_2O, Na_2O by flame spectrophotometer by R. B. Ellestad.

the sample was carefully picked, small amounts of halotrichite and alunogen may have been present. The 0.32% of Al_2O_3 and slightly high value for H_2O might be explained by these impurities. An impure sample was tested for FeO, and little or none was found. The SO_3 percentage is very likely a little low. The insoluble residue consists of quartz and clay minerals.

Goldichite is only very slightly soluble is cold water; soluble in hot water with hydrolysis; and readily soluble in dilute mineral acids.

The only closely related mineral is the monohydrate of the same compound, krausite (Foshag, 1931), from which goldichite can be readily distinguished by its physical properties.

Associated Minerals

The sulfate minerals found at the Dexter No. 7 Mine comprise the cementing material of the rock fragments in the talus. They range from well crystallized vug fillings to solid crystalline masses completely cementing the rock fragments. The trench exposing these minerals is dug to a depth of perhaps thirty to thirty-five feet measured perpendicular to the slope surface. There is a crude but distinct mineralogical zoning parallel to the slope surface. Figure 3 shows, qualitatively, the distribution and abundance of the various minerals.

Many of the minerals are exceptionally well crystallized and some are sufficiently rare to merit a brief description.

Coquimbite, $Fe_2(SO_4)_3 \cdot 9H_2O$

Stout hexagonal prisms of purple coquimbite up to half an inch long are abundant in the upper zone of the deposit. The crystals are modified by large basal pinacoids and small unequally developed pyramidal faces. In some cases these large crystals are encrusted with a thick, sugary mass of very small, colorless coquimbite crystals having well developed pyramidal faces. In slightly deeper zones coquimbite occurs as incomplete, colorless to pale lavender crystals up to one quarter inch in length. The refractive indices are $\epsilon = 1.546$, $\omega = 1.537$, and are the same for all of the types.

Alunogen, $Al_2(SO_4)_3 \cdot 18H_2O$

Large crystalline plates of colorless to white alunogen are common in the upper zone of the deposit. Some of the plates enclose small clusters of goldichite crystals.

Halotrichite, $Fe''Al_2(SO_4)_4 \cdot 22H_2O$

Long, white, silky fibers of halotrichite are common through most of

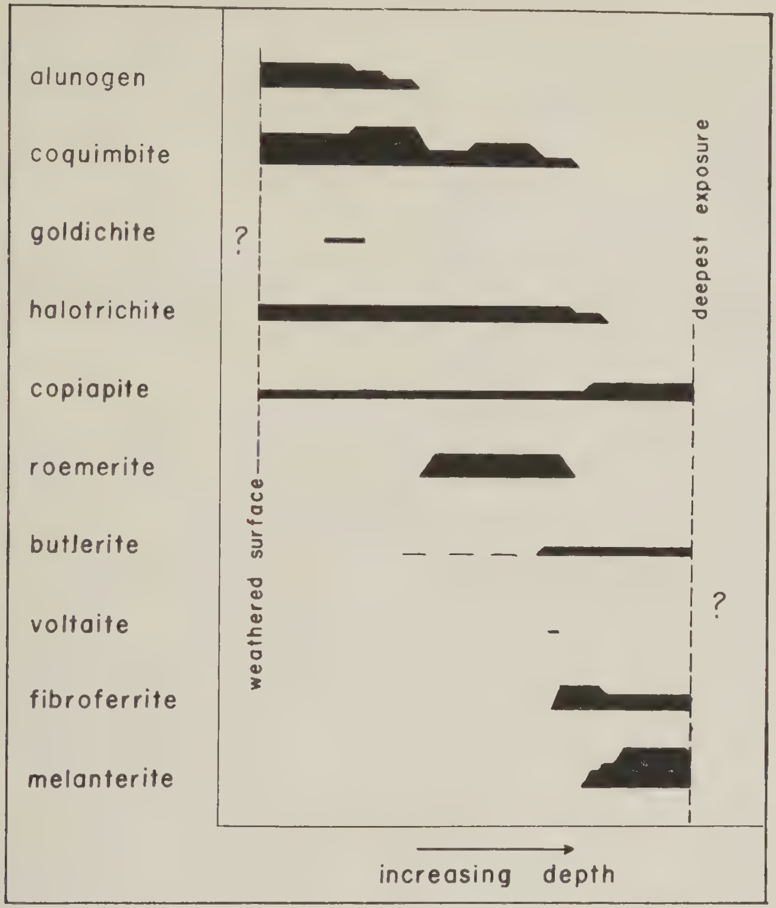

FIG. 3. Relative abundance of minerals in the talus deposit with respect to distance perpendicular to the surface. The abundance representation is qualitative.

the deposit, though almost absent from the deepest exposed zone. Halotrichite fibers are often found growing out of crystals of coquimbite and goldichite. The refractive indices are $\alpha=1.481$, $\beta=1.488$, $\gamma=1.489$; these are at the upper limit for halotrichite and indicate that the amount of magnesium is very small.

Copiapite, $Fe''Fe_4'''(SO_4)_6(OH)_2 \cdot 20H_2O$

Small, brilliant yellow plates of copiapite are common in all zones. The plates are often stacked one upon another in large numbers forming wormy or rod-like structures. The copiapite found in the deepest zone is extremely sensitive to changes in room temperature and humidity. The crystals become dark, bronzy brown on standing in warm dry air. The color change is reversible and can be made to take place several times before finally becoming permanent. The refractive indices are variable; $\alpha = 1.525$–1.530, $\beta = 1.539$–1.550, $\gamma = 1.585$–1.582. The indices suggest that little or no magnesium is present.

Roemerite, $Fe''Fe_2'''(SO_4)_4 \cdot 14H_2O$

Crystalline masses and very crude, equant crystals of dark brown roemerite are common in the intermediate zone. The refractive indices are $\alpha = 1.521$–1.525, $\beta = 1.567$–1.569, $\gamma = 1.577$–1.580.

Melanterite, $FeSO_4 \cdot 7H_2O$

Melanterite is very abundant in the deepest exposed zone as crystalline masses of pale blue-green to blue color. The color suggests that traces of copper may be present. Melanterite dehydrates very rapidly to $FeSO_4 \cdot 4H_2O$.

Fibroferrite, $Fe(SO_4)(OH) \cdot 5H_2O$?

Masses of very small, straw yellow, fibrous crystals of fibroferrite are common in the deep zone. Solution pits in melanterite are often lined with fibroferrite crystals a millimeter or two in length, whose surface has an almost metallic luster and color closely resembling that of pyrrhotite.

Butlerite and Parabutlerite, $Fe(SO_4)(OH) \cdot 2H_2O$

The dimorphs butlerite and parabutlerite occur as encrustations of small orange crystals with copiapite or melanterite. The two minerals are closely associated and are difficult to separate from one another.

Voltaite, $(K, Fe'')_3Fe'''(SO_4)_3 \cdot 4H_2O$?

Voltaite occurs as black, poorly developed octahedra up to 3 mm. in diameter in a matrix of crystalline coquimbite. Microscopically it is dark olive-green, isotropic, with irregular, weakly anisotropic areas, and a refractive index of 1.603.

Chalcanthite

Thin crystalline encrustations of chalcanthite were found close to the slope surface in the upper part of the exposure. This is the only copper mineral observed in the talus deposit; metazeunerite and chalcopyrite are present in the uranium ore horizon.

Diadochite, $Fe_2(PO_4)(SO_4)(OH)\cdot 5H_2O$

An orange-brown, amorphous material containing both sulfate and phosphate has been tentatively identified as diadochite. It gives no diffraction pattern, and is isotropic with $n=1.622$.

Sulfur

Minute crystals of native sulfur were found closely associated with alunogen, copiapite and goldichite. It is present in very small amounts.

Several other sulfate minerals were found, but were not present in sufficient quantity to permit identification or careful study. Uranium minerals were not observed in the sulfate deposit. A Geiger counter scanning of the exposure indicated only a normal background radiation.

PARAGENESIS

The occurrence of the large suite of sulfate minerals as a cementing material in a near surface deposit indicates without doubt that surface water was the agent in its formation. Two mechanisms suggest themselves, and very likely both were involved in the deposition. First, surface waters could have traveled through fractures or permeable zones in the pyrite-rich Shinarump conglomerate, oxidized the pyrite, and carried the sulfates in solution along impermeable layers or the top of the Moenkopi to be discharged into the talus, where crystallization took place by evaporation. Second, surface waters could have percolated through the talus composed of pyrite-bearing Shinarump fragments and formed the sulfates in place. Small amounts of pyrite are still to be found in the deeper zones. The fragmentary nature of the talus material suggests that it has been disintegrated by the solution of its cement, possibly pyrite.

A time sequence for the sulfates cannot be established. The system has sufficient components to be quite complex, and the particular phase to crystallize might be very sensitive to both concentration and temperature. Since the deposit is near the surface, and dependent on surface waters for its formation, it is conceivable that stability conditions for any one phase might be attained several times during the history of the deposit. This is exemplified by the intergrowth of the minerals and the several stages of crystallization of some phases (e.g. coquimbite).

The zoning of sulfates and their relative abundance (Fig. 3) shows the near surface zones to be more highly oxidized than the deeper ones. Although both ferric and ferrous iron are found throughout, the latter increases in abundance with depth.

ACKNOWLEDGMENTS

The authors wish to express their appreciation to R. L. Akright for bringing the occurrence to their attention and for his guidance during their visit to the locality. Thanks are due to J. W. Gruner for his encouragement and for reading the manuscript, and to Wm. N. Lipscomb for his assistance in the single crystal studies. Clifford Frondel kindly supplied type samples of iron sulfate minerals for comparison.

REFERENCES

AKRIGHT, R. L., Geology of the Calf Mesa area, Emery County, Utah, with drilling recommendations: *RME-37, U. S. Atomic Energy Commission, 1953.*

FOSHAG, W. F., Krausite, a new sulfate from California: *Am. Mineral.*, **16,** 351 (1931).

ROSENZWEIG, A., Mineralogy of the Dexter 7 claim, San Rafael Swell, Utah, and the occurrence of a new potassium iron sulfate mineral; in Gruner, J. W., Rosenzweig, A., and Smith, D. K., Jr., Annual report for April 1, 1953 to March 31, 1954: *U. S. Atomic Energy Commission, April 1954.*

ROSENZWEIG, A., GRUNER, J. W., AND GARDINER, LYNN, Widespread occurrence and character of uraninite from the Triassic and Jurassic sediments of the Colorado Plateau: *Economic Geology,* **49,** 351 (1954).

Manuscript received June 21, 1954.

RADON LEAKAGE FROM RADIOACTIVE MINERALS*

Bruno J. Giletti and J. Laurence Kulp, *Lamont Geological Observatory (Columbia University), Palisades, New York.*

Abstract

The leakage of radon from a variety of primary and secondary uranium minerals has been measured. At room temperature pitchblende specimens show radon loss ranging from 0.064% to 16.6%; uraninite, 0.58 to 0.80%; samarskite, approximately 0.03%; carnotite, 17 to 27%; and zircon, 1.6 to 6.2%. These ranges are not maximal since only a few specimens of each type were measured, but they indicate the order of magnitude involved. Radon leakage increases with temperature such that at 150° C. it is about twice that at room temperature. Between 200 and 300° C. recrystallization ensues, reducing the internal surface area and the radon leakage.

Measurements were made under equilibrium and non-equilibrium conditions. These studies helped define the mechanism of radon leakage as one of gaseous diffusion through the microfissures of the mineral.

Application of a radon leakage correction to Pb^{206}/U^{238} ages of certain minerals brings them essentially into agreement with the Pb^{207}/U^{235} ages.

Introduction

The loss of radon from uranium minerals was first investigated at the beginning of this century in connection with studies of the various uranium and thorium decay schemes. In the process of working out the relationships between the different members of each decay series it was found that radium emanation, radon, leaked from naturally occurring minerals. This was confirmed when the daughter products were found in slightly lower abundance than expected.

Boltwood (1) obtained values of leakage ranging from 0.7% to 26% on a wide variety of uranium minerals. Lind and Whittemore (2) characterized pitchblende as leaking from three to eight per cent and carnotites from sixteen to fifty per cent.

Since these authors were interested in the decay series, they confined their attention to the material balance aspects of radon leakage relative to the other decay products. Boltwood did heat a uraninite sample in a cruicible to red heat and found that after this treatment the rate of radon loss was smaller. An investigation of the mechanism of the leakage process and of the factors affecting it was not attempted in this early work.

The present study has had a three-fold objective: (1) to study the mechanism of radon leakage; (2) to measure radon leakage as a function of temperature; (3) to define the average radon leakage for each specimen of a variety of uranium minerals, particularly those to be used for age determination. The last objective is required to correct Pb^{206}/U^{238}, $Pb^{207}/$

---

* Lamont Geological Observatory Contribution No. 162.

Pb^{206}, and Pb^{206}/Pb^{210} ages to the proper values. Loss of radon makes the 206/238 age low and the 207/206 high, whereas the effect on the 206/210 age depends on the history of the leakage. If the radon leakage has been constant for most of the lifetime of the mineral the 206/210 age will be correct.

It is postulated that radon leakage occurs by recoil of the radon atoms at "birth" from the lattice into the microfissures of the mineral. From this point, the radon is lost by gaseous diffusion through these fissures to the surrounding country rock. The relatively long half-life of radon (Em^{222}, $t\frac{1}{2} = 3.83$ days) gives time for a large fraction of the radon which enters the microfissures to escape. From the diffusion mechanism it is possible to calculate the leakage of the emanation isotopes from the other two decay series (thoron, Em^{220}, $t\frac{1}{2} = 54.5$ sec.; and actinon, Em^{219}, $t\frac{1}{2} = 3.92$ sec.). It is concluded that the leakage of these two isotopes is negligible.

EXPERIMENTAL PROCEDURE

In this investigation both equilibrium and non-equilibrium methods of measuring radon leakage were employed. All of the final results were obtained by the equilibrium method. However, the non-equilibrium methods produced results which aid in the understanding of the mechanism of radon loss.

Equilibrium Method

A suitable quantity (generally 0.5 to 30 grams) of a uranium-bearing mineral, or a rock containing such a mineral, is sealed in air in a small glass bulb. Care is taken to avoid heating the specimen while the bulb is being sealed. The bulb is stored at constant temperature for at least thirty days.

At the end of the thirty day period, the rate of leakage of radon from the specimen into the bulb should equal the rate of decay of the radon in the bulb. The reason for this steady state is that almost eight half-lives of radon will have elapsed ($t\frac{1}{2} = 3.83$ days) and it should be in secular equilibrium with its source. The size of the minerals is such that the rate of diffusion of radon out of the specimen will have reached a steady state in this time.

Now, the seal on the bulb is broken and the radon flows to an evacuated one-liter flask. The volumes of the bulb and the flask are known with sufficient accuracy so that the fraction of the radon in the flask can be defined to better than 1%. An aliquot of radon is transferred from the one-liter flask to a four-liter ionization chamber. The chamber is then filled with dry nitrogen (which has been stored at least thirty days to permit any radon originally present to decay) to a pressure of 76 cm. of mercury. Three such aliquots are taken for three chambers.

The alpha pulses, which occur in the ionization chamber as the result of the decay of radon and its daughters, are amplified and counted according to the method described by Bate, Volchok and Kulp (3). In general, the aliquots are about 0.5% of the total radon in the one-liter flask. This is sufficient to give count rates on the order of 200 to 1000 cph. Backgrounds are constant at about 20 cph. The absolute efficiency of the counting technique has been determined by the use of radium solutions of known concentration obtained from the U. S. Bureau of Standards.

Three hours after the chamber has been filled, the radon is in equilibrium with its decay products. The chamber is usually counted overnight. The radon activity in the specimen bulb at the time the seal was broken can be calculated from the counting data as follows:

Let

t_0 = time gas phase removed from mineral.
t_1 = time (in hrs.) from t_0 to start of counting.
t_2 = time (in hrs.) from t_0 at which counting is stopped.
N = number of atoms of radon in the gas phase (a subscript referring to the corresponding time).
λ = decay constant of radon (in hours).

$$N_1 = N_0 e^{-\lambda t_1} \tag{1}$$

$$N_2 = N_0 e^{-\lambda t_2}. \tag{2}$$

Subtracting

$$N_0 = \frac{N_1 - N_2}{e^{-\lambda t_1} - e^{-\lambda t_2}}. \tag{3}$$

The difference $(N_1 - N_2)$ = number of radon atoms that decayed in the counting interval. This difference is obtained experimentally by correcting the counts obtained in the interval for counter efficiency and daughter contribution. Hence, equation (3) gives the number of radon atoms initially present in the gas phase. At equilibrium (i.e. t_0), the rate of decay of these atoms = rate of diffusion from the mineral. The latter essentially is equal to the rate at which radon atoms enter the gas phase in the internal volume of the mineral.

Since

$$-\frac{dN_0}{dt} = N_0\lambda \tag{4}$$

or

$$\frac{dN_0}{dt} = \frac{(N_2 - N_1)\lambda}{e^{-\lambda t_1} - e^{-\lambda t_2}}. \tag{5}$$

Now, the rate of production of radon in the mineral grains can be assumed to be equal to the rate of decay of the uranium (i.e., secular equilibrium). Therefore

$$\frac{dN_u}{dt} = N_u \lambda u = N_{Rn}\lambda_{Rn} \tag{6}$$

where N_u is the number of uranium atoms in the specimen and $N_{Rn}\lambda_{Rn}$ is the rate of production of radon in the mineral.

$$N_u = \frac{\text{Weight } U}{238} \times 6.02 \times 10^{23} \times \frac{138}{139}. \tag{7}$$

The ratio 138/139 corrects for the U^{235} which is included in the original uranium analysis.

The radon leakage is,

$$L = \frac{N_0}{N_{RN}}, \tag{8}$$

or

$$\% L = (100) \frac{(N_2 - N_1)\lambda}{N_u \lambda_u (e^{-\lambda t_1} - e^{-\lambda t_2})} \tag{9}$$

when N_u is obtained from (7). Radon leakage is defined in (9) as the loss of radon per hour divided by the rate of production of radon from radium per hour.

Non-equilibrium Experiments

The non-equilibrium experiments were conducted in two ways—the sample was evacuated prior to accumulation or the sample was flushed with a flow of nitrogen at room temperature prior to accumulation.

Vacuum Technique

In this technique the specimen is placed in a small bulb which is part of the vacuum system. The sample bulb is evacuated four times to a pressure of less than 1 mm. Each time it is filled again to one atmosphere with dry, "old," nitrogen. This removes any radon in the container as well as some of the radon in the microfissures. After the last flush, the sample is isolated under one atmosphere of nitrogen for a definite time interval ranging from 3 to 120 minutes. At the end of this accumulation period, the N_2 and the radon which has leaked out of the mineral are flushed into the previously evacuated ionization chamber. The procedure from this point parallels that for the equilibrium method.

Flow Technique

The specimen is placed in a tube through which flows dry, old nitrogen. After the N_2 flows through for some time, the tube is isolated for the radon to accumulate. After this, the nitrogen flush is resumed, but the gases now go into the evacuated ionization chamber. The process and calculations from this point on are the same as for the vacuum technique.

THEORY AND MECHANISM OF RADON LEAKAGE

The fraction of radon generated which escapes from a mineral is dependent on the *total* surface area, the temperature, and the nature of the aggregate of mineral grains. Consider first the simplest case of isolated, homogeneous, fissure-free grains of spherical shape. The emission of such a single grain is a sum of the contributions from recoil and diffusion in the solid phase. Near room temperature the contribution from diffusion of radon in a nearly perfect crystal is entirely negligible, having values for the diffusion coefficient, D, of less than 10^{-22} cm²/sec. Even at several hundred degrees the diffusion contribution is of little importance (Keevil, 4).

A thorough theoretical investigation of the rate of escape of emanation from solids has been made by Flügge and Zimens (5). The theory given below follows their development, although the experimental investigation of the mechanism is entirely new.

If a mineral grain has a constant concentration C of radium, the number of atoms of radon generated per cc. per sec. will be $C\lambda_{Ra}$ which will equal the number of radon atoms decaying per cc. per sec. in the mineral plus the number that escape. Consider a grain of radius r_0. For geometrical reasons exactly one-half of the radon atoms generated in the surface monolayer will escape, the other half will be driven back into the grain. Of the radon atoms formed within a shell of thickness R, the recoil range, only a fraction (which must be less than $\frac{1}{2}$) will be able to escape. It can be shown that the fraction of radon atoms formed in a shell of radius r (where $r_0-R \leqq r \leqq r_0$) which will escape is

$$q(r) = \frac{2rR - (r_0^2 - R^2) + r^2}{4Rr}.$$

The total number of atoms escaping by recoil, N_r will be

$$N_r = C\lambda_{\mathrm{Ra}} 4\pi \int_{r_0-R}^{r_0} q(r) r^2 dr = C\lambda_{\mathrm{Ra}} 4\pi \left(r_0^2 R - \frac{1}{12} R^3 \right).$$

Dividing by $\frac{4}{3}\pi r_0^3 C\lambda_{\mathrm{Ra}}$, the total number of radon atoms formed per second, will give F_r, the fraction emitted due to recoil.

$$F_r = \frac{3}{4}\frac{R}{r_0} - \frac{1}{16}\left(\frac{R}{r_0}\right)^3 \quad \text{for } 2r_0 \geqq R.$$

If $2r_0 < R$, every radon atom formed will escape by recoil. R is of the order of 10^{-6} cm. for radon in minerals.

Consider the effect of total surface area on this relationship. If the density of pitchblende is taken as 10g/cc., a pitchblende composed of isolated homogeneous spheres of radius such that the surface area is $1.0\mathrm{m}^2/\mathrm{gm}$, the pitchblende would have a leakage rate (due to recoil) of about 2.5%. Actually the pitchblende is not composed of isolated spheres of UO_2, but rather is a highly irregular aggregate of microcrystals. This leads to a high total surface area, but the internal fissures are very narrow and tortuous. Therefore, a certain fraction of the radon atoms ejected from the crystals into the internal volume decay in the fissures before escaping to the exterior of the mineral. Under such conditions the observed leakage from the mineral as a whole must be less than the actual release of radon from the solid phase, but will be proportional to the total surface area.

Whatever detailed mechanism is assumed for radon leakage, the following experimental results must be satisfied.

(1) An equilibrium, or quasi-equilibrium, situation is reached in 30 days. Longer times of accumulation do not yield higher leakage rates (Table 1).

(2) Increasing the external volume surrounding the mineral from 5 cc. to 1 liter has no effect on the apparent leakage in the equilibrium (30 day) experiments. This, along with the temperature effect listed under (6), indicates that the partial pressure of radon in the external volume is negligible compared to that in the internal volume.

TABLE 1. RADON LEAKAGE AS A FUNCTION OF ACCUMULATION TIME

(Sample K-1-28)

Waiting Period (Days)	% Leakage
40	3.2 ± .1
53	3.5 ± .2
227	3.4 ± .1
	Av. = 3.3 ± .1

(3) A bulb containing a sample was connected to another bulb of equal volume by way of a stopcock and the stopcock was left open for the 30 day experiment. At the end of the experiment the stopcock was closed and the radon in the two bulbs measured separately. The radon concentration in each bulb was found to be the same, proving that a negligible additional quantity of radon is flushed out of the mineral during the evacuation to the ionization chamber after a 30 day accumulation.

(4) On the other hand, if a mineral which has been at atmospheric pressure for at least 30 days, is flushed with nitrogen at atmospheric pressure to remove radon from the external volume, then isolated to accumulate radon for 10 minutes at atmospheric pressure, and finally the gas phase evacuated into an ion chamber, the radon leakage measured in such a procedure is too high. This indicates that an appreciable quantity of the radon in the internal volume was carried out with the nitrogen when the mineral was evacuated. The reason that the radon from

TABLE 2. LEAKAGE AS A FUNCTION OF PREVIOUS HISTORY

(Sample K-1-28)

Date	Duration of accumulation time (minutes)	% Leakage	Prior Treatment
7/13/53	4.29	1.95	No prior flush
7/14	4.38	1.45	Single evacuation on 7/13
7/16	4.42	1.23	Evacuation on 7/13 and 7/14
7/18	4.42	1.27	Evacuation on 7/13, 14 and 16
7/20	4.50	.84	Four successive evacuations
7/21	4.46	.79	Four successive evacuations
7/22	4.40	.68	Four successive evacuations
7/23	4.49	.89	Four successive evacuations
7/24	4.56	1.18	Four successive evacuations

the interior is measurable in this case but not in experiment (3) is simply due to the much greater quantity of radon in the external gas phase in experiment (3).

(5) A mineral is repeatedly exposed to one atmosphere of nitrogen and evacuated. Then, after a ten minute accumulation at atmospheric pressure, the gas phase is evacuated to the ion chamber.

In this case the measured radon leakage may be higher or lower or equal to the equilibrium leakage depending on the relation of the efficiencies of the evacuations. If the last of the repeated evacuations is more efficient than the one at the end of the accumulation, the apparent radon leakage will be low. If it is less efficient, the apparent leakage will be high. Since it is difficult to control this effect, the method is not usable for quantitative leakage measurements. Table 2 shows the type of variation obtained under two conditions: (*A*) the sample was not flushed prior to accumulation and, (*B*) the sample was evacuated four times in rapid succession prior to accumulation. The identical sample was used successively and remained in vacuum between runs. All of these measurements were made on the same sample. These evacuations reduce the partial pressure of radon in the internal volume—at least in that portion which is connected with the external volume through orifices that are wide compared to several molecular diameters. The outrush of nitrogen due to the pressure gradient carries out much more radon than would leave the internal volume in the same time interval by gaseous diffusion at one atmosphere of nitrogen inside and outside.

Table 3. Comparison of Radon Leakage Measured by the Evacuation and Equilibrium Methods

Sample	% Leakage	
	Evacuation	Equilibrium
K-1	2.9	3.1
K-4	~0.1	.03
K-7	8.5	6.7
K-8	2.1	8.6
K-9	1.9	1.6
K-14	.086	.064
K-15	2.7	1.3

Table 3 shows the variation from the true (equilibrium) leakage rate obtained for a few representative samples by using the evacuation technique.

(6) If a mineral at atmospheric pressure and room temperature is isolated for 10 minutes while the temperature is raised, say from 25° C. to 100° C., radon leakage occurs which is far larger than the equilibrium value at the higher temperature. This appears due to the sudden expulsion of the expanded nitrogen in the internal volume which carries with it some of the radon. It cannot be due merely to the increase of the diffusion coefficient, or the partial pressure of radon which accompanies the temperature rise. Table 4 shows this effect for two consecutive series of runs using the evacuation technique. Prior to the first series the mineral had been left at room temperature and atmospheric pressure for several weeks so that equilibrium could be attained. There was a one day interval between series "*A*" and "*B*". The equilibrium value for this mineral is 3.3%.

TABLE 4. INITIAL RADON LEAKAGE AFTER TEMPERATURE INCREASE

Sample K-1-28

Equilibrium temperature (200° C.) attained after 20 min.

	Time from Room Temperature (Hours)	% Leakage
Run A	0:37	10.5
	1:36	6.1
	2:56	3.9
Run B	1:00	5.6
	2:14	3.2
	26:14	2.9
	53:00	3.2

(7) If equilibrium experiments are carried out as a function of temperature, the rate of radon leakage increases somewhere between $T^{3/2}$ and T^2. Results on three representative minerals are shown in Table 5. These data will be discussed in more detail later.

The temperature coefficient of the radon leakage strongly suggests that the rate determining step is that of gaseous diffusion (Jost, 6) since the rate of escape from the solid by recoil is essentially temperature independent and at temperatures of less than 400° C. the rate of diffusion in the solid is negligible. However, the diffusion coefficient for radon in air at room temperature, D, is .12 cm.^{2}/sec in an unrestricted volume. Hence, the diffusion is essentially immediate in the external volume. On the other hand, empirical D values for the rate of escape of radon from various materials have ranged as low as 10^{-22} cm.^{2}/sec. Thus the actual rate is determined by gaseous diffusion through pores of very limited cross sectional area. Consequently, a considerable fraction of the radon atoms ejected into the internal volume may decay before they have time to diffuse into the external volume.

For a given mineral the uranium concentration, surface area, cross sectional area, internal volume, and temperature determine the partial pressure of radon in the internal volume. Since the partial pressure of radon in the external volume is always essentially zero, the effective rate of radon loss from the geometrical surface of the mineral is determined only by the partial pressure of radon in the interior, the temperature, and the cross sectional area available for leakage. All three factors will influence the rate of diffusion.

TABLE 5. EFFECT OF TEMPERATURE ON RADON LEAKAGE

(Equilibrium values)

Sample	Temperature (° C.)	% Leakage
K-1-28	25	3.3 ± .1
K-1-28	100	5.1 ± .3
K-1-28	140	5.5 ± .5
K-1-28	200	5.8 ±1.0
K-1-28	320	2.6 ± .3
K-6	25	2.5 ± .3
K-6	85	3.5 ± .5
K-6	200	9.6 ±1.2
K-6	320	3.6 ± .1
K-14	25	.06 ± .01
K-14	200	.16 ± .03
K-14	320	.44 ± .04

There are then two ways to measure the actual radon leakage. First, to flush the external gas phase at one atmosphere, accumulate for a known interval of time, and then flush this quantity of radon out of the external volume at atmospheric pressure into a counter. Second, accumulate the radon for a sufficiently long period of time (i.e., 30 days) so that equilibrium is established between the number of radon atoms being emitted from the geometrical surface of the mineral per unit time and the number decaying in the external volume per unit time. Only the latter procedure has been employed in the present study.

Any non-equilibrium experiment involving evacuation of the sample and short accumulation times will yield variable apparent leakages depending on the previous history of the mineral and the efficiency of the evacuation.

If the internal volume and the total surface area can be measured, the average life of a radon atom in the internal volume and the partial pressure can be calculated. Both of these measurements are physically possible. A reconnaissance surface area determination by the *BET* gas adsorption method using the apparatus and procedure described elsewhere (Kulp and Carr, 7) on one pitchblende which had a leakage of several per cent, gave a surface area of about a square meter per gram in good agreement with theory. Further support for the large internal surface area of these pitchblendes is afforded by the data of Table 6 which shows that increasing the geometrical surface area does not change the leakage. This shows the external surface area to be a negligible fraction of the total surface area.

TABLE 6. VARIATION OF RADON LEAKAGE WITH SIZE OF SPECIMEN

Sample Number		% Leakage
K-1-L	Single Piece (34.8 gms.)	3.0±0.4
K-1-28	Between 28 and 48 Mesh	3.3±0.1
K-1-48	Between 48 and 100 Mesh	3.0±0.6
K-1-200	Finer than 200 mesh	3.8±0.5

RADON LEAKAGE MEASUREMENTS AT ROOM TEMPERATURE

The data obtained by measuring the radon leakage of a variety of minerals at room temperature are given in Tables 7 and 8.

The leakage from pitchblende varies from .064% to 16.6% depending on the structure of the specimen. The 16.6% leakage was obtained from a rock containing extremely finely dispersed pitchblende. The Contact Lake pitchblende occurs in narrow wavy bands up to .02 mm. across. The Marysvale, Utah, sample which gave a 7.5% leakage was a fine powder consisting of aggregates less than .03 mm. in diameter. The Sunshine Mine material is somewhat coarser, having an average grain diameter of .05 mm. The Eldorado Mine sample which had only 0.27% leakage was relatively massive, commonly showing unfractured areas up to 0.2 mm. in diameter. The Nicholson sample K-19 is similar to K-18 in polished sections. The lowest leakage was obtained from K-14 which was colloform pitchblende in hematite-carbonate gangue. The pitchblende is banded, the inner zones being largely unfractured. The width of the bands may be as large as 0.7 mm. Samples K-30 through K-68 are all pitchblende concentrates without detailed polished section descriptions. The radon leakage for these samples lies in the range of the more completely described samples above.

The radon leakage for a representative set of uranium-bearing minerals is shown in Table 8. The uraninite falls in the range of the more massive pitchblende samples. The carnotite is very high as expected for a porous, poorly-crystallized, secondary uranium mineral. The considerable leakage obtained from the zircon samples is somewhat surprising since the samples were single crystals with well-formed faces. The specimen from Brazil had about three times the α activity and was considerably more metamict than the one from Madagascar.

TABLE 7. RADON LEAKAGE OF PITCHBLENDE SPECIMENS

Sample Number	Location	Size	% Leakage
K-1	Sunshine Mine, Idaho; 3100 ft. level	28–48 mesh	3.1 ±.4
K-6	Rickards Mine, Gilpin Co., Colorado	Lump with silicates	2.5 ±.3
K-7	Contact Lake, N.W. Terr., Canada	Lump with silicates	6.7 ±.1
K-8	German and Belcher Mine, Central City, Colorado	Lump with silicates	8.6 ±.2
K-9	Katanga, Belgian Congo	Massive pitchblende	1.61 ±.05
K-13	Marysvale, Utah; 300 ft. level	Powder	7.5 ±.7
K-14	Eagle Mine, L. Athabasca, Canada; 200′–300′ level	Pea size	.064±.008
K-15	Joachimsthal	Pea size	1.3 ±.1
K-18	Eldorado Mine, Gt. Bear Lake, Canada; 913 Stope	Pea size	0.27 ±.08
K-19	Nicholson Mine	Pea size	0.34 ±.05
K-21	Upper Huronian Iron Formation, Michigan	Very finely disseminated in silicate matrix	16.6 ±.3
K-30	Pitch Ore Group	Pitchblende concentrate	2.9 ±.4
K-32	Martin Lake Mine, Canada	Pitchblende concentrate	.23 ±.02
K-34	Rix (Leonard Series) Adit, Goldfields, Canada	Pitchblende concentrate	.72 ±.05
K-45	Ace Mine, L. Athabasca, Canada	Pitchblende concentrate	1.90 ±.09
K-48	Ace Mine, 1st level, L. Athabasca, Canada	Pitchblende concentrate	2.51 ±.07
K-54	Ace Mine, L. Athabasca, Canada	Pitchblende concentrate	4.3 ±.4
K-55	Ace Mine, L. Athabasca, Canada	Pitchblende concentrate	0.26 ±.03
K-68	Lee Lake, Loc-Larange, Saskatchewan	Pitchblende concentrate	5.2 ±.3

RADON LEAKAGE AS A FUNCTION OF TEMPERATURE AND PRESSURE

As shown in Table 5 the radon leakage of radioactive minerals increases with temperature up to 200° C. with a functional relationship of about $T^{3/2}$ indicative of a gaseous diffusion process. The increase in leakage is largely due to the increase of the diffusion coefficient with temperature, although the partial pressure of radon may also contribute.

The sharp decrease in radon leakage at 320° C. is due to a phase change (recrystallization) presumably to U_3O_8 as shown by Kerr (8) which occurs somewhere between 200 and 400° C. depending on the nature of the pitchblende. This effect is enhanced in air but the reaction occurs even in vacuum since all pitchblende contains appreciable UO_3 due in part to auto-oxidation as the uranium decays into lead.

TABLE 8. RADON LEAKAGE OF VARIOUS MINERALS

Sample Number	Mineral	Description	Source	% Leakage
P-2	Uraninite	Lump	Flat Rock Mine, Spruce Pine, N.C.	.58 ± .09
P-3L	Uraninite	Lump	Crabtree Creek, Yancey Co., N.C.	.80 ± .08
K-3	Samarskite	Lump	Mitchell Co., N.C.	0.026±0.008
K-4	Samarskite	Lump	Wiseman Mine, Beaver Creek, Mitchell Co., N.C.	0.030±0.002
LL-1	Autunite	Flakes	Mt. Painter, So. Australia	5.9 ± .3
LL-2	Carnotite	Disseminated	Camp Marvel, Naturita, Colo.	17.3 ±1.0
LL-5	Carnotite	Disseminated	Copper Prince Mine, Rock Creek, Colo.	27.1 ±0.8
Z-16	Zircon	Crystal	Brazil	6.2 ±0.1
LL-6	Zircon	Crystal	Ambotofotsky, Madagascar	1.59 ±0.13
K-73	Brannerite	Pea Size	Crocker's Well, So. Australia	6.0 ±0.3

U_3O_8 has not been reported in natural uraninites so it may be presumed that at least those that have been studied by *x*-ray diffraction techniques have not been subjected to temperatures exceeding 200–300° C. since they were emplaced. To obtain the integrated radon leakage for the life history of a mineral it is necessary to measure the leakage as a function of temperature up to the temperature at which phase changes occur and to estimate the thermal history of the mineral.

In this study no experimental attempt has been made to assess the effect of pressure. The pressure effect on the velocity of radon atoms in the gas phase would be quite trivial. On the other hand, if the fissures were closed, the leakage would be reduced in proportion to the cross sectional area available for diffusion. However, the evidence suggests that most of the lifetime of the mineral has been spent at temperatures less than 200° C., which is equivalent to a depth of about 7 km. At this depth rocks are still quite porous and unmetamorphosed, hence, it is not likely that the pressure effect is an important one. An independent confirmation of this conclusion comes from the application of radon leakage to correct the 206/238 ages as will be discussed in the following section. The radon leakage correction never overcorrects the age, which would be the case if the average radon leakage during the life of the mineral was measurably less than that observed in the laboratory at one atmosphere confining pressure.

APPLICATION TO AGE DETERMINATION

As has been pointed out in some detail (Kulp, Bate and Broecker, 9) the leakage of radon from radioactive minerals can explain several of the important and consistent anomalies in the ages obtained from the isotopic ratios Pb^{206}/U^{238}, Pb^{207}/U^{235}, Pb^{207}/Pb^{206}, and Pb^{206}/Pb^{210}. In almost all of the reported ages based on these ratios, the 206/238 age is lower than the 207/235. The 207/206 age which is dependent on these two is exponentially affected by slight differences in the ratio, hence the loss of small quantities of radon make this age very high. It is only for minerals older than 1×10^9 years that the percentage error in the 207/206 age due to radon loss approaches the error in the 206/238 age.

The 206/210 age bears a more complex relation to the radon leakage since Pb^{210} occurs below radon in the uranium decay series. Therefore, if the radon leakage has remained constant throughout the life of the mineral the 206/210 age will be correct. If the leakage was much higher during most of the history of the mineral than it was during the past million years, the age derived from this ratio will be low and will approach the 206/238 age. In most cases the 206/210 age will be between the 206/238 and 207/235 ages.

In all cases, the correction for radon leakage improves the agreement of the ages. The minimum correction can be obtained by simply measuring the leakage at room temperature. On the other hand, the correction derived from the radon leakage at the average temperature at which the mineral has existed for its history should give complete agreement unless other factors are influencing the isotopic ratios.

Since the half-life of radon is 3.83 days while that of thoron is 5.45 sec. and actinon 3.92 sec., the quantity of these two cousins which will leak will be 10^{-4} and 10^{-5} times as much as radon respectively. It is clear, therefore, that of these three noble gases only radon leakage need be considered in age determination work.

A few selected age determinations are shown in Table 9.

The ages are given uncorrected for radon leakage, corrected for the radon leakage at room temperature and in two cases (K-6 and K-14) for the experimental values at higher temperatures. The Gilpin County pitchblendes which have presumably had average temperatures during their geologic history of some 100° C. or less, yield good agreement in the isotopic ages when corrected for radon leakage. The correction for room temperature radon leakage for the Katanga sample is not quite enough to bring agreement, but this value is probably only about half of that for the average temperature for the life of the pitchblende.

TABLE 9. EFFECT OF RADON LEAKAGE ON AGES FROM VARIOUS ISOTOPIC RATIOS

(Ages in Millions of Years)

Lamont Sample No.	Locality	% Radon Leakage	206/238	207/235	207/206	210/206
K-6	Gilpin Co., Colo.	U	55 ± 2	64 ± 15	—	61 ± 3
		(25° C.) 2.5	56 ± 2	—	—	—
		(100° C.) 4.0	57 ± 2	—	—	—
K-8	Central City, Colo.	U	51 ± 1	56 ± 5	—	58 ± 3
		(25° C.) 8.6	55 ± 1	—	—	—
		(100° C.) 12*	57 ± 1	—	—	—
K-9	Katanga, Belgian Congo	U	575 ± 4	595 ± 5	630 ± 40	—
		(25° C.) 1.6	585 ± 4	—	595 ± 40	—
K-7	Contact Lake	U	840 ± 5	960 ± 15	1220 ± 50	864 ± 35
		(25° C.) 6.7	896 ± 5	—	1100 ± 45	—
K-14	Eagle Mine, 200′–300′, L. Athabasca, Canada	U	1425 ± 10	1450 ± 20	1530 ± 40	1448 ± 35
		(25° C.) .06	1425 ± 10	—	—	—
		(150° C.) .1	1430 ± 10	—	1525 ± 40	—

* Estimated from K-6.

The radon leakage of the Contact Lake specimen is high even at room temperature. By analogy with other similar specimens, taking into account the average temperature estimated at 150° C., the actual integrated leakage should approach 15% which would bring the 206/238 and 207/206 ages into line with the 207/235. This suggests that leaching of uranium or lead has been negligible. It is noteworthy that in this case, the uncorrected 210/206 age agrees with the uncorrected 206/238 age. This is expected whenever the average radon leakage for the mineral is much greater than the present room temperature leakage.

The Eagle Mine sample is an unusually compact specimen, showing low radon leakage. The integrated radon leakage would only have to be about 1.5% to account for the discrepancies in the ages.

The importance of radon leakage in age determination can also be seen in the results obtained on minerals of intermediate radioactive content analyzed for uranium and lead by isotope dilution techniques by Aldrich et al. (11). For zircons from the Essonville granite and the Cape granite, the radon leakage required to bring the 206/238 up to the 207/235 age would be 3% and 7%, respectively. It is noteworthy that the required radon leakage for these zircons lies approximately within the range shown by the zircons measured in this study.

It is concluded that radon leakage measurements are necessary in order to estimate the correction to be applied to 206/238 ages. If this is done as a function of temperature, if the average temperature of the mineral can be approximated, and if no leaching has occurred, the 207/206 age agrees with the corrected 206/238 and the 207/235 age for a considerable variety of specimens. If leaching is absent it appears that the 207/235 age is the most reliable. Conversely, if these three isotopic ages agree after correction for the radon leakage, leaching of uranium and lead are probably absent.

ACKNOWLEDGMENTS

The uranium analyses used to calculate the radon leakage were done by Ledoux and Co., Teaneck, N. J., and the A.E.C. Analytical Laboratory, New Brunswick, N. J. The authors are particularly grateful for the cooperation of Drs. C. J. Rodden and J. J. Tregoning of the New Brunswick Laboratory. At various stages in the study laboratory assistance was supplied by G. L. Bate, H. L. Volchok, and Dr. R. Holtzman. Discussions with D. R. Carr, G. L. Bate, H. L. Volchok, and W. R. Eckelmann were profitable. Mr. Wolfgang Elston examined polished sections of several of the specimens under the polarizing microscope. This research was supported by the Atomic Energy Commission under Contract *AT(30-1)-1114.*

REFERENCES

1. Boltwood, B. B., On the radioactivity of uranium minerals: *Am. Jour. Sci.* **25,** 4th Series, 269–298 (1908).
2. Lind, S. C., and Whittemore, C. F., The radium: uranium ratio in carnotities: *Jour. Am. Chem. Soc.*, **36,** 2066–2082 (1914).
3. Bate, G. L., Volchok, H. L., and Kulp, J. L., A low level radon counting system: *Rev. Sci. Instr.*, **25,** No. 2, 153–157, (1954).

4. Keevil, N. B., Interatomic forces and helium in rocks: *Proc. Am. Acad. of Arts and Sciences*, **73,** 311–359 (1940).
5. Flüge, S., and Zimens, K. E., *Z. Physik. Chem.*, **B42,** 179 (1939).
6. Jost, W., Diffusion in solids, liquids and gases: Academic Press, Inc., New York, (1952)
7. Kulp, J. L., and Carr, D. R., Surface area of deep sea sediments: *Jour. Geol.*, **60,** 148–159 (1952).
8. Kerr, P. F., Mineralogical studies of uraninite and uraninite-bearing deposits: *A.E.C., N.Y. Operations Office Interim Technical Report,* July 1, 1949–June 30, 1950.
9. Kulp, J. L., Bate, G. L., and Brocker, W. S., Present status of the lead method of age determination: *Am. Jour. Sci.* (in press for June 1954.)
10. Aldrich, L. T., Davis, G. L., Nicolaysen, L. O., and Tilton, G. R., Isotope dating of ancient igneous intrusives: *Dept. of Terr. Mag., Carnegie Inst., Annual Report for 1953.*

Manuscript received June 14, 1954.

WAVELLITE SPHERULITES IN THE BONE VALLEY FORMATION OF CENTRAL FLORIDA[1,2]

M. H. BERGENDAHL, *U. S. Geological Survey, Washington, D.C.*

ABSTRACT

Megascopic spherulitic aggregates of wavellite have been recently found in the Florida land-pebble phosphate field.

Petrographic studies were made to establish the identity of the mineral. Chemical and spectrographic data revealed the spherulites to be practically pure wavellite; the remainder is composed of phosphatic cement partly altered to wavellite.

The origin of wavellite is considered to be secondary, a replacement of apatite that has undergone ground-water leaching.

ACKNOWLEDGMENTS

The writer appreciates greatly the assistance and cooperation rendered by J. C. Rabbitt and Z. S. Altschuler, U. S. Geological Survey. Acknowledgments are due to the following for the chemical and spectrographic analyses made in the laboratories of the Geological Survey: Alexander Sherwood, B. A. McCall, and Charles Annell. The writer appreciates the courtesies extended by the F. S. Royster Guano Company. This report concerns work done on behalf of the Division of Raw Materials of the U. S. Atomic Energy Commission.

INTRODUCTION

An unusual occurrence of crystalline wavellite has been recently discovered in a sample taken from a phosphate prospect hole on the Royster tract, Sec. 14, T. 30 S., R. 25 E., in Polk County, Fla. The mineral was found in the leached zone of the Pliocene Bone Valley formation. Although clay-sized and barely visible wavellite has been described previously in the upper part of the Bone Valley formation (Altschuler and Boudreau, 1949), this mineral has never before been reported there as megascopic crystalline aggregates. The large size of the wavellite aggregates permitted isolation of the pure mineral for petrographic studies without the inconvenience of contamination by quartz sand or phosphate nodules.

GENERAL GEOLOGY

The rocks exposed within the Florida land-pebble phosphate field are considered by most writers to range from lower middle Miocene to Pleis-

---

[1] This report concerns work done on behalf of the Division of Raw Materials of the U. S. Atomic Energy Commission.

[2] Publication authorized by the Director, United States Geological Survey.

tocene age. All are thin, nearly flat-lying sediments. The oldest stratigraphic unit is the Hawthorn formation of Miocene age, a fossiliferous phosphatic limestone, interbedded with sand and clay. The Hawthorn formation is overlain unconformably by the Pliocene Bone Valley formation, a karst topography having been developed on the Hawthorn during late Miocene time. The Bone Valley formation is composed of two major lithologic units: the lower, a bedded marine phosphorite, containing phosphate nodules, quartz sand, and clay; and the upper, a leached zone, a white to gray-brown clayey sand, cemented in places into porous nodules and boulders by secondary phosphate, pseudowavellite, and wavellite. Near the bottom of the leached zone, crumbly gray phosphate pebbles are present. The lower part of the Bone Valley formation constitutes the economic phosphate deposit of the land-pebble phosphate field.

Cathcart and others consider the leached zone to have been formed during the interval between post-Bone Valley and pre-Pleistocene inundation, during which time the phosphate deposits were exposed at the surface. Downward-percolating ground water removed the soluble calcium phosphate and redeposited aluminum phosphate. Channels were eroded into the upper part of the Bone Valley formation before the encroachment of Pleistocene seas.

Pleistocene deposition is represented by loose quartz sands which are exposed at the surface throughout most of the land-pebble field.

More complete discussions of the geology may be found elsewhere (Cathcart 1950; Altschuler and Boudreau 1949; Cathcart and Davidson 1952; Cooke 1945).

DESCRIPTION

The wavellite crystals are in the form of spherulitic aggregates ranging in diameter from 1 mm. to 11 mm. Some individual spherulites attain diameters of 9 mm. Both concentric and radial structures occur. Radial structures are produced by the arrangement of individual bladed crystals about a core or nucleus of short doubly terminated crystals, often of different orientation from the radiating crystals.

The spherulites are composed of several concentric layers of large crystals. The cores of some spherulites consist of groups of feathery crystals. Each layer of large radial crystals in a spherulite is separated from the next by sheaves of bladed crystals which appear megascopically as a concentric line (Fig. 1). These tiny sheaves fill interstices around the outer edges of the larger crystals. Many of them seem to radiate about a nucleus. The small size and concentric arrangement of these small aggregates of crystals suggest an interruption of crystallization during the growth of the spherulite caused possibly by a change of environmental conditions.

PETROGRAPHY

Indices of refraction which were determined from crushed fragments ($-100+120$ mesh) are as follows: α 1.52–1.53, β 1.53–1.54, γ 1.55. All crystals examined exhibited parallel extinction under crossed nicols (Fig. 2). The only distinguishable interference figure obtained was a centered optic axis figure, from which the positive characteristics of the mineral were determined. The dispersion was $r > v$, barely perceptible.

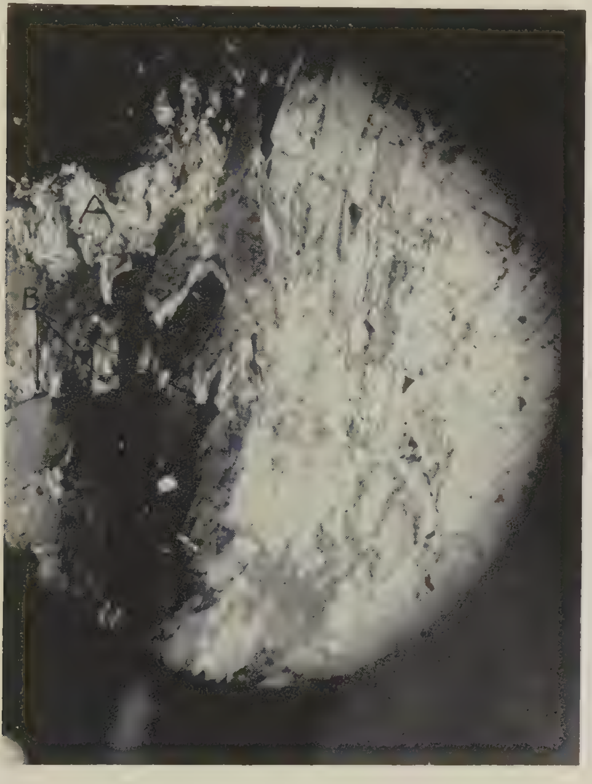

FIG. 1. Portion of spherulite showing radial arrangement of wavellite crystals. Part of concentric structure marked by cryptocrystalline sheaves of wavellite at *B*. Partly replaced phosphatic cement in upper left at *A*. Crossed nicols, ×70.

Five thin sections were made of individual spherulites and aggregates. All of these except one (Fig. 3) were almost pure wavellite. Figure 3 is a thin section made from a spherical aggregate of detrital quartz grains cemented by a network of microscopic wavellite rosettes. The spherical form is due to the habit of wavellite crystal growth, radially in all dimensions about a central nucleus or core. All five thin sections reveal the presence of a brown secondary phosphatic cement (described by Altschuler and Boudreau, 1949) which forms an irregular thin coating around the spherulites and also lines cracks and fills interstices between wavellite crystals. Most thin sections show this phosphatic cement partly replaced by cryptocrystalline wavellite.

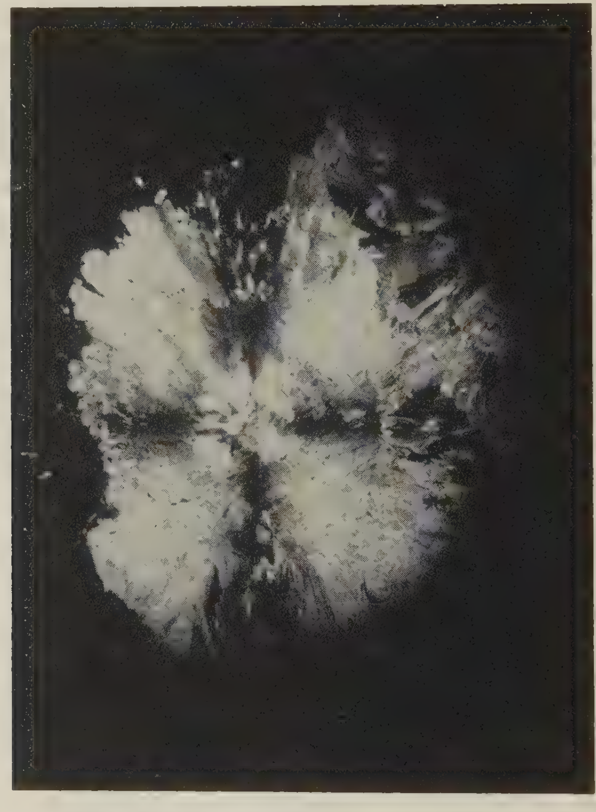

Fig. 2. Spherulite exhibiting extinction cross by radiating wavellite crystals. Crossed nicols, ×20.

Mineralogy and Chemistry

Both chemical and spectrographic analyses (Tables 1 and 2) were made of the wavellite.

Using the formula for wavellite, $Al_6(F,OH)_6(PO_4)_4 \cdot 9H_2O$ (Winchell, 1951), the molecular percentages of Al_2O_3 and P_2O_5 were computed as

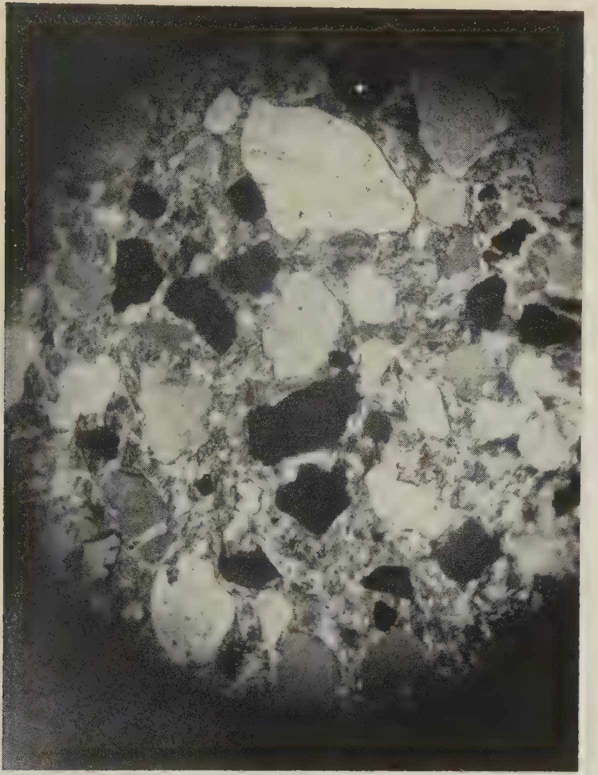

FIG. 3. Quartz grains cemented by cryptocrystalline wavellite. Section of a spherical aggregate. Crossed nicols, ×70.

TABLE 1. PARTIAL CHEMICAL ANALYSIS*

	Per Cent
Equivalent U	0.002
Al_2O_3	33.3
CaO	0.00
F	0.93
Fe	0.16
P_2O_5	33.0
SiO_2	1.62
U	0.003
Total	69.015

* Analysts: Alexander Sherwood, chemistry; B. A. McCall, radiation.

TABLE 2. SPECTROGRAPHIC ANALYSIS*

Elements	Per Cent
Al, P	Over 10
———	1–10
Si	0.1 – 1.0
Fe, Mg	0.01 – 0.1
Sr, Cr, V, Ti	0.001 – 0.01
———	0.0001– 0.001

* Analyst: Charles Annell.

38 per cent and 35.2 per cent, respectively. The formula for wavellite given in Dana's System of Mineralogy (Palache et al., 1951) is $Al_3(OH)_3(PO_4)_2\cdot 5H_2O$, with the constituents in the following percentages:

Al_2O_3	37.11
P_2O_5	34.47
H_2O	28.42
Total	100.00

Analyses of wavellite in Dana list Al_2O_3 from 31.01 to 37.44 per cent and P_2O_5 from 32.72 to 34.16 per cent. The chemical analysis (Table 1) lists Al_2O_3 as 33.3 per cent and P_2O_5 as 33.0 per cent, well within the limits of the analyses cited in Dana.

This departure of Al_2O_3 and P_2O_5 from the theoretical formula percentages can be explained. Altschuler states (written communication, Sept. 9, 1952) that small amounts of constituents not detectable spectrographically and not listed in the chemical analysis, or small amounts of one or more additional secondary hydrous aluminum phosphates, could alter the theoretical ratio of Al_2O_3 to P_2O_5, even though the sample is essentially pure wavellite. In addition, excess water could account for the P_2O_5 and Al_2O_3 deficiency.

The 1.62 per cent SiO_2 in Table 1 is assumed to be detrital quartz. Figure 3 shows that quartz is incorporated in some of the spherulites. The sample analyzed was composed of a number of spherulites, none of which were examined microscopically. It is not improbable that some detrital quartz could have been present in the sample. Fluorine can substitute for OH, and Fe may be present in small amounts in wavellite, substituting for Al_2O_3 (Altschuler and Boudreau, 1949). The absence of CaO in the analysis precludes the possibility that apatite, $Ca_5(F,Cl)P_3O_{12}$, or pseudowavellite, hydrous phosphate of Al and Ca, is present in the phosphatic cement. The chemistry and mineralogy of uranium in the leached zone are under study by others and are beyond the scope of this paper.

ORIGIN AND SIGNIFICANCE

Altschuler and Boudreau (1949) have discussed the origin of wavellite. They state that wavellite is formed by the leaching action of ground water on apatite; CaO is removed in solution, and Al^{+++}, presumably introduced from clay minerals, combines with the P_2O_5 from apatite to form wavellite. Prior to leaching, the apatite was present as phosphate pebbles and possibly also as a primary cement. Leaching resulted in redeposition of a secondary cement or glazed phosphate composed of varying percentages of apatite, pseudowavellite, and wavellite.

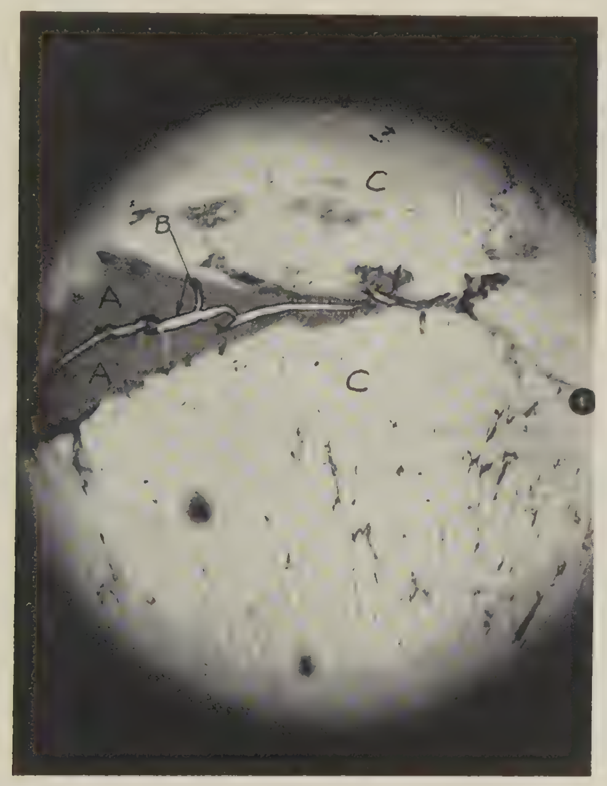

FIG. 4. Section of two spherulites with phosphatic cement filling space between them. Two generations of phosphatic cement line the cavity, the earlier (*A*) partly replaced by wavellite. The later generation (*B*) lines the large crack and fills small cracks and cavities in the earlier generation. The later phosphatic cement is darker. Wavellite crystals designated by *C*. Uncrossed nicols, ×70.

Figure 4 shows two generations of phosphatic cement lining a cavity between two wavellite spherulites. The earlier generation is partly replaced by wavellite; the later coating lines the cavity and is unreplaced. It is apparent from these relationships that some phosphatic cement was deposited after the wavellite crystallization ceased. Possibly a rise in the water table was responsible for the later deposition.

It is reasonably evident that the development of the large wavellite spherulites was dependent on three conditions:

1. The presence of sufficient phosphatic cement or phosphate nodules to supply the necessary P_2O_5.
2. High permeability in the leached zone to permit adequate circulation of ground water and enable the growth of large crystals.
3. The proximity of clay minerals or some other source of Al_2O_3.

The chemical composition of the sample (Table 1) shows the absence of CaO, thus removing the possibility of pseudowavellite being present as an intermediate mineral in the alteration, and also the consideration of the brown phosphatic cement as apatite.

REFERENCES

ALTSCHULER, Z. S., AND BOUDREAU, C. E. (1949), A mineralogical and chemical study of the leached zone of the Bone Valley formation of Florida: a progress report: *U. S. Geol. Survey Trace Elements Investigations Rept.* **102**.

CATHCART, J. B. (1950), Notes on the land-pebble phosphate deposits of Florida: *Symp. on min. res. of the southeastern U. S., Univ. of Tenn. Press.*

CATHCART, J. B., AND DAVIDSON, D. F. (1952), Distribution and origin of phosphate in the land-pebble phosphate district of Florida: *U. S. Geol. Survey Trace Elements Investigations Rept.* **212**.

COOKE, C. W. (1945), Geology of Florida: *Florida Geol. Survey, Bull.* **29**.

PALACHE, CHARLES, BERMAN, HARRY, AND FRONDEL, CLIFFORD (1951) Dana's System of Mineralogy, vol. 2, seventh edition, pp. 962–964.

WINCHELL, A. N. (1951), Elements of Optical Mineralogy, fourth edition, Part II, p. 209.

Manuscript received April 24, 1955.

SCAWTITE FROM CRESTMORE, CALIFORNIA

JOSEPH MURDOCH, *University of California at Los Angeles, California.*

ABSTRACT

An occurrence of scawtite has been discovered in the contact zone at Crestmore, California. This is the first on record for California, and the fourth known anywhere, to date. The mineral is in bundles of thin tabular crystals, strongly resembling in habit and mode of occurrence the original find at Scawt Hill. Crystals are in general poor, but it has been possible to make approximate measurements on selected individuals, and to confirm these with x-ray study of single crystals. The forms present are as follows: {100}, {110}, {120}, {130}, {010}, and {101}. The a-pinacoid is always dominant, with the prisms narrow and poorly developed. The mineral is monoclinic, probable space group $I\ 2/m$, with the following unit cell dimensions:

$$a_0 = 10.22\ \text{Å}, \quad b_0 = 15.42\ \text{Å}, \quad c_0 = 6.70\ \text{Å}$$
$$a:b:c \quad 0.6628:1:0.4345 \quad \beta = 100°29'$$

Powder photographs, which can be completely indexed, show the following spacings and intensities for the stronger lines: 3.04 Å—10, 3.01 Å—5, 2.49 Å—5, 2.236 Å—5, 1.898 Å—6.

The crystals have been oriented with Tilley's {001} as {100}, giving simpler indices for the forms, and a less oblique unit cell.

OCCURRENCE

Specimens collected on the 910 foot level of the Commercial quarry, Crestmore, California, showed a colorless mineral in thin veins in a matrix of massive diopside-wollastonite-spurrite rock. Where the veins are incompletely filled, crystals of this mineral are abundantly developed. Examination showed these crystals to be nearly square tablets with one edge always bevelled, and almost invariably occurring in sub-parallel aggregates, exactly like bundles of shingles. Chemical and optical tests showed the mineral to be scawtite, which has been found in similar crystalline groups only at Scawt Hill, County Antrim, Ireland, Tilley (1930), and Ballycraigy, Larne, N. Ireland, McConnell (1954). One other occurrence is known, but only as microscopic lath-like grains in a thin section of contact zone material from south of Neihart, Montana, Taylor (1935).

The Crestmore occurrence matches closely that described by Tilley, the mineral being one of the latest in the hydrothermal series, and having precisely the same habit. In general, the scawtite is the latest mineral to form in the veins in which it appears, overlying and enveloping calcite crystal. However, in at least one specimen, small bead-like calcite crystals were noted perched on the surface and edges of the scawtite. In another, delicate tufts of white needles and blades of an unidentified mineral occur closely associated with the scawtite, and seem to be essentially contemporaneous with it. Many scawtite veins show a zone of radiating clusters of a bladed unidentified mineral usually along one side of the vein, upon which the scawtite has been deposited. The blades of the unknown mineral are extremely thin obliquely rhombic plates, with extinction parallel to the longer edge of the rhomb.

Associated with the massive scawtite in one or two of the veins, are fine-grained sugary aggregates of bultfonteinite, which also appears in similar massive veins of afwillite, which was recently identified from Crestmore by Switzer and Bailey (1953). A description of this mineral, with *x*-ray study, is in preparation, and will be presented shortly.

PROPERTIES AND MORPHOLOGY

Sections parallel to the broad plates show parallel extinction, with the acute bisectrix emerging just outside the field of view, and giving a positive figure. 2 V is large (Tilley notes 74° ±.) A fair cleavage is present parallel to {010}, and sections with this orientation show an extinction angle of approximately 28°. Tilley records a cleavage parallel to {100}, but this may well be a parting, due to twinning on this face. Many rod-like inclusions with much lower index were observed in some sections. Indices of refraction of the Crestmore material check satisfactorily with recorded values.

The Crestmore scawtite is readily soluble in HCl, with moderate effervescence, leaving a residual skeleton of silica. It gives good microchemical tests for SiO_2 and CaO. In the closed tube the mineral decrepitates, and gives off water. Before the blowpipe it is infusible, but whitens and glows when heated intensely. No strong flame coloration was observable.

Using the large face as the front pinacoid, the following forms were observed: {100} always present and dominant, but usually somewhat uneven, and showing thin slabs of subsidiary crystals, {010} usually present, very shiny; {101} always present, normally shiny, and almost always giving multiple reflections, due to the aggregation of many flat crystals; {130} narrow, but often present as one or two faces; {120} and {110} narrow, and rarely present. Two faces of {011} are present on one crystal. It was possible to select crystals which were simple enough to measure on the reflecting goniometer, although without any great degree of precision. Only doubtful numerical indices could be assigned to the prisms from these measurements, but these could be confirmed from the *x*-ray measurements. Using these *x*-ray data, the angle table for observed forms has been calculated, and is presented below in Table 1.

Actual measurements for rho of {101} range from 39° 15′ to 43° 40′, with best probable values of about 42°. For {130} several readings gave 26° 33′ or 27° 18′; for {120} 40° 12′; and for {110} 56° 31′.

TABLE 1. SCAWTITE ANGLE TABLE

Monoclinic, Space Group *I* 2/*m*

$a_0:b_0:c_0=10.22:15.42:6.70$, $\beta=100°29'$
$a:b:c=0.6628:1:0.4345$
$p_0:q_0:r_0=0.6556:0.4273:1$
$r_2:p_2:q_2=2.3406:1.5344:1$
$p_0'=0.6667$, $q_0'=0.4345$, $e_0'=0.1850$

	ϕ	ρ	ϕ_2	$\rho_2=B$	A	C
b 010	90°00′	0°00′	—	0°00′	90°00′	90°00′
a 100	90 00	90 00	0 00	90 00	79 31	0 00
k 130	27 05	90 00	0 00	27 05	85 14	62 55
l 120	37 29½	90 00	0 00	37 29½	83 37½	52 30½
m 110	56 54½	90 00	0 00	56 54½	81 12	33 05½
011	23 04	25 17	79 20	66 52	80 22	23 08
d 101	90 00	40 25	49 35	90 00	29 54	49 35

One poor prism face with $\phi=18°03'$ was observed. This might doubtfully be {290} (calculated $\phi=18°50'$).

Transformation formula, Murdoch/Tilley $=00\bar{1}/010/100$.

X-RAY STUDY

By careful selection it was possible to isolate two crystals which were satisfactory for single crystal *x*-ray measurement, although even these were multiple, but with orientations so slightly varied as not to make trouble. One of these was rotated about *c*, and the other about *b*, so that all three directions could be adequately measured. Rotation, equator and first-layer line Weissenberg photographs were taken with filtered iron radiation, and the three cell-dimensions were calculated from these. Translations on the *b* and *c* axes were measured on the rotation photographs, and the layer-line pictures measured, using both top and bottom halves of the films. From these measurements, using as many as four or five orders of diffraction, and correcting for lack of uniformity in crystal dimensions, the values of a_0, b_0 and c_0 were calculated. The values thus arrived at are as follows:

$$a_0\ 10.22 \pm 01\ \text{Å}, \qquad b_0\ 15.42 \pm 01\ \text{Å}, \qquad c_0\ 6.70 \pm 01\ \text{Å}.$$

μ, measured directly on the Weissenberg film, and checked on the Schneider construction, is 79°31′, so that beta is 100°29′. Systematic

TABLE 2. *X*-RAY POWDER DATA FOR SCAWTITE

Cu K_α radiation, Angstrom units

d/n		*hkl*	*I*
Obs.	*Calc.*		
8.40	8.418	110	1
7.75	7.71	020	½
6.05	6.06	011	3
	6.037	$\bar{1}01$	
5.03	5.11	200	2
	5.103	101	
4.76	4.778	210	½
	4.753	$\bar{1}21$	
4.56	4.576	130	4
4.22	4.256	121	3
	4.232	$\bar{2}11$	
	4.211	220	
4.05	4.052	031	½
3.83	3.81	040	2
3.57	3.594	240	3
	3.584	211	
3.357 Fe	3.35	002	½
3.24	3.24	$\bar{1}12$	3
	3.274	310	
3.04	3.03	022	10
	3.057	240	
	3.076	141	
3.017 Fe	3.018	$\bar{2}02$	5
2.97 Fe	2.982	$\bar{3}21$	1
	2.963	$\bar{2}12$	
2.91	2.92	112	½
	2.90	$\bar{2}41$	
2.837	2.81	$\bar{2}22$	½
2.79	2.806	330	4
	2.793	051	
2.56 Fe	2.57	060	½
	2.561	$\bar{3}12$	
	2.555	400	
2.543	2.55	202	2
	2.526	$\bar{2}51$	
2.495	2.505	042	5
	2.472	$\bar{4}11$	
2.41	2.422	222	½
2.35	2.365	251, $\bar{1}61$	½
2.307 Fe	2.318	332	½
2.285 Fe	2.288	260	½
2.24	2.251	$\bar{4}31$	5
	2.259	341	
2.224 Fe	2.232	$\bar{1}03$	1
2.199 Fe	2.200	$\bar{4}02$	½
	2.197	152	
2.175	2.174	013	½
2.164	2.151	170	½
2.13	2.141	$\bar{2}13$	2
	2.1395	312	
2.107	2.107	440	3
	2.036	431	
2.007 Fe	2.012	$\bar{3}03$	
1.938	1.944	$\bar{4}51$	½
1.898	1.927	080	6
	1.891	271	
1.871	1.876	213	1
	1.872	530	
1.817	1.811	262	½
1.791 Fe	1.801	451	1
	1.789	053	
1.778 Fe	1.782	521	½
1.756	1.761	$\bar{5}32$	½
	1.743	$\bar{2}53$	
1.682	1.683	550	½
1.640	1.637	620	1
	1.638	014	
1.610	1.618	$\bar{2}24$	2
	1.611	024, 253	
	1.613	$\bar{6}31$	
	1.609	$\bar{2}04$	
1.589 Fe	1.590	$\bar{3}14$	½
	1.584	512	
1.577	1.576	$\bar{6}02$	½
1.566 Fe	1.572	114	½
1.560	1.553	291	½
1.543	1.547	381	2
	1.542	0.10.0	
1.530	1.537	282	½
	1.526	$\bar{3}34$	
1.508	1.515	413, 044	1
	1.510	134	
	1.509	$\bar{4}04$	
1.486 Fe	1.488	$\bar{6}51$	½
1.479	1.477	1.10.1	1
1.457	1.459	$\bar{7}01$	1
	1.460	$\bar{6}13$	
1.443	1.442	224	1
1.375	1.376	314	½
1.319			1
1.270			1
1.244			½
1.237			½
1.228			½
1.212			½
1.1515			½
1.132			½
1.111			½
1.102			½
1.094			½
1.0887			½
1.0687			½
1.0578			½
1.0375			½
1.008			½
.9836			½
.9277			½
.8882			½
.7890			½
.7780			½

extinctions in the chosen orientation, leaving only $h+k+l$ even, indicate a body-centered lattice. Other possible settings, with beta about 107°, or Tilley's orientation, with beta 115°24′ would give a base centered lattice, but the first was chosen as following a common custom of employing the unit cell with least possible obliquity. In addition this orientation gives simpler indices.

Powder photographs were taken with copper and with iron radiations and can be satisfactorily indexed. In the following, Table 2, giving the spacings and intensities, the symbol Fe indicates the presence of multiple lines shown on the copper film as single, or broadened lines, which have been resolved by the iron radiation. For example, a very strong, broad line on the copper film at about 3.04 Å is resolved in the iron into a definite triplet, 10, 5 and 1 in intensity.

Independently of the author, Mr. J. D. C. McConnell (this journal, pp. 510–514), working in the laboratory of the Department of Mineralogy at Cambridge University, has completed a study of scawtite from the Scawt Hill and Ballycraigy occurrences. Our results are in close agreement, and are interesting as showing practically identical conditions of formation, habit, etc., in two widely separated localities.

His observation of water in the mineral, overlooked in the original description, has been confirmed by the author for the Crestmore occurrence.

References

Tilley, C. E. (1930), Scawtite, a new mineral from Scawt Hill, Co. Antrim: *Mineral. Mag.*, **22**, 223–224.

Taylor, J. H. (1935), A contact metamorphic zone from the Little Belt Mountains, Montana: *Am. Mineral.*, **20**, 120–128.

Switzer, George, and Bailey, E. H. (1953), Afwillite from Crestmore: *Am. Mineral.*, **38**, 629–633.

McConnell, J. D. C. (1954), The hydrated calcium silicates riversideite, tobermorite and plombierite: *Mineral. Mag.*, **30**, 293–305.

Manuscript received July 14, 1954.

A CHEMICAL, OPTICAL AND *X*-RAY STUDY OF SCAWTITE FROM BALLYCRAIGY, LARNE, N. IRELAND

J. D. C. McConnell, *Department of Mineralogy and Petrology, Cambridge University, Cambridge, England.*

Abstract

A new chemical analysis of scawtite shows that this mineral is a carbonated calcium silicate hydrate. The scawtite examined was collected at Ballycraigy, Larne, N. Ireland, where it occurs in a vesicle in larnite rocks in association with the mineral tobermorite. Proof of the identity of the material from Ballycraigy and scawtite from Scawt Hill was provided by comparing the optical and cell constants of the two minerals.

The following data were obtained for scawtite from Ballycraigy:

Optical constants: $\alpha=1.595$, $\beta=1.605$, $\gamma=1.622$, all $\pm .001$.

$$2V = 75°5' \qquad 2V \text{ calculated} = 74°$$

Unit cell constants: An *A*-face centered cell was chosen adopting the orientation originally proposed by Tilley.

$$a = 6.61 \text{ Å}, \quad b = 15.22 \text{ Å} \quad \text{and} \quad c = 10.98 \text{ Å}, \quad \beta = 115°24'$$

The optical and crystallographic directions were related thus:

$$\beta = b, \quad \gamma \wedge a = 30°, \quad \text{and} \quad \gamma \wedge c = 34.5°.$$

The formula unit for scawtite, as found from the new analysis, was

$$Ca_6Si_6O_{18}2H_2O:CaCO_3 \cdot Z = 2.$$

Evidence is presented which suggests that scawtite is related structurally to wollastonite.

Occurrence

The occurrence of scawtite at Ballycraigy, Larne, N. Ireland, has already been noted (McConnell 1954, p. 295). Scawtite was found lining a single vesicle in larnite rocks from the dolerite-chalk contact at this locality. The mineralogy of this contact has not yet been described in detail but is closely similar to that of the Scawt Hill contact described by Tilley (1931).

Scawtite also occurs at Ballycraigy as an alteration product of some other mineral. Scawtite pseudomorphs after spurrite have been described by Tilley (1938). Consequently the primary mineral at Ballycraigy may well have been spurrite.

The vesicle examined was lined with transparent crystals of scawtite which were covered with delicate tuft-like aggregates of tobermorite. The crystal habit of scawtite was not observed for this reason.

Scawtite was found to have an H. of 5, G. of 2.77, and two cleavages at right angles. The cleavages were observed in crushed material.

Optical Properties

The optic axial plane was parallel to the poorer of the two cleavages and fragments orientated parallel to the perfect cleavage showed an off-centered optic axial interference figure. The optical constants as determined by the immersion technique were: $\alpha=1.595$, $\beta=1.605$ and $\gamma=1.622$, all ± .001. 2V was positive and universal stage measurements indicated a value of 75°5′ for this angle. The calculated value for 2V was 74°.

X-Ray Study

A single crystal *x*-ray study was carried out on a small but perfect single crystal of scawtite from the vesicle described above. The mineral was found to be monoclinic as suggested by Tilley (1930, p. 223) and the cleavage zone axis was selected as *a* in agreement with the orientation figured by him. The cell constants were determined from *b* axis zero, first and sixth layer line Weissenberg photographs, a *c* axis zero layer line Weissenberg and oscillation photographs for all three axes. The *b* axis Weissenberg photographs indicated that either an *A*-face centered or an *I* lattice could be chosen. The cell dimensions of both as determined from these photographs were;

Table 1. The *d* Spacings of Scawtite from Ballycraigy

8.36	vw	2.54	vw	1.81	w
7.93	vw	2.52	w	1.777	w
5.99	m	2.49	m	1.766	w
4.99	vw	2.39	vw	1.671	vw
4.52	m	2.33	vw	1.632	vw
4.19	m	2.23	m	1.602	vw
3.80	m	2.21	w	1.554	vw
3.55	m	2.17	vvw	1.535	w
3.21	m	2.15	vvw	1.503	w
3.03	vs	2.12	vw	1.472	vw
2.99	vs	2.01	m	1.320	w
2.96	w	1.89	s	1.313	w
2.78	m	1.87	m	1.141	vw

The *x*-ray powder photograph was taken on a 19 cm. powder camera using Cu-K_α radiation. The *d* spacings are given in Å units. Scale of decreasing intensities vs, s, m, w, vw, and vvw as estimated from visual comparison.

A cell; 115°24′, $a = 6.64$ Å, $c = 11.09$ Å
I cell; 100°48′, $a = 6.64$ Å, $c' = 10.18$ Å.

Oscillation photographs about *a*, *b* and *c* gave the following values for the cell dimensions of the *A* cell.

$$a = 6.61\text{ Å},\quad b = 15.22\text{ Å}\quad\text{and}\quad c = 10.98\text{ Å},\quad\text{all } \pm.05\text{ Å}$$

Both I and A cells had a calculated mass of $2743 \cdot 10^{-24}$ gms. The optical directions of scawtite had the following orientation to the crystallographic axes chosen:

$$\beta = b,\quad \gamma\wedge c = 34.5°,\quad \gamma\wedge c' = 71°\quad\text{and}\quad \gamma\wedge a = 30°.$$

A list of the d spacings of scawtite from Ballycraigy are given in Table 1·

Chemical Study

Attempts were made to find the correct formula unit for scawtite using the molar ratios of SiO_2, CaO and CO_2 given by Tilley and Hey (1930, p. 223). This proved to be impossible. From this it was inferred that either the mineral from Ballycraigy was not scawtite or the analysis cited was in error. The only crystals of the original scawtite sample available were preserved in a crystal mount. One of these crystals was mounted on the Weissenberg camera. An oscillation photograph about b and a zero layer line Weissenberg photograph about the same axis proved conclusively that scawtite and the mineral from Ballycraigy were identical. It was concluded that the original analysis was in error. Since the original analysis was carried out on a very small sample using ordinary analytical techniques the possibility of such an error has been admitted by Hey (personal communication).

In order to determine, qualitatively, the composition of scawtite the scawtite rock mentioned in the first section was analyzed. This analysis was made by J. H. Scoon of the Department of Mineralogy and Petrology, Cambridge. Optical examination of the analyzed material showed that it consisted essentially of scawtite. Minor amounts of calcite were present. X-ray powder photographs of the material were identical with those of pure scawtite. This analysis showed that the CO_2 content of scawtite could not be greater than 9% and that scawtite contained water. It was also shown that the total combined H_2O and CO_2 could be determined as loss in weight on ignition.

Approximately 30 milligrams of pure scawtite were separated from the vesicle from Ballycraigy. A preliminary separation of scawtite and tobermorite was effected by using heavy liquids and the product was then handpicked under a microscope.

Using the information derived from the preliminary analysis described above, the following microtechnique was developed for the analysis of the pure scawtite sample.

The apparatus consisted of a silica glass ignition tube to which an H_2O absorption tube was attached by means of a ground glass joint. A second absorption tube was added to collect the CO_2 evolved. Each of these absorption tubes weighed approximately three grams and weight increase was determined by means of a semimicrochemical balance.

When in use a platinum boat containing the sample to be analyzed was placed in the ignition tube and a gentle current of dried CO_2 free air was drawn through the apparatus. After ignition the sample was analyzed in the normal way for CaO and SiO_2.

During the ignition of the pure scawtite sample a delicate film of moisture was seen to travel along the ignition tube indicating that water had been evolved.

The results of this analysis, as shown below, were considered to be sufficiently accurate to warrant the calculation of a formula unit from the determined cell constants and density.

Chemical Analysis of Scawtite from Ballycraigy

	Per Cent	
SiO_2	43.5	6.00
R_2O_3	1.2	
CaO	46.1	6.80
H_2O^-	0.1	
H_2O^+	4.3	1.98
CO_2	4.4	0.83
	99.6	

This analysis was carried out jointly by J. H. Scoon and the author. All weighings were made on a semimicrochemical balance. The formula unit chosen was 7CaO, $6SiO_2$, $2H_2O$, CO_2, $Z=2$. This formula unit may also be written $Ca_6Si_6O_{18}2H_2O:CaCO_3$ and when written in this way indicates that scawtite may be regarded as a carbonated xonotlite ($Ca_6Si_6O_{18}2H_2O$).

Single crystals of scawtite when heated to a temperature of 850° C. were found to have their optical birefringence reduced. This was thought to be associated with decarbonation. *X*-ray powder photographs of the heated material were identical with those of wollastonite. The orientation of the wollastonite to the parent scawtite has not yet been determined.

The author wishes to thank Dr. A. M. B. Douglas of the Department of Mineralogy and Petrology, Cambridge, for assistance with the *x*-ray work. The *x*-ray photographs were taken by Mr. Kenneth Rickson. The research was done in the Department of Mineralogy and Petrology, Cambridge, under the direction of Professor C. E. Tilley. The author holds a Research Grant from the Ministry of Education for N. Ireland.

On completing the above research the author was informed that Professor Murdoch of the Department of Geology, University of California at Los Angeles was also working on the mineral scawtite.

The author is indebted to Professor Murdoch for subsequently sending him a specimen of scawtite from Crestmore and a manuscript copy of his results. The two investigations overlap to an extent sufficient to prove the identity of the minerals studied, and taken together, provide an integrated account of the morphology, occurrence and chemistry of the mineral scawtite.

REFERENCES

TILLEY, C. E., AND HEY, M. H. (1930), Scawtite, a new mineral from Scawt Hill, Co. Antrim: *Mineral. Mag.* **22,** 222–224.

TILLEY, C. E. (1931), The dolerite-chalk contact of Scawt Hill, Co. Antrim: *Mineral Mag.*, **22,** 439–468.

TILLEY, C. E. (1938), On scawtite pseudomorphs after spurrite at Scawt Hill, Co. Antrim: *Mineral. Mag.*, **25,** 38–40.

MCCONNELL, J. D. C. (1954), The hydrated calcium silicates riversideite, tobermorite and plombierite: *Mineral., Mag.*, **30,** 293–305.

Manuscript received July 14, 1954.

NOTES AND NEWS

STUDIES OF URANIUM MINERALS (XVII): SYNTHETIC SCHROECKINGERITE*

VIRGINIA ROSS,** *Harvard University, Cambridge, Massachusetts.*

Schroeckingerite, $Ca_3Na(UO_2)(CO_3)_3SO_4F \cdot 10H_2O$, has been described from several different localities, associated generally with gypsum. The unit cell and morphological constants were obtained by Hurlbut (1953) from pseudohexagonal platelets of the mineral.

Synthesis

The synthesis of schroeckingerite was initially undertaken by C. Ruggles in the autumn of 1953. Attempts to prepare the mineral from calcite immersed in solutions of NaF and $UO_2SO_4 \cdot 3H_2O$ were unsuccessful. The synthesis was enacted by dissolving.

1. 0.05 m. NaF and 0.15 m. $Na_2CO_3 \cdot 10H_2O$ in 600 ml. H_2O,
2. 0.05 m. $UO_2SO_4 \cdot 3H_2O$ in 200 ml. H_2O,
3. 0.15 m. $CaCl_2$ in 100 ml. H_2O,

and combining all three solutions. The resultant precipitate was greenish-yellow, highly fluorescent and the mother liquor, neutral (pH-7). Since the precipitate was exceedingly fine-grained, accurate optical data were unobtainable.

This work was recently continued by the writer. The original synthesis was repeated successfully by reducing the acidity of the resultant solutions with NH_4OH and by avoiding the slow reaction between the salts of the latter two solutions, by rapid combination. Since chlorine invariably may have substituted for fluorine in the crystals of schroeckingerite synthesized in this manner, $Ca(NO_3)_2 \cdot 4H_2O$ was substituted for $CaCl_2$. The precipitation of schroeckingerite was evident on approaching the neutral pH range, and the yield was increased by further reducing the acidity and depressing the solubility of the Na^+ ions by adding 0.1 *N* NaOH. The precipitate consisted of very fine-grained schroeckingerite and gypsum. The final reaction between uranyl sulfate and calcium nitrate was avoided by substituting for the former, uranyl nitrate and sodium sulfate in the stoichiometric proportions.

Repeated crystallizations of the schroeckingerite by evaporation at 40° C. from distilled water solutions reduced the gypsum contamination

---

* Contribution No. 351 of the Department of Mineralogy and Petrography, Harvard University, Cambridge, Massachusetts.

** Present address: Department of Chemistry, Brown University, Providence, Rhode Island.

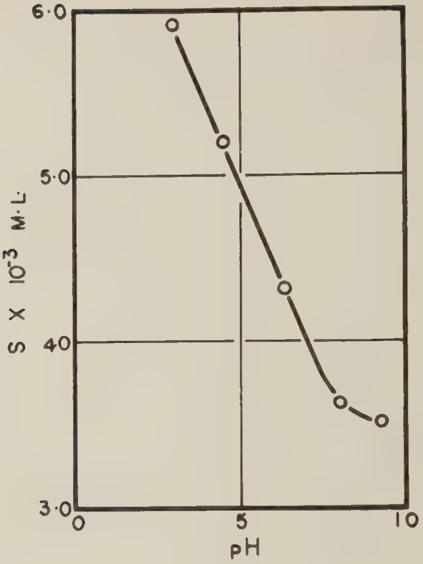

FIG. 1. The solubility of synthetic schroeckingerite as a function of pH at 22° C.

of the samples and yielded tiny, pseudohexagonal plates of schroeckingerite, measuring about 0.5 mm. in size and suitable for optical study.

Solubility

The solubility of schroeckingerite as functions of pH and temperature is indicated in Fig. 1 and Table 1. The solubility is slight, increasing with decreasing pH and it is roughly doubled between 22° and 50° C. This information was of value in obtaining sufficient concentrations of the mineral for recrystallization.

Trial Syntheses of Schroeckingerite Analogues

Attempts, all of which were unsuccessful, based upon the original synthesis, were made to prepare chloride, hydroxyl, potassium, magnesium, and lithium analogues of schroeckingerite.

TABLE 1. SOLUBILITY OF SCHROECKINGERITE

Temperature, °C.	pH	Solubility
22° C.	3.0	5.91×10^{-3} mols/liter
22° C.	4.5	5.20×10^{-3} mols/liter
22° C.	6.4	4.32×10^{-3} mols/liter
22° C.	8.0	3.64×10^{-3} mols/liter
22° C.	9.3	3.51×10^{-3} mols/liter
50° C.	4.5	10.17×10^{-3} mols/liter

(*a*) Chloride Analogue. Solutions containing 0.05 m. NaCl, 0.15 m. $Na_2CO_3 \cdot 10H_2O$ and 0.05 m. $UO_2SO_4 \cdot 3H_2O$, and 0.15 m. $CaCl_2$ were combined with slight evolution of CO_2 gas. On adding 0.1 *N* NaOH a precipitate of gypsum was obtained. The mother liquor (pH-6.5) was evaporated at 40° C. for three days and a fluorescent, yellowish-green precipitate of andersonite, $Na_2CaUO_2(CO_3)_3 \cdot 6H_2O$, and traces of $CaCO_3$ were obtained. (Andersonite has been synthesized previously by Axelrod *et al.* (1951) from solutions of K_2CO_3 and uranyl, sodium and calcium nitrates.)

(*b*) Hydroxyl Analogue. The precipitation of a hydroxyl analogue of schroeckingerite failed from neutral solutions of sodium carbonate, uranyl sulfate, and calcium nitrate.

(*c*) Potassium Analogue. The replacement of sodium by potassium in the original formula, using 0.05 m. KF and 0.15 m. K_2CO_3 combined with uranyl sulfate and calcium nitrate in solution yielded only gypsum through slow evaporation in the neutral range.

(*d*) Magnesium Analogue. From the evaporation of solutions of NaF, $Na_2CO_3 \cdot 10H_2O$, $UO_2(NO_3)_2 \cdot 6H_2O$ and $MgSO_4 \cdot 7H_2O$, rendered more alkaline with the addition of 0.1 *N* NaOH, only a colloidal precipitate of uranyl sulfate was ultimately obtained.

(*e*) Lithium Analogue. The corollary synthesis of a lithium analogue of schroeckingerite was hampered by the very great insolubility of lithium fluoride. However, no trace of lithium was apparent in any of the natural material as reported by Axelrod and co-workers.

Optical and X-ray Data of Pure, Synthetic Schroeckingerite

The optical constants obtained for pure, synthetic schroeckingerite are compared with those recorded by several other analysts on naturally-occurring material.

TABLE 2. SCHROECKINGERITE, OPTICAL DATA

Source	Wamsutter, Wyoming	Moab, Utah	San Isidro, Argentina	Pure Synthetic
Analyst	Larsen	Hurlbut	Hurlbut	Ross
Character	Biaxial (−)	Biaxial (−)	Biaxial (−)	Biaxial (−)
$nX=c$ (Pale yellow)	1.489 ± .002	1.490 ± .001	1.492 ± .001	1.495 ± .001
$nY=b$ (yellow-green)	1.542 ± .001	1.537 ± .001	1.543 ± .001	1.543 ± .001
$nZ=a$ (yellow-green)	1.542 ± .001	1.538 ± .001	1.544 ± .001	1.544 ± .001
2V	5°	18°	10°	16°
Dispersion not perceivable	—	—	—	—

The crystals from Argentina were reported by Hurlbut to alter on de-

TABLE 3. SYNTHETIC SCHROECKINGERITE. *X*-RAY POWDER DIFFRACTION DATA
Space Group-*Cmmm*, a_0 −9.69 Å, b_0−16.83 Å, c_0 −14.26 Å.
I/I_0− Relative Intensity, d_{hkl}-interplanar spacing

I/I_0	$d_{meas.}$	*hkl*	$d_{calc.}$
3	14.28	001	14.26
10	7.26	021 111	7.25 7.24
2	5.421	022 112	5.439 5.434
8	4.796	200 003	4.845 4.752
2	4.167	220 113 023	4.199 4.139 4.138
1	4.044	041 221 132	4.036 4.028 4.013
1	3.591	042 222 004	3.624 3.618 3.564
2	3.362	203	3.393
1B	3.303	024 114	3.282 3.281
<1 VB	3.13	310 043 223 151 241 311	3.172 3.150 3.147 3.101 3.101 3.096
7	2.876	134 204	2.873 2.871
1	2.767	061 331	2.753 2.747
1	2.706	025 115	2.701 2.700
2	2.393	261 401	2.393 2.388
<1	2.304	171 351 262 421	2.302 2.300 2.298 2.297

B—Broad, VB—Very Broad.

hydration to: $Ca_3NaUO_2(CO_3)_3SO_4F \cdot 4H_2O$, which is hexagonal, nO $=1.581$, nE$=1.532$. The loss of water was found to exert a marked decrease in the nY index of refraction. The synthetic material, which was apparently fully hydrated, exhibited maximum refraction.

The complete x-ray analysis of synthetic schroeckingerite required the combined use of film and recording diffractometer techniques to compensate for the absence of high-angle reflections, which is characteristic of the mineral. From the unit cell dimensions and space-group provided by Hurlbut from single crystal analysis, the various powder reflections were accordingly indexed and are listed in Table 3.

It appears that the synthetic material is more fully hydrated as evidenced from the slightly larger d-spacings than those calculated on the basis of the natural single-crystal data, and from the comparatively higher refractive indices. The natural material was undoubtedly slightly dehydrated on constant exposure to the air. The d-spacings of the synthetic material are in fair agreement with those reported by Jaffe (1948) with the exception of a few lines which have been omitted. The latter lines, which were very weak, could not be indexed on the basis of the single crystal data and were attributed ultimately to traces of gypsum. It was observed during the synthesis of schroeckingerite that the water content, and consequently, the d-spacings of the co-precipitated gypsum were highly variable.

ACKNOWLEDGMENT

This investigation was carried out on behalf of the Division of Raw Materials of the U. S. Atomic Energy Commission, *Contract No. AT (30-1) 1403*. The method of synthesis was suggested by Dr. C. Frondel.

REFERENCES

1. AXELROD, J. M., GRIMALDI, F. S., MILTON, C., AND MURATA, K. J., The uranium minerals from the Hillside Mine, Yavapai County, Arizona: *Am. Mineral.*, **36**, 1–21, (1951).
2. HURLBUT, C. S., JR., Studies of uranium minerals (XV): Schroeckingerite from Argentina and Utah: *Am. Mineral.*, **39**, 901–907.
3. JAFFE, H. W., SHERWOOD, A. M., AND PETERSON, M. J., New data on schroeckingerite: *Am. Mineral.*, **33**, 152–157, (1948).
4. LARSEN, E. S., JR., AND GONYER, F. A., Dakeite, a new uranium mineral from Wyoming: *Am. Mineral.*, **22**, 561–563, (1937).

A DISCUSSION ON "MECHANISM OF SOLUTION OF QUARTZ IN PURE WATER AT ELEVATED TEMPERATURES AND PRESSURES"

W. S. Fyfe, *Institute of Geophysics, University of California, Los Angeles, California.*

Recently Frederickson and Cox (1) have measured the solubility of quartz in water between 200 and 370° C. at a pressure of 300 bars. The solubility was determined by removing samples of the solution from the bomb at given P and T and determining the amount of solute by weighing the dry residue. An innovation in technique was introduced in that samples could be withdrawn from the top and near the bottom of the vertical bomb.

The important experimental finding reported by these workers in their studies on quartz and albite (2) is that the "solubility" differs in different parts of the bomb, being much greater at the bottom than at the top. Based on these findings a mechanism of solution is postulated. If the results are correct, they must throw considerable doubt on the "absolute" values of solubility as found by Kennedy (3) and Morey and Hesselgesser (4).

Unfortunately, some experimental data which are critical in evaluating the results of the experiments are not given in the paper. In particular, the volume of the samples withdrawn and the magnitude of the "temporary pressure drop" during sampling should have been recorded. If, however, the techniques and procedures used are as stated in the text of the paper, these may be calculated and if this is done we need not look far for an explanation of the solubility anomalies reported and certainly there is no justification for postulating any special mechanism of solution to explain the results.

There are a great number of experimental difficulties in determining the solubility of a substance in water at high pressures and temperatures. There are objections to the methods used by Kennedy and Morey and Hesselgesser, but both studies illustrate that some of the objectionable features are not significantly affecting the results. Such objections might be (*a*) diffusion out of the system along a cold gauge line is possible (a function of time); (*b*) there might be reaction with materials of the bomb (a function of time); (*c*) solution might be reprecipitated on the crystals during cooling (a function of the available surface and rate of cooling—a difficulty not encountered in Morey's work). In general, the data presented by these workers clearly shows that such effects under the conditions studied are trivial.

The inherent difficulty with sampling techniques lies in the possibility of changes in the system caused by the sampling. In this respect we must look more closely at the experiments of Frederickson and Cox. We are told that a pressure of 300 bars at 200° C. was produced in the 195 cc. bomb by the degree of initial filling. The technique of sampling used was such that sufficient sample was removed at 200° C. to leave enough water to give a pressure of 300 bars at 250° C., this procedure being repeated at approximately 50° intervals till a temperature of 350–370° C. was attained. If this is the procedure used, then during sampling at each temperature, the state of the system will be profoundly changed. At 300 bars, at all temperatures a homogeneous fluid phase will exist in the bomb. If enough water is removed at each of the intervals mentioned above, then at the end of the sampling, and during much of the sampling, a liquid-vapor system will be created. In Table 1 are listed some calculations on this problem from *P.V.T.* data of Kennedy (5) and Keenan and Keyes (6).

TABLE 1

I T° C.	II Vol. of water at *N.T.P.* to fill bomb	III cc's removed in sampling	IV Vol. of water at *N.T.P.* to fill with satd. liquid	V Minimum sample to enter liquid-vapor region
200	172.5 cc.	11.5 cc.	168.6 cc.	3.9 cc.
250	161.0	14.5	155.3	5.7
300	146.5	21.1	138.8	7.7
350	125.4	—	111.6	13.8

In column II are listed the volumes of water needed at *N.T.P.* to fill the 195 cc. bomb to give 300 bars at the temperatures of column I. In column III are listed the volumes of the samples removed if the successive sampling technique described is followed. In column IV are listed the volumes of water at *N.T.P.* needed to fill the bomb with liquid water at a pressure corresponding to the liquid-vapor equilibrium pressure. In column V are listed the maximum volumes of sample which could be removed without entering the liquid-vapor region. It is obvious when columns III and V are compared, that during much of the sampling, a vapor phase exists in the bomb. In each case this will occur when approximately $\frac{1}{3}$ of the sample has been removed. It is immediately obvious why the samples removed from the top of the bomb give lower solubilities than those removed from the bottom for much of these samples consist of vapor saturated with quartz and the solubility in the vapor will be small compared with that in the homogeneous fluid originally present. In the same way, the evaporation of part of the water will cause rapid precipitation of silica which may be collected in the bottom sampling. The effects will occur independently of the order of sampling.

The removal of the samples will also cause pronounced cooling of the bomb, depending in part on the rate of sampling. If this is fast, then as the latent heat of vaporization of water is in the range 8–6 k. cals/gram mol over this temperature range, and as approximately a gram mol of water is removed at each sampling, then one might expect cooling of the order of 20–30° C. during the sampling. This effect will further tend to throw the system into the liquid-vapor region and the volumes of sample which could be removed without causing inhomogeneity of the fluid phase will be even smaller than indicated in column V of Table 1.

The conclusion which must be reached from the description of the experiments given by the authors is that the anomalous results for the solubility of albite and quartz found are in all probability related to the drastic changes in the state of the aqueous solvent caused by the sampling technique. With this doubt in mind it would be unwise to place too much weight on the deductions made from the experimental findings.

References

1. Frederickson, A. F., and Cox, Joseph E., Mechanism of "solution" of quartz in pure water at elevated temperatures and pressures: *Am. Mineral.*, **39**, 886 (1954).
2. ———, Solubility of albite in hydrothermal solutions: *Am. Mineral.*, **39**, 738 (1954).
3. Kennedy, George C., A portion of the system silica-water: *Economic Geology*, **45**, 629 (1950).
4. Morey, G. W., and Hesselgesser, J. M., The solubility of quartz and some other substances in superheated steam at high pressures: *Transactions of the A.S.M.E.*, 865 (1951).
5. Kennedy, George C., Pressure-volume-temperature relations in water at elevated temperatures and pressures: *Am. Jour. Sci.*, **248**, 540 (1950).
6. Keenan, J. H., and Keyes, F. G., *Thermodynamic Properties of Steam*. John Wiley and Sons (1936).

DIRECTIONAL HARDNESS VARIATION IN TUNGSTEN CARBIDE (WC) MONOCRYSTALS

J. A. Kohn,* Perry G. Cotter, and R. A. Potter,
U. S. Bureau of Mines, Norris, Tennessee.

Introduction

During a series of experiments designed to increase the hardness and density of tungsten carbide-cobalt alloys, microhardness tests were made on tungsten carbide single crystals.† Measurement of oriented microindentations showed a hardness variation of almost 50 per cent on the *prism face;* no variation was detected on the *basal pinacoid.* Although accounts of directional hardness variation have been given for diamond (references 1–9), corundum (10–13), silicon carbide (10, 14, 15), and other substances (10, 16), no such property has been reported for tungsten carbide.

---

* Present address, Chemical-Physics Branch, Signal Corps, Engineering Laboratory, Ft. Monmouth (Hexagon) N. J.

† Crystals supplied by Kennametal Inc., Latrobe, Pa.

PROCEDURE

The crystals used in the investigation displayed trigonal symmetry, having fairly well developed basal pinacoid (0001) and first order prism $(10\bar{1}0)$ faces. The specimens varied in shape from equidimensional to tabular and had testing surface areas of 0.15 to 1.5 mm². The crystals were black and showed a distinct conchoidal fracture. An *x*-ray powder pattern of the crushed single crystals showed the presence of only one phase—the monocarbide of tungsten (WC). The specimens for hardness testing were selected on the basis of the quality of their natural faces and the sharpness of their interfacial edges. In a few instances the orientation was confirmed by single-crystal *x*-ray exposures. The selected crystal faces were cemented to a mounting block by a trace of Canada balsam to maintain their orientation during the setting in bakelite.

Surfaces suitable for microindenting were prepared by grinding first on a resin-bonded diamond wheel, next on a glass plate with 600-grit silicon carbide, and finally on a teakwood wheel with 0- to 2-micron diamond paste. It is believed that this procedure resulted in a minimum of polishing (surface-flow) action.

Indentations were made with a Tukon microhardness tester using a Knoop indenter and a 100-gram load. The mounted crystals were oriented on the Microton stage of the instrument by aligning the sharp interfacial edges with the long dimension of the pyramidal diamond indenter. Indentations were made on both the prism and basal pinacoid. For each crystal, the hardness of a particular azimuth was determined by a series of five microindentations. The latter were measured by three observers, giving 15 readings from which the hardness of each crystal-azimuth was averaged. The microindentations were measured with an oil-immersion objective in the optical system of the Tukon apparatus at an effective magnification of approximately 1600 ×. Orientations were verified on the revolving stage of a petrographic microscope fitted with a vertical illuminator.

RESULTS

The data obtained from this study are summarized in Table 1.

Measurements made parallel and perpendicular to an *a* axis on the *basal pinacoid* of three crystals (*a*, *b*, *c*) indicated no discernible hardness

Table 1. Knoop Microhardness Data (K_{100})

Basal Pinacoid (0001)

Specimen	Parallel *a* axis	Perpendicular *a* axis
a	1830	1770
b	1780	1800
c	1845	1945
Average	1820	1840

*Prism Face** ($10\bar{1}0$)

Specimen	0°	22½°	45°	60°	70°	80°	86°	88°	90°	94°	100°	110°
d	975	1035	1195	—	1565	1810	—	—	1890	—	—	—
e	1105	1135	1255	1425	1650	1830	—	—	2090	—	1836	1660
f	1030	1140	1240	—	1565	1785	—	—	1935	—	—	—
g	1130	—	1285	—	—	—	—	—	2015	—	—	—
h	1115	—	1225	—	—	—	—	—	2075	—	—	—
i†	—	—	—	—	—	—	1900	1970	2000	1945	—	—
j†	—	—	—	—	—	—	1900	1985	2000	1905	—	—
Average	1070	1105	1240	—	1595	1810	1900	1980	2000	1925	—	—

* Angles denote azimuth with reference to *c* axis.

† Corrected values—see text.

variation. Indentations made on the *prism face* of three additional crystals (*d*, *e*, *f*) showed a hardness variation of almost 50 per cent. On the basis of these data, no further measurements were made on the basal pinacoid, and attention was directed toward refining and expanding the data obtained from the prism face.

Figure 1 shows graphically the hardness variation observed on the first order prism face. After the general shape of the function had been determined, it seemed advisable to examine directions immediately adjacent to the hard vector (90° from the *c* axis). Accordingly, two additional crystals (*i*, *j*) were indented at the 86°-, 88°-, and 90°-positions. For correlation purposes, the hard vector measurements were compared with the previously determined average for this direction (based on five crystals). The corrections thus derived (averaging +35 Knoop units) were applied to the measurements at 86° and 88° and the corrected values plotted in Fig. 1. Paired measurements made on either side of the hard vector (crystals *e*, *i*, *j*) demonstrated that the hardness function follows the crystal symmetry, and accordingly the curve was drawn symmetrically about the 90°-position. The average microhardness dif-

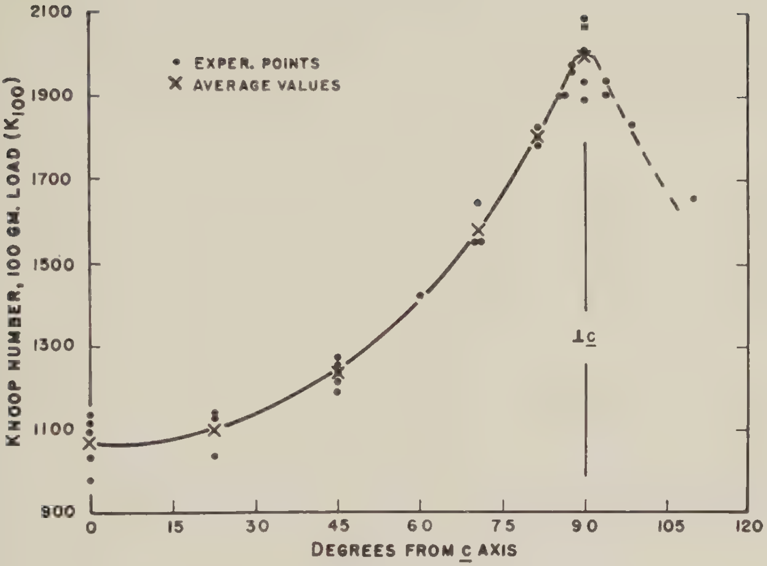

FIG. 1. Variation of Knoop hardness number on the first order prism face of tungsten carbide (WC).

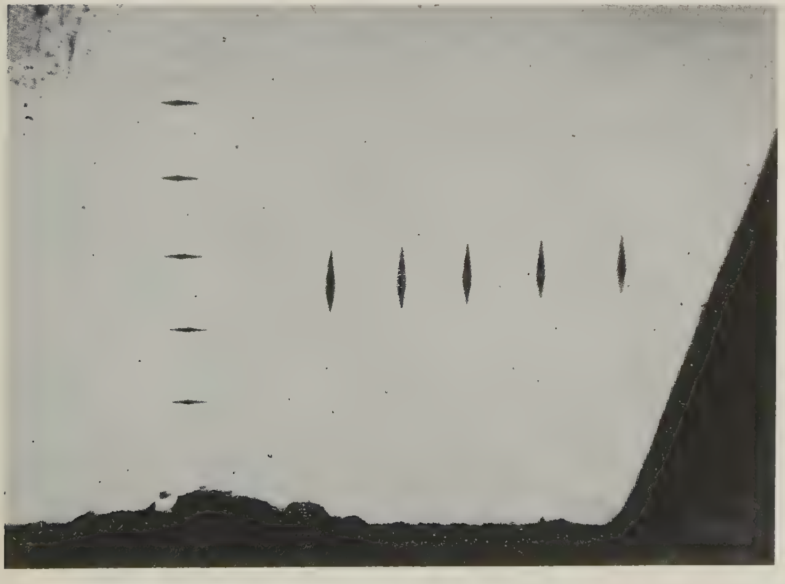

FIG. 2. Knoop microindentations on the first order prism face of tungsten carbide (WC, crystal *d*). The larger indentations are parallel to the *c* axis and approximately 39 microns in length.

ference between the soft direction, parallel to the *c* axis (1070 K_{100}), and the hard direction, perpendicular to the *c* axis (2000 K_{100}), is 930 Knoop units, or approximately 47 per cent. This striking hardness variation is shown clearly by the two sets of microindentations pictured in Fig. 2.

ACKNOWLEDGMENTS

The authors are indebted to J. C. Redmond, Kennametal Inc., Latrobe, Pennsylvania, for the single crystals used in this investigation. Thanks are due to M. V. Denny for the photomicrograph and the reproduction of the curve.

REFERENCES

1. TOLKOWSKY, M. (1920), Research on the abrading, grinding, or polishing of diamond: *Unpublished Doctoral Dissertation*, University of London, cited by Grodzinski, P. (1949), Diamond and gemstone industrial production methods—XII: *Ind. Diamond Rev.*, **9**, 118–122.
2. KRAUS, E. H., AND SLAWSON, C. B. (1939), Hardness variation in the diamond: *Am. Mineral.*, **24**, 661–676.
3. PETERS, C. G., NEFFLEN, K. F., AND HARRIS, F. K. (1945), Diamond cutting accelerated by an electric arc: *J. Res. Nat. Bur. Standards*, **34**, 587–593, RP 1657.
4. WHITTAKER, HARRY, AND SLAWSON, C. B. (1946), Third symposium on diamonds—Vector hardness in diamond tools: *Am. Mineral.*, **31**, 143–149.
5. WINCHELL, HORACE (1946), Third symposium on diamonds—Observations on orientation and hardness variations: *ibid.*, **31**, 149–152.
6. GRODZINSKI, P., AND STERN, W. (1949), Abrasion tests on diamonds; directional properties: *Nature*, **164**, 193–194.
7. SLAWSON, C. B., AND KOHN, J. A. (1950), Maximum hardness vectors in the diamond: *Ind. Diamond Rev.*, **10**, 168–172.
8. DENNING, REYNOLDS M. (1953), Directional grinding hardness in diamond: *Am. Mineral.*, **38**, 108–117.
9. HUKAO, Y. (1953), Abrading diamond: *Ind. Diamond Rev.*, **13**, 182–183.
10. WINCHELL, HORACE (1945), The Knoop microhardness tester as a mineralogical tool: *Am. Mineral.*, **30**, 583–595.
11. ATTINGER, C. (1951), Orientation and hardness of synthetic corundum: *Bull. Soc. suisse de chronométrie* (June), cited in *Ind. Diamond Rev.*, **12**, 136–137.
12. KASPAR, J. (1951), Syntheticke Korundy: Prague, cited as synthetic corundum: *Ind. Diamond Rev.*, **13**, 102–104.
13. STERN, W. (1952), Directional hardness and abrasion resistance of synthetic corundum: *Ind. Diamond Rev.*, **12**, 137–140.
14. KOHN, J. A. (1951), Directional variation of grinding hardness in silicon carbide: *ibid.*, **11**, 211–212; 235–237.
15. STERN, W. (1951), Directional hardness differences in silicon carbide crystals: *ibid.*, **11**, 237–239; 255.
16. DUCH-BERNELIN (1934), The study of the hardness of crystals in different directions: *Zeit. Krist.*, **88**, 323–324.

HORNBLENDE IN DIORITE PEGMATITE NEAR CAMP IRWIN, SAN BERNARDINO COUNTY, CALIFORNIA*

Robert D. Allen and Henry Kramer, *U. S. Geological Survey, Claremont, California.*

Introduction

Coarsely crystalline hornblende is the principal dark mineral in a diorite pegmatite 4 miles southeast of Camp Irwin in the Mojave Desert of California. The sample was collected by F. M. Byers, Jr., of the U. S. Geological Survey, near the summit of a low mountain in the SE ¼ sec. 11, T. 13 N., R. 3 E., San Bernardino base and meridian (lat. 35°14′ N., long. 116°38′ W., northernmost part of the Alvord Mountain quadrangle). According to Byers (personal communication) the diorite pegmatite is intrusive into diorite gneiss as (1) lit-par-lit injections parallel to foliation that strikes northwest and dips southwest, and less commonly as (2) cross cutting dikes as much as 6 inches wide. Three quarters of a mile southwest of the pegmatite locality a small granodiorite stock is in contact with the diorite gneiss.

Hornblende crystals in the diorite pegmatite average 1 to 2 cm. in length and 0.5 to 1 cm. in width. Although the crystals exhibit random orientation in two dimensions, their *c* axes tend to parallel a single plane. The mode (Chayes, 1954) of the diorite, determined by point-counting three mutually perpendicular thin sections and averaging the results, is given below, in per cent.

Sodic andesine	59.2
Hornblende	35.5
Biotite	2.1
Sphene	1.3
Quartz	0.8
Apatite	0.6
Calcite	0.6
Total	100.1

This mode was substantiated by counting light and dark minerals on three other mutually perpendicular polished surfaces of a hand specimen.

Optical Data

For convenient use, optical data are presented in tabular form.

α_{Na}	1.654 ± 0.001
β_{Na}	1.668 ± 0.001
γ_{Na}	1.676 ± 0.001

---

* Publication authorized by the Director, U. S. Geological Survey.

Birefringence $(\gamma-\alpha)$	0.022 ± 0.002
Optic sign	Negative
$2V_{\text{measured}}$	$67° \pm 2°$
$2V_{\text{calculated}}$	$73\frac{1}{2}°$
Dispersion	Inclined, strong, $r > v$
$Z \wedge c$	$23° \pm 2°$
X	Pale yellow
Y	Pale yellowish green
Z	Deep grass green
Absorption	$Z > Y > X$
Orientation	$Y = b$

ANALYTICAL DATA

The hornblende was purified by (1) sieving to minus 60 plus 200 mesh to remove biotite, (2) acid leaching to remove apatite and calcite, (3) bromoform separation to remove plagioclase and quartz, and (4) methylene iodide separation to remove sphene. A grain count of the purified sample gave the following percentages: hornblende 97.1 ± 0.1; quartz 2.9 ± 0.1. The chemical analysis and specific gravity were recalculated to eliminate the effect of quartz on the original analytical data. Both original and recalculated data are contrasted below.

	Original (*per cent*)	*Recalculated* (*per cent*)
SiO_2	47.01	45.43
Al_2O_3	7.73	7.96
Fe_2O_3	5.29	5.45
FeO	10.62	10.94
MgO	12.78	13.16
CaO	12.51	12.88
Na_2O	1.00	1.03
K_2O	0.52	0.54
H_2O (+)	0.89	0.92
H_2O (−)	nil	nil
TiO_2	1.14	1.17
MnO	0.29	0.30
F	0.51	0.53
Cl	nil	nil
NiO	0.02	0.02
BaO	nil	nil
V_2O_5	0.09	0.09
Total	100.40	100.42
Less O for F	0.21	0.22
Total	100.19	100.20
Specific gravity at 24° C.	3.19	3.21

Analyst: *Henry Kramer*

The most noteworthy chemical features of this hornblende are the relatively small amounts of sodium, potassium, and fluorine.

The spectrographic analysis, in per cent, is tabulated below.

0.X	Ti, Na, K, Mn
0.0X	V, Ni, Zr
0.00X	Cu, Co
0.000X	Cr

The formula for the Camp Irwin hornblende calculated from the above analysis is:

$$(\mathrm{Ca, Na, K})_{2.47}(\mathrm{Fe}'', \mathrm{Mg}, \mathrm{Mn}'', \mathrm{Ni})_{4.32}(\mathrm{Fe}''', \mathrm{Ti}, \mathrm{Al}, \mathrm{V})_{0.92}(\mathrm{Si}, \mathrm{Al})_{8.00}\mathrm{O}_{22.84}(\mathrm{OH}, \mathrm{F})_{1.16}.$$

This formula is patterned after the structural type proposed by Berman (1937): $W_3(X, Y)_5(Z_4O_{11})_2(OH, F)_2$.

This hornblende from Camp Irwin is classified as pargasite because the ratio of silicon to aluminum is 4.83, intermediate between edenite and hastingsite (Larsen and Berman, 1934).

Chemical Relation to the Host Rock

In a study of amphiboles from the Purcell sills, British Columbia, Rice (1935) reports data indicating that the ratio FeO/MgO is higher for hornblendes associated with sodic plagioclase than for those associated with calcic plagioclase. Buddington and Leonard (1953) report similar findings on hornblendes from the Adirondack igneous rocks. The ratio FeO+MnO/MgO, in molecular proportions, is 1.89 for femaghastingsite from granite, whereas it is 0.78 for pargasite from amphibolite. For the Camp Irwin pargasite in diorite pegmatite the ratio FeO+MnO/MgO is 0.48.

A second ratio that might be useful in characterizing a hornblende expresses the molar proportions in the "W" group of the structural formula: Na_2O+K_2O/CaO. The femaghastingsite referred to above gives a value of 0.59, but the Camp Irwin pargasite gives 0.29. Here again, the composition of the hornblende is related to the composition of the rock in which it occurs.

Acknowledgments

An *x*-ray diffraction verification of hornblende was made by Arthur Chodos, Department of Geology, California Institute of Technology. The spectrographic analysis was made by Hal W. Johnson, Pacific Spectrochemical Laboratory, Los Angeles, California.

References

Berman, H. (1937), Constitution and classification of the natural silicates: *Am. Mineral.*, **22**, 342–408.

Buddington, A. F., and Leonard, B. F. (1953), Chemical petrology and mineralogy of hornblendes in northwest Adirondack granitic rocks: *Am. Mineral.*, **38,** 891–902.

Chayes, F. (1954), The theory of thin-section analysis: *Jour. Geol.*, **62,** 92–101.

Larsen, E. S., and Berman, H. (1934), The microscopic determination of the nonopaque minerals: *U. S. Geol. Survey, Bull.* **848,** 2d Ed., 219–227.

Rice, H. M. A. (1935), Amphibole from the Purcell sills, British Columbia: *Am. Mineral.*, **20,** 307–309.

LATTICE SPACINGS IN CLEAR CRYSTALLINE QUARTZ AND THEIR VARIABILITY

H. D. Keith, *H. H. Wills Physical Laboratory,*
University of Bristol, England.

Although quartz has been widely used as a standard substance for the calibration of *x*-ray diffraction cameras and, to a lesser extent, for admixture with specimen materials in routine *x*-ray analysis, it appears that no fully indexed list of its lattice spacings has yet been published. The purpose of this note is (*a*) to present such a list of spacings, and (*b*) to discuss its reliabillty for calibration purposes in the light of a recently observed variability in the properties of quartz.

Attention was first drawn to variations in the lattice-parameters of clear crystalline quartz by the author (Keith, 1950) who, on the basis of a limited number of accurate measurements, suggested that they are more likely to be caused by impurities than by some form of lattice defect. More extensive researches have since been carried out on the variable behavior of large numbers of quartz samples in the neighborhood of the $\alpha \rightleftharpoons \beta$ inversion temperature (Keith and Tuttle, 1952; McDowell and Vose, 1952; Fieldes, 1952; and Sabatier, 1953) and also on variations in lattice spacings (Keith and Tuttle, *loc. cit.*); these have yielded results which agree well with earlier work, and which support the view that impurities are primarily responsible for the observed variations. In view of this agreement and of the considerable interest now shown in the properties of quartz, a brief discussion of the variability of its lattice-parameters—with particular reference to the quartz calibration standard—will now be given.

Bradley and Jay (1933) were the first workers to realize the practical advantage of establishing the lattice-parameters of clear quartz as a standard with which other lattice spacings may be compared experimentally, and they therefore tabulated values of the Bragg angles observed for some fifteen high angle reflections with CuK_α radiation. Lipson and Wilson (1941) later determined the lattice-parameters of one particular quartz specimen with greater accuracy (1 part in 10^5 relative to Siegbahn's values of the characteristic *x*-ray wave-lengths), and then revised the existing table of Bragg angles accordingly. The possible occurrence of appreciable variations in the lattice spacings of different samples of mineral quartz was not, apparently, considered seriously by these authors: it seems likely that they relied upon the results of the measurements made by Bradley and Jay, on two clear and two slightly contaminated colored quartzes, as having established an adequate degree of constancy in the lattice-parameters.

However, it was later pointed out by the author (*loc. cit.*) that the method adopted by Bradley and Jay, which depended upon the assumption of a constant and slightly incorrect value for the axial ratio (c/a), would have tended to obscure rather than bring to light, any slight variations which may have existed. Being led by indirect evidence to suspect the reliability of the quartz calibration standard for very accurate work, he used a 19 cm. powder camera, which had been calibrated by two independent direct methods, in order to determine the lattice-parameters of a very large single crystal of Brazilian quartz, and also of three synthetic samples grown at different temperatures. These measurements, in which an accuracy of 1 part in 10^5 was attained, revealed variations in the lattice-parameters of at least 1 part in 10^4; and gave results for the Brazilian quartz which were considerably smaller than those published by Lipson and Wilson but which agreed moderately well with Bradley and Jay's values. Analysis of these results, which are tabulated in Table 1, indicates a progressive decrease in the axial ratio as the lattice parameters increase. The significance of this variation becomes at once apparent if the differences in the lattice-parameters of the various samples, taken in pairs, are used to derive values for the ratio

TABLE 1

Sample (all at 18° C.)	"a" Angstroms	"c" Angstroms	Axial Ratio c/a
Brazilian quartz	4.91248_8	5.40422_7	1.10010
Synthetic quartz (Grown at 292° C.)	4.91312_3	5.40471_3	1.10006
Synthetic quartz (Grown at 369° C.)	4.91274_2	5.40442_5	1.10008
Synthetic quartz (Grown at 388° C.)	4.91263_6	5.40439_6	1.10010

$$\left(\frac{\Delta a}{a}\Big/\frac{\Delta c}{c}\right),$$

of which the mean is found to be 1.39 (neglecting pairs of parameters not different by more than the experimental error). Inclusion in this scheme of Bradley and Jay's and of Lipson and Wilson's figures for the lattice-parameters increases the mean ratio to 1.70, which differs by only 30% from the known ratio $(S_{11}/S_{33}) = 1.307$ of the isothermal strain components, or moduli of compliance, of quartz (Cady, 1946). The interpretation of the results which immediately suggests itself is one in terms of the distortion of the lattice by impurities. It is known (Bragg and Gibbs, 1925) that fairly wide channels, which are parallel to the optic axis, exist in the quartz lattice; these may account for the large observed ratio of the relative increments in lattice-parameters, since it is probable that their influence would be such as to cause any stresses, set up by impurity atoms or ions imprisoned within the lattice, to have a larger effect in the plane normal to the optic axis than in the direction parallel to it. It is implied in this interpretation that the impurities normally found in quartz tend to increase its lattice-spacings, a result which would be expected regardless of whether the impurities are accommodated interstitially or substitutionally (as a solid solution), the radius of Si^{4+} ion being smaller than that of any other ion likely to replace it. On this basis, the Brazilian quartz which was studied would seem to be of fairly high purity, having lattice-parameters smaller than those given by Lipson and Wilson, and smaller than almost all other quoted values.

In their recent paper, Keith and Tuttle have listed the spacings of the (234) planes of some twenty quartz specimens of diverse origins, and these show considerable variations approaching, in a few cases, 1 part in 10^3. Concerning their results it is significant that:

(*a*) the lowest spacing which they record (for an unspecified temperature) is only 1 part in 2×10^4 larger than that obtained by the author for Brazilian quartz at 18° C.,

(*b*) the spacing recorded for a synthetic sample, not believed to contain any marked impurity, agrees extremely well with the author's values for similar synthetic samples, and

(*c*) all the samples known to be impure (notably germanium-bearing synthetic crystals) have spacings considerably larger than the majority of other samples, and they also exhibit anomalous inversion temperatures.

From this evidence it seems reasonable to conclude (i) that it is correct to attribute the variability of the lattice-parameters of quartz to the presence of impurities as has previously been done by Keith and Tuttle and by the author, and (ii) that the lattice spacings determined for the large single crystal of Brazilian quartz are probably very close to the correct values for pure uncontaminated material. The well-known reluctance of crystals to maintain relative perfection and grow to large sizes in the presence of impurities, and also their tendency to reject impurities during growth, would support the latter conclusion.

For the calibration of x-ray diffraction cameras, the use of fragments of large single crystals of clear quartz is advisable and, even then, the reliability of the method is limited to an accuracy of about 0.01%. Where greater accuracy than this is not required, as is generally the case, quartz calibrations are very convenient, and the inclusion of further relevant data may well be of assistance to other workers.

Table 2. Lattice Spacings of Quartz at 18° C.

Index $hk \cdot l$	Spacing Å	Relative Intensity	2θ	Index $hk \cdot l$	Spacing Å	Relative Intensity	2θ
100	4.2544	80	20.862	402	.98967	20	102.209
101	3.3428	100	26.526	115	.98930		102.262
110	2.4563	60	36.550	313	.98705	20	102.587
102	2.2809	60	39.474	304	.97819	15	103.890
111	2.2361	50	40.298	230	.97602	15	104.217
200	2.1272	60	42.458	231	.96047	30	106.634
201	1.9794	50	45.802	232	.91796	10	114.088
112	1.8176	80	50.146	403	.91587	20	114.492
202	1.6714	40	54.882	411	.91497	10	114.668
103	1.6588	20	55.336	224	.90877	10	115.858
211	1.5412	70	59.970	215	.89703	20	118.334
113	1.4526	20	64.046	314	.88873	15	120.152
300	1.4182	10	65.792	106	.88118	5	121.880
212	1.3818	40	67.756	412	.87800	15	122.632
203	1.3747	40	68.154	305	.85962	5	127.284
301	1.3717	30	68.324	116	.84564	5	131.246
104	1.2893	30	73.370	501	.84051	3	132.813
302	1.2557	40	75.672	404	.83570	3	134.346
220	1.2281	30	77.686	206	.82941	20	136.458
213	1.1996	30	79.898	413	.82523	20	137.935
221	1.1976	10	80.056	330	.81875	10	140.360
114	1.1838	30	81.182	502	.81159	40	143.268
310	1.1800	40	81.500	225	.81138		143.358
311	1.1528	30	83.850	331	.80951	20	144.166
312	1.0814	40	90.840	240	.80399	30	146.681
400	1.0635	10	92.814	315	.79701	20	150.222
105	1.0476	20	94.656	241	.79524	10	151.196
401	1.0436	20	95.136	234	.79117	40	153.588
214	1.0344	25	96.256	216	.78582	20	157.151
223	1.0147	25	98.768				

The spacings given in the Table 2 were determined for the sample of Brazilian quartz mentioned above. They refer to 18° C., are expressed in Angstrom units (relative to the following wavelengths CuK$_{\alpha_1}$

$=1.540501$ Å, $\text{CuK}_{\alpha_2}=1.544345$ Å, $\text{CuK}_\alpha=1.541782$ Å), and have been corrected for eccentricity and absorption errors; they are given to five significant figures which corresponds to the limit of their probable accuracy when applied to quartz samples chosen at random. The relative intensities of the *x*-ray reflections are approximate, having been estimated visually from a powder photograph. A table of values of 2θ is also included, where θ is the Bragg angle for the reflection of CuK_{α_1} radiation by a given lattice plane.

The author gratefully acknowledges the assistance he has received from Professor G. W. Brindley, who drew his attention to the recent work on this subject; and also from Dr. D. R. Hale, who kindly supplied the synthetic quartz samples studied in the earlier work.

References

Bradley, A. J., and Jay, A. H. (1933), *Proc. Phys. Soc.*, **45**, 407.
Bragg, W. H., and Gibbs, R. E. (1925), *Proc. Roy. Soc.*, **A.109**, 405.
Cady, W. G. (1946), "Piezoelectricity," McGraw-Hill Book Co. p. 137.
Fieldes, M. (1952), *Nature*, **170**, 366.
Keith, H. D., (1950), *Proc. Phys. Soc.*, **63B**, 208, 1034.
Keith, M. L., and Tuttle, O. F. (1952), *Am. J. Sci.*, Bowen Volume, 203.
Lipson, H., and Wilson, A. J. G. (1941), *Proc. Phys. Soc.*, **53**, 245.
McDowell, I., and Vose, W. (1952), *Nature*, **170**, 366.
Sabatier, G. (1953), *C. R. Acad. Sci. Paris*, **236**, 720.

Note by G. W. Brindley

Dr. H. D. Keith's statement that "no fully indexed list of its lattice spacings has yet been published" requires modification in view of the recently issued *A.S.T.M.* *x*-ray index card No. 5-0490 which contains accurate indexed data for quartz obtained by Swanson and Fuyat (*NBS circular* **539**, Vol. III, 1953) who give the lattice spacings *a* 4.913, *c* 5.405 Å at 25° C. relative to λ 1.5405 Å (CuK_{α_1}). This, of course, does not detract from Dr. Keith's discussion of the accuracy of quartz spacing determinations and of their suitability for calibrating *x*-ray diffraction cameras.

Note by M. L. Keith

The small sample of quartz received from Dr. H. D. Keith has a simple, sharp inversion (H 573.4°, C 573.3°). The thermal record shows no evidence of multiple or complex inversion.

Tuttle and I found growth zoning and resultant complex inversion to be common in samples from Brazilian crystals; of course, recognition of growth zoning by thermal methods requires a sample representative of all zones, ideally a granular sample prepared by crushing a slice cut normal to the *c* axis.

ABSORPTION SPECTRA OF SMOKY QUARTZ FROM AN ARKANSAS VEIN DEPOSIT AND FROM A SIERRAN MIAROLITIC GRANITE

Royal R. Marshall, *California Institute of Technology, Pasadena, California.**

The absorption spectrum of a moderately colored smoky quartz crystal from the John Brown prospect in Blakely sandstone, Jessieville, Arkansas, has been determined for the wave length range 220–1000 mμ using a Beckman model DU spectrophotometer. A section 1.30 cm. thick was cut parallel to the basal pinacoid and the surfaces polished. The light path was parallel to the *c* axis. Zoning of the coloration parallel to the prism faces and also at a low angle to the (0001) plane is readily observed in the section. The measured optical densities have been corrected for small reflection losses and converted to absorption coefficient (K) values. The term absorption as used in this note must be qualified since a significant amount of light passing through smoky quartz is scattered (1) and the apparent absorption curve (Fig. 1) has this effect superimposed upon true absorption. K (in cm^{-1}) plotted against wavelength (in mμ) in Fig. 1 illustrates the continuous increase in absorption with decreasing wavelength (2, 3). There is a readily discernible shoulder on the curve at wavelengths somewhat greater than 400 mμ and a less pronounced one

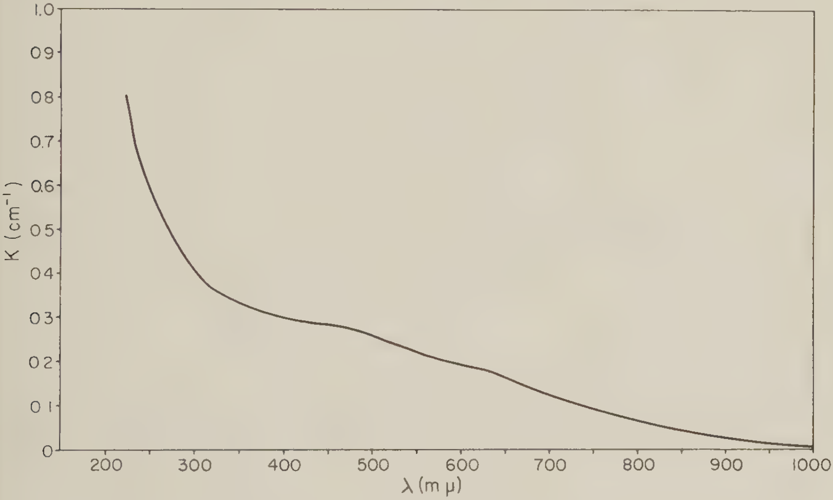

Fig. 1. Absorption coefficient versus wavelength for Arkansas smoky quartz.

---

* Publications of the Division of the Geological Sciences, California Institute of Technology, Pasadena, California. Contribution No. 722.

near 600 mμ. The measurements were made at 5 mμ intervals from 220 to 600 mμ and at 10 mμ intervals from 600 to 1000 mμ in a continuous run at constant temperature. The remarkably smooth curve formed by these numerous points indicates that these shoulders are significant.

Cohen (4) has studied smoky quartz from the Dinkey Lakes region, Fresno County, California, and his (5) spectrophotometric curve and confirmation of an absorption peak near 600 mμ by the photographic plate method agree with the data presented in Fig. 1. The writer has subsequently visited the Dinkey Lakes region and found that the material which Cohen used in his studies occurs in numerous miarolitic cavities typically 2 to 3 inches in diameter scattered throughout a ridge of granite. Potash feldspar and intensely colored smoky quartz crystals protrude into these cavities. Hamilton (6) has examined in detail the alaskite pluton containing these crystals.

The Arkansas specimen was obtained from a different geologic environment. This crystal formed in a quartz vein in Ordovician sandstone (the maximum age possible for the vein is middle Pennsylvanian since this and other veins cut rocks as young as middle Pennsylvanian; the minimum, lowermost Cretaceous; the inferred age is middle Pennsylvanian). Nevertheless, it exhibits the thermolabile and x-ray inducible coloration typical of pegmatitic smoky quartz (7). The absorption spectrum data reported in this note further substantiate the contention that there is a fundamental interpretation of the coloration of these crystals. Apparently small local concentrations of radioactive elements can darken quartz although the effects of irradiation may have to accumulate over millions of years. Some evidence (8) has appeared indicating that an impurity is required. This impurity would have to be a rather common one in view of the extensive distribution and diverse geologic environments of smoky quartz and quartz which can be artificially darkened. In accord with this is some paramagnetic resonance data suggesting that aluminum is closely connected with the magnetic centers obtained in irradiated quartz (9).

In any case it should be emphasized that the mechanism by which quartz darkens is more complicated than that generally involved in the development of the thermolabile coloration of other minerals. Mohler (3) found well-defined absorption peaks in freshly irradiated quartz which became less pronounced with time while absorption at short wavelengths increased. Also natural smoky quartz has been found to be only slightly thermoluminescent (10), an anomaly which Daniels and Saunders (11) have confirmed. However, they found that freshly irradiated quartz is very thermoluminescent. Irradiation seems to be initially accompanied by the formation of metastable electron centers. With time some reaction occurs transforming these centers to a different type (perhaps of a colloidal or light-scattering nature (1)). These centers can be annealed out in a non-radiative process.

I am grateful to Dr. A. E. J. Engel, California Institute of Technology, for his interest in this study and to him and Mr. H. D. Miser, U. S. Geological Survey, for the donation of smoky quartz crystals.

References

1. Strutt, R. J. (1919), Scattering of light by solid substances: *Proc. Roy. Soc. London*, **95A,** 476–479.
2. Holden, E. F. (1925), The cause of color in smoky quartz and amethyst: *Am. Mineral.*, **10,** 203–252.
3. Mohler, N. (1936), A spectrophotometric study of smoky quartz: *Am. Mineral.*, **21,** 258–263.
4. Cohen, A. J. (1954), Regularity of the *F*-center maxima in fused silica and α quartz: *J. Chem. Phys.*, **22,** 570.
5. Cohen, Alvin J., Mellon Institute (private communication).
6. Hamilton, Warren B. (1951), Granitic rocks of the Huntington Lake area, Fresno County, California: *Ph.D. thesis,* University of California, Los Angeles.
7. Engel, A. E. J. (1952), Quartz crystal deposits of western Arkansas: *U. S. Geol. Survey, Bull.* **973-E,** 260 pp.
8. Brown, C. S., and Thomas, L. A. (1952), Response of synthetic quartz to *x*-ray irradiation: *Nature,* **169,** 35–36.
9. Griffiths, J. H. E., Owen, J., and Ward, I. M. (1954), Paramagnetic resonance in neutron-irradiated diamond and smoky quartz: *Nature,* **173,** 439–440.
10. Köhler, A., and Leitmeir, H. (1934), Die natürliche Thermolumineszenz bei Mineralien und Gesteinen: *Zeit. Krist.*, **87,** 146–180.
11. Daniels, F., and Saunders, D. F. (1950), The thermoluminescence of crystals: Final Report, *A.E.C. Contract AT(11-1)-27.*

A NEW PARALLEL RULER FOR ADAPTING THE UNIVERSAL STAGE FOR PETROFABRIC ANALYSIS

A. W. Kleeman, *Mawson Laboratories,*
University of Adelaide, Adelaide, South Australia.

In adapting the universal stage for petrofabric analysis, it is necessary to fix to the upper hemisphere a parallel rule device to enable the slice to be moved into parallel positions across the field of view. (cf. Fairbairn p. 258, Fig. 20.4). Leitz has designed a special hemisphere mount with the "Schmidt Ruler" built in. In both of these devices the arm that holds the slice is parallel to the long axis of the hemisphere mount and is necessarily in contact with the shortest edge of the glass slip on which the slice is mounted. In order to cover a large area of the rock slice it is frequently necessary to change the Schmidt ruler from one end to the other of the slip, which means that the ends must be parallel.

A new type of parallel ruler in which the reference arm is at right angles to the long axis of the hemisphere mount, and hence parallel to

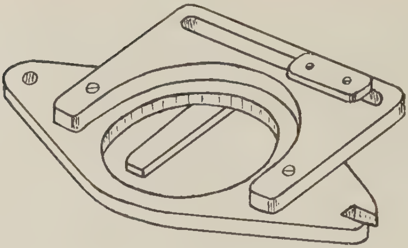

Fig. 1

the long edge of the slip has been designed in the Mawson Laboratories. An isometric sketch showing the parallel ruler attached to a standard Leitz hemisphere mount is shown in Fig. 1. In this sketch the hemisphere itself is not shown so that the position of the reference arm can be seen below the hemisphere mount. Figure 2 is a copy of the working drawing from which the device was built. Only a few dimensions are given, the rest can easily be scaled from the drawing. The dimensions will vary slightly depending on the exact size of the hemisphere mount to which the ruler is to be fitted. The horseshoe shaped yoke was made of aluminium alloy "dural" about 2.5 mm. thick but it could easily be thinner. The semi-circular opening can be as large as is consistent with the rest of the design, as well as being an opening large enough to clear the hemisphere. It should also give enough room for the microscope objective when the stage is tilted. This does not apply so much when objectives such as the Leitz U.M. series are used as it does when using the normal short mount objective (e.g. Leitz P2).

The reference arm must of necessity be thinner than the thinnest thin section used. In general the glass slip upon which the rock is mounted is

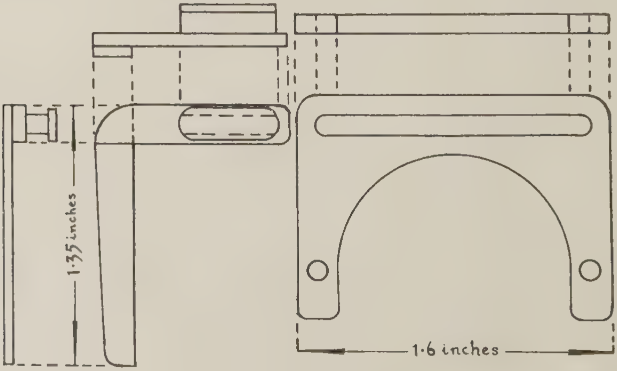

Fig. 2

1.0±0.10 mm.; to this must be added 0.20 mm. for the combined thickness of the slice and cover glass. The arm therefore was designed at 1.00 mm. This arm is fixed to another piece of dural, a little thicker than the hemisphere mount, in our model 2.0 mm. thick. Upon this is the cursor which runs in the slot of the yoke. This cursor should be just a little thicker than the yoke to allow for adjustment when the device is assembled. The top plate screwed above the cursor is necessary unless some other artifice is used to keep the cursor in place in the slot. The yoke is fixed to the hemisphere mount by two set screws, for which it is necessary to tap two holes in the hemisphere mount. These two screws should be countersunk to prevent them coming into contact with the objective when the stage is tilted.

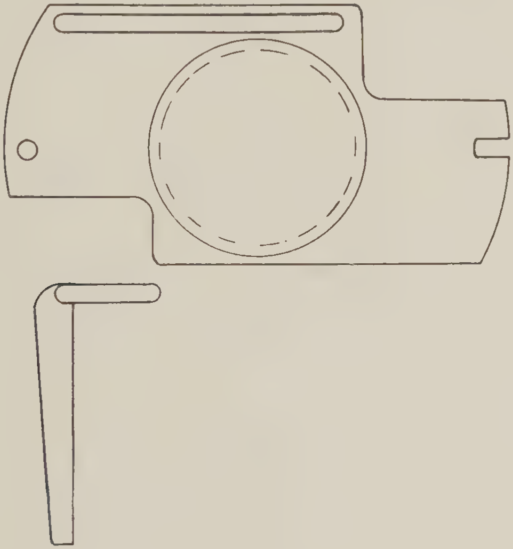

FIG. 3

The new design has several advantages. As mentioned above, the reference arm is in contact with the long edge of the thin section and the whole available area can be traversed in one set-up. Also it is not necessary to cut the glass slip as short as when the Schmidt ruler is used. The device can be designed so that the reference arm does not prevent the thin section being moved into any position in which the design of the Leitz U.T.4 allows it to be manipulated, but in the original model the movement was limited slightly. Thin sections in the Mawson Laboratories are made in the first instance on 3 inch by 1 inch microscope slides and covered by $\frac{7}{8}$ inch square cover glasses. It was, therefore, decided to limit the movement of the reference arm to 0.90 inch, (23 mm.). The distance that the thin section can move parallel to the reference arm is limited by the length of the thin section because the corners hit the mounting of the inner circle of the universal stage during manipulation. For universal stage work thin sections are cut to length between 1.6 and 1.8 inches, i.e. producing 25 mm.×45 mm. to 25 mm.×40 mm. thin sections. With the larger size the square area that can be brought beneath the crosswires is 14×14 mm. and with the smaller 19×19 mm. Allowing for the fact that it is not necessary to bring the grains beneath the crosswires the use of the smaller (25 mm.×40 mm.) glass slip will permit as much rock slice as can be mounted below a $\frac{7}{8}$ inch square (22 mm.) cover glass to be examined.

This device is designed to be fitted on the normal hemisphere mount of the Leitz U.T.4 or similar universal stage. The same principle of having the reference arm at right angles to the long axis of the hemisphere mount can be adopted in making up special hemisphere mounts as is indicated by the sketch in Fig. 3. In this design the hemisphere mount is cut away to enable the thin section to be moved more easily.

Reference

Fairbairn, H. W. (1951), The Structural Petrology of the Deformed Rocks. Cambridge, Mass.

ACTIVATION OF PHOTOLUMINESCENCE IN ARTIFICIAL CALCITE BY STANNOUS ION

Stewart J. Carlson, *Tulsa, Oklahoma.**

Introduction

Activation of calcite fluorescence has received a great deal of attention in the past, although the results and interpretations have been contradictory. Headen (1906) suggested the yttrium group as possible activators but presented little definite evidence. Nichols (1918) confirmed manganese activation and suggested that heat might be necessary for fluorescence. Tanaka (1924), analyzing calcite cathodoluminescence with a spectrophotometer, decided the "active agent" was manganese and suggested as other "active agents," dysprosium, yttrium, thallium, samarium, and strontium. Brown (1934), analyzing natural calcite, found that 3.4 mole per cent manganese gave the most intense luminescence.

---

* Present address: Box 40, U. S. NAVCOMMFAC, Navy 214, c/o FPO, New York, New York.

On the other hand Northup (1940), also using natural specimens, found no definite relation between manganese content and luminescent intensity, but found that the sample with the most intense luminescence had 0.2 per cent lead while the others had only a trace. Fonda (1940) artificially precipitated luminescent calcite using manganese as an activator. Schulman and others (1947), following Fonda's (1940) method of preparation, determined that manganese does not activate alone but requires an auxiliary activator such as lead, thallium, or samarium.

This study was intended to establish other possible activators of calcite photoluminescence by synthesis under carefully controlled chemical and physical conditions. The experiments were carried out in the Mineralogical Laboratory of the Department of Geology, Cornell University, Ithaca, New York.

PREPARATION OF PHOSPHORS

The method of preparation was patterned after Fonda (1940). A cold solution of 0.150 molar $(NH_4)_2CO_3$ was added to one containing 0.075 molar $CaCl_2$ and other cations, and the resulting precipitate was heated for 10 minutes to refine the crystals and to insure uniform solid solution. Letting the precipitate stand in cold solution for 10 hours gives equal luminescence. The precipitate was examined under a microscope to determine crystal form, then filtered, washed, and dried. The precipitates were pure white in color. Luminescent intensity and color were observed at room temperature using a cold quartz ultraviolet source.

EXPERIMENTAL RESULTS

Addition of stannous ion to calcite activates a bright white fluorescence. The limits of visible fluorescence are 0.02 and 19.0 mole per cent, with the most intense fluorescence at 0.6 mole per cent. A trace of bismuth alters the stannous-activated fluorescence to green, lanthanum and neodymium to pale yellow, manganese to deep orange, and magnesium to bluish green. Stannic ion fails to activate.

Co-activation of manganese with other ions was confirmed. Many other ions were tried in various combinations and concentrations, without inducing visible fluorescence.

CONCLUSIONS

Tin activation of calcite appears to be substitutional since only the stannous ion produces fluorescence and relatively large mole percentages are necessary for activation. The color shifts caused by the addition of other ions are probably examples of partially or completely sensitized activation, as discussed by Schulman and others (1947) for the case of manganese-lead activation of calcite.

In general, natural luminescence results from an impurity ion having an absorption spectrum close to the wavelength of the source used for examination. This impurity ion either acts as a dominant activator and controls the emission spectrum, or acts as an auxillary activator and sensitizes the fluorescence by transferring its absorbed energy to one or more dominant activators. Thus many of the additional impurity ions in a natural phosphor may modify the fluorescent spectrum, and make indiscriminate use of fluorescence for mineral identification or correlation of doubtful value.

References

Brown, W. L. (1934), *University Toronto Studies, Geol. Ser.*, No. **36,** 45–54.

Fonda, G. R. (1940), *Jour. Phys. Chem.*, **44,** 435-441.

Headen, W. T. (1906), *Am. Jour. Sci.*, **221,** 301–306.

Nichols, E. L., Howes, H. L., and Wilber, D. T. (1918), *Phys. Rev.*, **12,** 351–353.

Northrup, M. A., and Lee, O. I. (1940), *Jour. Opt. Soc. Am.*, **30,** 206–223.

Schulman, J. H., Evans, L. W., Ginter, R. J., and Murata, K. J. (1947), *Jour. Appl. Phys.*, **18,** 732–740.

Tanaka, T. (1924), *Jour. Opt. Soc. Am.*, **8,** 411–418.

ON THE STABILITY AND HYDROTHERMAL SYNTHESIS OF BENITOITE

D. E. Rase and Rustum Roy, *College of Mineral Industries,** *The Pennsylvania State University, State College, Pennsylvania.*

Although extremely rare, the mineral benitoite ($BaTiSi_3O_9$) is of considerable interest since it represents one main type of chain structure in silicates; it also has some value as a gem stone. Furthermore, its temperature and pressure range of stability could perhaps assist in understanding the formation of the rocks in which it occurs.

No previous work has been reported on the synthesis or stability of benitoite although numerous papers have appeared dealing with its physical and optical properties and crystalline structure. These aspects are thoroughly reviewed by Dana (1949) and Bragg (1937). The work reported here has been done in conjunction with a study of the equilibrium relations in the system barium titanate-silica. The experimental conditions and results obtained are presented in detail in another paper by the authors (1954).

The most prominent interplanar spacings for benitoite are presented in Table 1, since none are available in the literature. These data were obtained from the natural mineral found in San Benito County, California, using a Norelco hi-angle x-ray diffractometer, CuK_α radiation and Ni filter. The indexing of the pattern followed from a consideration of the axial ratio reported in the literature and the use of Bunn charts.

---

* Contribution No. 54-57.

On the basis of x-ray data alone, the maximum temperature of stability of benitoite under dry conditions, as determined by heating the natural mineral to higher and higher temperatures, appears to be 1050° C. Above this temperature the x-ray diffraction pattern definitely indicated the presence of another phase, $BaTiSi_2O_7$. However, microscopic observation indicated that at least partial dissociation had occurred well below 1050° C. and as low as 1000° C. Dissociation in the mineral is evidenced by minute "worms" appearing throughout the crystalline benitoite fragments when observed microscopically. Extended heat treatment induced the "worms" to grow until they began to appear as individual and distinct crystals within the benitoite itself.

TABLE 1. SELECTED INTERPLANAR SPACINGS FOR THE MINERAL BENITOITE ($BaTiSi_3O_9$)

(Natural and synthetic identical)

d	I/I_0	$hk\cdot l$
5.75	45	100
3.733	100	102
3.329	10	110
3.156	10	111
2.883	35	200
2.771	65	201
2.252	30	104
2.179	25	210
2.125	5	211
1.990	10	212
1.972	15	114
1.925	10	300
1.860	25	204
1.788	40	302
1.665	5	220
1.628	85	310
1.576	10	222, 311, 106

Hydrothermally, the stability maximum of benitoite was not defined as distinctly by means of x-rays as in the case of the dry investigations. However, similar growth of crystals within the benitoite was observed in the hydrothermal runs as in the dry runs.

Attempts to synthesize benitoite "dry" by heating a mixture of oxides or "gel" of its own composition, or by devitrifying a glass of the correct composition were always unsuccessful. When the completely melted and quenched stoichiometric mixtures (having a $BaTiSi_3O_9$ composition) were treated hydrothermally above about 965° C. at 5000 psi water pressure and only as long as 4 hours, benitoite was not observed as a stable phase. In all cases the x-ray pattern indicated mainly the presence of the compound $BaTiSi_2O_7$ with tridymite appearing only in the longer runs. At temperatures below 965° and at 5000 psi however, these same mixtures converted readily to a crystalline phase having an x-ray diffraction pattern identical to that of the natural benitoite. Furthermore, it was possible to obtain the benitoite pattern from mixtures slightly off the stoichiometric composition. In the latter case, the patterns for both benitoite and the compound $BaTiSi_2O_7$ were obtained thus indicating that equilibrium had been attained since these appear to be the stable phases at these temperatures as determined in the study of the system $BaTiO_3$-SiO_2. It appears therefore that the maximum stability temperature of benitoite as determined hydrothermally is about 100° lower than the apparent maximum under dry conditions, a situation not uncommon in hydrothermal literature and one which might well be expected. Although benitoite can be synthesized quite easily by a hydrothermal devitrification process, in no case was it possible to obtain any indication of its presence from the initial sintered oxide mixtures even when treated at temperatures and pressures known to favor the synthesis.

Thus we have been able to synthesize benitoite hydrothermally and to fix its upper stability limit as $965° \pm 10°$ C. at 5000 psi.

REFERENCES

BRAGG, W. L., (1937), Atomic Structure of Minerals, Cornell University Press, Ithaca, New York, Chap. XII, pp. 179–181, 292 pgs.

DANA, E. S., (1949), Dana's Textbook of Mineralogy, John Wiley and Sons, New York, 4th Edition edited by W. E. Ford, p. 691, 851 pgs.

RASE, D. E., AND ROY, RUSTUM, (1955), The System $BaTiO_3$-SiO_2; *Jour. Am. Cer. Soc.* (In Press).

FAULTS IN GYPSUM ACCESSORY PLATES

WILLIAM T. HOLSER, *Cornell University, Ithaca, N. Y.*

It may not occur to some petrographers to question the accuracy of the engraving on an accessory plate, unless they begin to get anomalous results. A beginning student may not even realize that his results are anomalous. Our experience suggests that all such plates should be closely inspected when received from the manufacturer or from overhaul.

In 1951 a new gypsum full-wave plate was received with a microscope returned from factory overhaul. Although the plate was given a brief visual inspection, only during subsequent use was it discovered to have an interference color in deep blue instead of magenta. Investigation revealed that the plate was actually gypsum, oriented in the correct way, but of too great a thickness. The plate was also found to have its fast direction at an angle of 18° with the edge of the holder. Further tests on our seven other plates showed a maximum angle of 8°, with an average of 3 degrees. All these plates are from the same manufacturer, who states that the inspection tolerances are:

Retardation—535 ± 15 mμ,
Orientation—fast ray parallel to edge of plate within ±1°.

Of course the manufacturer graciously replaced the defective plate, and the new plate was found to have a satisfactory thickness, and parallel extinction. Unfortunately, and almost incredibly, the parallel extinction was found later to be slow instead of fast, in other words, the plate with an 18° deviation had been replaced with one of 90°.

According to Wright (1911, p. 133) the orientation of the plate does not impair its usefulness in determining the extinction position, in fact the optimum orientation is almost parallel to the nicols. Furthermore, the small deviations make no difference in work with interference figures. However, in determining whether the elongation of a crystal is nearest to the slow or fast ray ("sign of elongation"), a deviation of the plate as large as 18°, or even 8°, might give wrong answers for minerals of large extinction angle. Of course the deviation of 90° should soon be noticed by even a poor student.

REFERENCE

WRIGHT, F. D. (1911), The Methods of Petrographic Microscope Research: *Carnegie Inst., Publ.* **109**.

THE DIAMOND TOOL INDUSTRY IN 1954

This is the 10th successive report in this series on the Diamond Tool Industry. It is divided into 18 sections, for instance, scientific aspects, hardness and microhardness, surface finish testing, fine boring and turning, truing of grinding wheels, etc. In each of these sections it is referred to outstanding work published during 1954 and in some instances also to publications in 1953. The publication of 12 pages contains about 200 references. The literature referred to in this report can be obtained on loan, in England only, on application to: the Industrial Diamond Information Bureau, St. Andrew's House, 32-34 Holborn Viaduct, London, EC 1.

The American Crystallographic Association will hold its annual meeting on the campus of the California Institute of Technology, Pasadena, California, during the week of June 27, 1955.

BOOK REVIEWS

THE OPTICAL PROPERTIES OF ORGANIC COMPOUNDS, by A. N. WINCHELL. Second Edition. Academic Press, Inc., New York (1954). xviii+487 pages, 153 figs., 2 diagrams in pocket. Price $12.00.

The second edition of this very useful compilation contains descriptions of some 900 more compounds (total, 2500) than were in the original (1943) edition. Almost twice as many (ca. 2000) are included on one or both of the two diagrams for determination of compounds than were on the single diagram of the first edition.

In its manner of treatment, classification of the compounds, and explanation of the diagrams this edition is essentially identical with the first edition. The remarks in Faust's review[1] of that edition still apply, therefore, with one important exception noted below.

Most of the changes made are very minor ones:

1. The key to the diagrams has been placed in a table in the text rather than on the margins of the diagrams themselves.

2. N_x, N_y and N_z are used for indices of refraction of biaxial crystals instead of N_p, N_m and N_g.

3. The systematic part of the treatise begins with a two page summary of the properties of the various forms of carbon: diamond, graphite, and coal.

4. Faust's criticism that it is commonly difficult to obtain maximum and minimum indices of refraction from cleavage fragments has been considered and a brief supplement on this subject added to the explanation of the diagrams. Also, a second diagram based on N, N_0, or N_y, the optic angle, and the optic sign has been added, which simplifies the use of the diagram(s) and key a great deal.

It should be realized that the chances of finding a given organic compound in the tables or diagrams is comparatively remote. This is in no wise the fault of the compiler; he has done a remarkable job of getting together a mass of optical data from the literature and has included unpublished information on some 200 compounds. It is rather a reflection of the general failure of organic chemists to realize the importance and usefulness of optical properties in the characterization of compounds. Some 500,000 solid crystalline organic compounds are known; with approximately 2500 such compounds in the volume under review it would appear that the chances are about 200 to 1 against finding a given compound described in it. Actually, the chances are considerably better than this, because many more relatively common compounds are included than rare ones.

Optical properties of gases are meaningless for the purpose of this volume, but for organic compounds that are liquids at room temperature it would have been very useful to include such data as are available on indices of refraction and variation thereof with temperature, dispersion, optical activity (power of rotation), etc. The fact that liquids were not included raises the question as to whether the title should have been "The Optical Properties of Crystalline Organic Compounds."

Winchell's compilation is far and away the best single source of information on the optical properties of solid organic compounds. It should be widely used in identifying them, but from the comparatively few optical descriptions that have been published since the first edition appeared it is evident that Faust's hope that "this book will stimulate a wider interest amongst chemists in the useful methods of microscopic-petrographic research" has not yet been fulfilled.

Earl Ingerson
U. S. Geological Survey,
Washington, D. C.

---

[1] *Am. Mineral.*, **30**, 545–546 (1945).

TEXTURES OF THE ORE MINERALS AND THEIR SIGNIFICANCE, by A. B. Edwards.

242+xiii pp., 31 tables, 204 figures. Australasian Inst. Min. and Met. (Inc.). Melbourne, Australia. 2nd ed. (revised), 1954. Costs are as follows: Members Aus. I.M.M. (one copy only) £2-, plus postage; Student Members Aus. I.M.M. (one copy only) 30/-, plus postage; Non-members £3-, plus postage; Bona-fide Students (non-members) £2-, plus postage. The above prices are in Australian currency.

The first edition of this book, which appeared in 1947, was a welcome addition to the scanty modern literature, *in English*, on the interpretation of ore-mineral textures. Despite little publicity or advertising, copies became widely distributed. The reviewer found the book highly useful as assigned collateral reading in a course on ore-mineral paragenesis. The second edition follows faithfully the plan of the first; no significant alterations have affected the mode of presentation. New data have been included throughout, however, and a final chapter on the textures of smelter products has been added. Since the first edition was not reviewed in *The American Mineralogist*, readers may obtain an idea of the scope and arrangement of the book from the following list of chapter headings and some of the topics:

I. The textures of native metals—silver, gold, bismuth, arsenic and antimony.
II. Primary zoning and banding in oxide and sulfide ores—growth zoning, magmatic layering, crustification, colloform banding.
III. Textures due to deformation—banding, twinning, recrystallization, fracturing.
IV. Solid solutions—in native metals, in oxides, in sulfides and sulfosalts.
V. Replacement textures—rim, core and zonal replacements, veins, relicts, pseudo-eutectic textures.
VI. Application to ore geology—paragenesis (simultaneous, successive and overlapping deposition), temperature determinations.
VII. Application to ore dressing.
VIII. The transparent gangue minerals.
IX. Smelter products.

The numerous photomicrographs are generally pertinent, and many are clear reproductions, although some are sufficiently lacking in detail so that they should be replaced or drawings substituted (e.g., figures 14, 15, 89, 103, 106 and 126). A number are taken from Schneiderhöhn and Ramdohr, *Lehrbuch der Erzmikroskopie*, as well as from other published sources. To all workers in ore-mineral microscopy the book may be recommended as a very good summation of the textures of the opaque minerals and interpretations of their genetic significance.

E. Wm. Heinrich,
University of Michigan,
Ann Arbor, Michigan

MINERALS IN WORLD INDUSTRY by Walter H. Voskuil,

324 pp., 38 tables, 26 figures. McGraw-Hill Book Co., New York City. $5.75, 1955.

Of considerable interest to many mineralogists, geologists, mining engineers and mineral economists will be *Minerals in World Industry*, an up to date summary of the participation and importance of minerals in economic systems, with particular emphasis on their significance in the founding and development of high living standards, especially in that of the United States. Unusually well organized, the book appears to be designed principally as a text for mineral economics, although its content is sufficiently detailed and modern to permit its use as a general work of reference.

After a brief discussion of mineral economy, six chapters are devoted to iron and its alloys—its relations to man, the geographic pattern of steel empires, iron in the Americas, in Europe and in Asia, Australasia and Africa. Chapters 8 to 16 deal with mineral fuels, coal, petroleum and natural gas, with brief comments on solar energy, water power and nuclear energy. Then follow chapters on copper, lead and zinc, aluminum and magnesium, building materials, three on mineral plant foods—nitrogen, phosphates and potash, one on sulfur, and one on minerals used in minor tonnages. The last two chapters are entitled American Mineral Policy and Relation of Industrial Nation to Undeveloped Areas. The whole is a well integrated and highly readable, fact-crammed account of world-wide mineral economics.

Although the author realizes the importance of adequate water supplies in promoting high living standards, it is disappointing that no discussion whatsoever of this vital material is included. Here and there the tone, particularly of some of the topic headings, becomes somewhat pedagogical. Significant omissions appear to be few—no mention of Br or I, of light weight concrete aggregate material, of synthetic mica or of the importance of Li in nuclear reactions, but these and others are all minor. More serious is the inadequacy of the index in which many topics and materials, touched on briefly in the text, find no reference. Beyond these the book is comprehensive and comprehensible. Its particular forte is its outstanding exposition of the interrelations of economic geology and *geopolitik*.

E. WM. HEINRICH,
University of Michigan,
Ann Arbor, Mich.

A HISTORICAL SURVEY OF PETROLOGY by F. Y. LOEWINSON-LESSING, translated from the Russian by S. I. Tomkeieff. 112 pp. Oliver and Boyd Ltd., Tweeddale Court, Edinburgh 1, Scotland. 12/6, 1954.

This book, which was originally written in Russian by the late Professor Loewinson-Lessing and published in 1936 under the title of *Vvedenie v Istoriu Petrografi* (An Introduction to the History of Petrography), has at last appeared in an English edition. The only possible regret on its appearance is that it was not available earlier, for although the translation was completed in 1939, World War II delayed its publication. The translator, Dr. S. I. Tomkeieff, who is Reader in Mineralogy, King's College, University of Durham, was a student of Professor Loewinson-Lessing and in his own words, has " . . . translated rather freely, curtailing some parts, amplifying others, and including additional material drawn from Professor Loewinson-Lessing's latest papers."

The book is primarily a synthesis of the evolution of petrogenetic thinking, assembled in the light of the author's own experience and considerable contribution to the science, rather than a detailed chronological record of the development of petrology. Thus, after an introductory chapter, the book outlines the major concepts and important discoveries separately under the different lines of approach to petrology—geological, petrographical, chemical, experimental and synthetic. Although the author refers to his work as " . . . simply a modest introduction . . . ," the book is so concise and so well organized that it encompasses easily and skillfully the entire lifetime of the science, without descending to mere tabulation of dates, men and ideas. It is not only worthwhile reading, but also interesting reading. No review can do justice to its wealth of detail, naturally arranged.

So often today, because of the looming mass of factual material whose mastery is required of students, an appreciation of the work of our predecessors tends to be neglected. Graduate students in particular should be encouraged to look beyond their textbooks and acquaint themselves with the original classical monographs that spelled out, one by one, the basic laws and theories of the science. A Historical Survey of Petrology is recommended as required reading in petrology and petrography; it is a stimulating summary, the only adequate one available in English.

E. WM. HEINRICH,
University of Michigan,
Ann Arbor, Mich.

GUIDEBOOK TO THE GEOLOGY OF UTAH, NUMBER 9, URANIUM DEPOSITS AND GENERAL GEOLOGY OF SOUTHEASTERN UTAH. Ed. Wm. Lee Stokes. Utah Geol. Soc., 115 pp., 18 figures, 5 plates, 2 tables, 1954. Distributed by Utah Geol. Mineral. Survey, Mines Bldg., Univ. Utah, Salt Lake City, Utah. $3.00.

This up-to-date guidebook to the geology and uranium deposits of the Thompson district (Grand Co.) and Big Indian-Lisbon Valley area (San Juan Co.) in southeastern Utah is divided into the following chapters: History of radium-uranium mining in the Plateau Province (R. Clare Coffin); Summary of events in the Colorado Plateau since 1924 (anonymous); Stratigraphy of the southeastern Utah uranium region (Wm. Lee Stokes); Structural features of southeastern Utah and adjacent parts of Colorado, New Mexico and Arizona (Eugene M. Shoemaker); The uranium mineralogy of the Colorado Plateau and adjacent regions (John W. Gruner); Geology and uranium deposits of the Thompson area, Grand County, Utah (Wm. Lee Stokes and C. M. Mobley); Ore deposits of the Big Indian Wash-Lisbon Valley area (Y. Wm. Isachsen); Side trip to Arches National Monument (U. S. Park Service); and Itinerary and road logs. With the wealth of detailed information it contains, this guidebook should prove invaluable to geologists and prospectors working in this and adjacent regions. Mineralogists will be particularly interested in Gruner's discussion of the mineralogical relations between the oxidized and unoxidized uranium ores.

E. Wm. Heinrich,
University of Michigan,
Ann Arbor, Mich.

PRACTICAL REFRACTOMETRY BY MEANS OF THE MICROSCOPE, by Roy M. Allen. 76 pp., 15 fig., paper bound. R. P. Cargille Laboratories, Inc., 117 Liberty St., N. Y., N. Y. 1954. $1.00.

This is a handy manual that will be useful to all students of microscopic crystallography, mineralogy and petrography as well as to ceramicists and chemists, or anyone attempting to identify translucent crystalline materials by means of their optical properties under ordinary and polarized light. The discussion of refractive index determinations deals with indices of liquids, of solids and the various comparison techniques (Becke line, oblique illumination, half-illumination and Emmons double variation methods). Information follows on lighting sources, procedures for uniaxial and biaxial crystalline substances, dispersion and accuracy. A final section describes index liquids.

E. Wm. Heinrich,
University of Michigan,
Ann Arbor, Mich.

DIE EIGENSCHAFTEN DER MINERALE, TEIL II, MINERALCHEMISCHE TABELLEN UND QUALITATIV-CHEMISCHE NACHWEISVERFAHREN, by Arno Schüller. 602 pp. Akademie-Verlag, 39 Mohren Street, Berlin W. 8, Germany. 1954. DM42.00.

This voluminous work is essentially a series of mineral determinative tables based primarily on chemical composition, particularly on the recognition of one of the cations present. Parts I and II of Section *A* include general information on the calculation of mineral formulas from chemical analyses and examples of mineral determination with the help of multi-component-system diagrams. Part III is a group of chemical tables—colors in melts; borax and microcosmic salt bead colors; general solubilities of mineral groups in acids; colors of HCl solutions; tests for important cations with certain standard reagents; lists of reagents, both alphabetical and according to the elements for which they test; an alphabetical list of the elements, with symbols, atomic members and weights and atomic and ionic radii; an alphabetical list of the cations and their ionic radii; several figures and a table showing size relations of atoms and ions; and chemical and physical periodic tables of the elements. Several of the figures, particularly figures 6*a* and 6*b*, are reduced to a point at which they cease to be useful. Section *A* concludes with a short list of references and with another of abbreviations employed in the mineral tables that follow.

Most of the mass of the book (522 pages) is included in the first part of Section *B*. Here are presented 49 subdivisions under the various main elements that form cations in minerals, arranged alphabetically (aluminum to zirconium). For each of these elements the following data are listed: atomic weight and number, valence, atomic and ionic radii, distribution of mineral species containing that element as a cation among the major groups of minerals (elements; sulfides; haloids and oxyhaloids; oxides and hydroxides; carbonates, borates and nitrates; sulfates, phosphate-haloid-sulfates; phosphates and arsenates; tungstates, molybdates, vanadates and uranates; silicates; and organic compounds), reactions in melts, characteristic crystal precipitate (with sketches of crystal shapes), characteristic color reactions, and flame colors. Thereafter are listed by groups the individual mineral species in which that element is a cation. For each species is given a brief description embodying composition, color, optical properties, hardness, specific gravity, crystal system and a short paragenetic designation. The volume concludes with a systematic listing of minerals by groups.

Patently the book represents a prodigious effort in compilation and arrangement of mineralogical data. Yet it can hardly be considered to serve adequately as a tool for mineral identification primarily by chemical techniques. For a great many species identification is much more rapidly advanced and facilitated if the major *anion* is first identified, for anion isomorphism is normally more restricted than cation isomorphism. For example, the book does not list borates under boron. Surely the initial recognition that a species is a sulfide, or a phosphate, or a carbonate is, for identification purposes, more useful than that it contains Mn, perhaps coupled with unknown amounts of Mg and Fe^2 as well.

The scheme of this book requires multitudinous repetition and duplication, both because of complex isomorphism and because of cations in various structural positions in complex minerals. Thus most aluminum silicates require entry under Al and at least one other element, and many species are listed in three places or even four. Extreme cases are represented by such a mineral as polymignite, which is repeated, properties and all, under Ca, Cb, Ce, Mn, Ta, Th, Ti, W and Zr.

Further burdening the task of identification is the retention of numerous varietal names, including some synonyms and some of trivial varieties (falkmanite, lotrite, oellacherite, keilhauite, lusakite, pyrrhite, magnesiumorthite, cleveite, etc.). The paragenetic assignment for some species is, of course, difficult to express adequately in a few words or even in several phrases and such curtailed genetic generalizations may be of little value as an identification aid. A mechanical shortcoming appears in the grouping of species under a series heading without a typographical break appearing at the end of the series (e.g. for Scapolites, under Ca, pp. 190–191).

The chief value of the book lies in its collection of information on chemical tests for the various elements. The arrangement of the tables is turgid and viscous and mineral identification by means of them will be difficult and hardly direct—rather by hint and anacoluthon.

E. Wm. Heinrich,
University of Michigan,
Ann Arbor, Mich.

NEW MINERAL NAMES

Lodochnikovite

E. I. Nefedov, Report on new minerals discovered by him p. 317 in V. A. Mokievsky. The scientific session of the Federov Institute together with the All-Union Mineralogical Society. *Zapiski Vses. Mineral. Obshch.* (*Mem. Soc. russe mineral.*) Vol. **82,** No. 4, 311–317 (1953), through *Mineralog. Abs.,* **12,** 352–353 (1954).

A complex oxide of Al, Mg, Ca, and F. Insol. in acids. Monoclinic, optically neg., 2 V small, *N*s, alpha 1.732, beta 1.744, gamma 1.746, X bluish-green, Y light yellowish-green, Z almost colorless, Z perpendicular to (010), *r* less than *v*. H. 7½. Found in skarn with calcite, spinel, titanomagnetite, idocrase, and corundum.

Michael Fleischer

Mikheevite

E. I. Nefedov, *op. cit.* Composition $K_2Ca_4(SO_3)_5 \cdot H_2O$. Triclinic with *a* 6.70 ± .001, *b* 9.12 ± .02, *c* 16.63 ± .06, alpha 100° 30′, beta 75°18′, gamma 110°44′, *a*:*b*:*c* 0.734:1:1.825. Habit prismatic, fragile, cleavage imperfect. H. 3½, G. 2.93, colorless to white, m.p. 1000° C.; *N*s, alpha 1.557, beta 1.568, gamma 1.580. Found among salts.

Discussion: Despite differences in composition, crystal system, and G., this is almost certainly identical with görgeyite, see *Am. Mineral.*, **39**, 403–404 (1954). The name görgeyite seems to have priority by a few months.

M. F.

Knipovichite

E. I. Nefedov, *op. cit.* A hydrous carbonate of Ca, Al and Cr, containing CaO, 15.00; Al_2O_3, 21.8; Cr_2O_3, 8.8; ignition loss (H_2O+CO_2)45; insol. 2.9%.

Infusible, soluble in acids with effervescence. H. 2–3, G. 2.229. Optically neg., 2V small, *N*s, alpha 1.540, gamma 1.592, X yellowish-pink, Z pink, parallel to elongation. Occurs in pink fibrous radial aggregates in dolomite and quartz veins.

M. F.

Stepanovite

E. I. Nefedov, *op. cit.* Composition $Na\,Mg\,Fe^{+3}\,(C_2O_4)_3 \cdot 8\text{–}9\,H_2O$. Trigonal, with *a* 9.82, *c* 36.67 kX. H.3, G. 1.61. Optically neg., *N*s, omega 1.515, epsilon 1.417, E colorless, O yellowish-green. Fuses with difficulty; soluble in water. Occurs in yellowish-green granular aggregates in coal.

M. F.

Vladimirite

E. I. Nefedov, *op. cit.* Composition $Ca_3(AsO_4)_2 \cdot 4H_2O$. Monoclinic (?), in acicular radial aggregates with good cleavage. H. 3½, G. 3.21, sol. in acids, fusible with difficulty. Optically neg., *N*s, alpha 1.560, beta 1.656, gamma 1.661, 2 V 70°. Found in the zone of oxidation of ore deposits.

Discussion: If the figure for 2V is correct, that for alpha is wrong. Perhaps a misprint for 1.650?

M. F.

Volkovite

E. I. Nefedov, *op. cit.* A hydrous borate of Sr and K. Monoclinic, in colorless cruciform intergrowth twins; *a* 12.90, *b* 14.37, *c* 12.76 kX, beta 100° 27′, cleavage (010) good. Fragile,

H. 3–4. Optically neg., *N*s, alpha 1.513, beta 1.524, gamma 1.580, 2V 44°, Y perpendicular to (010). Sol. in HCl, easily fusible. Found in salts of Inder borate deposits.

M. F.

Belovite

E. I. Nefedov, *op. cit.* Composition given as $Ca_3(Ca, Mg)(AsO_4)_2 \cdot 2H_2O$ (this does not balance. MF). Belongs to the roselite group. In colorless or white druses and fine crystalline aggregates. H.5, G. 3.50, sol. in acids, fusible to a white enamel, *N*s, alpha 1.670, beta 1.688, gamma 1.704, 2V 90°. Found in the zone of oxidation.

Discussion: This is not the same as belovite (a member of the apatite group), recently described. See *Am. Mineral*, **40**, 367 (1955).

M. F.

Ivanovite

E. I. Nefedov, *op. cit.* A hydrous chloro-borate of Ca (and K?). Monoclinic (pseudohexagonal), with *a* 8.60, *b* 8.02, *c* 14.72 kX, beta 91° 08′, short prismatic or tabular, cleavage (010) good. Optically neg., 2V 58–72°, *N*s, alpha 1.504, beta 1.523, gamma 1.531, $r<v$. Soluble in water and acids. Found in salts of the Inder borate deposits.

M. F.

Shubnikovite

E. I. Nefedov, *op. cit.* Composition—a hydrous chloro-arsenate of Cu, Ca, and K, contains CuO 37.32, CaO 7.33, Cl 2.7, As_2O_5 41.43; insol. 1.66%. Orthorhombic (?), platy, light blue. Easily fusible, sol. in acids. H. 2. Optically neg., *N*s, alpha 1.640, beta = gamma 1.690, 2 V small, $r<v$, X light blue, $Y=Z$ greenish-blue. Found in the zone of oxidation.

M. F.

Ammersooite

H. W. van Der Marel, Potassium fixation in Dutch soils: Mineralogical analyses, *Soil Sci.*, **78**, 163–179 (1954).

The name ammersooite is given to the principal clay mineral separated from the less than 2 micron fraction of strongly potassium-fixing soils of the Netherlands, Belgium, France, and Surinam. It is apparently a variety of illite that has an open layer structure. It has a basal spacing *d* (001) of 15.6 Å in air, 17.9 Å when saturated with glycerol. It retains this 15.6 Å spacing when saturated with H^+, Li^+, Na^+, Mg^{++}, Ca^{++}, Sr^{++}, or Ba^{++}. Saturation with K^+, Li^+, Cs^+, or NH_4^+ reduces the basal spacing to 10.8 Å. Vermiculite shows a similar behavior, but is also partly contracted when saturated with Li^+, Na^+, Ca^{++}, Sr^{++}, or Ba^{++}. The *x*-ray and *D.T.A.* data clearly differentiate ammersooite from vermiculite. When heated to 500° C., ammersooite gives the basal spacing of illite (10.6 Å).

Analyses of fractions less than 2 microns with strong power to fix K (about 80% ammersooite) give: SiO_2 50 to 52, Al_2O_3 19 to 22, Fe_2O_3 9 to 11, CaO 1.1 to 1.5, MgO 2.6 to 2.9, K_2O 2.1 to 2.3, Na_2O 0.3 to 0.6, Mn_3O_4 0.1 to 0.2, TiO_2 0.6 to 0.8, P_2O_5 0.2 to 0.4, H_2O 6.5 to 7.5%. Ammersooite is apparently formed from illite in environments with excess Ca^{++}, Mg^{++}, or H^+ and a deficiency in K^+, conditions commonly found in Dutch river sediments or in peaty river and marine sediments.

The name is for "the potash experimental field near Armmerzoden, locally known as 'Ammersooien,' where the K-fixing phenomenon was first observed in Dutch agricultural practice."

Discussion: There is urgent need for the attempt to be made to reach international agreement among soil scientists and mineralogists on the nomenclature of the clay minerals.

The present bad situation cannot be resolved by unilateral decisions by any one society or group; recent attempts of this nature have only made the situation worse. Re-definition is needed, not new names.

M. F.

Hagendorfite

H. Strunz, Hagendorfit, ein neues Mineral der Varulith-Hühnerkobelit-Reihe. *Neues Jahrb. Mineral., Montash.* (1954) 252–255.

The name hagendorfite is given to the mineral of composition $(Na, Ca)(Fe, Mn)_2(PO_4)_2$ with $Na > Ca$ and $Fe > Mn$. Varulite and hühnerkobelite belong to the same group; varulite has $Na > Ca$ and $Mn > Fe$; hühnerkobelite has $Ca > Na$ and $Fe > Mn$. A new analysis from the Hagendorf-South pegmatite gave P_2O_5 42.26, FeO 15.44, Fe_2O_3 13.30, MnO 18.50, MgO 0.66, CaO 1.68, K_2O 0.17, Na_2O 8.47%. An analysis from Norrö, Sweden (Erikson, 1946) previously given as arrojadite is of hagendorfite. The mineral is probably triclinic, pseudo-orthorhombic. It has 3 cleavages, one good, one less good, and the third poor. G. 3.71. H. $3\frac{1}{2}$. Strongly pleochroic, X yellow-brown, Y green, Z blue-green; α 1.739, β and $\gamma > 1.74$. *X*-ray powder data are given. Hagendorfite occurs at the Hagendorf-South pegmatite, Bavaria, with triphylite, wolfeite, and hematite.

M. F.

ANNUAL MEETING OF THE MINERALOGICAL SOCIETY OF AMERICA

The thirty-sixth annual meeting of The Mineralogical Society of America will be held in New Orleans, Louisiana, Monday through Wednesday, November 7–9, 1955. A series of field trips is being planned, one to precede and several to follow the meeting.

Abstracts of papers to be presented at the annual meeting must be received by the Secretary on or before *July 15, 1955*. Abstract blanks may be obtained from the Secretary.

NOMINATIONS OF OFFICERS FOR 1956

President: Clifford Frondel, Harvard University, Cambridge, Massachusetts.
Vice-President: D. Jerome Fisher, University of Chicago, Chicago, Illinois.
Secretary: C. S. Hurlbut, Jr., Harvard University, Cambridge, Massachusetts.
Treasurer: Earl Ingerson, U. S. Geological Survey, Washington, D. C.
Editor: Walter F. Hunt, University of Michigan, Ann Arbor, Michigan.
Councilors (1956–58): Chester B. Slawson, University of Michigan, Ann Arbor, Michigan; Alfred O. Woodford, U. S. Geological Survey, Menlo Park, California.

The above Fellows have been nominated by the Council as officers of The Mineralogical Society of America for 1956. They will be voted on at the election in October 1955.

On the ballot in 1954 the Fellows voted to change Article III, Section 1 of the Constitution so that two Councilors will be elected each year for a term of three years.

C. S. Hurlbut, Jr., *Secretary*

Corrections

The norm was incorrectly given for three chemical analyses (Nos. 1, 3, and 5, page 722) in the paper on "Origin of dunites and of olivine-rich inclusions in baslatic rocks" in the September–October (1954) issue of this journal. The following table gives the analyses and their corrected norms.

Due to typographical errors involving misplaced decimal points, the second sentence, the third paragraph, page 720, should read as follows: "A comparison shows that the average ratio of NiO to MgO is 0.0063 in olivine, 0.0023 in enstatite, and 0.002 in diopside."

Nodule Bearing Rocks*

	Chemical Analysis				*Norms*		
	1	3	5		1	3	5
SiO_2	46.64	41.72	51.24	Q	—	—	—
Al_2O_3	14.45	13.04	17.98				
Fe_2O_3	3.18	2.68	3.30	or	5.57	5.01	12.24
FeO	9.77	10.00	6.61	ab	24.12	26.22	35.65
TiO_2	2.35	2.73	1.51	an	23.92	16.69	18.64
Cr_2O_3	—	0.06	—				
CaO	9.86	10.82	6.98	lc	—	—	—
MgO	9.33	9.00	4.62	ne	—	2.56	5.40
Na_2O	2.84	3.74	5.39				
K_2O	0.97	0.88	2.10	hl	—	0.12	—
MnO	0.19	0.18	—				
NiO	—	—	—	wo	9.64	5.46	6.74
BaO	—	0.07	—	en	3.71	—	—
ZrO_2	—	0.03	—	fs	1.85	—	—
CO_2	0.01	3.19	—				
P_2O_5	0.34	0.58	—	fo	13.65	15.69	8.09
H_2O-	0.00	0.27	—	fa	7.74	9.27	5.30
H_2O+	0.06	0.92	0.35				
				mt	4.63	3.94	4.86
				il	4.40	5.16	2.88
				hm	—	—	—
				ap	0.67	1.35	—
				cc	—	7.31	—
Total	99.99	100.02†	100.08		99.90	98.78	99.80

* See *American Mineralogist*, Vol. 39, 722 (1954).

† Includes 0.11 per cent Cl.